

# Out of time ordered effective dynamics of a Brownian particle

A Thesis

Submitted to the  
Tata Institute of Fundamental Research, Mumbai  
for the Degree of Doctor of Philosophy  
in Physics

by  
Soumyadeep Chaudhuri

International Centre for Theoretical Sciences  
Tata Institute of Fundamental Research  
Bangalore  
August, 2019

## DECLARATION

This thesis is a presentation of my original research work. Wherever contributions of others are involved, every effort is made to indicate this clearly, with due reference to the literature, and acknowledgement of collaborative research and discussions. The work was done under the guidance of Professor R. Loganayagam, at the International Centre for Theoretical Sciences (ICTS), Bangalore of the Tata Institute of Fundamental Research (TIFR), Mumbai.

*Soumyadeep Chaudhuri*  
(Soumyadeep Chaudhuri)

In my capacity as supervisor of the candidate's thesis, I certify that the above statements are true to the best of my knowledge.

*R. Loganayagam*  
(R. Loganayagam)

Date: 29<sup>TH</sup> AUG 2019 .

# List of publications

## Publications relevant to the thesis:

1. Soumyadeep Chaudhuri, R. Loganayagam, “*Probing Out-of-Time-Order Correlators*”, *J. High Energ. Phys.* 07, 006 (2019), [arXiv:1807.09731 \[hep-th\]](#).
2. Soumyadeep Chaudhuri, Chandramouli Chowdhury, R. Loganayagam, “*Spectral representation of thermal OTO correlators*”, *J. High Energ. Phys.* 02, 018 (2019), [arXiv:1810.03118 \[hep-th\]](#).
3. Bidisha Chakrabarty, Soumyadeep Chaudhuri, R. Loganayagam, “*Out of Time Ordered Quantum Dissipation*”, *J. High Energ. Phys.* 07, 102 (2019), [arXiv:1811.01513 \[cond-mat.stat-mech\]](#).
4. Bidisha Chakrabarty, Soumyadeep Chaudhuri, “*Out of time ordered effective dynamics of a quartic oscillator*”, *SciPost Phys.* 7, 013 (2019), [arXiv:1905.08307 \[hep-th\]](#).

## Other publications:

1. Soumyadeep Chaudhuri, Victor I. Giraldo-Rivera, Anosh Joseph, R. Loganayagam, Junggi Yoon, “*Abelian Tensor Models on the Lattice*”, *Phys. Rev. D* 97, 086007, [arXiv:1705.01930 \[hep-th\]](#).
2. Bidisha Chakrabarty, Joydeep Chakravarty, Soumyadeep Chaudhuri, Chandan Jana, R. Loganayagam, Akhil Sivakumar, “*Nonlinear Langevin dynamics via holography*”, [arXiv:1906.07762 \[hep-th\]](#).

## **ACKNOWLEDGEMENTS**

I would like to begin by thanking my advisor Dr. R. Loganayagam for his constant encouragement, guidance and support during my Ph.D. I am also thankful to all the past and present members of ICTS for creating a wonderful ambience for scientific research. I would like to express my gratitude to my collaborators for their cooperation and enthusiastic participation in the research projects. It has been a delightful experience to work with them. I am deeply grateful to Dr. Goutam Pal, Mr. Tapas Ghosh, and my mother, Dr. Chitrita Chaudhuri, for their encouragement and support throughout my academic career. Finally, I would like to acknowledge my debt to the people of India for their steady and generous support to research in the basic sciences.

# Contents

<b>1</b>	<b>Introduction</b>	<b>1</b>
1.1	A brief review of our present understanding of OTOCs . . . . .	2
1.2	An overview of the work described in this thesis . . . . .	5
<b>2</b>	<b>Cubic OTO effective theory</b>	<b>8</b>
2.1	Introduction . . . . .	8
2.2	Cubic Schwinger-Keldysh effective theory . . . . .	10
2.3	Extension to the OTO effective theory . . . . .	17
2.4	Conclusion and Discussion . . . . .	26
<b>3</b>	<b>Spectral representation of thermal OTO correlators</b>	<b>29</b>
3.1	Introduction . . . . .	30
3.2	Spectral representation of SK two point functions . . . . .	33
3.3	Spectral representation of generalised SK two point functions . . . . .	39
3.4	Spectral representation of higher point correlators . . . . .	47
3.5	Conclusion and Discussion . . . . .	53
<b>4</b>	<b>Cubic OTO effective theory for thermal environment</b>	<b>55</b>
4.1	Motivation . . . . .	56
4.2	Review of Caldeira-Leggett model . . . . .	58
4.3	Introduction to Non-linear Langevin equation . . . . .	67
4.4	Introduction to the qXY model . . . . .	83
4.5	Effective theory of the Brownian particle . . . . .	92
4.6	Relations between effective couplings . . . . .	99
4.7	Conclusion and discussion . . . . .	110

<b>5</b>	<b>Quartic OTO effective theory</b>	<b>113</b>
5.1	Introduction . . . . .	113
5.2	Description of the $qXY$ model . . . . .	115
5.3	Schwinger-Keldysh effective theory of the oscillator . . . . .	117
5.4	Extension to the effective theory for OTO correlators . . . . .	129
5.5	Conclusion and discussion . . . . .	149
<b>6</b>	<b>Conclusion</b>	<b>153</b>
6.1	Summary of the thesis . . . . .	153
6.2	Future directions . . . . .	156
<b>A</b>	<b>Appendices to Chapter 3</b>	<b>158</b>
A.1	Basis of column vectors . . . . .	158
A.2	Rules of contraction for general $k$ . . . . .	160
A.3	Orthogonal tensors and Column Vector Representation . . . . .	173
<b>B</b>	<b>Appendices to Chapter 4</b>	<b>195</b>
B.1	Dimensional analysis . . . . .	195
B.2	Contour integrals and Poles for the Effective Couplings . . . . .	196
<b>C</b>	<b>Appendices to Chapter 5</b>	<b>199</b>
C.1	Cumulants of the bath operator that couples to the particle . . . . .	199
C.2	Argument for the validity of the Markovian limit . . . . .	202
C.3	Relations between the OTO effective couplings and the bath's OTOCs . . . . .	203
C.4	Quartic couplings in the high temperature limit . . . . .	205

# Chapter 1

## Introduction

The effective theory framework is a very useful tool for studying the dynamics of quantum systems. In any such study, it is important to first identify the appropriate set of degrees of freedom for the observables of interest. Then, based on the symmetries of the system, one can try to construct an effective theory which governs the dynamics of these relevant degrees of freedom. Such an effective theory enables one to compute physically interesting quantities in a scenario where a microscopic computation is not feasible.

Traditionally, this effective theory paradigm has been employed to study the evolution of a system given some data on its initial conditions.<sup>1</sup> The physical observables associated with this forward evolution (in time) of the system are determined by the time-ordered correlators of its operators (in the Heisenberg picture).

However, quite recently, a different class of problems have drawn the attention of physicists. These involve the sensitivity of the evolution of a quantum system to small changes in the initial conditions<sup>2</sup>. In such problems, one needs to compare two states of the system which are connected by a succession of backward and forward evolutions in time accompanied with insertions of operators in the middle. Consequently, such delicate comparisons require information of correlation functions where the insertions violate time-ordering.

These Out-of-Time-Order Correlators (OTOCs) have been studied in varied contexts. They have been found to be useful in determining the rate of scrambling of information in quantum systems [1–4], and have been used as diagnostic measures for related phenomena such as chaos

---

<sup>1</sup>For a closed quantum system, such an initial condition would be the initial quantum state of the system. More generally, for open systems, such initial conditions are typically encapsulated in the initial reduced density matrix of the system.

<sup>2</sup>Such a small change in the initial state can be accomplished by the action of an operator close to identity.

[1, 5–8], thermalisation and many-body localisation [9–13], and spread of entanglement [14–16]. Parallely, several experimental protocols [4, 17–19] have been suggested to measure these OTOCs which may lead to a set of new observables that encode hitherto unknown features of quantum systems. We will now briefly discuss some of these progresses in our understanding of OTOCs.

## 1.1 A brief review of our present understanding of OTOCs

The first systematic analysis of OTOCs arose in the study of scrambling of information in black holes [1, 2]. The notion of scrambling of information in a system involves the spread/delocalisation of an initially local perturbation introduced into the system. For instance, in the context of black holes, one can consider some small object being thrown into the horizon. The information contained in this object eventually gets delocalised in the Hawking quanta emitted by the black hole. Similar scrambling of information takes place in most physical systems where there are many degrees of freedom interacting with each other. In such systems, a small perturbation introduced to a local degree of freedom eventually gets delocalised to other degrees of freedom via the interactions between these degrees of freedom.

A natural question to ask in this context is how does one quantify the rate at which such a spread of information takes place in a system. In recent years, it was found that a particular kind of OTOC can actually capture this rate. To illustrate this, let us consider a generic  $d$ -dimensional QFT in some state  $|\psi\rangle$ . Now, suppose we perturb this state by an operator  $V(\vec{x}_1, t_0)$  which is purely a function of the fields at the point  $(\vec{x}_1, t_0)$ . If we consider some other operator  $W(\vec{x}_2, t_0)$  at the same time instant  $t_0$  but localised at a different spatial point  $\vec{x}_2$ , then the commutation of the fields at these two points leads to the vanishing of the commutator of the two operators  $V(\vec{x}_1, t_0)$  and  $W(\vec{x}_2, t_0)$ . Therefore, we have

$$\langle\psi|[W(\vec{x}_2, t_0), V(\vec{x}_1, t_0)]^\dagger[W(\vec{x}_2, t_0), V(\vec{x}_1, t_0)]|\psi\rangle = 0. \quad (1.1)$$

Note that the operator whose expectation value appears in the LHS of the above equation is positive semi-definite.

Now, one can evolve the operator  $V(x_1, t_0)$  to a later instant  $t$  as follows

$$V(\vec{x}_1, t) = e^{iH(t-t_0)}V(\vec{x}_1, t_0)e^{-iH(t-t_0)}, \quad (1.2)$$



where  $H$  is the Hamiltonian of the system. For sufficiently large values of  $t$ , the operators  $V(\vec{x}_1, t)$  and  $W(\vec{x}_2, t_0)$  would have a nontrivial commutator, and hence we will have

$$\mathcal{F}(t, t_0) \equiv \langle \psi | [W(\vec{x}_2, t_0), V(\vec{x}_1, t)]^\dagger [W(\vec{x}_2, t_0), V(\vec{x}_1, t)] | \psi \rangle > 0. \quad (1.3)$$

The magnitude of the above quantity represents the overlap of the two operators  $V(\vec{x}_1, t)$  and  $W(\vec{x}_2, t_0)$  as witnessed in the state  $|\psi\rangle$ . Therefore it can serve as a measure of delocalisation of the initial perturbation applied at  $(\vec{x}_1, t_0)$  to the degrees of freedom at the point  $\vec{x}_2$  in the time span  $(t - t_0)$ .

Notice that the above function  $\mathcal{F}(t, t_0)$  can be written as a sum of 4 correlators as follows:

$$\begin{aligned} \mathcal{F}(t, t_0) = & \langle \psi | V^\dagger(\vec{x}_1, t) W^\dagger(\vec{x}_2, t_0) W(\vec{x}_2, t_0) V(\vec{x}_1, t) | \psi \rangle \\ & + \langle \psi | W^\dagger(\vec{x}_2, t_0) V^\dagger(\vec{x}_1, t) V(\vec{x}_1, t) W(\vec{x}_2, t_0) | \psi \rangle \\ & - \langle \psi | W^\dagger(\vec{x}_2, t_0) V^\dagger(\vec{x}_1, t) W(\vec{x}_2, t_0) V(\vec{x}_1, t) | \psi \rangle \\ & - \langle \psi | V^\dagger(\vec{x}_1, t) W^\dagger(\vec{x}_2, t_0) V(\vec{x}_1, t) W(\vec{x}_2, t_0) | \psi \rangle. \end{aligned} \quad (1.4)$$

The last two correlators in this sum has the interesting property that the insertions violate time-ordering twice in each of them. Such correlators are examples of what are now known as Out-of-Time-Order-Correlators (OTOCs). So, we see how the evaluation of such OTOCs is important in determining the rate of scrambling of information among the degrees of freedom of a system.

A particular case where such scrambling is of special interest is the class of systems which demonstrate quantum chaos. In such systems, OTOCs like the function  $\mathcal{F}(t, t_0)$  grow exponentially as the time interval  $(t - t_0)$  is increased<sup>3</sup>. In fact, such exponential growth of OTOCs allows one to identify and quantify chaos in quantum systems. This is a direct extension of similar measures of chaos in classical systems as we explain below.

Consider a classical particle which is governed by a chaotic dynamics. For simplicity, let us restrict our attention to the case where the particle is constrained to move in only one direction. Let the position of the particle as a function of time  $t$  be represented by  $q(t)$  and the corresponding momentum be given by  $p(t)$ . Now, if we change the particle's position at some initial time  $t_0$  by a very small amount  $\delta q(t_0)$  (keeping the initial momentum fixed), then the

---

<sup>3</sup>This exponential growth persists upto a timescale beyond which it starts to saturate.

corresponding change in its position at some later time  $t$  is given by

$$\delta q(t) = \left. \frac{\partial q(t)}{\partial q(t_0)} \right|_{p(t_0)} \delta q(t_0) = \{q(t), p(t_0)\} \delta q(t_0) \quad (1.5)$$

where  $\{q(t), p(t_0)\}$  denotes the Poisson bracket between these  $q(t)$  and  $p(t_0)$ . Therefore, we have

$$\left( \frac{\delta q(t)}{\delta q(t_0)} \right)^2 = \{q(t), p(t_0)\}^2. \quad (1.6)$$

For a chaotic system, the above ratio increases exponentially with time. The exponent which determines the rate of this growth is known as the Lyapunov exponent.

Notice that the RHS of the above equation goes to the square of a commutator under the standard rules of quantisation as shown below:

$$\{q(t), p(t_0)\}^2 \longrightarrow \left( \frac{1}{i\hbar} [q(t), p(t_0)] \right)^2 = -\frac{1}{\hbar^2} [q(t), p(t_0)]^2 = \frac{1}{\hbar^2} [p(t_0), q(t)]^\dagger [p(t_0), q(t)]. \quad (1.7)$$

Thus, a natural way to extend the measure of chaos to quantum systems is to consider the expectation value of the above operator. This expectation value has a structure quite similar to the function  $\mathcal{F}(t, t_0)$  that we introduced earlier. Hence, we find that OTOCs can serve as nice diagnostic measures of quantum chaos.

The Lyapunov exponents that determine the rate of growth of such OTOCs in chaotic systems satisfy the following interesting property [5]: For thermal states, these exponents have an upper bound which is given by  $\frac{2\pi k_B T}{\hbar}$ , where  $T$  is the temperature. Moreover, this bound is saturated for holographic QFTs whose thermal states (at sufficiently high temperature) are dual to black holes in the corresponding gravitational theories. This result has led to investigations of potential holographic duals of several quantum mechanical models where the chaos bound is saturated [7, 20–27].

A phenomenon that is intimately related to scrambling and chaos in quantum systems is *thermalisation*. To understand this phenomenon, consider a system with many degrees of freedom that are in thermal equilibrium. Now, suppose one perturbs this system slightly away from equilibrium. Then, in most cases, the system eventually goes to a new state where many observables approximately behave as they would in a thermal state. This approximate equilibration of the system is commonly known as thermalisation. There are some known exceptions where the system actually fails to achieve such an equilibration (see [28] for a review on such systems).

In such cases, the system is said to be in a *many-body localised phase*. Whether a system thermalises or not depends on whether the information contained in the perturbation gets delocalised in its degrees of freedom. If such a delocalisation happens, then one has to perform very fine measurements to recover information about the details of this perturbation. For more coarse-grained observables, the system roughly appears to be in thermal equilibrium. Thus, scrambling of information plays a central role in the thermalisation of a system, and OTOCs can serve as good diagnostic measures of thermalisation. In situations where the system does thermalise, such OTOCs can also be used to quantify the rate of thermalisation [11–13]. In other cases, they can be used to diagnose many-body localisation [9, 10].

Another interesting aspect of OTOCs that has been explored in recent years is their relation to the structure of entanglement between different components of a system. Intuitively, it seems plausible that as some information gets scrambled in the degrees of freedom of a many-body system, there is also a build-up of entanglement between these degrees of freedom. To detect such entanglement, one has to look at very fine measures such as the Renyi entropies or multipartite quantum information between different components of the system [14–16]. However, as we will briefly discuss in chapter 6, there is still a need to find appropriate generalisations of standard information theoretic quantities which can fully capture the essence of OTOCs.

## 1.2 An overview of the work described in this thesis

Despite the progresses in the study of OTOCs discussed in the previous section, we still lack a convenient framework to compute them as many familiar tools of effective theory are yet to be extended to include the information contained in them. In this thesis, we will discuss the results of some recent works [29–32] which are aimed towards filling this gap.

To develop the basic ideas behind the construction of an effective theory for OTOCs, we will consider a very simple system viz. a Brownian particle interacting with a large environment. In this setup, we will discuss the OTO dynamics of the particle in a path integral formalism defined on a contour with multiple time-folds<sup>4</sup>. We will see that couplings in this effective dynamics receive contributions from the OTOCs of the environment. These relations between the particle’s effective couplings and the environment’s OTOCs provide a convenient way to extract information of these OTOCs by performing measurements on the particle. Moreover, these

---

<sup>4</sup>This is a generalisation [33, 34] of the Schwinger-Keldysh formalism [35–37].

relations also allow one to study the effects of symmetries in the environment's microscopic dynamics on the particle's effective theory. We will consider the effects of one such symmetry, viz. microscopic time-reversal invariance, and show that it leads to OTO generalisations of the Onsager-Casimir reciprocal relations [38–40] between the particle's effective couplings.

Apart from the generalised Onsager-Casimir relations, there are some additional constraints on the effective couplings when the environment is in a thermal state. These constraints follow from the Kubo-Martin-Schwinger relations [41–43] between the thermal correlators of the environment. At the level of the quadratic effective couplings in the high temperature limit, the KMS relations imply the well-known fluctuation-dissipation relation [44–47] which connects the thermal random force experienced by the particle to its damping coefficient. We will show that the cubic and quartic couplings in the effective dynamics satisfy some generalisations of this fluctuation-dissipation relation which connect the non-Gaussianity in the thermal noise experienced by the particle to a thermal jitter in its damping coefficient. We will argue that these generalised fluctuation-dissipation relations arise due to a combined effect of microscopic reversibility in the environment's dynamics and its thermality.

### **Organisation of the thesis:**

In chapter 2, we will lay down the structure of a cubic OTO effective action of a Brownian particle interacting with a general environment. We will see that certain cubic couplings in this effective action receive contributions from the environment's 3-point OTOCs. We will provide the expressions of these couplings in terms of the environment's OTOCs. Such expressions may be useful in extracting information about the OTOCs of the environment by performing measurements on the particle.

From chapter 3 onwards, we will focus on the case where the environment is a thermal bath. The OTOCs of such a thermal bath satisfy some relations between its correlators. These relations are based on microscopic unitarity and thermality of the bath. We will show that these relations can be encapsulated concisely by expressing the bath's correlators in terms of a minimal set of independent spectral functions. Such representations of the bath's OTOCs are useful for exploring the constraints imposed on the particle's effective dynamics due to thermality of the bath. In addition, they simplify the perturbative analysis of thermal OTOCs in an interacting theory.

In chapter 4, we will discuss the constraints imposed on the particle's cubic effective dy-

namics by microscopic reversibility and thermality of the bath. To illustrate these constraints with a concrete model, we will consider a bath comprising of two sets of harmonic oscillators coupled nonlinearly to the particle. We will show that the bath's microscopic reversibility leads to a set of generalised Onsager relations which connect the particle's cubic OTO couplings to its Schwinger-Keldysh (SK) couplings. Moreover, the bath's thermality induces an OTO generalisation of the fluctuation-dissipation relation (FDR) between a cubic OTO coupling and a Schwinger-Keldysh coupling. Combining these two kinds of relations, we will obtain a generalised fluctuation-dissipation relation between two cubic SK couplings. We will show that the SK effective couplings enter as parameters in a dual non-linear Langevin dynamics, where the generalised FDR connects the non-Gaussianity in the noise distribution with a thermal jitter in the particle's damping.

In chapter 5, we will discuss the quartic terms in the OTO effective action. There, we will extend many of the results obtained in the previous chapters to obtain some generalised Onsager relations and a generalised fluctuation-dissipation relation between the quartic couplings.

In chapter 6, we will conclude with a brief summary of the contents of this thesis and some discussion on future directions.

# Chapter 2

## Cubic OTO effective theory

This chapter is based on the paper [29] written by the author in collaboration with R. Loganayagam.

### Comment on the conventions followed in this chapter:

In this chapter, we will work in units where  $\hbar = 1$  and the mass of the particle coupling to the environment is unity.

### 2.1 Introduction

In this chapter, we will develop the basic framework of the out of time ordered effective theory of a Brownian particle interacting with an environment in a generic state. The usual approach towards studying the effective dynamics of an open system (like the Brownian particle in this case) is to look at the evolution of the reduced density matrix of the system. We will first discuss this effective dynamics and systematically take into account the contributions of 3-point correlators of the environment in this dynamics. While this effective dynamics is useful to study a host of phenomena such as decoherence, dissipation, thermalisation, etc. [48–50], it fails to capture the effects of the OTO correlators of the environment. In addition, it is also insufficient for the computation of OTO correlators of the particle.

To overcome these limitations, we will extend the effective dynamics by including the contributions of the 3-point OTOCs of the environment <sup>1</sup>. We will see that these 3-point OTOCs of the environment contribute to some cubic couplings in this extended effective theory. These

---

<sup>1</sup>The effects of the 4-point OTOCs of the environment will be discussed later in chapter 5.

cubic couplings do not appear in the effective dynamics of the particle's reduced density matrix. However, they do contribute to the OTO correlators of the particle (see the discussion in 2.3.4). For this reason, we would call them 'OTO couplings' of the particle. We will determine the relations between these cubic OTO couplings and the 3-point OTOCs of the environment. Such relations provide a way to extract information about the environment's OTOCs by measuring the particle's effective OTO couplings. It would be interesting to extend the currently existing OTOC measurement protocols [4, 15, 17–19, 51, 52] to this context.

### **Organisation of the chapter:**

In section 2.2, we develop the cubic Schwinger-Keldysh effective theory of a Brownian particle. We start by reviewing the evolution of the reduced density matrix of the particle. We show that this evolution is determined by a path integral in the Schwinger-Keldysh formalism. We discuss a Markovian regime where the influence phase in this SK path integral can be taken to be approximately local in time. Corresponding to this effective dynamics, we lay down the rules for constructing a cubic 1-PI effective action. These rules are based on the microscopic unitarity of the (particle+environment) combined system and the Hermiticity of the operator representing the position of the particle. Although the effective action derived from these rules correctly describes the evolution of the reduced density matrix and allows one to compute the Schwinger-Keldysh correlators of the particle, we argue that it is inadequate to compute the OTO correlators of the particle.

In section 2.3, we extend the effective dynamics to include the OTOCs of the particle in the analysis. This is done through a path integral formalism defined on a double-folded time contour. By integrating out the environment's degrees of freedom on this contour, we show that one gets a generalisation of the influence phase of the particle which encodes the effects of the OTOCs of the environment. Corresponding to this OTO dynamics of the particle, we write down a cubic OTO 1-PI effective action. We identify the cubic couplings in this OTO effective action which receive contributions of the environment's 3-point OTOCs. We express these OTO couplings in terms of the environment's OTOCs upto leading order in the particle-environment coupling. We also show how these OTO couplings appear in the OTOCs of the particle.

In section 2.4 we conclude with some discussion on future directions.

## 2.2 Cubic Schwinger-Keldysh effective theory

### 2.2.1 Evolution of the reduced density matrix of the particle

Consider the situation where a Brownian particle ( $q$ ) is coupled to an environment with a large number of degrees of freedom. Let us denote these degrees of freedom collectively by  $X$ . The Lagrangian of the combined system of the particle and the environment is given by <sup>2</sup>

$$L[q, X] = \frac{1}{2}(\dot{q}^2 - m_0^2 q^2) + L_E[X] + \lambda Oq. \quad (2.1)$$

Here,  $m_0$  is the frequency of the particle and  $L_E[X]$  is the Lagrangian of the environment. The environment couples to the particle's position via an operator  $O$ .  $\lambda$  is the strength of this coupling. We will take  $\lambda$  to be small i.e. the particle to be weakly coupled to the environment. This allows us to employ perturbation theory in obtaining an effective dynamics of the particle.

Let us assume that the particle and the environment are initially unentangled and the interaction between them is switched on at a time  $t_0$ . Then the state of the (particle+environment) combined system at  $t_0$  is given by

$$\rho_0 = \rho_{E0} \otimes \rho_{p0}, \quad (2.2)$$

where  $\rho_{E0}$  and  $\rho_{p0}$  are the density matrices of the environment and the particle respectively at the time  $t_0$ .

After the particle starts interacting with the environment, an effective description of its state can be given in terms of its reduced density matrix which is obtained by tracing out the environment's degrees of freedom in the density matrix of the combined system. The evolution of the reduced density matrix is given by the quantum master equation [49] of the particle. An equivalent description of this evolution can be developed in terms of an effective action of the particle <sup>3</sup> in the Schwinger-Keldysh formalism [35–37, 43, 54, 55].

In this formalism, one can determine the density matrix of the combined system at some later time  $t_f$  from a path integral on the contour shown in figure 2.1. This contour has two legs which we label as 1 and 2. For each of these legs, we need to take a copy of the degrees of freedom of both the particle and the environment:  $\{q_1, X_1\}$  and  $\{q_2, X_2\}$ . The evolution of the density matrix of the combined system is then obtained from a path integral with a Lagrangian

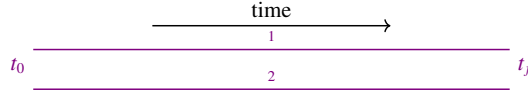
---

<sup>2</sup>In this chapter we work in units where the bare mass of particle is unity, and  $\hbar = 1$ .

<sup>3</sup>We refer the reader to [53] for a discussion on how the quantum master equation is related to the Schwinger-Keldysh effective action.



Figure 2.1: Contour for evolution of the density matrix



of the following form<sup>4</sup>

$$L_{\text{SK}} = L[q_1, X_1] - L[-q_2, X_2]. \quad (2.3)$$

Let us denote all the degrees of freedom of the combined system collectively by  $Q$ . Then, the two copies of these degrees of freedom can be expressed as

$$\{q_1, X_1\} \rightarrow Q_1, \{-q_2, X_2\} \rightarrow Q_2. \quad (2.4)$$

Now, given the information that the initial density matrix at time  $t_0$  is  $\rho_0(Q_{10}, Q_{20})$ , the density matrix at the later time  $t_f$  is given by the following path integral:

$$\rho_f(Q_{1f}, Q_{2f}) = \int dQ_{10} \int dQ_{20} \rho_0(Q_{10}, Q_{20}) \int_{\substack{Q_1(t_0)=Q_{10}, \\ Q_2(t_0)=Q_{20}}}^{\substack{Q_1(t_f)=Q_{1f}, \\ Q_2(t_f)=Q_{2f}}} [DQ_1][DQ_2] e^{i \int_{t_0}^{t_f} dt L_{\text{SK}}[Q_1(t), Q_2(t)]}. \quad (2.5)$$

To get the reduced density matrix ( $\rho_{pf}$ ) of the particle at the time  $t_f$ , we need to trace out the environment's degrees of freedom at  $t_f$ . This can be achieved in the above path integral by setting

$$X_{1f} = X_{2f} = X_f, \quad (2.6)$$

and then integrating over  $X_f$ .

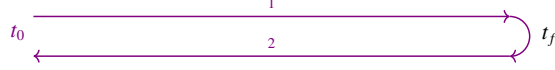
This path integral representation of the reduced density matrix still involves integrals over the environment's degrees of freedom. One can, however, express this integral in terms of only the particle's degrees of freedom by integrating out the environment's coordinates. Such an integral over the environment's coordinates leads to a correction to the particle's action. This additional piece in the action which encapsulates the influence of the environment on the particle's dynamics is called the 'influence phase' of the particle [37]. Next, we discuss the form of this influence phase.

<sup>4</sup>Here we find it convenient to put an extra minus sign in  $q_2$  over the standard convention followed in texts on the Schwinger-Keldysh formalism [43, 54].

## 2.2.2 The influence phase of the particle

In the previous subsection we argued that the expression for the reduced density matrix  $\rho_{pf}$  can be obtained from the path integral in (2.5) by identifying the environment's degrees of freedom on the two legs at the time  $t_f$ . Therefore, in this expression, the environment's coordinates have to be integrated over a contour of the following form: This is the usual Schwinger-Keldysh

Figure 2.2: Schwinger-Keldysh contour



contour where the two legs are connected by a future-turning point. Path integrals over such a contour give correlators where the insertions are contour-ordered according to the arrow indicated in figure 2.2. Therefore, such contour-ordered correlators of the environment would contribute to the effective action of the particle when the environment's coordinates are integrated out.

The contributions of the environment's correlators are imprinted in the influence phase ( $W_{\text{SK}}$ ) which appears in the path integral for  $\rho_{pf}$  as follows

$$\rho_{pf}(q_{1f}, -q_{2f}) = \int dq_{10} \int dq_{20} \rho_{p0}(q_{10}, -q_{20}) \int_{\substack{q_1(t_f)=q_{1f}, \\ q_2(t_f)=q_{2f} \\ q_1(t_0)=q_{10}, \\ q_2(t_0)=q_{20}}} [Dq_1][Dq_2] e^{i \left[ \frac{1}{2} m_p \int_{t_0}^{t_f} dt \left\{ (\dot{q}_1^2 - \bar{\mu}_0^2 q_1^2) - (\dot{q}_2^2 - \bar{\mu}_0^2 q_2^2) \right\} + W_{\text{SK}} \right]} \quad (2.7)$$

The influence phase in the above expression can be expanded as a perturbation series in  $\lambda$ :

$$W_{\text{SK}} = \sum_{n=1}^{\infty} \lambda^n W_{\text{SK}}^{(n)}, \quad (2.8)$$

where

$$W_{\text{SK}}^{(n)} = i^{n-1} \sum_{i_1, \dots, i_n=1}^2 \int_{t_0}^{t_f} dt_1 \cdots \int_{t_0}^{t_{n-1}} dt_n \langle \mathcal{T}_C O_{i_1}(t_1) \cdots O_{i_n}(t_n) \rangle_c q_{i_1}(t_1) \cdots q_{i_n}(t_n). \quad (2.9)$$

Here  $\langle \mathcal{T}_C O_{i_1}(t_1) \cdots O_{i_n}(t_n) \rangle_c$  is the cumulant (connected part) of a contour-ordered correlator of  $O(t)$  where the insertion at time  $t_j$  is on the  $i_j^{\text{th}}$  leg.

In this chapter, we will restrict our attention to up to cubic terms in this influence phase.

These terms are given below:

$$W_{\text{SK}}^{(2)} = i \sum_{i_1, i_2=1}^2 \int_{t_0}^{t_f} dt_1 \int_{t_0}^{t_1} dt_2 \langle \mathcal{T}_C O_{i_1}(t_1) O_{i_2}(t_2) \rangle_c q_{i_1}(t_1) q_{i_2}(t_2), \quad (2.10)$$

$$W_{\text{SK}}^{(3)} = - \sum_{i_1, i_2, i_3=1}^2 \int_{t_0}^{t_f} dt_1 \int_{t_0}^{t_1} dt_2 \int_{t_0}^{t_2} dt_3 \langle \mathcal{T}_C O_{i_1}(t_1) O_{i_2}(t_2) O_{i_3}(t_3) \rangle_c q_{i_1}(t_1) q_{i_2}(t_2) q_{i_3}(t_3). \quad (2.11)$$

Plugging these expressions for the quadratic and cubic terms in the influence phase into the path integral given in (2.7), one can determine the evolution of the reduced density matrix of the particle. The action that appears in this path integral can also be used to compute the correlators of the particle.<sup>5</sup> From the form of the influence phase in (2.9), we can see that this action is non-local in time. Next, we discuss a certain limit in which one may get an approximately local form for this action.

### 2.2.3 Markovian limit

The coefficient functions appearing in the influence phase given in (2.9) are the cumulants of the operator  $O$  which couples to the particle. Now, if these cumulants decay sufficiently fast compared to the time-scales in which the particle evolves, then one can get an approximately local dynamics of the particle. This regime is commonly known as the Markovian limit.<sup>6</sup>

In such a limit, the information about the particle's state that gets transmitted to the bath (via the operator  $O$ ) is quickly forgotten by the bath. Hence, there is very little feedback of this information on the particle's later dynamics. Therefore, the effective dynamics of the particle at any given instant is mostly determined by its state in the immediate past. This approximation of a local effective dynamics is tantamount to Taylor-expanding the different  $q$ 's in the terms of the influence phase about a single time instant (say,  $t_1$ ), and truncating at some finite order. We

---

<sup>5</sup>To compute the particle's correlators from path integrals with this effective action, one needs to put  $q_1 = -q_2$  at some time in the future of all the insertions.

<sup>6</sup>In chapter 4, we will discuss an explicit example of such a regime.

show the forms of such approximately local terms in the influence phase below:

$$\begin{aligned}
W_{SK}^{(2)} \approx & i \sum_{i_1, i_2=1}^2 \int_{t_0}^{t_f} dt_1 \left[ \left\{ \int_{t_0}^{t_1} dt_2 \langle \mathcal{T}_C O_{i_1}(t_1) O_{i_2}(t_2) \rangle_c \right\} q_{i_1}(t_1) q_{i_2}(t_1 - \epsilon) \right. \\
& + \left\{ \int_{t_0}^{t_1} dt_2 \langle \mathcal{T}_C O_{i_1}(t_1) O_{i_2}(t_2) \rangle_c t_{21} \right\} q_{i_1}(t_1) \dot{q}_{i_2}(t_1 - \epsilon) \\
& \left. + \left\{ \int_{t_0}^{t_1} dt_2 \langle \mathcal{T}_C O_{i_1}(t_1) O_{i_2}(t_2) \rangle_c \frac{t_{21}^2}{2} \right\} q_{i_1}(t_1) \ddot{q}_{i_2}(t_1 - \epsilon) \right], \tag{2.12}
\end{aligned}$$

$$\begin{aligned}
W_{SK}^{(3)} \approx & - \sum_{i_1, i_2, i_3=1}^2 \int_{t_0}^{t_f} dt_1 \left[ \left\{ \int_{t_0}^{t_1} dt_2 \int_{t_0}^{t_2} dt_3 \langle \mathcal{T}_C O_{i_1}(t_1) O_{i_2}(t_2) O_{i_3}(t_3) \rangle_c \right\} \right. \\
& q_{i_1}(t_1) q_{i_2}(t_1 - \epsilon) q_{i_3}(t_1 - 2\epsilon) \\
& + \left\{ \int_{t_0}^{t_1} dt_2 \int_{t_0}^{t_2} dt_3 \langle \mathcal{T}_C O_{i_1}(t_1) O_{i_2}(t_2) O_{i_3}(t_3) \rangle_c t_{21} \right\} \\
& q_{i_1}(t_1) \dot{q}_{i_2}(t_1 - \epsilon) q_{i_3}(t_1 - 2\epsilon) \\
& + \left\{ \int_{t_0}^{t_1} dt_2 \int_{t_0}^{t_2} dt_3 \langle \mathcal{T}_C O_{i_1}(t_1) O_{i_2}(t_2) O_{i_3}(t_3) \rangle_c t_{31} \right\} \\
& \left. q_{i_1}(t_1) q_{i_2}(t_1 - \epsilon) \dot{q}_{i_3}(t_1 - 2\epsilon) \right]. \tag{2.13}
\end{aligned}$$

Here, we have kept up to second order derivative terms in the quadratic piece to take into account the correction to the kinetic term in the particle's action. For the cubic piece, we have kept terms with at most a single derivative. To preserve the information about the original ordering of the different time instants, we have kept a small point-split regulator  $\epsilon > 0$ .<sup>7</sup>

Using this approximate local form of the influence phase, one can determine the particle's correlators. The same correlators can be obtained from a local 1-PI effective action [56]<sup>8</sup>. The utility of such a local effective action is that its form is heavily constrained by the unitarity of the (particle+environment) combined system. Hence, this form is quite insensitive to the microscopic details of the environment's dynamics. Next, we discuss this form of the particle's 1-PI effective action and the constraints that lead to it.

<sup>7</sup>It is important to keep this regulator as otherwise one can get wrong answers while computing contributions of loop diagrams where two of the  $q$ 's on the same vertex contract with each other.

<sup>8</sup>Only the connected tree level diagrams obtained from the 1-particle irreducible effective (1-PI) action contribute to the connected parts of the particle's correlators.

## 2.2.4 The Schwinger-Keldysh 1-PI effective action

In the previous subsection we discussed an approximately local form of the influence phase which is obtained by perturbatively expanding the effects of the particle-environment interaction on the particle's dynamics. By putting appropriate initial conditions on path integrals with this influence phase one can calculate the correlators of the particle. However, as we saw, the influence phase has a slight non-locality due to the presence of the point-split regulator. It is cumbersome to keep track of this ordering of the time instants for the different  $q$ 's in the effective action. To avoid this, we introduce a 1-PI effective action for the particle which can be employed to compute its correlators.<sup>9</sup> An additional advantage of developing this 1-PI effective action is that its structure is constrained by some general principles which do not rely on the explicit form of the particle-environment interaction given in (2.1). We discuss these constraints below:

- **Collapse rule:**

The effective action should vanish under the following identification:

$$q_1 = -q_2 = \tilde{q}. \quad (2.14)$$

As discussed in [43, 57], this condition is based on the fact that the particle is a part of a closed system governed by a unitary dynamics. At the level of correlators, it makes sure that the value of a contour-ordered correlator of the particle just picks up a sign when one slides the future-most insertion from one leg to the other without changing its temporal position. The sign is introduced because we are putting an extra minus sign in the definition of  $q_2$  over the convention followed in [43, 57].

- **Reality condition:**

The effective action should become its own negative under complex conjugation along with the following exchange:

$$q_1 \leftrightarrow -q_2. \quad (2.15)$$

This condition is based on the Hermiticity of the operator  $q(t)$  which implies that the correlators of  $q$  should remain unchanged under a reversal of the ordering of the inser-

---

<sup>9</sup>The issue of contraction of  $q$ 's on the same vertex does not arise in the 1-PI effective theory framework because the correlators receive contributions only from tree-level diagrams. Hence, there is no need for a point-split regulator in the terms of the 1-PI effective action.

tions followed by a complex conjugation. The above reality condition ensures that such relations between the particle's correlators are satisfied.

The most general effective action (up to cubic terms with at most single time derivatives) which is consistent with the above conditions is as follows:

$$\begin{aligned}
L_{\text{SK,1-PI}} = & \widehat{F}(q_1 + q_2) + \frac{1}{2}Z\dot{q}_1^2 - \frac{1}{2}Z^*\dot{q}_2^2 + iZ_\Delta\dot{q}_1\dot{q}_2 - \frac{m^2}{2}q_1^2 + \frac{(m^2)^*}{2}q_2^2 - im_\Delta^2q_1q_2 + \frac{\widehat{\gamma}}{2}(q_1\dot{q}_2 - \dot{q}_1q_2) \\
& - \frac{\lambda_3}{3!}q_1^3 - \frac{\lambda_3^*}{3!}q_2^3 + \frac{\sigma_3}{2!}q_1^2q_2 + \frac{\sigma_3^*}{2!}q_1q_2^2 + \frac{\sigma_{3\gamma}}{2!}\dot{q}_2(q_1^2 - q_2^2) - \frac{\sigma_{3\gamma}^*}{2!}\dot{q}_1(q_1^2 - q_2^2).
\end{aligned} \tag{2.16}$$

The collapse rules further impose the following conditions [57] on the couplings:

$$Z_\Delta = \text{Im}[Z], \quad m_\Delta^2 = \text{Im}[m^2], \quad \text{Im}[\lambda_3 + 3\sigma_3] = 0. \tag{2.17}$$

The reality condition implies that  $\widehat{F}$  and  $\widehat{\gamma}$  are real.

The quadratic terms in the SK effective action have been studied previously in detail by Caldeira-Leggett [58] and Hu-Paz-Zhang [59, 60]. This quadratic effective theory has been shown to be equivalent to a stochastic dynamics governed by a linear Langevin equation with a Gaussian noise [55] following the methods developed by Martin-Siggia-Rose [61], De Dominicis-Peliti [62] and Janssen [63]. In this Langevin dynamics, the coupling  $\widehat{\gamma}$  is the coefficient of damping, whereas  $m_\Delta^2$  is the strength of the noise experienced by the particle. The real parts of  $m^2$  and  $Z$  are the renormalised frequency (squared) and mass of the particle respectively. The linear term in (2.26) augments this dynamics by introducing a constant force on the particle.

Among the cubic terms given in (2.30), the term associated with the real part of  $\lambda_3$  is the usual cubic potential in a unitary dynamics of the particle. The non-unitary couplings  $\sigma_3$  and  $\sigma_{3\gamma}$  are coefficients of terms that mix the degrees of freedom on different legs. These cubic terms introduce a nonlinearity in the equivalent stochastic theory. We will discuss this nonlinear Langevin dynamics later in chapter 4.

## 2.2.5 Limitation of the Schwinger-Keldysh effective theory

The Schwinger-Keldysh effective theory developed in the previous subsections suffers from the following limitations:

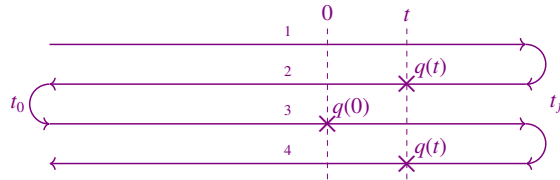
1. It allows one to compute only correlators of the particle which can be obtained from path integrals on the Schwinger-Keldysh contour shown in figure 2.2.
2. The effective couplings receive contributions only from similar Schwinger-Keldysh correlators of the bath.

However, it is possible to consider more general correlators of the particle which cannot be obtained from path integrals on the Schwinger-Keldysh contour. For example, consider the correlator

$$\langle q(t)q(0)q(t) \rangle \equiv \text{Tr}[\rho_0 q(t)q(0)q(t)], \quad (2.18)$$

where  $t_f > t > 0 > t_0$ . Starting from the initial density matrix in the above expression, one has to go forward and backward in time twice to include all the insertions. To get a path integral representation for such correlators, one needs to consider a contour with two time folds [33,34] as shown in figure 2.3. The positions of the insertions that would give the correlator in (2.18) are indicated in this diagram by the crosses. These insertions are contour-ordered according to the arrow indicated in the diagram.

Figure 2.3: Contour-ordered correlator for  $\langle q(t)q(0)q(t) \rangle$



Correlators which can only be obtained by putting insertions on such a contour with multiple time-folds are known as out-of-time-order correlators (OTOCs). The construction of an effective theory for computing such OTOCs requires incorporating the effects of similar OTOCs of the environment.

In the next section, we will first extend the effective theory to include the particle's OTOCs. We will see that this extension requires the introduction of some additional couplings. We will show how these OTO couplings are dependent on the OTO correlators of the environment.

## 2.3 Extension to the OTO effective theory

In this section, we will extend the effective theory of the particle to one that

- a) allows computation of the particle's OTOCs, and
- b) takes into account the contributions of the environment's OTOCs.

In particular, we will see that certain cubic effective couplings in this extended framework receive contributions from the 3-point OTOCs of the operator  $O$  that couples to the particle.

### 2.3.1 Generalised influence phase of the particle

At the end of the last section, we saw that a path integral representation for the OTOCs requires us to introduce a contour with two time-folds as shown in figure 2.3. Then following the strategy developed for obtaining the Schwinger-Keldysh effective dynamics, here we will have to consider a copy of the microscopic degrees of freedom for each of the four legs in this contour:  $\{q_1, X_1\}$ ,  $\{q_2, X_2\}$ ,  $\{q_3, X_3\}$  and  $\{q_4, X_4\}$ .

The Lagrangian of the combined system in this generalised Schwinger-Keldysh path integral is given by<sup>10</sup>

$$L_{\text{GSK}} = L[q_1, X_1] - L[-q_2, X_2] + L[q_3, X_3] - L[-q_4, X_4]. \quad (2.19)$$

While computing OTO correlators of the particle from path integrals with the above Lagrangian, we can first integrate out the environment's degrees of freedom. This would give us a generalisation of the influence phase which encodes the effect of the OTOCs of the bath on the particle's effective dynamics. This generalised influence phase is given by

$$W_{\text{GSK}} = \sum_{n=1}^{\infty} \lambda^n W_{\text{GSK}}^{(n)} \quad (2.20)$$

where

$$\begin{aligned} & W_{\text{GSK}}^{(n)} \\ &= i^{n-1} \sum_{i_1, \dots, i_n=1}^4 \int_{t_0}^{t_f} dt_1 \int_{t_0}^{t_1} dt_2 \cdots \int_{t_0}^{t_{n-1}} dt_n \langle \mathcal{T}_C O_{i_1}(t_1) \cdots O_{i_n}(t_n) \rangle_c q_{i_1}(t_1) \cdots q_{i_n}(t_n). \end{aligned} \quad (2.21)$$

Notice that the cumulants of the environment's contour-ordered correlators on the double-folded contour contribute to the generalised influence. In this chapter, we will focus on the contributions of the cumulants of the environment's 3-point correlators. Out of these cumulants,

---

<sup>10</sup>Here we again put extra minus signs while defining the  $q$ 's on the even legs.



there are only two independent ones which cannot be obtained from the Schwinger-Keldysh contour. These OTO cumulants are as follows:  $\langle O(t_1)O(t_3)O(t_2) \rangle_c$  and  $\langle O(t_2)O(t_3)O(t_1) \rangle_c$ , for  $t_1, t_2, t_3$ . These OTO cumulants can be obtained by putting insertions on the double-folded time contour as shown in figures 2.4 and 2.5.

Figure 2.4: Insertions corresponding to  $\langle O(t_1)O(t_3)O(t_2) \rangle_c$

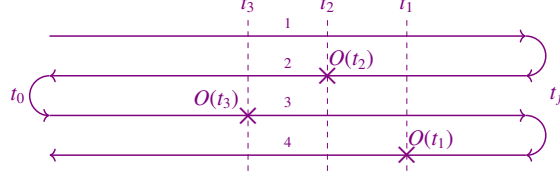
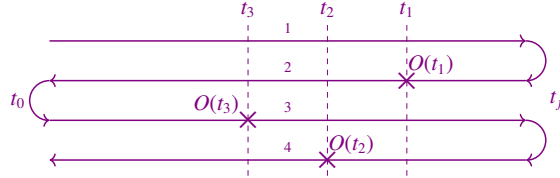


Figure 2.5: Insertions corresponding to  $\langle O(t_2)O(t_3)O(t_1) \rangle_c$



We assume that, just like the cumulants of the SK correlators, these OTO cumulants also saturate to sufficiently small values much faster than the time-scales in which the particle evolves (See the discussion in section 2.4). In such a situation, one can get an approximately local form for the generalised influence phase. The quadratic and the cubic terms in this approximately local form are as follows:

$$\begin{aligned}
W_{\text{GSK}}^{(2)} \approx i \sum_{i_1, i_2=1}^4 \int_{t_0}^{t_f} dt_1 & \left[ \left\{ \int_{t_0}^{t_1} dt_2 \langle \mathcal{T}_C O_{i_1}(t_1) O_{i_2}(t_2) \rangle_c \right\} q_{i_1}(t_1) q_{i_2}(t_1 - \epsilon) \right. \\
& + \left\{ \int_{t_0}^{t_1} dt_2 \langle \mathcal{T}_C O_{i_1}(t_1) O_{i_2}(t_2) \rangle_c t_{21} \right\} q_{i_1}(t_1) \dot{q}_{i_2}(t_1 - \epsilon) \\
& \left. + \left\{ \int_{t_0}^{t_1} dt_2 \langle \mathcal{T}_C O_{i_1}(t_1) O_{i_2}(t_2) \rangle_c \frac{t_{21}^2}{2} \right\} q_{i_1}(t_1) \ddot{q}_{i_2}(t_1 - \epsilon) \right], \tag{2.22}
\end{aligned}$$

$$\begin{aligned}
W_{\text{GSK}}^{(3)} \approx & - \sum_{i_1, i_2, i_3=1}^4 \int_{t_0}^{t_f} dt_1 \left[ \left\{ \int_{t_0}^{t_1} dt_2 \int_{t_0}^{t_2} dt_3 \langle \mathcal{T}_C O_{i_1}(t_1) O_{i_2}(t_2) O_{i_3}(t_3) \rangle_c \right\} \right. \\
& q_{i_1}(t_1) q_{i_2}(t_1 - \epsilon) q_{i_3}(t_1 - 2\epsilon) \\
& + \left\{ \int_{t_0}^{t_1} dt_2 \int_{t_0}^{t_2} dt_3 \langle \mathcal{T}_C O_{i_1}(t_1) O_{i_2}(t_2) O_{i_3}(t_3) \rangle_c t_{21} \right\} \\
& q_{i_1}(t_1) \dot{q}_{i_2}(t_1 - \epsilon) q_{i_3}(t_1 - 2\epsilon) \\
& + \left\{ \int_{t_0}^{t_1} dt_2 \int_{t_0}^{t_2} dt_3 \langle \mathcal{T}_C O_{i_1}(t_1) O_{i_2}(t_2) O_{i_3}(t_3) \rangle_c t_{31} \right\} \\
& \left. q_{i_1}(t_1) q_{i_2}(t_1 - \epsilon) \dot{q}_{i_3}(t_1 - 2\epsilon) \right]. \tag{2.23}
\end{aligned}$$

This approximately local generalised influence phase can be used to compute the OTO correlators of the particle. But just like the influence phase, it suffers from the problem of having point-split regulators to preserve the original time-ordering in the non-local form. To avoid this complication, we will construct a local 1-PI effective action of the particle on the 2-fold contour. As we will see next, this OTO 1-PI effective action is a straightforward extension of the Schwinger-Keldysh effective action discussed in the previous section.

### 2.3.2 Out of time ordered 1-PI effective action of the particle

The 1-PI effective action for OTOCs has to satisfy some constraints which are based on similar principles as those mentioned in section 2.2.4. We summarise these constraints below:

- **Collapse rules:**

The 1-PI effective action should become independent of  $\tilde{q}$  under any of the following identifications:

1.  $q_1 = -q_2 = \tilde{q}$ ,
2.  $q_2 = -q_3 = \tilde{q}$ ,
3.  $q_3 = -q_4 = \tilde{q}$ .

Moreover, under any of these collapses, the OTO effective action should reduce to the Schwinger-Keldysh effective action introduced in section 2.2.4.

- **Reality conditions:**

The effective action should become its own negative under complex conjugation along with the following exchanges:

$$q_1 \leftrightarrow -q_4, \quad q_2 \leftrightarrow -q_3 . \quad (2.24)$$

Just as before, these conditions are based on the microscopic unitarity of the (particle+environment) combined system and the hermiticity of the operator  $q$ .

We will write down a local 1-PI effective Lagrangian consistent with the above conditions which has the following expansion:

$$L_{1\text{-PI}} = L_{1\text{-PI}}^{(1)} + L_{1\text{-PI}}^{(2)} + L_{1\text{-PI}}^{(3)} + \dots , \quad (2.25)$$

where the  $L_{1\text{-PI}}^{(1)}$ ,  $L_{1\text{-PI}}^{(2)}$  and  $L_{1\text{-PI}}^{(3)}$  are the terms linear, quadratic and cubic in  $q$ 's respectively. The linear and quadratic terms are given in (2.26) and (2.27) respectively.

$$L_{1\text{-PI}}^{(1)} = \widehat{F}(q_1 + q_2 + q_3 + q_4) , \quad (2.26)$$

$$\begin{aligned} L_{1\text{-PI}}^{(2)} = & \frac{1}{2}Z(\dot{q}_1^2 + \dot{q}_3^2) - \frac{1}{2}Z^*(\dot{q}_2^2 + \dot{q}_4^2) + i Z_\Delta \sum_{i<j} \dot{q}_i \dot{q}_j \\ & - \frac{m^2}{2}(q_1^2 + q_3^2) + \frac{(m^2)^*}{2}(q_2^2 + q_4^2) \\ & - im_\Delta^2 \sum_{i<j} q_i q_j + \frac{\widehat{\gamma}}{2} \sum_{i<j} (q_i \dot{q}_j - \dot{q}_i q_j) . \end{aligned} \quad (2.27)$$

It is easy to see that these terms go to their negative under the exchange of the degrees of freedom given in (2.24) and the complex conjugation of the coefficients <sup>11</sup>, thus satisfying the reality conditions. Under any of the collapses mentioned above, these terms reduce to linear and the quadratic terms in the SK 1-PI effective action given in (2.16). For any of these collapses, the two residual degrees of freedom play the role of the right-moving and the left-moving coordinates in the SK effective theory. As an example, consider the identification of the degrees of freedom on the 3<sup>rd</sup> and the 4<sup>th</sup> leg, i.e.  $q_3 = -q_4 = \widetilde{q}$ , under which the quadratic

<sup>11</sup>Note that the coefficients  $Z_\Delta$ ,  $m_\Delta^2$  and  $\widehat{\gamma}$  are real.

part of the Lagrangian reduces to

$$L_{1\text{-PI}}^{(2)} \rightarrow \frac{1}{2}Z\dot{q}_1^2 - \frac{1}{2}Z^*\dot{q}_2^2 + iZ_\Delta\dot{q}_1\dot{q}_2 - \frac{m^2}{2}q_1^2 + \frac{(m^2)^*}{2}q_2^2 - im_\Delta^2q_1q_2 + \frac{\widehat{\gamma}}{2}(q_1\dot{q}_2 - \dot{q}_1q_2) + \left[ \left\{ \frac{1}{2}(Z - Z^*) - iZ_\Delta \right\} \dot{\bar{q}}^2 - \left\{ \frac{1}{2}(m^2 - (m^2)^*) - im_\Delta^2 \right\} \bar{q}^2 \right]. \quad (2.28)$$

The last line (within the brackets) in the above expression vanishes due to the relations given in (2.17). Consequently, this quadratic action becomes independent of  $\bar{q}$  and reduces to the quadratic part of the SK effective action given in (2.16).

The cubic terms in the OTO 1-PI effective Lagrangian can be split into 2 parts: one part which reduces to the terms in the SK 1-PI effective Lagrangian under any of the collapses mentioned above, and another part which vanishes under such collapses. These 2 sets of terms are given in (2.30) and (2.31).

$$L_{1\text{-PI}}^{(3)} = L_{1\text{-PI,SK}}^{(3)} + L_{1\text{-PI,OTO}}^{(3)}, \quad (2.29)$$

where

$$\begin{aligned} L_{1\text{-PI,SK}}^{(3)} = & -\frac{\lambda_3}{3!}(q_1^3 + q_3^3) - \frac{\lambda_3^*}{3!}(q_2^3 + q_4^3) \\ & + \frac{\sigma_3}{2!}[q_1^2(q_2 + q_3 + q_4) - q_2^2(q_3 + q_4) + q_3^2q_4] \\ & + \frac{\sigma_3^*}{2!}[q_1(q_2^2 - q_3^2 + q_4^2) - q_2(q_3^2 - q_4^2) + q_3q_4^2] \\ & + \frac{\sigma_{3\gamma}}{2!}[q_1^2(\dot{q}_2 + \dot{q}_3 + \dot{q}_4) - q_2^2(\dot{q}_3 + \dot{q}_4) + q_3^2\dot{q}_4 - (q_2^2\dot{q}_2 + q_4^2\dot{q}_4)] \\ & + \frac{\sigma_{3\gamma}^*}{2!}[q_1(\dot{q}_2^2 - \dot{q}_3^2 + \dot{q}_4^2) - \dot{q}_2(\dot{q}_3^2 - \dot{q}_4^2) + \dot{q}_3\dot{q}_4^2 - (q_1^2\dot{q}_1 + q_3^2\dot{q}_3)], \end{aligned} \quad (2.30)$$

$$\begin{aligned} L_{1\text{-PI,OTO}}^{(3)} = & -\left(\kappa_3 + \frac{1}{2}\text{Re}[\lambda_3 - \sigma_3]\right)(q_1 + q_2)(q_2 + q_3)(q_3 + q_4) \\ & - (q_2 + q_3)\left[\left(\kappa_{3\gamma} - \text{Re}[\sigma_{3\gamma}]\right)(\dot{q}_1 + \dot{q}_2)(q_3 + q_4) \right. \\ & \left. + \left(\kappa_{3\gamma}^* - \text{Re}[\sigma_{3\gamma}]\right)(q_1 + q_2)(\dot{q}_3 + \dot{q}_4)\right]. \end{aligned} \quad (2.31)$$

The reality condition implies that  $\kappa_3$  is real.

The couplings  $\kappa_3$  and  $\kappa_{3\gamma}$  are the new couplings in the OTO effective theory that are not

present in the SK 1-PI effective action. In the next subsection, we will see that these OTO couplings encode information about the 3-point OTOCs of the operator  $O(t)$  (see Table 2.1). In subsection 2.3.4, we will show how these couplings enter in the OTO correlators of the particle (see equations (2.40) and (2.41)).

### 2.3.3 Relations between 1-PI effective couplings and environment's correlators

The relations between the 1-PI effective couplings and the environment's correlators can be derived by comparing the particle's correlators obtained from the 1-PI effective action with the same obtained from the generalised influence phase given in (2.21). These couplings will generally be functions of time. But we focus on the particle's dynamics at a sufficiently late time when the effective couplings have saturated to constant values. Moreover, we assume that

$$\lim_{t-t_0 \rightarrow \infty} \langle O(t) \rangle = 0. \quad (2.32)$$

If this is not true, then one can give a constant shift to the centre of oscillation of the particle. This effectively introduces a shift in the operator  $O(t)$  when the Lagrangian is recast into the form given in (2.1). By appropriately choosing this shift, one can make sure that the condition given in (2.32) is satisfied by the shifted operator. This condition implies that the  $O(\lambda)$  term in the linear coupling vanishes. However, we expect a subleading contribution at  $O(\lambda^3)$ . A correct computation of this subleading term requires taking into account the perturbative corrections to the state of the particle. We will consistently ignore such subleading corrections in what follows.

We restrict our attention to the relations connecting the leading order forms of the quadratic and the cubic couplings to the correlators of the operator  $O(t)$ . These relations are given in equations (2.36), (2.37) and Table 2.1.

**Notational conventions:** While expressing the couplings in terms of the correlators of  $O(t)$ , we have followed some notational conventions which are given below:

1. The interval between two time instants  $t_i$  and  $t_j$  is expressed as

$$t_{ij} \equiv t_i - t_j. \quad (2.33)$$

2. We express the cumulant  $\langle O(t_{i_1})O(t_{i_2})\cdots O(t_{i_n})\rangle_c$  as  $\langle i_1 i_2 \cdots i_n \rangle$ . For example,

$$\langle 123 \rangle \equiv \langle O(t_1)O(t_2)O(t_3) \rangle_c . \quad (2.34)$$

3. The cumulant corresponding to a single-nested structure with commutators and anti-commutators is expressed by angle brackets enclosing a pair of square brackets [64]. The insertions that one encounters while going outwards through the nested structure are arranged from left to right within the square brackets. Positions of anti-commutators are indicated by (+) signs. For example,

$$\begin{aligned} \langle [123] \rangle &\equiv \langle [[O(t_1), O(t_2)], O(t_3)] \rangle_c , \\ \langle [12_+3] \rangle &\equiv \langle \{[O(t_1), O(t_2)], O(t_3)\} \rangle_c , \\ \langle [321_+] \rangle &\equiv \langle \{[O(t_3), O(t_2)], O(t_1)\} \rangle_c . \end{aligned} \quad (2.35)$$

### Quadratic couplings:

$$\begin{aligned} Z &= 1 - i \lambda^2 \lim_{t_1-t_0 \rightarrow \infty} \left[ \int_{t_0}^{t_1} dt_2 \langle 12 \rangle t_{12}^2 \right] + \mathcal{O}(\lambda^4), \\ m^2 &= m_0^2 - 2i \lambda^2 \lim_{t_1-t_0 \rightarrow \infty} \left[ \int_{t_0}^{t_1} dt_2 \langle 12 \rangle \right] + \mathcal{O}(\lambda^4), \\ \widehat{\gamma} &= i \lambda^2 \lim_{t_1-t_0 \rightarrow \infty} \left[ \int_{t_0}^{t_1} dt_2 \langle [12] \rangle t_{12} \right] + \mathcal{O}(\lambda^4). \end{aligned} \quad (2.36)$$

**Cubic couplings:** Any cubic coupling  $g$  can be expanded in powers of  $\lambda$  as

$$g = \lambda^3 \lim_{t_1-t_0 \rightarrow \infty} \int_{t_0}^{t_1} dt_2 \int_{t_0}^{t_2} dt_3 \mathcal{I}[g] + \mathcal{O}(\lambda^5) . \quad (2.37)$$

We enumerate the integrand  $\mathcal{I}$  for the cubic couplings in Table 2.1.

Notice that  $\kappa_3$  and  $\kappa_{3\gamma}$  are the only two cubic couplings that receive contributions from the OTO cumulants  $\langle 132 \rangle$  and  $\langle 231 \rangle$  which appear in the expansions of the nested structures  $\langle [321] \rangle$  and  $\langle [321_+] \rangle$ . In the next section, we give examples of two OTOCs of the particle where these two couplings show up.

Table 2.1: Relations between the particle's 1-PI effective couplings and the correlators of  $O(t)$

$g$	$\mathcal{I}[g]$
$\lambda_3$	$6\langle 123 \rangle$
$\text{Re}[\lambda_3 + \sigma_3]$	$2\langle [123] \rangle$
$\kappa_3$	$-\langle [321] \rangle$
$2 \text{Re}[\sigma_{3\gamma}]$	$-\langle [123] \rangle (t_{12} + t_{13})$
$2 \text{Re}[\kappa_{3\gamma}]$	$\langle [321] \rangle (t_{32} + t_{31})$
$2i \text{Im}[\kappa_{3\gamma}]$	$-\left(\langle [123_+] \rangle + \langle [321_+] \rangle\right)t_{12} - \langle [12_+3] \rangle t_{13}$
$2i \text{Im}[\sigma_{3\gamma}]$	$\langle [12_+3] \rangle (t_{32} + t_{31}) + \langle [123_+] \rangle (t_{21} + t_{23})$

### 2.3.4 OTOCs of the particle

The 1-PI effective action introduced in subsection 2.3.2 can be used to express the particle's OTOCs in terms of the effective couplings. The tree level diagrams in the effective theory provide these expressions of the OTOCs. To fix the values of the propagators in such diagrams, one needs to find the appropriate initial condition of the particle at some time when the local effective dynamics has set in. We choose this initial condition to be that of the ground state of the unperturbed oscillator (with frequency  $m_0$ ). Given this initial state, we express the cumulants of two OTOCs of the particle in (2.40) and (2.41). The OTO couplings  $\kappa_3$  and  $\kappa_{3\gamma}$  appear in these cumulants.

While computing these OTOCs, we take the  $O(\lambda^3)$  terms in the effective couplings and neglect the terms which are higher order in  $\lambda$ . Similarly, we take the propagators to be those corresponding to the ground state of the unperturbed oscillator and neglect  $O(\lambda^2)$  corrections to them. This gives us the correct 3-point cumulants upto  $O(\lambda^3)$ .

We find it convenient to express the time-dependence of the cumulants in terms of the phases defined below:

$$\phi_n \equiv \phi_0 + n\Delta, \quad (2.38)$$

where

$$\phi_0 \equiv m_0(t_1 + t_2 - 2t_3), \quad \Delta \equiv m_0(t_3 - t_2). \quad (2.39)$$

For  $t_1 > t_2 > t_3 \gg t_0$ , we get the following forms for the cumulants:

$$\begin{aligned}
& \langle [[q(t_3), q(t_2)], q(t_1)] \rangle_c \\
&= \frac{\kappa_3}{3m_0^4} \left\{ -\cos \phi_0 + 3 \cos \phi_1 - 3 \cos \phi_2 + \cos \phi_3 \right\} \\
&+ \frac{\text{Re}[\kappa_{3\gamma}]}{3m_0^3} \left\{ -2 \sin \phi_0 + 3 \sin \phi_1 - \sin \phi_3 \right\} + \text{O}(\lambda^5),
\end{aligned} \tag{2.40}$$

$$\begin{aligned}
& \langle q(t_1)q(t_3)q(t_2) \rangle_c - \langle q(t_2)q(t_3)q(t_1) \rangle_c \\
&= -\frac{i \text{Im}[2\kappa_{3\gamma} - \sigma_{3\gamma}]}{2m_0^3} \left\{ -\sin \phi_1 + 2 \sin \phi_2 - \sin \phi_3 \right\} \\
&+ \frac{i \text{Re}[\lambda_3 + \sigma_3]}{6m_0^4} \left\{ -\sin(\phi_1 + \phi_2) + 3 \sin \phi_2 - \sin \phi_3 \right\} \\
&+ \frac{i \text{Re}[\sigma_{3\gamma}]}{6m_0^3} \left\{ -4 \cos(\phi_1 + \phi_2) + 3 \cos \phi_1 + \cos \phi_3 \right\} + \text{O}(\lambda^5).
\end{aligned} \tag{2.41}$$

The couplings that appear in these cumulants are truncated to their leading order values in  $\lambda$  whose forms were given in (2.37) and Table 2.1.

The above expressions together with Table 2.1 demonstrate how the OTOCs of the particle encode information about the OTOCs of the operator  $O(t)$ .

## 2.4 Conclusion and Discussion

In this chapter, we have developed an OTO effective action of a Brownian particle interacting with a generic environment. The couplings appearing in this effective action have been expressed in terms of the environment's correlators integrated over a certain time domain. Focusing on the cubic terms in the action, we have identified the couplings that encode information about the 3-point OTOCs of the environment.

We would like to emphasize that this information about the environment's OTOCs is only partial. As evident from equation (2.37) and table 2.1, the particle's effective couplings depend only on certain moments of the environment's OTOCs. More information about these OTOCs can be extracted by including higher derivative terms in the particle's effective action. To determine the complete expressions for the environment's OTOCs, one would have to work with the full non-local effective action of the particle.

Although we have restricted our analysis here to cubic terms in the effective action, in



chapter 5 we will extend this formalism to take into account the quartic terms as well. We will see that the corresponding couplings at leading order in  $\lambda$  would receive contributions from the 4-point OTOCs of the system.

While discussing the Markovian limit for the effective theory, we demanded a sufficiently fast decay of the environment's cumulants (including the OTOCs). Such a decay can happen in several ways. For instance, the 3-point cumulants may be exponentially damped as  $(e^{-\alpha_1|t_i-t_j|-\alpha_2|t_j-t_k|})$  where  $t_i, t_j, t_k$  are some permutations of the time instants  $t_1, t_2, t_3$  and  $\alpha_1, \alpha_2$  are positive numbers. Such a damping of the environment's cumulants will be discussed for a toy model in chapter 4. A similar damping of 4-point cumulants for another model will be discussed in chapter 5. But for more generic systems, this kind of exponential damping of OTOCs may not hold in all time-regimes.

In fact, for several chaotic systems [65–68], the 4-point OTO cumulants show an exponentially rapid fall-off (the Lyapunov regime) before saturating to some constant values. Now, if these values at which the cumulants saturate are sufficiently small and the saturation time-scales are much shorter than the time-scales at which the particle's correlators evolve, then we expect a local dynamics of the particle. The effective couplings in this dynamics would then receive contributions from the cumulants in all the different time-regimes mentioned above. It may be useful to take a simple model of a chaotic system and determine the relative significance of contributions from the different regimes to see whether information about the Lyapunov exponent can be extracted from the OTO effective couplings of the probe particle.

We would like to draw attention to the fact that although we assume a weak particle-environment coupling, no restriction has been imposed on the strength of couplings within the environment. In particular, the environment may be strongly coupled (as long as its cumulants decay sufficiently fast). For such an environment, it is not possible to employ the standard methods of perturbation theory to compute the particle's correlators directly from the microscopic dynamics. However, using the effective theory framework introduced here, one can derive the particle's correlators in terms of the effective couplings. As we have shown, these couplings encode information about the correlators of the environment. Hence, a measurement of the effective couplings can provide valuable insight into the correlators of strongly coupled systems.

The effective OTO dynamics of the particle presented in this chapter holds for any generic state of the system where its cumulants decay sufficiently fast. In chapter 4, we would specialise

to the case where the environment is in a thermal state. There, we will see that the KMS relations [64] between the thermal correlators of the environment imply additional relations between the the effective couplings of the particle which are generalisations of the fluctuation dissipation relation [64, 69]. In the context of such an OTO effective dynamics of a system in a thermal environment, it may be interesting to study the time-scale of thermalisation of the system's OTOCs vis a vis its time-ordered correlators.

# Chapter 3

## Spectral representation of thermal OTO correlators

In the previous chapter we saw that the couplings in the OTO effective theory of the Brownian particle receive contributions from the OTO correlators of the environment. Now, suppose this environment is in a thermal state. In such a situation, the environment can be considered as a thermal bath. As we discussed in chapter 2, the OTOCs of such a bath can be obtained from path integrals on a contour with multiple time-folds. We saw that such contour-ordered OTOCs appear in the generalised influence phase of the particle given in (2.21). In this chapter we will demonstrate that there are certain relations between these contour-ordered OTOCs of the bath due to its microscopic unitarity and thermality. Such relations allow one to express the bath's OTOCs in terms of a minimal set of independent objects viz. a set of spectral functions. These spectral representations of the thermal OTOCs clarifies one's understanding of the effects of the thermality of bath on the particle's dynamics. In addition, they also provide a convenient basis for developing perturbation theory for OTOCs of a system in a thermal state.

The relations that lead to the spectral representations of the thermal OTOCs hold quite generally for bosonic operators in arbitrary quantum systems. In particular, they are also valid for systems with a continuum of degrees of freedom which are governed by quantum field theories. Therefore, to keep the discussion general, we deviate from the (0+1)-dimensional case in this chapter, and develop the spectral representations of thermal OTOCs of scalar operators in a field theory defined on a general  $d$ -dimensional spacetime. In chapters 4 and 5 we will again go back to considering thermal baths defined on a (0+1)-dimensional space.

The material of this chapter is drawn from the paper [30] written by the author in collabo-

ration with Chandramouli Chowdhury and R. Loganayagam.

### 3.1 Introduction

The dynamics of quantum field theory at finite temperature is of fundamental interest in fields ranging from dynamical critical phenomena to cosmology, in blackhole physics/quantum gravity. Until recently, it had been conventional to assume that, in principle all the observables of real time, finite temperature quantum field theory are encoded in its Schwinger Keldysh correlators [35–37, 43, 53–55, 70–72]. This statement has been upended by the advent of out of time ordered correlators (OTOCs) [73] which fall beyond the conventional Schwinger-Keldysh formalism and the usual edifice of intuitions, approximations and computations built around it. These OTOCs require that we extend the standard Schwinger-Keldysh formalism to path integrals with many time-fold contours [33, 34].

From the viewpoint of a non-equilibrium field theorist, three crucial questions could be asked regarding OTOCs :

- What new *physics* do these OTOCs encode ? A growing literature has shown relations to notions of chaos vs ergodicity say in blackholes [1, 5] via its relation to Loschmidt echo<sup>1</sup>, thermalisation vs localisation [10, 74–76], quantum information measures related to joint quasi-probabilities in weak measurements [14, 69, 77–79], generalised discontinuities of the correlators [80–82] which encode useful spectral information in CFTs. The analytic structure of OTOCs in quantum thermal systems has led to bounds on chaos [5, 83–86], generalised FDTs [64] and in generalising Eigenstate hypothesis [87]. This fast growing array of ideas show the usefulness of studying OTOCs.
- Secondly, how are they to be *measured* in experiments ? The dogma that only time-ordered correlators can be measured in an experiment has yielded ground to an ingenious set of experiments/ experimental proposals aimed at reverse time evolution/weak measurements [19, 88]. Despite, this, we are far from having experimental protocols to measure OTOCs in complex systems.
- Thirdly, What are the most efficient ways to *compute* these correlators ? Any attempt at setting up a naive diagrammatic perturbation theory, even in the simplest of quantum

---

<sup>1</sup>See [http://www.scholarpedia.org/article/Loschmidt\\_echo](http://www.scholarpedia.org/article/Loschmidt_echo) for a description.

field theories, runs aground with a proliferation of fields and their Feynman vertices. This definitely calls for new computational frameworks to systematise such calculations.

In this chapter, we will primarily address the last issue by constructing a practical framework to compute and classify OTOCs of a system at thermal equilibrium. Stated briefly, this can be done by recognising that the core physics of the system can be encoded in certain *spectral functions* and the structure of thermal correlators naturally admit *spectral representations* in terms of them. This statement is a finite-temperature generalisation of the Kallen-Lehmann spectral representations in the zero temperature quantum field theory (See, for example, §§10.7 of [89] for a textbook discussion).

The idea of spectral representation for Schwinger-Keldysh real time correlators has a long history [90–97] (for a discussion in terms of discontinuities see [98, 99]). Such spectral representations have been found useful in developing efficient perturbative formalisms [100–103]. They have found applications in transport computations at finite temperature and in developing effective methods to truncate to kinetic theory descriptions (including effective actions encoding hard thermal loops of gluons at high temperature ala Braaten-Pisarski [104]). Our aim in this chapter is to develop a similarly useful formalism for out of time ordered thermal perturbation theory.

We will now describe in slightly more detail, the idea of spectral functions/representations. For example, in the above mentioned works, it was recognised that the 2-pt and 3-pt SK correlators in the thermal state can be written down in terms of thermal expectation values of fully nested time-ordered commutators (also termed fully retarded Green functions [92]) of the form:

$$\langle \Theta_{12}[O(t_1), O(t_2)] + \Theta_{21}[O(t_2), O(t_1)] \rangle_\beta, \quad \langle \Theta_{123}[[O(t_1), O(t_2)], O(t_3)] + \text{permutations} \rangle_\beta.$$

Here  $\Theta_{ij\dots}$  are step functions enforcing time-ordering  $t_i > t_j > \dots$ . These are the aforementioned spectral functions which are nicer objects to compute than the full real-time correlators and they are also easiest to obtain by analytic continuation from Euclidean correlators [92, 105]. Commutators have nice causality properties in time domain which, via Kramers-Kronig type arguments, enforce good analytic behaviour in appropriate regions of the frequency domain.

Another key insight relevant to our discussion in this chapter is the following : there is a natural formalism in terms of arrays of certain column vectors which provides a convenient way to organise and use such spectral representations [95, 96, 100–102]. This column vector

basis is also naturally related to what is termed retarded-advanced (RA) basis [105–108] in the thermal SK formalism.

When we move to 4-pt correlators, the time-ordered commutators are no more sufficient to capture all thermal correlations [64], and OTO commutators/spectral functions should be added to the set of spectral functions. The addition of OTO spectral functions into the analysis, clears up the complexity visible in older analysis of thermal SK correlators. The authors of [64] showed that, by adding in the OTO spectral functions, one can indeed reconstruct all n-point Wightman correlators. In fact, the constraints imposed by thermal periodicity can be completely solved for an arbitrary n-pt function, and a simple formula can be written down expressing arbitrary Wightman correlators in terms of spectral functions [64].

Wightman correlators, however, are not natural objects to formulate perturbation theory or to set up diagrammatics. Diagrammatics and path integral formalism naturally work with contour-ordered correlators on the multi-time-fold contours. In principle, this is a simple matter of expressing contour correlators in terms of Wightman functions and using the relations derived in [64]. In practice, however, combinatorics overwhelm this exercise, resulting in complicated looking expressions which hide much of the structure.

Inspired by the previous work on SK correlators, in this chapter, we will extend the column vector/retarded-advanced formalism to generalised SK correlators. Our basis is chosen such that, *on a time contour with  $k$  timefolds, we have  $k$  ‘retarded’ combinations which can occur within a correlator only in the causal past of some other operators and  $k$  advanced combinations which can occur only in the causal future.* This is a natural generalisation of the usual retarded-advanced formalism with a single retarded and a single advanced field. Our primary aim here is to express the contour correlators in terms of spectral functions within such a formalism.

### **Organisation of the chapter:**

We will begin in 3.2 by reviewing spectral representation of Schwinger-Keldysh two point functions in terms of column vectors. The material here is well-known and is discussed in a variety of reviews and textbooks (see, for example [54]). We write down many equivalent expressions for the two point functions and note their underlying structure. Our notation and emphasis here are aimed towards further generalisation. The reader familiar with this material may wish to skim these sections and move ahead to 3.3 where we extend this spectral represen-

tation to two point functions in the generalised SK contour. This section brings out the main ideas behind the construction of these representations which is then applied to higher point functions. This is followed by section 3.4 where we quote the results for higher point functions within generalised Schwinger-Keldysh formalism. We end with a discussion of future directions in 4.7.

For the convenience of the reader, many of the technical details are relegated to the appendices : in appendix A.1, we summarise the basis of column vectors on which our spectral representations are based. The appendix A.2 details the structure of arguments used to constrain the structure of the contour-ordered thermal correlators. In appendices A.3.1, A.3.2 and A.3.3, we present the analyses of 2 point, 3 point and 4 point functions respectively.

## 3.2 Spectral representation of SK two point functions

### 3.2.1 Example of a free scalar field

Before going into the general contour correlators and their relations, let us begin with a simple example. Consider the contour-ordered, thermal two point functions of a free real scalar field in SK formalism (in the mostly plus metric convention) :

$$\begin{aligned}
\langle \mathcal{T}_C \phi_1(x_1) \phi_1(x_2) \rangle &= \langle \mathcal{T} \phi(x_1) \phi(x_2) \rangle = \int_p \rho_p (\Theta_{12} + \check{f}_p) e^{ip \cdot (x_1 - x_2)} , \\
\langle \mathcal{T}_C \phi_1(x_1) \phi_2(x_2) \rangle &= \langle \phi(x_2) \phi(x_1) \rangle = \int_p \rho_p \check{f}_p e^{ip \cdot (x_1 - x_2)} , \\
\langle \mathcal{T}_C \phi_2(x_1) \phi_1(x_2) \rangle &= \langle \phi(x_1) \phi(x_2) \rangle = \int_p \rho_p (1 + \check{f}_p) e^{ip \cdot (x_1 - x_2)} , \\
\langle \mathcal{T}_C \phi_2(x_1) \phi_2(x_2) \rangle &= \langle \mathcal{T}^* \phi(x_1) \phi(x_2) \rangle = \int_p \rho_p (\Theta_{21} + \check{f}_p) e^{ip \cdot (x_1 - x_2)} .
\end{aligned} \tag{3.1}$$

Here,  $\phi_1$  is the ‘ket’ field with time-ordered propagator whereas  $\phi_2$  is the ‘bra’ field of Schwinger formalism with anti-time-ordered propagators. The symbol  $\mathcal{T}_C$  denotes SK contour ordering and  $\Theta_{12}$  denotes Heaviside step function in time. We have written down the corresponding correlators in the single-copy notation (with the time-ordering operator  $\mathcal{T}$  and anti-time-ordering operator  $\mathcal{T}^*$ ) for the convenience of the reader.

The symbol  $\rho_p$  in the above equation stands for the *spectral function* which in a free scalar

theory takes the form

$$\rho_p \equiv 2\pi \operatorname{sign}(p^0) \delta(p^2 + m^2) = \frac{2\pi}{2\omega_p} [\delta(\omega - \omega_p) - \delta(\omega + \omega_p)] .$$

Here  $\omega_p = \sqrt{\mathbf{p}^2 + m^2}$ . The spectral function is also directly related to the Fourier-transform of commutators in the theory, viz.,

$$\int_p \rho_p e^{ip \cdot (x_1 - x_2)} = \langle [\phi(x_1), \phi(x_2)] \rangle$$

and it neatly encodes all the theory-dependent information. The factor  $\mathfrak{f}_p$  is the Bose-Einstein factor

$$\mathfrak{f}_p \equiv \frac{1}{e^{\beta p^0} - 1}$$

which obeys  $1 + \mathfrak{f}_p + \mathfrak{f}_{-p} = 0$  and  $\mathfrak{f}_p = e^{-\beta p^0} (1 + \mathfrak{f}_p)$ . These Bose-Einstein factors are universal and the way they occur in the correlators are completely fixed by general arguments.

Further, we have used the notation

$$\int_p \equiv \int \frac{d^d p}{(2\pi)^d}$$

to denote the momentum integrals in  $d$  spacetime dimensions. Using these relations, we get the more familiar two point correlators :

$$\begin{aligned} \langle \mathcal{T}_C \phi_1(x_1) \phi_1(x_2) \rangle &= \langle \mathcal{T} \phi(x_1) \phi(x_2) \rangle \\ &= \int \frac{d^{d-1} p}{(2\pi)^{d-1} 2\omega_p} \left[ (\Theta_{12} + \mathfrak{f}_p) e^{ip \cdot (x_1 - x_2)} + (\Theta_{21} + \mathfrak{f}_p) e^{-ip \cdot (x_1 - x_2)} \right]_{p^0 = \omega_p} , \\ \langle \mathcal{T}_C \phi_1(x_1) \phi_2(x_2) \rangle &= \langle \phi(x_2) \phi(x_1) \rangle \\ &= \int \frac{d^{d-1} p}{(2\pi)^{d-1} 2\omega_p} \left[ \mathfrak{f}_p e^{ip \cdot (x_1 - x_2)} + (1 + \mathfrak{f}_p) e^{-ip \cdot (x_1 - x_2)} \right]_{p^0 = \omega_p} , \\ \langle \mathcal{T}_C \phi_2(x_1) \phi_1(x_2) \rangle &= \langle \phi(x_1) \phi(x_2) \rangle \\ &= \int \frac{d^{d-1} p}{(2\pi)^{d-1} 2\omega_p} \left[ (1 + \mathfrak{f}_p) e^{ip \cdot (x_1 - x_2)} + \mathfrak{f}_p e^{-ip \cdot (x_1 - x_2)} \right]_{p^0 = \omega_p} , \\ \langle \mathcal{T}_C \phi_2(x_1) \phi_2(x_2) \rangle &= \langle \mathcal{T}^* \phi(x_1) \phi(x_2) \rangle \\ &= \int \frac{d^{d-1} p}{(2\pi)^{d-1} 2\omega_p} \left[ (\Theta_{21} + \mathfrak{f}_p) e^{ip \cdot (x_1 - x_2)} + (\Theta_{12} + \mathfrak{f}_p) e^{-ip \cdot (x_1 - x_2)} \right]_{p^0 = \omega_p} . \end{aligned} \tag{3.2}$$

The reader can readily verify the correctness of the above expressions by starting with the



free theory mode expansion

$$\phi(x) = \int \frac{d^{d-1}p}{(2\pi)^{d-1} \sqrt{2\omega_p}} \left[ a_p e^{ip \cdot x} + a_p^\dagger e^{-ip \cdot x} \right]_{p^0 = \omega_p} \quad (3.3)$$

and using the thermal expectation values  $\langle a_{p_1}^\dagger a_{p_2} \rangle = (2\pi)^{d-1} \delta^{d-1}(\vec{p}_1 - \vec{p}_2) \check{f}_{p_1}$  and  $\langle a_{p_1} a_{p_2}^\dagger \rangle = (2\pi)^{d-1} \delta^{d-1}(\vec{p}_1 - \vec{p}_2)(1 + \check{f}_{p_1})$ .

### 3.2.2 The column vector structure

For a general scalar operator  $\Phi(x)$  instead of the free field, the above form of two point functions in (3.1) still holds in SK formalism, just with a different spectral function still defined by

$$\int_p \rho_p e^{ip \cdot (x_1 - x_2)} \equiv \langle [\Phi(x_1), \Phi(x_2)] \rangle .$$

This is the SK analog of the famous Kallen-Lehman representation in zero temperature QFT and is a direct consequence of periodicity in imaginary time of thermal correlators, viz.,

$$\langle \Phi(x_1 - i\beta) \Phi(x_2) \rangle = \langle \Phi(x_2) \Phi(x_1) \rangle .$$

Here  $\beta^\mu$  is a time-like vector defining thermal equilibrium with its direction giving the rest frame and its magnitude (also denoted by  $\beta$ ) giving rest frame inverse temperature.

The statement of periodicity is also termed Kubo-Martin-Schwinger(KMS) relations and is the underlying reason behind fluctuation-dissipation theorems in QFTs. Using these relations along with the second equation of (3.1) (which can be taken as the definition of  $\rho_p$ ), the rest of (3.1) follows. Thus, the *four* two point functions of SK formalism depend eventually on only *one* system-dependent spectral function and thermality fixes the rest, as advertised.

We will find it convenient to write the above correlators as an array :

$$\begin{aligned} \langle \mathcal{T}_C \Phi_i(x_1) \Phi_j(x_2) \rangle &= \int_p \rho_p \begin{pmatrix} \Theta_{12} + \check{f}_p & \check{f}_p \\ 1 + \check{f}_p & \Theta_{21} + \check{f}_p \end{pmatrix} e^{ip \cdot (x_1 - x_2)} \\ &= \Theta_{12} \int_p \rho_p \begin{pmatrix} 1 + \check{f}_p & \check{f}_p \\ 1 + \check{f}_p & \check{f}_p \end{pmatrix} e^{ip \cdot (x_1 - x_2)} + \Theta_{21} \int_p \rho_p \begin{pmatrix} \check{f}_p & \check{f}_p \\ 1 + \check{f}_p & 1 + \check{f}_p \end{pmatrix} e^{ip \cdot (x_1 - x_2)} \\ &= \Theta_{12} \int_p \rho_p \begin{pmatrix} 1 \\ 1 \end{pmatrix} e^{ip \cdot x_1} \otimes \begin{pmatrix} 1 + \check{f}_p \\ \check{f}_p \end{pmatrix} e^{-ip \cdot x_2} + \Theta_{21} \int_p \rho_p \begin{pmatrix} \check{f}_p \\ 1 + \check{f}_p \end{pmatrix} e^{ip \cdot x_1} \otimes \begin{pmatrix} 1 \\ 1 \end{pmatrix} e^{-ip \cdot x_2} , \end{aligned} \quad (3.4)$$

where in the last line we have re-written the answer as tensor products of certain set of column vectors for later convenience. The first term in the above expression corresponds to the retarded propagator as it is nonzero only when  $x_1^0 \geq x_2^0$ . Similarly, the second term corresponds to the advanced propagator as it is nonzero only when  $x_2^0 \geq x_1^0$ . Thus, this basis of column vectors appears naturally when we decompose the contour ordered correlators into retarded and advanced pieces. This is the origin of the name ‘retarded-advanced’ or RA basis for this basis of column vectors.<sup>2</sup>

Such arrays and the column vectors have various structural features which generalise to the case of OTOCs as well as higher point functions. Note that the array that appears along with the step function  $\Theta_{21}$  can be obtained from *transposing* the array that appears with the step function  $\Theta_{12}$ , followed by a map  $p \mapsto -p$  under which  $\rho_p \mapsto -\rho_p$  and  $\check{f}_p \mapsto -(1 + \check{f}_p)$ . At the level of tensor products, the transpose appears as a permutation in the order of tensor products as the time-order changes.

A more symmetric representation is obtained by defining

$$\int_{p_1} \int_{p_2} \rho[12] e^{i(p_1 \cdot x_1 + p_2 \cdot x_2)} \equiv \langle [\Phi(x_1), \Phi(x_2)] \rangle$$

in terms of which we can write a spectral representation [91, 94–96]

$$\begin{aligned} \langle \mathcal{T}_C \Phi_i(x_1) \Phi_j(x_2) \rangle &= \int_{p_1} \int_{p_2} \{ \rho[12] \Theta_{12} \begin{pmatrix} -1 \\ -1 \end{pmatrix} e^{ip_1 \cdot x_1} \otimes \begin{pmatrix} \check{f}_2 \\ 1 + \check{f}_2 \end{pmatrix} e^{ip_2 \cdot x_2} \\ &\quad + \rho[21] \Theta_{21} \begin{pmatrix} \check{f}_1 \\ 1 + \check{f}_1 \end{pmatrix} e^{ip_1 \cdot x_1} \otimes \begin{pmatrix} -1 \\ -1 \end{pmatrix} e^{ip_2 \cdot x_2} \}, \end{aligned} \quad (3.7)$$

<sup>2</sup>Note that our basis is closely related to RA basis (as it appears for example in [95]) upto overall normalisations. In the notations of [95], the column vectors appearing in this expression can be written as

$$[e_R(p)]_{\text{Hou-Wang-Heinz}} \equiv \begin{pmatrix} 1 + \check{f}_p \\ \check{f}_p \end{pmatrix}, [e_A(p)]_{\text{Hou-Wang-Heinz}} \equiv -\begin{pmatrix} 1 \\ 1 \end{pmatrix}. \quad (3.5)$$

Using, these column vectors, (3.4) can be rewritten as

$$\begin{aligned} \langle \mathcal{T}_C \Phi_i(x_1) \Phi_j(x_2) \rangle &= -\Theta_{12} \int_p \rho_p [e_A(-p)]_{\text{Hou-Wang-Heinz}} \otimes [e_R(p)]_{\text{Hou-Wang-Heinz}} e^{ip \cdot (x_1 - x_2)} \\ &\quad + \Theta_{21} \int_p \rho_p [e_R(-p)]_{\text{Hou-Wang-Heinz}} \otimes [e_A(p)]_{\text{Hou-Wang-Heinz}} e^{ip \cdot (x_1 - x_2)}. \end{aligned} \quad (3.6)$$

We will find it convenient to work with a slightly different RA basis in the following.

where we have used the notation  $\check{f}_1 \equiv \check{f}_{p_1}$ ,  $\rho[12] \equiv \rho[p_1, p_2]$  etc. For a free scalar,

$$\rho[12] \equiv 2\pi \operatorname{sign}(p_1^0) \delta(p_1^2 + m^2) \times (2\pi)^d \delta^d(p_1 + p_2) = -\rho[21] .$$

In this presentation, the action on the array can be described as the joint permutation of the time ordering, the array indices and the momenta.

### 3.2.3 The Wightman array

At the end of the last subsection, we had obtained

$$\langle \mathcal{T}_C \Phi_i(x_1) \Phi_j(x_2) \rangle = \Theta_{12} \mathbf{M}(x_1, x_2) + \text{permutation} \quad (3.8)$$

where

$$\mathbf{M}(x_1, x_2) \equiv \int_{p_1} \int_{p_2} \rho[12] \begin{pmatrix} -1 \\ -1 \end{pmatrix} e^{ip_1 \cdot x_1} \otimes \begin{pmatrix} \check{f}_2 \\ 1 + \check{f}_2 \end{pmatrix} e^{ip_2 \cdot x_2} . \quad (3.9)$$

The permutation in (3.8) refers to the term given by

$$\Theta_{21} \int_{p_1} \int_{p_2} \rho[21] \begin{pmatrix} \check{f}_1 \\ 1 + \check{f}_1 \end{pmatrix} e^{ip_1 \cdot x_1} \otimes \begin{pmatrix} -1 \\ -1 \end{pmatrix} e^{ip_2 \cdot x_2} . \quad (3.10)$$

Thus, the permutation involves summing over all possible time-ordering. This is accompanied by a simultaneous transpositions of the column vectors, thus changing the order in which they appear in the tensor product. We also exchange the momenta ( $p_1 \leftrightarrow p_2$ ) appearing in the argument of spectral function as well as the column vectors. As we will see later, this kind of a permutation structure is common to higher point contour-ordered correlators whether time-ordered or out of time-ordered.

The array  $\mathbf{M}$  is actually an array of Wightman correlators :

$$\mathbf{M}(x_1, x_2) = \begin{pmatrix} \langle \Phi_1(x_1) \Phi_2(x_2) \rangle & \langle \Phi_2(x_2) \Phi_1(x_1) \rangle \\ \langle \Phi_1(x_1) \Phi_2(x_2) \rangle & \langle \Phi_2(x_2) \Phi_1(x_1) \rangle \end{pmatrix} = \begin{pmatrix} \langle 12 \rangle & \langle 21 \rangle \\ \langle 12 \rangle & \langle 21 \rangle \end{pmatrix} . \quad (3.11)$$

Here we have introduced a useful notation for Wightman correlators [64] whereby only insertion points and their ordering are retained. The Fourier representation is then obtained by using

KMS relations :

$$\begin{aligned}\langle 12 \rangle &= - \int_{p_1} \int_{p_2} \rho[12] \check{f}_2 e^{ip_k \cdot x_k} , \\ \langle 21 \rangle &= - \int_{p_1} \int_{p_2} \rho[12] (1 + \check{f}_2) e^{ip_k \cdot x_k} .\end{aligned}\tag{3.12}$$

Note that the array of Wightman correlators above is constructed so as to agree with the contour-ordered correlators for a particular time-ordering of insertions, viz.,

$$\Theta_{12} \langle \mathcal{T}_C \Phi_i(x_1) \Phi_j(x_2) \rangle = \Theta_{12} \mathbf{M}(x_1, x_2) .\tag{3.13}$$

Such an arrangement of Wightman correlators play a crucial role throughout this chapter and we will henceforth refer to it as the *Wightman array corresponding to a time-ordering* and denote it by  $\mathbf{M}$ . Often, it is convenient to deal with the Fourier transform of the Wightman array which we will denote by  $\tilde{\mathbf{M}}$  :

$$\mathbf{M}(x_1, x_2) \equiv \int_p \tilde{\mathbf{M}}(p) e^{ip \cdot (x_1 - x_2)} \quad \text{with} \quad \tilde{\mathbf{M}}(p) \equiv \rho_p \begin{pmatrix} 1 + \check{f}_p & \check{f}_p \\ 1 + \check{f}_p & \check{f}_p \end{pmatrix} .\tag{3.14}$$

or

$$\mathbf{M}(x_1, x_2) \equiv \int_{p_1} \int_{p_2} \tilde{\mathbf{M}}(p_1, p_2) e^{ip_k \cdot x_k} ,$$

with

$$\tilde{\mathbf{M}}(p_1, p_2) \equiv \rho[12] \begin{pmatrix} -1 \\ -1 \end{pmatrix} \otimes \begin{pmatrix} \check{f}_2 \\ 1 + \check{f}_2 \end{pmatrix} .\tag{3.15}$$

This formula is the basic building block out of which spectral representations are constructed via Fourier transforms and sum over time-orderings. We note the following features :

- First of all, there is a clear separation here between the theory dependent information in the spectral function (viz. the Fourier transform of the commutators) and *the array structure imposed by KMS relations* captured by the column vectors . In practical terms, it is always easier to compute  $\rho[12]$  and use the above representation than computing each of these thermal correlators in turn.
- Next one notes the *causal structure* of these correlators made manifest via step-functions

in time. We note that the correlators here are written as a sum over various time-orderings. Within each time-ordering, specific spectral functions appear in conjunction with a particular tensor product of column vectors.

- As we permute across time-orderings, the arguments of spectral functions get permuted along with a permutation in the order in which the tensor products are taken.

As we will see later on, all these features directly generalise to spectral representations of higher point thermal correlators (whether time-ordered or out of time-ordered).

Before we move to the generalisation of these results, let us focus on an example of how causal structure is encoded in these column vectors : consider taking either the first field to be a SK difference field  $\Phi_d \equiv \Phi_1 - \Phi_2$ . This is equivalent to contracting the first vector of the product with a row vector  $(1 \ -1)$  resulting in

$$\langle \mathcal{T}_C(\Phi_1(x_1) - \Phi_2(x_1))\Phi_j(x_2) \rangle = \Theta_{21} \int_{p_1} \int_{p_2} \rho[21] \begin{pmatrix} 1 \\ 1 \end{pmatrix} e^{ip_1 \cdot x_1} e^{ip_2 \cdot x_2} . \quad (3.16)$$

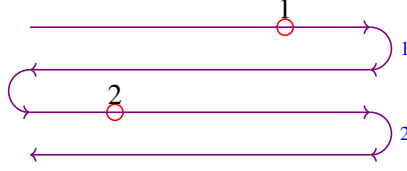
We note that this vanishes unless the difference operator at  $x_1$  is actually in the past of  $x_2$ . What we have shown is the *largest time equation* for difference operators : *any correlator with the future-most operator being the difference operator, vanishes [54]*.

The structure of the two-point thermal correlators that we just reviewed raises a variety of questions : how much of these structures could be generalised to higher point functions ? What is the systematic way to derive similar results ? Could one systematically understand the structure of the column vectors whose tensor-products appear in such formulae ? How do we generalise these results in the context of out of time order correlators beyond the usual SK formalism ?

### 3.3 Spectral representation of generalised SK two point functions

#### 3.3.1 Structure of generalised SK two point functions

We would now like to generalise the column vector representation in Eqn(3.7) to two point functions on a generalised SK contour like the one shown below :



Each of the two insertions can lie on any of the four legs of the contour thus resulting in a  $4 \times 4$  array of contour ordered two point functions. This is a simple enough correlator that all the contour-ordering can be explicitly worked out. We obtain

$$\langle \mathcal{T}_C \Phi_i(x_1) \Phi_j(x_2) \rangle = \Theta_{12} \mathbf{M}(x_1, x_2) + \text{permutation} \quad (3.17)$$

with the Wightman array

$$\mathbf{M} = \begin{pmatrix} \langle 12 \rangle & \langle 21 \rangle & \langle 21 \rangle & \langle 21 \rangle \\ \langle 12 \rangle & \langle 21 \rangle & \langle 21 \rangle & \langle 21 \rangle \\ \langle 12 \rangle & \langle 12 \rangle & \langle 12 \rangle & \langle 21 \rangle \\ \langle 12 \rangle & \langle 12 \rangle & \langle 12 \rangle & \langle 21 \rangle \end{pmatrix}. \quad (3.18)$$

In Fourier domain, we have

$$\mathbf{M}(x_1, x_2) \equiv \int_{p_1} \int_{p_2} \tilde{\mathbf{M}}(p_1, p_2) e^{ip_k \cdot x_k}$$

with

$$\tilde{\mathbf{M}} = -\rho[12] \begin{pmatrix} \tilde{f}_2 & 1 + \tilde{f}_2 & 1 + \tilde{f}_2 & 1 + \tilde{f}_2 \\ \tilde{f}_2 & 1 + \tilde{f}_2 & 1 + \tilde{f}_2 & 1 + \tilde{f}_2 \\ \tilde{f}_2 & \tilde{f}_2 & \tilde{f}_2 & 1 + \tilde{f}_2 \\ \tilde{f}_2 & \tilde{f}_2 & \tilde{f}_2 & 1 + \tilde{f}_2 \end{pmatrix}. \quad (3.19)$$

We want to now choose a judicious ‘RA-like’ basis of column vectors which make the causal structure of this array manifest. To see why a good basis is required, note that, a generic  $4 \times 4$  array decomposed in a general basis is a sum of 16 tensor products. In the context of perturbation theory, using the above two point function as the propagator, this is the statement that, naively we seem to have 4 fields in the path-integral which all get changed into each other during time-evolution, thus producing 16 propagators. The concomitant proliferation of diagrams arising from this fact seems to be intimidating to all but profligate diagrammarians.

This way of proceeding is, however, excessively inefficient for the array under question. For example, here is a column vector decomposition which does much better (with only two tensor products) :

$$\tilde{\mathbf{M}} = \rho[12] \left\{ \begin{pmatrix} -1 \\ -1 \\ 0 \\ 0 \end{pmatrix} \otimes \begin{pmatrix} \check{f}_2 \\ 1 + \check{f}_2 \\ 1 + \check{f}_2 \\ 1 + \check{f}_2 \end{pmatrix} + \begin{pmatrix} 0 \\ 0 \\ -1 \\ -1 \end{pmatrix} \otimes \begin{pmatrix} \check{f}_2 \\ \check{f}_2 \\ \check{f}_2 \\ 1 + \check{f}_2 \end{pmatrix} \right\}. \quad (3.20)$$

This is the OTO analogue of the familiar statement in real time SK perturbation theory: by a judicious choice of basis which exploits the causal/KMS structure, the number of propagators/diagrams can be reduced drastically.

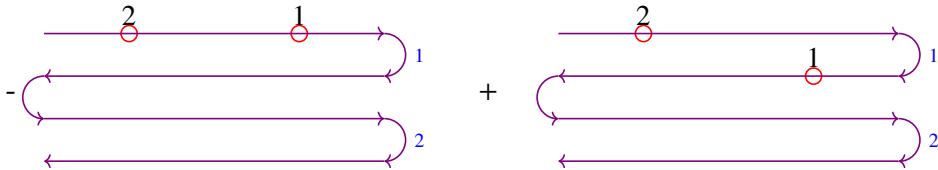
### 3.3.2 A basis of row vectors from causality and KMS

Let us pause to examine why such a simplification is made possible. By analysing the array in Eq.(3.19), we note that  $\tilde{\mathbf{M}}$  is annihilated by the following row vectors contracted to its first index (i.e., the index corresponding to its future-most operator) :

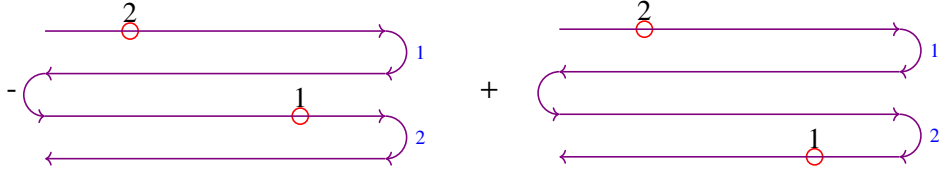
$$\begin{aligned} e_F^{(1)}(\omega_1) &\equiv (-1, 1, 0, 0), \\ e_F^{(2)}(\omega_1) &\equiv (0, 0, -1, 1). \end{aligned} \quad (3.21)$$

Here the subscript  $F$  is to remind us that these vectors annihilate the future-most index. This is the multi time-fold analogue of the largest time equation, whereby if the future-most operator is set to be a difference operator, the correlator vanishes.

In pictures, the annihilation by the row vector  $e_F^{(1)}$  is the statement that the following combination of correlators vanish (irrespective of the position of the operator insertion 2, provided it is in the past of insertion 1) :



Thus, we say row vector  $e_F^{(1)}$  encodes the sliding of operators against the first future turning point. A similar picture of the row vector  $e_F^{(2)}$  describing the sliding across the *second* future turning point is :



These statements immediately generalise to any number of time-fold contours. In the case of  $k$  time-folds, the row-vectors that annihilate the future most index are  $2k$  dimensional and they are  $k$  in number :

$$\begin{aligned}
e_F^{(1)}(\omega) &\equiv (-1, 1, 0, \dots, 0), \\
e_F^{(2)}(\omega) &\equiv (0, 0, -1, 1, 0, \dots, 0), \\
&\dots, \\
e_F^{(j)}(\omega) &\equiv (0, 0, 0, \dots, -1_{2j-1}, 1_{2j}, 0, \dots, 0), \\
&\dots, \\
e_F^{(k)}(\omega) &\equiv (0, 0, \dots, -1, 1) .
\end{aligned} \tag{3.22}$$

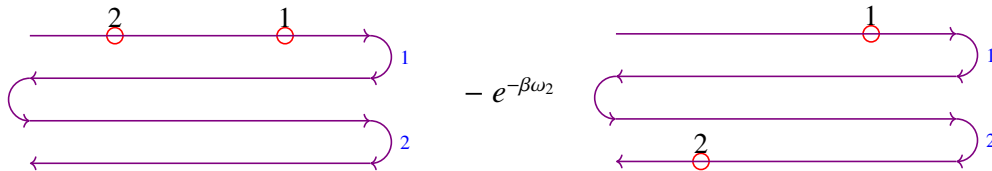
Here, the row vector  $e_F^{(j)}$  describes the sliding across the  $j$ 'th future turning point.

The array  $\tilde{\mathbf{M}}$  is also annihilated by the following row vectors contracted to its second index (i.e., the index corresponding to its past-most operator) :

$$\begin{aligned}
e_P^{(1)}(\omega_2) &\equiv (1, 0, 0, -e^{-\beta\omega_2}), \\
e_P^{(2)}(\omega_2) &\equiv (0, -1, 1, 0),
\end{aligned} \tag{3.23}$$

where we have used  $\mathfrak{f}_2 = e^{-\beta\omega_2}(1 + \mathfrak{f}_2)$ . Here the subscript  $P$  is to remind us that these vectors annihilate the past-most index.

In pictures, the annihilation by the row vector  $e_P^{(1)}$  is the statement that the following combination of correlators vanish (irrespective of the position of the operator insertion 1, provided it is in the future of insertion 2) :



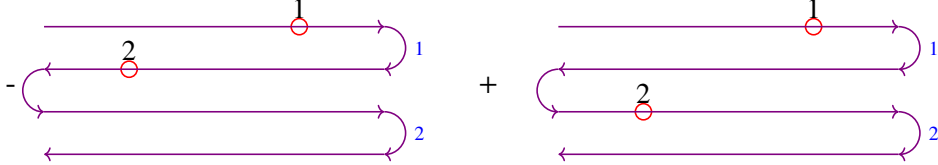
This is a frequency domain version of the KMS relation

$$\langle \mathbb{O}_1(t_1)\mathbb{O}_2(t_2) \rangle = \langle \mathbb{O}_2(t_2 - i\beta)\mathbb{O}_1(t_1) \rangle . \tag{3.24}$$



The readers familiar with the thermal SK formalisms will recognise the above as the combination which occurs in the retarded-advanced (RA) formalism for SK correlators [105–108]. Thus, the row vector  $e_p^{(1)}$  describes the sliding across the thermal density matrix, which, by convention, is treated as the first past turning point.

A similar picture of the row vector  $e_p^{(2)}$  describing the sliding across the *second* past turning point is :



These statements again generalise to any number of time-fold contours. In the case of  $k$  time-folds, the row-vectors that annihilate the past most index are  $2k$  dimensional and they are  $k$  in number :

$$\begin{aligned}
e_p^{(1)}(\omega) &\equiv (1, 0, 0, 0, \dots, 0, -e^{-\beta\omega}), \\
e_p^{(2)}(\omega) &\equiv (0, -1, 1, 0, \dots, 0), \\
e_p^{(3)}(\omega) &\equiv (0, 0, 0, -1, 1, 0, \dots), \\
&\dots, \\
e_p^{(j)}(\omega) &\equiv (0, 0, 0, \dots, -1_{2j-2}, 1_{2j-1}, 0, \dots, 0) .
\end{aligned} \tag{3.25}$$

Here, the row vector  $e_p^{(j)}$  describes the sliding across the  $j^{\text{th}}$  past turning point. Thus causality and KMS conditions naturally choose a basis<sup>3</sup> of  $2k$  row vectors  $\{e_F^{(j)}, e_p^{(j)}\}$  which annihilate the future-most and past-most indices, thus implementing largest and smallest time equations.

Returning back to the case of  $k = 2$  time-folds, we conclude that, due to causality and KMS conditions,  $\widetilde{\mathbf{M}}$  contracted with the following 12 of the 16 basis tensors vanish :

$$\begin{aligned}
&e_F^{(1)} \otimes e_p^{(1)}, & e_F^{(1)} \otimes e_p^{(2)}, & e_F^{(1)} \otimes e_F^{(1)}, & e_F^{(1)} \otimes e_F^{(2)}, \\
&e_F^{(2)} \otimes e_p^{(1)}, & e_F^{(2)} \otimes e_p^{(2)}, & e_F^{(2)} \otimes e_F^{(1)}, & e_F^{(2)} \otimes e_F^{(2)}, \\
&e_p^{(1)} \otimes e_p^{(1)}, & e_p^{(1)} \otimes e_p^{(2)}, & & \\
&e_p^{(2)} \otimes e_p^{(1)}, & e_p^{(2)} \otimes e_p^{(2)}. & & 
\end{aligned} \tag{3.26}$$

We will call such tensor structure orthogonal to  $\widetilde{\mathbf{M}}$  as *orthogonal tensors*. We will also introduce

<sup>3</sup>More precisely, one obtains a basis at non-zero frequencies  $\omega \neq 0$ . Throughout this chapter, we will stay away from the special points where any one or more of the external frequencies go to zero. The expressions we write down, in general, receive contact term corrections at these special loci.

the following notation to denote the array  $\widetilde{\mathbf{M}}$  contracted against these row vectors

$$\widetilde{\mathbf{M}}_{AB}^{rs} \equiv \widetilde{\mathbf{M}}_{ij} (e_A^{(r)})^i (e_B^{(s)})^j \equiv \widetilde{\mathbf{M}} \cdot e_{AB}^{rs}, \quad (3.27)$$

where  $A, B \in \{P, F\}$  and  $i, j \in \{1, 2\}$  (or more generally  $i, j \in \{1, 2, \dots, k\}$ ). We have also introduced the convenient notation  $e_{AB}^{rs} \equiv e_A^{(r)} \otimes e_B^{(s)}$ .

For example, the orthogonal tensors listed above imply that the following contractions of the array  $\widetilde{\mathbf{M}}$  are zero :

$$\begin{aligned} & \widetilde{\mathbf{M}}_{FP}^{11}, & \widetilde{\mathbf{M}}_{FP}^{12}, & \widetilde{\mathbf{M}}_{FF}^{11}, & \widetilde{\mathbf{M}}_{FF}^{12}, \\ & \widetilde{\mathbf{M}}_{FP}^{21}, & \widetilde{\mathbf{M}}_{FP}^{22}, & \widetilde{\mathbf{M}}_{FF}^{21}, & \widetilde{\mathbf{M}}_{FF}^{22}, \\ & \widetilde{\mathbf{M}}_{PP}^{11}, & \widetilde{\mathbf{M}}_{PP}^{12}, & & \\ & \widetilde{\mathbf{M}}_{PP}^{21}, & \widetilde{\mathbf{M}}_{PP}^{22}. & & \end{aligned} \quad (3.28)$$

### 3.3.3 Dual basis of Column vectors

We concluded the previous subsection with the result that contractions of the array  $\widetilde{\mathbf{M}}$  with many of the basis tensors vanish. By elementary linear algebra, these contractions are essentially components of the array in the *dual* basis. This dual basis will also provide us a natural generalisation of the Retarded-Advanced basis of the SK formalism.

To see this, let us begin by computing the basis of column vectors which is dual to the basis of 4-dimensional row vectors mentioned above. We have

$$\begin{aligned} \bar{e}_P^{(1)}(\omega) &\equiv (1 + \bar{f}(\omega), 1 + \bar{f}(\omega), 1 + \bar{f}(\omega), 1 + \bar{f}(\omega))^T, \\ \bar{e}_P^{(2)}(\omega) &\equiv (\bar{f}(\omega), \bar{f}(\omega), 1 + \bar{f}(\omega), 1 + \bar{f}(\omega))^T, \\ \bar{e}_F^{(1)}(\omega) &\equiv (\bar{f}(\omega), 1 + \bar{f}(\omega), 1 + \bar{f}(\omega), 1 + \bar{f}(\omega))^T, \\ \bar{e}_F^{(2)}(\omega) &\equiv (\bar{f}(\omega), \bar{f}(\omega), \bar{f}(\omega), 1 + \bar{f}(\omega))^T, \end{aligned} \quad (3.29)$$

for any frequency  $\omega \neq 0$ , where  $\bar{f}(\omega) \equiv \frac{1}{e^{\beta\omega} - 1}$  is the Bose-Einstein distribution. These dual column vectors satisfy the following:

$$\begin{aligned} e_P^{(i)}(\omega) \cdot \bar{e}_F^{(j)}(\omega) &= e_F^{(i)}(\omega) \cdot \bar{e}_P^{(j)}(\omega) = 0, \\ e_P^{(i)}(\omega) \cdot \bar{e}_P^{(j)}(\omega) &= e_F^{(i)}(\omega) \cdot \bar{e}_F^{(j)}(\omega) = \delta^{ij}, \end{aligned} \quad (3.30)$$

for  $i, j \in \{1, 2\}$ . A dual basis for  $k$  time-folds can also be constructed and takes the form :

$$\begin{aligned}\bar{e}_p^{(j)}(\omega) &\equiv \underbrace{\{\check{f}(\omega), \check{f}(\omega), \dots, \check{f}(\omega)\}}_{2j-2 \text{ times}} \underbrace{\{1 + \check{f}(\omega), 1 + \check{f}(\omega), \dots, 1 + \check{f}(\omega)\}}_{2k-2j+2 \text{ times}}^T, \\ \bar{e}_F^{(j)}(\omega) &\equiv \underbrace{\{\check{f}(\omega), \check{f}(\omega), \dots, \check{f}(\omega)\}}_{2j-1 \text{ times}} \underbrace{\{1 + \check{f}(\omega), 1 + \check{f}(\omega), \dots, 1 + \check{f}(\omega)\}}_{2k-2j+1 \text{ times}}^T.\end{aligned}\tag{3.31}$$

This furnishes the generalised Retarded-Advanced (RA) basis for  $k$  time-folds.

One can then expand the array  $\tilde{\mathbf{M}}$  in the basis of tensor products of these column vectors defined at  $\omega_1$  and  $\omega_2$  :

$$\begin{aligned}\tilde{\mathbf{M}} &= \tilde{\mathbf{M}}_{PP}^{ij} \bar{e}_p^{(i)}(\omega_1) \otimes \bar{e}_p^{(j)}(\omega_2) + \tilde{\mathbf{M}}_{FP}^{ij} \bar{e}_F^{(i)}(\omega_1) \otimes \bar{e}_p^{(j)}(\omega_2) \\ &\quad + \tilde{\mathbf{M}}_{FF}^{ij} \bar{e}_F^{(i)}(\omega_1) \otimes \bar{e}_F^{(j)}(\omega_2) + \tilde{\mathbf{M}}_{PF}^{ij} \bar{e}_p^{(i)}(\omega_1) \otimes \bar{e}_F^{(j)}(\omega_2) \\ &= \tilde{\mathbf{M}}_{PF}^{ij} \bar{e}_p^{(i)}(\omega_1) \otimes \bar{e}_F^{(j)}(\omega_2).\end{aligned}\tag{3.32}$$

Here  $\tilde{\mathbf{M}}_{AB}^{rs}$  denotes the array contracted against the basis row vectors and in the last step, we have used the fact that many of these contractions vanish. So, we have to fix the 4 coefficients -  $\tilde{\mathbf{M}}_{PF}^{11}$ ,  $\tilde{\mathbf{M}}_{PF}^{12}$ ,  $\tilde{\mathbf{M}}_{PF}^{21}$  and  $\tilde{\mathbf{M}}_{PF}^{22}$ .

Let us look at the expansion of these coefficients in terms of the elements of the array  $\tilde{\mathbf{M}}$  (i.e., the usual contour ordered correlators):

$$\begin{aligned}\tilde{\mathbf{M}}_{PF}^{11} &= -\tilde{\mathbf{M}}_{11} + \tilde{\mathbf{M}}_{12} + e^{-\beta\omega_1} \tilde{\mathbf{M}}_{41} - e^{-\beta\omega_1} \tilde{\mathbf{M}}_{42} = -\rho[12], \\ \tilde{\mathbf{M}}_{PF}^{12} &= -\tilde{\mathbf{M}}_{13} + \tilde{\mathbf{M}}_{14} + e^{-\beta\omega_1} \tilde{\mathbf{M}}_{43} - e^{-\beta\omega_1} \tilde{\mathbf{M}}_{44} = e^{-\beta\omega_1} \rho[12], \\ \tilde{\mathbf{M}}_{PF}^{21} &= \tilde{\mathbf{M}}_{21} - \tilde{\mathbf{M}}_{22} - \tilde{\mathbf{M}}_{31} + \tilde{\mathbf{M}}_{32} = \rho[12], \\ \tilde{\mathbf{M}}_{PF}^{22} &= \tilde{\mathbf{M}}_{23} - \tilde{\mathbf{M}}_{24} - \tilde{\mathbf{M}}_{33} + \tilde{\mathbf{M}}_{34} = -\rho[12].\end{aligned}\tag{3.33}$$

Here, we have computed the correlators directly term by term. We note a few salient aspects of this result : first, many of the contractions with these basis vectors naturally evaluate to the spectral function  $\rho[12]$ . Second, since all the components are proportional to  $\rho[12]$ , we can deduce additional linear combinations which vanish :

$$\tilde{\mathbf{M}}_{PF}^{11} + \tilde{\mathbf{M}}_{PF}^{21}, \quad \tilde{\mathbf{M}}_{PF}^{22} + e^{\beta\omega_1} \tilde{\mathbf{M}}_{PF}^{12}, \quad \tilde{\mathbf{M}}_{PF}^{22} - \tilde{\mathbf{M}}_{PF}^{11}.\tag{3.34}$$

This is equivalent to the statement that there are three additional, non-trivial orthogonal tensors

to  $\widetilde{\mathbf{M}}$  :

$$e_p^{(1)} \otimes e_F^{(1)} + e_p^{(2)} \otimes e_F^{(1)}, \quad e_p^{(2)} \otimes e_F^{(2)} + e^{\beta\omega_1} e_p^{(1)} \otimes e_F^{(2)}, \quad e_p^{(2)} \otimes e_F^{(2)} - e_p^{(1)} \otimes e_F^{(1)}. \quad (3.35)$$

If we could somehow deduce the complete set of orthogonal tensors independently, then the only explicit computation needed is that of  $\widetilde{\mathbf{M}}_{PF}^{11}$ . We will develop a method to do so in the appendix A.2, using which we systematically tabulate all the orthogonal tensors for 2, 3 and 4 point functions in the appendices A.3.1, A.3.2 and A.3.3 respectively.

Returning to the array  $\widetilde{\mathbf{M}}$ , it can be expressed as

$$\begin{aligned} \widetilde{\mathbf{M}} = \rho[12] & \left( \bar{e}_p^{(2)}(\omega_1) \otimes \bar{e}_F^{(1)}(\omega_2) - \bar{e}_p^{(1)}(\omega_1) \otimes \bar{e}_F^{(1)}(\omega_2) \right. \\ & \left. + e^{-\beta\omega_1} \bar{e}_p^{(1)}(\omega_1) \otimes \bar{e}_F^{(2)}(\omega_2) - \bar{e}_p^{(2)}(\omega_1) \otimes \bar{e}_F^{(2)}(\omega_2) \right). \end{aligned} \quad (3.36)$$

Let us define

$$\begin{aligned} e_p^{(3)}(\omega) & \equiv (e^{\beta\omega}, 0, 0, -1) = e^{\beta\omega} e_p^{(1)}(\omega), \\ \bar{e}_p^{(3)}(\omega) & \equiv e^{-\beta\omega} \bar{e}_p^{(1)}(\omega) = \frac{\check{f}(\omega)}{1 + \check{f}(\omega)} \bar{e}_p^{(1)}(\omega) = (\check{f}(\omega), \check{f}(\omega), \check{f}(\omega), \check{f}(\omega))^T. \end{aligned} \quad (3.37)$$

Then, the final expression of the array  $\widetilde{\mathbf{M}}$  in terms of tensor products of the column vectors is as follows:

$$\begin{aligned} \widetilde{\mathbf{M}} & = \rho[12] \sum_{i=1}^2 \left( \bar{e}_p^{(i+1)}(\omega_1) \otimes \bar{e}_F^{(i)}(\omega_2) - \bar{e}_p^{(i)}(\omega_1) \otimes \bar{e}_F^{(i)}(\omega_2) \right) \\ & = \rho[12] \sum_{i=1}^2 \left( \bar{e}_p^{(i+1)}(\omega_1) - \bar{e}_p^{(i)}(\omega_1) \right) \otimes \bar{e}_F^{(i)}(\omega_2) \end{aligned} \quad (3.38)$$

One can check that these two terms correspond exactly to the terms encountered in Eq.(3.20):

$$\underbrace{\begin{pmatrix} -1 \\ -1 \\ 0 \\ 0 \end{pmatrix}}_{\bar{e}_p^{(2)} - \bar{e}_p^{(1)}} \otimes \underbrace{\begin{pmatrix} \check{f}_2 \\ 1 + \check{f}_2 \\ 1 + \check{f}_2 \\ 1 + \check{f}_2 \end{pmatrix}}_{\bar{e}_F^{(1)}} + \underbrace{\begin{pmatrix} 0 \\ 0 \\ -1 \\ -1 \end{pmatrix}}_{\bar{e}_p^{(3)} - \bar{e}_p^{(2)}} \otimes \underbrace{\begin{pmatrix} \check{f}_2 \\ \check{f}_2 \\ \check{f}_2 \\ 1 + \check{f}_2 \end{pmatrix}}_{\bar{e}_F^{(2)}}.$$

As we will show in appendix [A.3.1](#), for  $k$  time folds, the above result simply generalises to

$$\boxed{\tilde{\mathbf{M}}(2\text{-Pt}) = \rho[12] \sum_{r=1}^k \left( \bar{e}_p^{(r+1)} - \bar{e}_p^{(r)} \right) \otimes \bar{e}_F^{(r)}} . \quad (3.39)$$

Here, as in  $k = 2$ , we have defined

$$\begin{aligned} e_p^{(k+1)}(\omega) &\equiv (e^{\beta\omega}, 0, 0, 0, \dots, 0, -1) = e^{\beta\omega} e_p^{(1)}(\omega) , \\ \bar{e}_p^{(k+1)}(\omega) &\equiv \{\check{f}(\omega), \check{f}(\omega), \dots, \check{f}(\omega)\}^T = e^{-\beta\omega} \bar{e}_p^{(1)}(\omega) . \end{aligned} \quad (3.40)$$

Instead of  $4k^2$  tensor products, only  $2k$  tensor products appear, illustrating how much of simplification a judicious choice of basis can achieve.

### 3.4 Spectral representation of higher point correlators

We will now move on to the question of how we get a spectral representation for the higher point functions. Given the description in the previous sections, the basic logic on how to proceed is clear.

First, we systematically construct all the orthogonal tensors of the Wightman array in Fourier domain. This constrains the form of the array to a great extent with a few undetermined coefficients. In fact, we can count the number of orthogonal tensors using the following fact derived in [\[64\]](#): after KMS conditions are imposed, for sufficiently large  $k$ , there are  $(n-1)!$  independent  $n$  point correlators. Thus, among  $(2k)^n$  tensors,  $(2k)^n - (n-1)!$  linear combinations would be orthogonal to the Wightman array. While the logic is straightforward, one needs to proceed systematically and algorithmically. We will describe precisely such a systematic method to list the orthogonal tensors in the appendix [A.2](#), where the curious reader can find the details behind our results.

Once the orthogonal tensors have been enumerated and the most general form with  $(n-1)!$  undetermined coefficients is written down, we can then fix the undetermined coefficients by  $(n-1)!$  calculations.

### 3.4.1 Spectral representation of three point functions

Implementing the above logic for three point functions, we find a simple expression in the column vector basis :

$$\begin{aligned} \widetilde{\mathbf{M}}(3\text{-Pt}) = & \rho[321] \sum_{r=1}^k (\bar{e}_P^{(r+1)} \otimes \bar{e}_P^{(r+1)} - \bar{e}_P^{(r)} \otimes \bar{e}_P^{(r)}) \otimes \bar{e}_F^{(r)} \\ & - \rho[123] \sum_{r=1}^k (\bar{e}_P^{(r+1)} - \bar{e}_P^{(r)}) \otimes \bar{e}_F^{(r)} \otimes \bar{e}_F^{(r)}. \end{aligned} \quad (3.41)$$

Here, the spectral functions that appear in the Wightman array are defined by

$$\begin{aligned} \int_{p_1} \int_{p_2} \int_{p_3} \rho[123] e^{i(p_1 \cdot x_1 + p_2 \cdot x_2 + p_3 \cdot x_3)} & \equiv \langle [[\Phi(x_1), \Phi(x_2)], \Phi(x_3)] \rangle, \\ \int_{p_1} \int_{p_2} \int_{p_3} \rho[321] e^{i(p_1 \cdot x_1 + p_2 \cdot x_2 + p_3 \cdot x_3)} & \equiv \langle [[\Phi(x_3), \Phi(x_2)], \Phi(x_1)] \rangle. \end{aligned} \quad (3.42)$$

The contour ordered correlators are then given by

$$\begin{aligned} \langle \mathcal{T}_C \Phi_i(x_1) \Phi_j(x_2) \Phi_k(x_3) \rangle & \equiv \int_{p_1} \int_{p_2} \int_{p_3} \Theta_{123} \widetilde{\mathbf{M}}(3\text{-Pt}) e^{i(p_1 \cdot x_1 + p_2 \cdot x_2 + p_3 \cdot x_3)} \\ & + (\text{Rest of the } 3! \text{ permutations}). \end{aligned} \quad (3.43)$$

In the above expression, when the time-orderings are permuted, the tensors should also be permuted as before. We note again the drastic reduction in number of tensor products due to the choice of the basis : we go from  $8k^3$  possible terms to only  $4k$  non-zero terms. Among the 8 possible set of permutations of  $\{P, F\}$  that can occur, causality forbids all combinations except two :  $PPF$  and  $PFF$ . This justifies the claim that the above basis encodes causality constraints quite efficiently. And when we contract  $\widetilde{\mathbf{M}}$  with row vectors in these two sectors, we naturally obtain the two independent spectral functions that characterise 3-pt. functions.

Let us look at some examples. Consider the example of  $k = 1$  (Schwinger-Keldysh). We get :

$$\begin{aligned} \widetilde{\mathbf{M}}(3\text{-Pt}) = & -\rho[123] \begin{pmatrix} -1 \\ -1 \end{pmatrix} \otimes \begin{pmatrix} \check{f}_2 \\ 1 + \check{f}_2 \end{pmatrix} \otimes \begin{pmatrix} \check{f}_3 \\ 1 + \check{f}_3 \end{pmatrix} \\ & + \rho[321] \left[ \begin{pmatrix} \check{f}_1 \\ \check{f}_1 \end{pmatrix} \otimes \begin{pmatrix} \check{f}_2 \\ \check{f}_2 \end{pmatrix} \otimes \begin{pmatrix} \check{f}_3 \\ 1 + \check{f}_3 \end{pmatrix} - \begin{pmatrix} 1 + \check{f}_1 \\ 1 + \check{f}_1 \end{pmatrix} \otimes \begin{pmatrix} 1 + \check{f}_2 \\ 1 + \check{f}_2 \end{pmatrix} \otimes \begin{pmatrix} \check{f}_3 \\ 1 + \check{f}_3 \end{pmatrix} \right]. \end{aligned} \quad (3.44)$$

This structure, when multiplied by the step function  $\Theta_{123}$  and then summed over all its permutations, yields the contour-ordered 3-point functions of the Keldysh contour. For example, here is the term obtained by  $1 \leftrightarrow 3$  exchange (i.e., the combination that multiplies  $\Theta_{321}$ ) :

$$\begin{aligned}
& -\rho[321] \begin{pmatrix} \tilde{f}_1 \\ 1 + \tilde{f}_1 \end{pmatrix} \otimes \begin{pmatrix} \tilde{f}_2 \\ 1 + \tilde{f}_2 \end{pmatrix} \otimes \begin{pmatrix} -1 \\ -1 \end{pmatrix} \\
& + \rho[123] \left[ \begin{pmatrix} \tilde{f}_1 \\ 1 + \tilde{f}_1 \end{pmatrix} \otimes \begin{pmatrix} \tilde{f}_2 \\ \tilde{f}_2 \end{pmatrix} \otimes \begin{pmatrix} \tilde{f}_3 \\ \tilde{f}_3 \end{pmatrix} - \begin{pmatrix} \tilde{f}_1 \\ 1 + \tilde{f}_1 \end{pmatrix} \otimes \begin{pmatrix} 1 + \tilde{f}_2 \\ 1 + \tilde{f}_2 \end{pmatrix} \otimes \begin{pmatrix} 1 + \tilde{f}_3 \\ 1 + \tilde{f}_3 \end{pmatrix} \right].
\end{aligned} \tag{3.45}$$

The Wightman array for the  $k = 2$  contour is given similarly by

$$\begin{aligned}
\tilde{\mathbf{M}}(3\text{-Pt}) = & -\rho[123] \left[ \begin{pmatrix} -1 \\ -1 \\ 0 \\ 0 \end{pmatrix} \otimes \begin{pmatrix} \tilde{f}_2 \\ 1 + \tilde{f}_2 \\ 1 + \tilde{f}_2 \\ 1 + \tilde{f}_2 \end{pmatrix} \otimes \begin{pmatrix} \tilde{f}_3 \\ 1 + \tilde{f}_3 \\ 1 + \tilde{f}_3 \\ 1 + \tilde{f}_3 \end{pmatrix} + \begin{pmatrix} 0 \\ 0 \\ -1 \\ -1 \end{pmatrix} \otimes \begin{pmatrix} \tilde{f}_2 \\ \tilde{f}_2 \\ \tilde{f}_2 \\ 1 + \tilde{f}_2 \end{pmatrix} \otimes \begin{pmatrix} \tilde{f}_3 \\ \tilde{f}_3 \\ \tilde{f}_3 \\ 1 + \tilde{f}_3 \end{pmatrix} \right] \\
& + \rho[321] \left[ \begin{pmatrix} \tilde{f}_1 \\ \tilde{f}_1 \\ 1 + \tilde{f}_1 \\ 1 + \tilde{f}_1 \end{pmatrix} \otimes \begin{pmatrix} \tilde{f}_2 \\ \tilde{f}_2 \\ 1 + \tilde{f}_2 \\ 1 + \tilde{f}_2 \end{pmatrix} \otimes \begin{pmatrix} \tilde{f}_3 \\ 1 + \tilde{f}_3 \\ 1 + \tilde{f}_3 \\ 1 + \tilde{f}_3 \end{pmatrix} - \begin{pmatrix} 1 + \tilde{f}_1 \\ 1 + \tilde{f}_1 \\ 1 + \tilde{f}_1 \\ 1 + \tilde{f}_1 \end{pmatrix} \otimes \begin{pmatrix} 1 + \tilde{f}_2 \\ 1 + \tilde{f}_2 \\ 1 + \tilde{f}_2 \\ 1 + \tilde{f}_2 \end{pmatrix} \otimes \begin{pmatrix} \tilde{f}_3 \\ 1 + \tilde{f}_3 \\ 1 + \tilde{f}_3 \\ 1 + \tilde{f}_3 \end{pmatrix} \right] \\
& + \left[ \begin{pmatrix} \tilde{f}_1 \\ \tilde{f}_1 \\ \tilde{f}_1 \\ \tilde{f}_1 \end{pmatrix} \otimes \begin{pmatrix} \tilde{f}_2 \\ \tilde{f}_2 \\ \tilde{f}_2 \\ \tilde{f}_2 \end{pmatrix} \otimes \begin{pmatrix} \tilde{f}_3 \\ \tilde{f}_3 \\ 1 + \tilde{f}_3 \\ 1 + \tilde{f}_3 \end{pmatrix} - \begin{pmatrix} \tilde{f}_1 \\ \tilde{f}_1 \\ 1 + \tilde{f}_1 \\ 1 + \tilde{f}_1 \end{pmatrix} \otimes \begin{pmatrix} \tilde{f}_2 \\ \tilde{f}_2 \\ 1 + \tilde{f}_2 \\ 1 + \tilde{f}_2 \end{pmatrix} \otimes \begin{pmatrix} \tilde{f}_3 \\ \tilde{f}_3 \\ \tilde{f}_3 \\ 1 + \tilde{f}_3 \end{pmatrix} \right].
\end{aligned} \tag{3.46}$$

As for the  $k = 1$  case, this structure when multiplied by the step function  $\Theta_{123}$ , summed over the permutations and Fourier transformed gives the contour ordered correlators.

### 3.4.2 Spectral representation of four point functions

We now turn to the 4-point correlators. Classifying the orthogonal tensors and fixing the remaining coefficients, we can write the column vector representation for 4pt functions. There are 16 combinations which are a priori possible, but most of them are forbidden by causality. Only 4 combinations  $PPPF, PFFF, PFPF, PFFP$  are allowed. We can thus write

$$\boxed{\tilde{\mathbf{M}}(4\text{-Pt}) = \tilde{\mathbf{M}}_{PPPF} + \tilde{\mathbf{M}}_{PFFF} + \tilde{\mathbf{M}}_{PFPF} + \tilde{\mathbf{M}}_{PFFP}} \quad (3.47)$$

where we obtain

$$\begin{aligned} \tilde{\mathbf{M}}_{PPPF} &= -\rho[4321] \sum_{r=1}^k (\bar{e}_p^{(r+1)} \otimes \bar{e}_p^{(r+1)} \otimes \bar{e}_p^{(r+1)} \otimes \bar{e}_F^{(r)} - \bar{e}_p^{(r)} \otimes \bar{e}_p^{(r)} \otimes \bar{e}_p^{(r)} \otimes \bar{e}_F^{(r)}), \\ \tilde{\mathbf{M}}_{PFFF} &= \rho[1234] \sum_{r=1}^k (\bar{e}_p^{(r+1)} - \bar{e}_p^{(r)}) \otimes \bar{e}_F^{(r)} \otimes \bar{e}_F^{(r)} \otimes \bar{e}_F^{(r)}, \\ \tilde{\mathbf{M}}_{PFPF} &= \sum_{r,s=1}^k (\theta_{r>s} \rho[12][34] + \theta_{r\leq s} \rho[34][12]) (\bar{e}_p^{(r+1)} - \bar{e}_p^{(r)}) \otimes \bar{e}_F^{(r)} \otimes \bar{e}_p^{(s+1)} \otimes \bar{e}_F^{(s)} \\ &\quad - \sum_{r,s=1}^k (\theta_{r\geq s} \rho[12][34] + \theta_{r<s} \rho[34][12]) (\bar{e}_p^{(r+1)} - \bar{e}_p^{(r)}) \otimes \bar{e}_F^{(r)} \otimes \bar{e}_p^{(s)} \otimes \bar{e}_F^{(s)}, \\ \tilde{\mathbf{M}}_{PFFP} &= \sum_{r,s=1}^k (\theta_{r>s} \rho[13][24] + \theta_{r\leq s} \rho[24][13]) (\bar{e}_p^{(r+1)} - \bar{e}_p^{(r)}) \otimes \bar{e}_p^{(s+1)} \otimes \bar{e}_F^{(r)} \otimes \bar{e}_F^{(s)} \\ &\quad - \sum_{r,s=1}^k (\theta_{r\geq s} \rho[13][24] + \theta_{r<s} \rho[24][13]) (\bar{e}_p^{(r+1)} - \bar{e}_p^{(r)}) \otimes \bar{e}_p^{(s)} \otimes \bar{e}_F^{(r)} \otimes \bar{e}_F^{(s)} \\ &\quad + \sum_{r,s=1}^k (\theta_{r\geq s} \rho[14][23] + \theta_{r<s} \rho[23][14]) \bar{e}_p^{(r+1)} \otimes (\bar{e}_p^{(s+1)} - \bar{e}_p^{(s)}) \otimes \bar{e}_F^{(s)} \otimes \bar{e}_F^{(r)} \\ &\quad - \sum_{r,s=1}^k (\theta_{r>s} \rho[14][23] + \theta_{r\leq s} \rho[23][14]) \bar{e}_p^{(r)} \otimes (\bar{e}_p^{(s+1)} - \bar{e}_p^{(s)}) \otimes \bar{e}_F^{(s)} \otimes \bar{e}_F^{(r)} \\ &\quad + \rho[2314] \sum_{r=1}^k (\bar{e}_p^{(r+1)} \otimes \bar{e}_p^{(r+1)} - \bar{e}_p^{(r)} \otimes \bar{e}_p^{(r)}) \otimes \bar{e}_F^{(r)} \otimes \bar{e}_F^{(r)}. \end{aligned} \quad (3.48)$$

Here we define the spectral functions via

$$\int_{p_1} \int_{p_2} \int_{p_3} \int_{p_4} \rho[1234] e^{i(p_1 \cdot x_1 + p_2 \cdot x_2 + p_3 \cdot x_3 + p_4 \cdot x_4)} \equiv \langle [ [\Phi(x_1), \Phi(x_2)], \Phi(x_3)], \Phi(x_4) \rangle,$$



$$\int_{p_1} \int_{p_2} \int_{p_3} \int_{p_4} \rho[12][34] e^{i(p_1 \cdot x_1 + p_2 \cdot x_2 + p_3 \cdot x_3 + p_4 \cdot x_4)} \equiv \langle [\Phi(x_1), \Phi(x_2)][\Phi(x_3), \Phi(x_4)] \rangle .$$

Our previous comments about the reduction of number of terms extend to the four point functions : the column vector basis reduces the  $16k^4$  terms that can potentially appear in the 4-pt vertices of a  $k$  time-fold contour to  $12k^2 + 6k = 6k(2k + 1)$  number of terms.

For example, in the Schwinger Keldysh case, the above formulae evaluates to

$$\begin{aligned} \widetilde{\mathbf{M}}(4\text{-Pt})_{\text{Nested}} = & \rho[1234] \begin{pmatrix} -1 \\ -1 \end{pmatrix} \otimes \begin{pmatrix} \check{f}_2 \\ 1 + \check{f}_2 \end{pmatrix} \otimes \begin{pmatrix} \check{f}_3 \\ 1 + \check{f}_3 \end{pmatrix} \otimes \begin{pmatrix} \check{f}_4 \\ 1 + \check{f}_4 \end{pmatrix} \\ & + \rho[4321] \begin{pmatrix} 1 + \check{f}_1 \\ 1 + \check{f}_1 \end{pmatrix} \otimes \begin{pmatrix} 1 + \check{f}_2 \\ 1 + \check{f}_2 \end{pmatrix} \otimes \begin{pmatrix} 1 + \check{f}_3 \\ 1 + \check{f}_3 \end{pmatrix} \otimes \begin{pmatrix} \check{f}_4 \\ 1 + \check{f}_4 \end{pmatrix} \\ & - \rho[4321] \begin{pmatrix} \check{f}_1 \\ \check{f}_1 \end{pmatrix} \otimes \begin{pmatrix} \check{f}_2 \\ \check{f}_2 \end{pmatrix} \otimes \begin{pmatrix} \check{f}_3 \\ \check{f}_3 \end{pmatrix} \otimes \begin{pmatrix} \check{f}_4 \\ 1 + \check{f}_4 \end{pmatrix} \\ & - \rho[2314] \begin{pmatrix} 1 + \check{f}_1 \\ 1 + \check{f}_1 \end{pmatrix} \otimes \begin{pmatrix} 1 + \check{f}_2 \\ 1 + \check{f}_2 \end{pmatrix} \otimes \begin{pmatrix} \check{f}_3 \\ 1 + \check{f}_3 \end{pmatrix} \otimes \begin{pmatrix} \check{f}_4 \\ 1 + \check{f}_4 \end{pmatrix} \\ & + \rho[2314] \begin{pmatrix} \check{f}_1 \\ \check{f}_1 \end{pmatrix} \otimes \begin{pmatrix} \check{f}_2 \\ \check{f}_2 \end{pmatrix} \otimes \begin{pmatrix} \check{f}_3 \\ 1 + \check{f}_3 \end{pmatrix} \otimes \begin{pmatrix} \check{f}_4 \\ 1 + \check{f}_4 \end{pmatrix} , \end{aligned} \tag{3.49}$$

and

$$\begin{aligned} \widetilde{\mathbf{M}}(4\text{-Pt})_{\text{Double}} = & \rho[12][34] \begin{pmatrix} 1 \\ 1 \end{pmatrix} \otimes \begin{pmatrix} \check{f}_2 \\ 1 + \check{f}_2 \end{pmatrix} \otimes \begin{pmatrix} 1 + \check{f}_3 \\ 1 + \check{f}_3 \end{pmatrix} \otimes \begin{pmatrix} \check{f}_4 \\ 1 + \check{f}_4 \end{pmatrix} \\ & - \rho[34][12] \begin{pmatrix} 1 \\ 1 \end{pmatrix} \otimes \begin{pmatrix} \check{f}_2 \\ 1 + \check{f}_2 \end{pmatrix} \otimes \begin{pmatrix} \check{f}_3 \\ \check{f}_3 \end{pmatrix} \otimes \begin{pmatrix} \check{f}_4 \\ 1 + \check{f}_4 \end{pmatrix} \\ & + \rho[13][24] \begin{pmatrix} 1 \\ 1 \end{pmatrix} \otimes \begin{pmatrix} 1 + \check{f}_2 \\ 1 + \check{f}_2 \end{pmatrix} \otimes \begin{pmatrix} \check{f}_3 \\ 1 + \check{f}_3 \end{pmatrix} \otimes \begin{pmatrix} \check{f}_4 \\ 1 + \check{f}_4 \end{pmatrix} \\ & - \rho[24][13] \begin{pmatrix} 1 \\ 1 \end{pmatrix} \otimes \begin{pmatrix} \check{f}_2 \\ \check{f}_2 \end{pmatrix} \otimes \begin{pmatrix} \check{f}_3 \\ 1 + \check{f}_3 \end{pmatrix} \otimes \begin{pmatrix} \check{f}_4 \\ 1 + \check{f}_4 \end{pmatrix} \\ & - \rho[14][23] \begin{pmatrix} \check{f}_1 \\ \check{f}_1 \end{pmatrix} \otimes \begin{pmatrix} 1 \\ 1 \end{pmatrix} \otimes \begin{pmatrix} \check{f}_3 \\ 1 + \check{f}_3 \end{pmatrix} \otimes \begin{pmatrix} \check{f}_4 \\ 1 + \check{f}_4 \end{pmatrix} \\ & + \rho[23][14] \begin{pmatrix} 1 + \check{f}_1 \\ 1 + \check{f}_1 \end{pmatrix} \otimes \begin{pmatrix} 1 \\ 1 \end{pmatrix} \otimes \begin{pmatrix} \check{f}_3 \\ 1 + \check{f}_3 \end{pmatrix} \otimes \begin{pmatrix} \check{f}_4 \\ 1 + \check{f}_4 \end{pmatrix} . \end{aligned} \tag{3.50}$$

The boxed equations of this and the previous subsections are the main results of this chapter. On one hand, they give an efficient way to parametrise the contour-ordered correlators in terms of spectral functions which are easier to compute. On the other hand, they give a basis in which the diagrammatics is simplified and the number of vertices/propagators are reduced drastically.

Here we would like to emphasise that our choice of the independent spectral functions was solely based on the fact that they appear as coefficients in the expansions of the Wightman arrays in our column-vector basis. Moreover, the fact that they are Fourier transforms of thermal expectation values of nested and double commutators means that generically they may be easier to compute than the Wightman correlators.

The expression of thermal OTOCs in terms of spectral functions was also explored in [109]. There the authors obtained a spectral representation for the bipartite statistical average of the following form:

$$\text{Tr}\left[\rho^{\frac{1}{2}}A(t)B(t')\rho^{\frac{1}{2}}A(t)B(t')\right], \quad (3.51)$$

where  $\rho$  is a thermal density matrix and  $A$  and  $B$  are two operators. It was also shown there that the Fourier transform of such a correlator can be obtained by an appropriate analytic continuation of an analogous Euclidean correlator in the frequency domain. The main differences in our approach from this work are as follows:

- Instead of the bipartite statistical averages of the above-mentioned form, we have considered the usual thermal correlators. Moreover, we have considered more general OTOCs where all the operator insertions and the corresponding time instants can be distinct.
- Instead of studying the analytic continuation of Euclidean correlators to obtain the thermal OTOCs, we have restricted our attention to the real time correlators themselves.
- We have worked in the generalised SK formalism where apart from the KMS relations, there are additional relations between the contour-ordered correlators due to unitarity of the underlying dynamics. Our main objective was to make these relations manifest by introducing the column vector basis.

**A brief comment on the generalisation of the RA basis:** We saw that the Wightman arrays on a  $k$ -fold contour simplify considerably when they are expanded in the generalised RA basis provided by tensor products of the column vectors introduced in (3.31). This suggests that while computing truncated correlators (correlators from which the external propagators are

removed) in momentum space, it is convenient to switch to a basis for the fields that is obtained by contraction with these column vectors as shown below:

$$\begin{aligned}\tilde{\Phi}_P^{(i)}(p) &\equiv \sum_{l=1}^{2k} \tilde{\Phi}_l(p) \left( \tilde{e}_P^{(i)}(p^0) \right)_l, \\ \tilde{\Phi}_F^{(i)}(p) &\equiv \sum_{l=1}^{2k} \tilde{\Phi}_l(p) \left( \tilde{e}_F^{(i)}(p^0) \right)_l,\end{aligned}\tag{3.52}$$

for  $i = 1, \dots, k$ . Here  $\tilde{\Phi}_l(p)$  is the field (in momentum space) on the  $l^{\text{th}}$  leg of the contour.

For a 1-fold contour (i.e. the SK contour) this basis reduces to the familiar Retarded-Advanced (RA) basis

$$\begin{aligned}\tilde{\Phi}_A(p) &\equiv \tilde{\Phi}_P^{(1)}(p) \equiv (1 + \mathfrak{f}_p) \left( \tilde{\Phi}_1(p) + \tilde{\Phi}_2(p) \right), \\ \tilde{\Phi}_R(p) &\equiv \tilde{\Phi}_F^{(1)}(p) \equiv \mathfrak{f}_p \tilde{\Phi}_1(p) + (1 + \mathfrak{f}_p) \tilde{\Phi}_2(p).\end{aligned}\tag{3.53}$$

Just as this RA basis simplifies the array of SK correlators by making use of the largest time equation and the KMS relations, its generalisation (3.52) achieves a similar simplification for correlators on the  $k$ -fold contour. Moreover, the diagrammatic analysis of thermal OTOCs in weakly interacting theories should be considerably simpler in this basis due to the drastic reduction in the number of propagators, and allowed vertices. We hope that such diagrammatic techniques for thermal OTOCs would be developed in more detail in the future.

### 3.5 Conclusion and Discussion

In this chapter, we have set up the basic formalism of spectral representations of thermal out of time order correlators. We have also explicitly worked out case of  $n = 2, 3, 4$  point functions which, in an appropriate basis, take a nice and useful form that automatically encodes the causality and KMS conditions. This opens up a way to simplify OTO perturbation theory, Feynman rules and diagrammatics at finite temperature. A particular application would be to develop a full-fledged OTO kinetic theory and hydrodynamics from a consistent truncation of OTO Schwinger Dyson equations. We hope our formalism can play the role RA formalism has played in traditional Schwinger-Keldysh applications [98].

While our final results for the spectral representations take a simple and compact form, their derivation as we sketch in our appendices is somewhat elaborate due to the combinatorics in-

volved. Perhaps, a simpler and shorter derivation of the spectral representations would provide more insight into the physics behind the simplifications we see in our final results.

A set of interesting questions for future research would be to derive cutting rules for OTOCs. Ideally, we would like to predict the OTO imaginary parts and give an ‘on-shell’ picture of the physics behind them. Such a work should extend the classic work of Kobes and Semenoff [110–112] in the SK formalism (See also [98]). It should also automatically incorporate the emerging understanding of the physics behind OTOCs via operator spreading/‘infection’ models or OTO combustion waves [6,33,113–115] as well as reveal the physical picture behind the OPE inversion formula and double discontinuities in CFTs [80–82]. From the viewpoint of thermal field theory, it would be interesting to extend the existing intuitions regarding hard thermal loops(HTL) [104, 116] to OTOCs and for example, enquire whether thermal OTOCs of QCD leave a signature in the heavy ion collision experiments.

Another set of interesting questions revolve around holography and black holes in AdS. It would be nice to have a derivation of the OTOC spectral representations from gravity, say along the lines of [117, 118]. Such a framework should allow us to compute OTO spectral functions of energy momentum tensor and currents in strongly coupled gauge theories and study their low frequency, high temperature behaviour that gives rise to OTO hydrodynamics.

Finally, the spectral representations we discussed in this chapter are valid modulo contact terms in the frequency domain (since the basis row vectors we use, become linearly dependent when any one of the external frequencies of a correlator is taken to vanish.) This is a limitation already in the RA formalism of SK correlators, which the extended formalism inherits. This is usually addressed by shifting to a Keldysh basis, in which only causality conditions are implemented (and not the KMS conditions). Consequently, the column vector type representations in such a basis contain more terms, but have the merit of being applicable in non-equilibrium situations. A Keldysh type basis for OTOCs was described by [34] and it would be interesting to see how our results can be extended away from equilibrium using similar basis [119].

# Chapter 4

## Cubic OTO effective theory for thermal environment

This chapter is based on the paper [31] written by the author in collaboration with Bidisha Chakrabarty and R. Loganayagam.

Here we return to the study of the effective dynamics of a Brownian particle. Henceforth we will restrict our attention mostly to the case where the environment is a thermal bath. For such a Brownian particle interacting in a thermal environment, we will show that the cubic Schwinger-Keldysh (SK) effective theory discussed in chapter 2 is dual to a stochastic dynamics governed by a non-linear Langevin equation. Our strategy will be to first discuss the form of this non-linear Langevin dynamics in detail, and then demonstrate its duality with the SK effective theory.

To discuss this non-linear effective dynamics, we will introduce a simple toy model where the oscillators of a harmonic bath are coupled nonlinearly to the particle. For this simple model, we will derive the explicit forms of the particle's cubic effective couplings in the high temperature limit of the bath. We will see that these couplings satisfy a generalised fluctuation-dissipation relation (FDR) which is based on microscopic reversibility and thermality of the bath. From the point of view of the non-linear Langevin dynamics, this generalised FDR would connect a thermal jitter in the particle's damping coefficient to a non-Gaussianity in the thermal noise experienced by the particle.

To derive this generalised FDR, we will consider the OTO extension of the effective dynamics. We will see that this will allow us to study the effects of the bath's microscopic reversibility and thermality separately. These effects would manifest in the OTO effective dynamics of the

particle in the form of some OTO generalisations of the Onsager-Casimir reciprocal relations and the fluctuation-dissipation relation. By combining these relations, we will obtain the aforementioned generalised FDR in the nonlinear Langevin dynamics.

### **Comment on the conventions followed in this chapter:**

In this chapter, we will deviate slightly from the conventions followed in chapter 2. We will not explicitly write the small parameter  $\lambda$  which represented the strength of the particle-environment coupling in chapter 2. Instead, we will implicitly assume that this coupling is weak and that the perturbative analysis of chapter 2 holds here as well. Apart from this, we will put appropriate powers of  $\hbar$  in all the expressions. We choose to introduce these powers of  $\hbar$  in this chapter as we would mention the classical limit of the particle's dynamics which is obtained by truncating the expressions at the leading order in  $\hbar$ .

## **4.1 Motivation**

The dynamics of a Brownian particle interacting with a thermal bath is a topic that has been studied for over a hundred years. A systematic understanding of a quantum Brownian particle emerged in the 1960s with the works of Schwinger [35] and Feynman-Vernon [37]. In these works, an effective theory was derived for a quantum Brownian particle by tracing out the thermal bath's degrees of freedom.

These analyses were later extended by Caldeira and Leggett [58] to a concrete model of a particle linearly coupled to a harmonic bath. The bath degrees of freedom can be exactly integrated out to get a non-local, non-unitary theory describing the evolution of the particle. In this simple model, Caldeira and Leggett managed to show the following interesting result: First, if the distribution of the bath oscillator frequencies is chosen appropriately then the bath correlators decay with time. Consequently, at sufficiently long time-scales, one obtains a local effective theory for the particle which in classical limit reduces to the standard Langevin dynamics. This model of Caldeira-Leggett and its generalisations [59, 60] (see [48–50] for textbook level discussion) have been crucial in understanding dissipation and decoherence in quantum systems.

In this chapter, we seek to generalise Caldeira-Leggett like models. We extend such models in two directions : one extension is to go beyond the linear Langevin description to non-linear

generalisations of Langevin equation. While the non-linear versions have indeed been considered in different contexts before (see references above), a systematic classification of all possible terms at the leading level of non-linearity for a Brownian particle coupled to a generic bath was lacking. Such a systematic study along with the concomitant generalisation of the famous fluctuation dissipation theorems and Onsager's reciprocal relations is one of our objectives.

The power of Caldeira-Leggett model lies in its ability to relate the effective couplings of a dissipative/open quantum system description to the underlying microscopic physics. At a superficial level, the idea is the one familiar in usual effective theories : one computes correlators in the effective description and in the microscopic description and then matches the two. But, in open quantum systems, the integrated out degrees of freedom are not quite the heavy degrees of freedom. Thus, the integrated degrees of freedom can go on-shell resulting in the non-unitarity of the effective description. For this reason, the matching is not merely one of comparing low frequency behaviour.

At high temperatures, a whole band of frequency domain contributes right upto the thermal scale. Further, this contribution is modulated by how effectively the particle couples to the various states of the bath. We will take these aspects into account by writing the effective couplings as frequency integrals over complex contours with appropriate  $i\epsilon$  prescription that picks up the correct causal response. The integrands would be the *spectral functions* of the bath which encode the effective number of bath states accessible to the particle in a given process. From a mathematical point of view, we will write down expressions that relate the effective couplings of the Langevin description to generalised discontinuities of the appropriate (in general, out of time ordered) bath correlators.

A second related objective is the generalisation of Caldeira-Leggett like models to take into account out of time order correlations(OTOCs) and how they get transmitted from the bath to the Brownian particle. In chapter 2, we showed how the OTOCs of the particle record information about the OTOCs of the environment. In this chapter, we will discuss a concrete realisation of the ideas discussed there.

The perspective provided by extending the ideas about open systems to include out of time order correlations is crucial to the content of this chapter. As we shall show explicitly, the fluctuation-dissipation theorems and Onsager's reciprocal relations relate parameters governing time-ordered correlations to those controlling out of time ordered correlations. The straightforward way to understand the relations between time-ordered couplings is via the relations

between out of time-ordered correlations and time-ordered correlations. This is the macroscopic counterpart to the observation that including out of time ordered correlations simplify the structure of thermal correlators in a general quantum field theory [30, 34, 64].

We illustrate our results about non-linear corrections to Langevin theory by considering a simple extension of Caldeira-Leggett model. Our model consists of a Brownian particle coupled to two sets of oscillators at the same temperature. Apart from the usual linear coupling, we will also turn on weak three-body interactions involving the particle and two other bath oscillators, one drawn from each set. We show that under appropriate distribution of couplings, the bath continues to be Markovian. We derive the non-linear corrections to Langevin equation that result from such an interaction in the Markovian limit and check that these couplings indeed satisfy the correct generalisations of fluctuation-dissipation/Onsager reciprocal relations.

In the following sections, we will elaborate on these ideas and summarise our results. We will begin by reviewing the model by Caldeira-Leggett in section 4.2. This is followed by a detailed description of a non-linear generalisation of Langevin theory in section 4.3, where we also summarise our main results on such non-linear corrections for a general bath. This is followed by a description of the particular model we work with. A complete specification of the qXY model is given in section 4.4. The derivation of the non-linear Langevin theory from qXY model is the subject of section 4.5. We give a general analysis of both the generalised Onsager and fluctuation-dissipation relations in the non-linear Langevin theory in section 4.6, before our concluding remarks in section 4.7.

In appendix B.1, we enumerate the dimension of various physical quantities that appear in this chapter. In appendix B.2, we summarise various contour integrals that are useful in computation of the effective Langevin couplings from our microscopic model.

## 4.2 Review of Caldeira-Leggett model

We will now begin with a brief review of the salient features of the quantum Brownian particle and later, how these get generalised in the context of our work. We will sketch the basic structural features postponing detailed derivations for later.



## 4.2.1 Review of Langevin theory and Fluctuation-Dissipation theorem

Consider, for definiteness, a Brownian particle whose evolution is described by Langevin equation :

$$\frac{d^2q}{dt^2} + \gamma \frac{dq}{dt} = \langle f^2 \rangle \mathcal{N}(t). \quad (4.1)$$

Here  $\gamma$  is the damping constant of the particle. The term  $\langle f^2 \rangle \mathcal{N}(t)$  is the fluctuating force ('the noise term') which is commonly approximated to be Gaussian and delta-correlated, viz., its only non-zero cumulant is taken to be of the form

$$\langle \mathcal{N}(t) \mathcal{N}(t') \rangle_{noise} \equiv \frac{1}{\langle f^2 \rangle} \delta(t - t'). \quad (4.2)$$

Here  $\mathcal{N}(t)$  is normalised to have the inverse dimension of velocity for later convenience, so that  $\langle f^2 \rangle$  measures the statistical variance of the fluctuating force per unit mass (and has the dimension of acceleration<sup>2</sup>×time). The cumulant statement above can also be recast into a statement about the probability distribution governing the noise ensemble :

$$P[\mathcal{N}] \propto \exp \left\{ -\frac{\langle f^2 \rangle}{2} \int dt \mathcal{N}^2 \right\}. \quad (4.3)$$

The significance of Caldeira-Leggett model is that it shows how such a system of equations can arise from an underlying quantum mechanical model, under appropriate approximations, via integrating out the effects of a harmonic bath.

Another triumph of Caldeira-Leggett model is that it can reproduce the well-known fluctuation-dissipation relation [44–46, 120] between the parameter  $\langle f^2 \rangle$  characterising thermal fluctuations and the parameter  $\gamma$  characterising dissipation. Let us remind the reader the classical argument why such a relation should be expected : the thermal fluctuations in the bath which source the noise also cause the dissipative effects of the bath. On one hand, the rate of damping  $\gamma$  is roughly determined by the effective number of degrees of freedom of the bath with which it interacts. On the other hand, the thermal noise is produced by the energy fluctuations in the bath which is roughly  $k_B T$  times the number of degrees of freedom (here,  $T$  denotes the temperature of the bath and  $k_B$  is the Boltzmann constant). This suggests a relationship of the form  $\langle f^2 \rangle \sim \gamma \frac{k_B T}{m_p}$  between the fluctuation and the dissipation parameters. Here, we have introduced

the mass of the particle  $m_p$  to match the dimensions.

A more precise argument is as follows : at the level of classical stochastic dynamics, one can integrate the Langevin equation to obtain

$$\frac{dq}{dt} = e^{-\gamma(t-t_0)} \left( \frac{dq}{dt} \right)_{t_0} + \langle f^2 \rangle \int_{t_0}^t dt' e^{-\gamma(t-t')} \mathcal{N}(t'). \quad (4.4)$$

We square this equation and average over the noise under the assumption that the initial velocity distribution and the fluctuating force are uncorrelated. At large times, this yields for the long-time average kinetic energy for a particle of mass  $m_p$  :

$$\lim_{t \rightarrow \infty} \left\langle \frac{1}{2} m_p \left( \frac{dq}{dt} \right)^2 \right\rangle_{noise} = \frac{m_p \langle f^2 \rangle}{4\gamma}. \quad (4.5)$$

Demanding that this average kinetic energy approach the thermal equipartition value  $\frac{1}{2}k_B T$ , we obtain the fluctuation-dissipation relation

$$\langle f^2 \rangle = 2\gamma \frac{k_B T}{m_p} \equiv 2\gamma v_{th}^2, \quad (4.6)$$

where we have introduced the rms thermal velocity  $v_{th}$  of the Brownian particle defined via

$$v_{th}^2 \equiv \frac{k_B T}{m_p}. \quad (4.7)$$

The physics behind such a classical stochastic argument is clear : the kicks of the fluctuating force should, on average, replenish the energy lost due to dissipation so that the eventual balance is achieved at the Maxwell-Boltzmann value for the average kinetic energy.

As pointed out by Kubo, Martin and Schwinger [41, 42], the origins of this relation can be traced back, in the underlying quantum description, to the mathematical structure of thermal correlators. In the linear response theory, both the fluctuating force and damping rate felt by the Brownian particle can be computed from a characteristic *spectral function* of the bath denoted by  $\rho(\omega)$ , related to the Fourier domain commutator of bath operators that couple to the particle

(see below). We then have the frequency integrals (often termed the *sum rules*):

$$\begin{aligned} m_p^2 \langle f^2 \rangle &= \int_{-\infty-i\epsilon}^{\infty-i\epsilon} \frac{d\omega}{2\pi i} \frac{\rho(\omega)}{\omega^2} (1 + 2\mathfrak{f}_\omega) \hbar\omega , \\ m_p \gamma &= \int_{-\infty-i\epsilon}^{\infty-i\epsilon} \frac{d\omega}{2\pi i} \frac{\rho(\omega)}{\omega^2} , \end{aligned} \quad (4.8)$$

where  $\beta \equiv \frac{\hbar}{k_B T}$  is the periodicity of the thermal circle and  $\mathfrak{f}_\omega \equiv \frac{1}{e^{\beta\hbar\omega} - 1}$  is the Bose-Einstein distribution. These relations make precise the afore-mentioned intuition that the same effective degrees of freedom (encoded in the single function  $\rho(\omega)$  of the bath) determine both  $\langle f^2 \rangle$  and  $\gamma$ .

Note the factor  $(1 + 2\mathfrak{f})$  whose three terms describe spontaneous emission, stimulated emission and absorption of the fluctuation of frequency  $\omega$ , all of which add incoherently into the variance of noise. At high temperature limit (i.e., small  $\beta$ ) one then recovers Eq.(4.6). The  $i\epsilon$  prescription for the frequency integral is the frequency domain analogue of step functions that appear in time domain retarded Green functions. For example, the formula above for  $\gamma$  can also be written in the form

$$m_p \gamma = \int d\tau (\tau - t) \Theta(t - \tau) \int \frac{d\omega}{2\pi i} \rho(\omega) e^{-i\omega(t-\tau)} , \quad (4.9)$$

which can be thought of as coming in turn from the approximation of a non-local retarded Green function :

$$m_p \gamma \dot{q}(t) \in \int d\tau \left\{ \Theta(t - \tau) \int \frac{d\omega}{2\pi i} \rho(\omega) e^{-i\omega(t-\tau)} \right\} q(\tau) . \quad (4.10)$$

While such time domain expressions clearly exhibit the causality properties, we will find it convenient to work in frequency domain where the structure of thermal correlators can be examined clearly. All our frequency domain contour integrals can, if needed, be readily converted into time domain integrals with appropriate step functions.

Let us examine in some more detail how this works : consider a probe particle coupled to a bath in a general time-independent state and assume that at long enough time scales, a local autonomous description is still possible for the particle (i.e., Markovian approximation can be justified and any effect of the memory of the bath can be ignored). Under these assumptions, the effect of the bath can be integrated out following the method of Schwinger [35] and Feynman-

Vernon [37] to get a local Schwinger-Keldysh effective action (or equivalently a local Feynman-Vernon influence functional). We can match this local effective action against the generating functional for the Langevin correlators following the method of Martin-Siggia-Rose [61]-De Dominicis-Peliti [62]-Janssen [63] (See [121] for a recent review). This results in a general expression for the Langevin couplings :

$$\begin{aligned} m_p^2 \langle f^2 \rangle &= \int_{-\infty-i\epsilon}^{\infty-i\epsilon} \frac{d\omega_1}{2\pi i} \int_{-\infty+i\epsilon}^{\infty+i\epsilon} \frac{d\omega_2}{2\pi} \frac{\rho[12_+]}{\omega_1}, \\ m_p \gamma &= \int_{-\infty-i\epsilon}^{\infty-i\epsilon} \frac{d\omega_1}{2\pi i} \int_{-\infty+i\epsilon}^{\infty+i\epsilon} \frac{d\omega_2}{2\pi} \frac{\rho[12]}{\omega_1^2}. \end{aligned} \quad (4.11)$$

Here the integrands are the Fourier transformed expectation values of the commutator/anti-commutator

$$\begin{aligned} \rho[12] &\equiv \frac{1}{\hbar} \int dt_1 \int dt_2 e^{i(\omega_1 t_1 + \omega_2 t_2)} \langle [O(t_1), O(t_2)] \rangle_B, \\ \rho[12_+] &\equiv \int dt_1 \int dt_2 e^{i(\omega_1 t_1 + \omega_2 t_2)} \langle \{O(t_1), O(t_2)\} \rangle_B. \end{aligned} \quad (4.12)$$

In the above,  $O$  is the bath operator that couples linearly to the Brownian particle position  $q$  and the expectation values are evaluated in an appropriate time-independent state of the bath.<sup>1</sup>

The reader should also note the specific energy-conserving  $i\epsilon$  prescription needed to write the sum-rules above :

$$\int_{C_2} \equiv \int_{-\infty-i\epsilon}^{\infty-i\epsilon} \frac{d\omega_1}{2\pi} \int_{-\infty+i\epsilon}^{\infty+i\epsilon} \frac{d\omega_2}{2\pi}. \quad (4.13)$$

The above expressions relating the microscopic dynamics of the bath degrees of freedom to the effective couplings can be obtained by standard procedures of effective theory : for instance by matching the correlators predicted by the effective theory against the microscopic computations. The  $i\epsilon$  prescription then naturally appears when comparing appropriately retarded correlators.

Another important property of the complex contour  $C_2$  is the following : it remains invariant under a simultaneous complex conjugation and the reversal of frequencies. It follows then that, if the integrands are similarly invariant (as the above integrands indeed are), the resultant

---

<sup>1</sup>In the following, we stick to the convention that every commutator is divided by  $\hbar$  in the definition of spectral functions. This has the advantage that the classical limit of the spectral function  $\rho[12]$  is just the Fourier transform of the Poisson bracket. For example, Eq.(4.11) is also valid in classical statistical mechanics, provided  $\rho[12]$  is computed via Poisson brackets.

answers are real.

The expressions above imply that, from the point of view of thermal correlators, whereas the damping constant  $\gamma$  is related to the *commutator* of bath operators, the fluctuation  $\langle f^2 \rangle$  is related to the *anti-commutator*. If the bath state is thermal, the Kubo-Martin-Schwinger(KMS) conditions relate these frequency domain functions as

$$\rho[12_+] = \hbar(1 + 2\tilde{f}_1)\rho[12] = -\hbar(1 + 2\tilde{f}_2)\rho[12] . \quad (4.14)$$

Using time translation invariance to write  $\rho[12] = \rho(\omega_1) 2\pi\delta(\omega_1 + \omega_2)$ , we then recover Eq.(4.8). The Eq.(4.14) can be motivated by the following relation between thermal averages in a harmonic oscillator of frequency  $\omega$  :

$$\langle \{a, a^\dagger\} \rangle_\beta = \hbar(1 + 2\tilde{f}_\omega) \frac{1}{\hbar} \langle [a, a^\dagger] \rangle_\beta . \quad (4.15)$$

KMS showed that such a relation continues to hold true for a general quantum system, thus giving rise to Eqs. (4.8) and (4.6) under very general assumptions.

To summarise, the microscopic justification of fluctuation-dissipation theorem lies in the following steps :

- In the first step, one identifies the relevant effective couplings of the system (here  $\langle f^2 \rangle$  and  $\gamma$  of the Brownian particle) and connects it with the appropriate bath correlators (via sum rules like the ones in Eq.(4.11)). This step already assumes the emergence of a Markovian description which can be checked explicitly in a simple model like that of Caldeira-Leggett.
- In the next step, one uses thermality to derive KMS relations akin to Eq.(4.14). Note that this step, by itself, does not immediately result in a simple relation between the effective couplings of the local Markovian description.

KMS condition merely says that two couplings are related to two *different moments* of the same spectral function (see Eq.(4.8)). These two moments are a priori two independent numbers provided by the theory behind the bath. Thus, the KMS condition alone is of limited utility to an experimentalist probing the local dynamics of the Brownian particle.<sup>2</sup>

---

<sup>2</sup>One could however imagine a fine-grained experiment sensitive to non-Markovian/memory effects of the bath (such experiments are within the realm of possibility [122–125]) and think of the integrands in Eq.(4.8) as part of

- In the last step, we take a high temperature limit to get a fluctuation-dissipation relation of the form Eq.(4.6). It is in this step that one obtains the fluctuation-dissipation relation between the effective couplings.

Apart from the fluctuation-dissipation relations, there are other useful relations that can be derived when one has more than one Brownian degree of freedom and when one can assume additional symmetries. An example of such a symmetry is the microscopic time-reversal invariance whose consequences were explored by Onsager [38, 39] and Casimir [40] (we refer the reader to the monograph by Stratonovich [126] for extensions and a detailed exposition). Say we had many degrees of freedom denoted by the coordinate  $q_A$ , which undergo coupled Langevin dynamics governed by a matrix of Langevin couplings  $\gamma_{AB}$  and  $\langle f_{AB}^2 \rangle$ . In that case, the sum rules of the discussion above generalise to

$$\begin{aligned} m_p^2 \langle f_{AB}^2 \rangle &= \int_{-\infty-i\epsilon}^{\infty-i\epsilon} \frac{d\omega_1}{2\pi i} \int_{-\infty+i\epsilon}^{\infty+i\epsilon} \frac{d\omega_2}{2\pi} \frac{\rho[1_A 2_{B+}]}{\omega_1}, \\ m_p \gamma_{AB} &= \int_{-\infty-i\epsilon}^{\infty-i\epsilon} \frac{d\omega_1}{2\pi i} \int_{-\infty+i\epsilon}^{\infty+i\epsilon} \frac{d\omega_2}{2\pi} \frac{\rho[1_A 2_B]}{\omega_1^2}. \end{aligned} \quad (4.16)$$

Here  $O_A$  is the bath operator that couples to the coordinate  $q_A$  and we have used a matrix of spectral functions

$$\begin{aligned} \rho[1_A 2_B] &\equiv \frac{1}{\hbar} \int dt_1 \int dt_2 e^{i(\omega_1 t_1 + \omega_2 t_2)} \langle [O_A(t_1), O_B(t_2)] \rangle, \\ \rho[1_A 2_{B+}] &\equiv \int dt_1 \int dt_2 e^{i(\omega_1 t_1 + \omega_2 t_2)} \langle \{O_A(t_1), O_B(t_2)\} \rangle. \end{aligned} \quad (4.17)$$

Say the dynamics and the initial state of the bath are microscopic time-reversal invariant and we will assume that the Hermitian operators  $\{O_A\}$  have definite time-reversal parities  $\{\eta_A\}$ . The microscopic time-reversal then acts by the simultaneous exchange of  $\omega_1$  and  $\omega_2$  along with complex conjugation.<sup>3</sup> One then obtains the famous *Onsager reciprocal relations* [38, 39]:

$$\langle f_{AB}^2 \rangle = \eta_A \eta_B \langle f_{BA}^2 \rangle, \quad \gamma_{AB} = \eta_A \eta_B \gamma_{BA}. \quad (4.18)$$

In this chapter, we will mainly confine ourselves to studying the dynamics of a single degree of freedom and the memory functions of the bath. For this reason, many authors (see, for example, Stratonovich [126, 127]) refer to equations like Eq.(4.14) as *non-Markovian* fluctuation-dissipation theorems.

<sup>3</sup>We note that the contour  $C_2$  is left invariant under this operation. Hence, the symmetry property of integrands under this operation is inherited by the effective couplings.

of freedom, which can in principle couple to many bath operators  $\{O_A\}$  with different couplings  $g_A$ . Then, the Onsager reciprocal relations can be interpreted as statements relating the contributions proportional to  $g_A g_B$  to the damping constant and the noise variance. We will later meet an example of similar relations, when we study non-linear corrections to the dynamics of a single degree of freedom (see the discussion in section 4.6.2).

## 4.2.2 Model of the harmonic bath in Caldeira-Leggett like models

We will now move from the general description to particular models of the bath. The equation (4.11) for the damping constant  $\gamma$  naively suggests the following: if we can engineer a bath of harmonic oscillators with a linear spectral function of the form<sup>4</sup>

$$\rho[12] \equiv \rho(\omega_1)2\pi\delta(\omega_1 + \omega_2) \sim m_p\gamma\omega_1 2\pi\delta(\omega_1 + \omega_2) , \quad (4.19)$$

a naive residue integral seems to pickup the required contribution. This is however misleading. In fact, the integral for  $\gamma$  with the linear spectral function is UV divergent and needs to be regulated appropriately. A simple and commonly used regulator is to assume a Lorentz-Drude form for the spectral function, with the linear growth at low frequencies :

$$\rho(\omega) = 2 \operatorname{Im} \left\{ m_p \gamma \frac{i\Omega^2}{\omega + i\Omega} \right\} = 2m_p\gamma\omega \frac{\Omega^2}{\omega^2 + \Omega^2} , \quad (4.20)$$

which does give back  $\gamma$  after the contour integral is performed.

How can such a distribution be obtained from the underlying microscopic dynamics of the harmonic bath ? Say we are interested in the thermal harmonic bath where  $q(t)$  of the Brownian particle is coupled linearly to the bath oscillators via

$$O(t) = \sum_i g_{x,i} X_i(t) . \quad (4.21)$$

We want to now examine what set of couplings  $g_{x,i}$  and masses  $m_{x,i}$  for the bath oscillators will result in a Lorentz-Drude spectral function. Computing the commutator of the bath operator in

---

<sup>4</sup>We note that, for Markovian approximation to hold, the spectral function should be sufficiently analytic near real axis of the frequency domain [59, 60, 128].

the thermal state and Fourier transforming yields

$$\begin{aligned}\rho[12] &= \frac{1}{2\omega_1} 2\pi\delta(\omega_1 + \omega_2) \sum_i \frac{g_{x,i}^2}{m_{x,i}} 2\pi\delta(|\omega_1| - \mu_i) \\ &\equiv 2\pi\delta(\omega_1 + \omega_2) \times \int_0^\infty \frac{d\mu_x}{2\pi} (2\pi) \operatorname{sgn}(\omega_1)\delta(\omega_1^2 - \mu_x^2) \left\langle\left\langle \frac{g_x^2}{m_x} \right\rangle\right\rangle,\end{aligned}\tag{4.22}$$

where we have defined a function of  $\mu_x$  :

$$\left\langle\left\langle \frac{g_x^2}{m_x} \right\rangle\right\rangle \equiv \sum_i \frac{g_{x,i}^2}{m_{x,i}} 2\pi\delta(\mu_x - \mu_i).\tag{4.23}$$

A spectral function  $\rho(\omega)$  as in Eq.(4.20) is then obtained, if we take a continuum of oscillators whose couplings add up to give

$$\left\langle\left\langle \frac{g_x^2}{m_x} \right\rangle\right\rangle = m_p \gamma \frac{4\mu_x^2 \Omega^2}{\mu_x^2 + \Omega^2}.\tag{4.24}$$

Thus, the continuum approximation with an infinite set of oscillators gives the required smooth form for the spectral function. Only in this limit can the set of bath oscillators be idealised as a perfect thermal bath into which the Brownian particle can irreversibly dissipate into. It is also only in this limit that the information about the particle is quickly forgotten by the thermal bath, thus allowing us to ignore any memory effect. This last point can be explicitly checked by computing the bath correlators and confirming that they indeed decay at time scales set by  $\Omega^{-1}$ . Thus, we expect a local description to be good when there is a hierarchy of frequency scales :

$$\gamma \ll \Omega \ll \frac{k_B T}{\hbar}.$$

The continuum approximation and the resultant irreversibility are good approximations at time scales much smaller than the inverse of the typical gap in the bath spectrum.

This ends our brief review of the standard Langevin theory. One main goal of this chapter is to see many of these ideas and expressions generalise to higher point functions, out of time order correlations and to non-linear Langevin dynamics.



### 4.3 Introduction to Non-linear Langevin equation

It is a natural question to ask how these results generalise once we go beyond the linear Langevin description. A particular non-linear generalisation is of relevance to this chapter, which we shall now describe. Consider a non-linear generalisation of Langevin theory described by the following stochastic equation :

$$\mathcal{E}[q] \equiv \frac{d^2 q}{dt^2} + (\gamma + \zeta_\gamma \mathcal{N}) \frac{dq}{dt} + (\bar{\mu}^2 + \zeta_\mu \mathcal{N}) q + \left( \bar{\lambda}_3 - \bar{\lambda}_{3\gamma} \frac{d}{dt} \right) \frac{q^2}{2!} - F = \langle f^2 \rangle \mathcal{N} . \quad (4.25)$$

Here, we will take  $\mathcal{N}$  to be a random noise drawn from the non-Gaussian probability distribution

$$P[\mathcal{N}] \propto \exp \left\{ -\frac{1}{2\langle f^2 \rangle} \int dt \left( \langle f^2 \rangle \mathcal{N} - \zeta_N \mathcal{N}^2 \right)^2 - \frac{1}{2} Z_I \int dt \dot{\mathcal{N}}^2 \right\} . \quad (4.26)$$

We will assume that the corrections to the Langevin equation are small : this is equivalent to assuming that the parameters  $\{\zeta_\gamma, \zeta_\mu, \bar{\lambda}_3, \bar{\lambda}_{3\gamma}, \zeta_N, Z_I\}$  are small.

The physical meaning of these non-linear parameters should be evident :  $\zeta_\gamma, \zeta_\mu$  characterise the thermal jitter in the damping constant  $\gamma$  and the (renormalised) natural frequency  $\bar{\mu}^2$  of the Brownian oscillator. The parameters  $\bar{\lambda}_3, \bar{\lambda}_{3\gamma}$  control the anharmonicity in the model whereas  $\zeta_N$  characterises the non-Gaussianity of the thermal noise. The above equation includes all terms upto quadratic in amplitudes of  $q$  and  $\mathcal{N}$  and upto one time derivative acting on  $q$  (except for the inertial term  $\frac{d^2 q}{dt^2}$  which was already present before the bath came into picture). In this sense, this is indeed the most generic leading non-linear correction to the linear Langevin theory.

Another equivalent way to define these couplings would be to state how they occur in the long-time three point cumulants of the Brownian particle which starts off from the harmonic oscillator vacuum at an initial time  $t = t_0$ . While specification in terms of cumulants does not have the immediate intuitive appeal of the description above, it is a very useful characterisation for computing these couplings from a microscopic model. Consider long enough time scales such that the memory effects of the bath can be ignored and the Markovian approximation is valid. We will however be interested in the time scales much smaller than  $\gamma^{-1}$ , the time scale at which damping effects become substantial. In this time window, one can write down universal expressions for the vacuum cumulants of the Brownian particle in terms of the effective Langevin couplings. In the semi-classical limit (i.e., ignoring  $O(\hbar)$  terms), they take

the following form [29] : for  $t_1 > t_2 > t_3$ , we get

$$\begin{aligned}
\frac{1}{\hbar^2} \langle [q(t_1)q(t_2)q(t_3)] \rangle_c &= (\bar{\lambda}_3 - \bar{\lambda}_{3\gamma} \frac{\partial}{\partial t_1}) Q_{123} + O(\hbar), \\
\frac{1}{\hbar^2} \langle [q(t_3)q(t_2)q(t_1)] \rangle_c &= (\bar{\kappa}_3 + \bar{\kappa}_{3\gamma} \frac{\partial}{\partial t_3}) Q_{321} + O(\hbar), \\
\frac{i}{\hbar} \langle [q(t_1)q(t_2)q(t_3)_+] \rangle_c &= O(\hbar), \\
\frac{i}{\hbar} \langle [q(t_3)q(t_2)q(t_1)_+] \rangle_c &= 2m_p \left[ \zeta_\mu + 2\zeta_\gamma \frac{\partial}{\partial t_1} - \frac{2}{3} \widehat{\kappa}_{3\gamma} \left( \frac{\partial}{\partial t_1} - \frac{\partial}{\partial t_2} \right) \right] Q_{321} + O(\hbar), \\
\frac{i}{\hbar} \langle [q(t_1)q(t_3)q(t_2)_+] \rangle_c &= -2m_p \left[ \zeta_\mu + 2\zeta_\gamma \frac{\partial}{\partial t_2} + \frac{2}{3} \widehat{\kappa}_{3\gamma} \left( \frac{\partial}{\partial t_1} - \frac{\partial}{\partial t_2} \right) \right] Q_{321} + O(\hbar), \\
\langle [q(t_1)q(t_2)_+q(t_3)_+] \rangle_c &= \frac{2}{\mu^4} \zeta_N \left[ 2 \cos(\bar{\mu}(t_{13} + t_{23})) + 6 \cos(\bar{\mu}t_{12}) + \cos(\bar{\mu}(t_{10} + t_{20} + t_{30})) \right. \\
&\quad \left. - 3 \cos(\bar{\mu}(t_{12} - t_{30})) - 3 \cos(\bar{\mu}(t_{23} - t_{10})) - 3 \cos(\bar{\mu}(t_{31} - t_{20})) \right] + O(\hbar).
\end{aligned} \tag{4.27}$$

In the above expressions, we have defined the function

$$Q_{ijk} \equiv \frac{1}{6(m_p \bar{\mu}^2)^2} \left\{ \cos[\bar{\mu}(t_{ij} + t_{ik})] - \cos[\bar{\mu}(t_{ji} + t_{jk})] - 3 \cos[\bar{\mu}t_{ik}] + 3 \cos[\bar{\mu}t_{jk}] \right\}, \tag{4.28}$$

with  $t_{ij} \equiv t_i - t_j$  and we have used the square bracket notation to indicate nested commutators (with a + subscript indicating anticommutator). For example,

$$\begin{aligned}
\langle [q(t_1)q(t_2)q(t_3)] \rangle_c &\equiv \langle [[q(t_1), q(t_2)], q(t_3)] \rangle_c, \\
\langle [q(t_1)q(t_2)q(t_3)_+] \rangle_c &\equiv \langle \{ [q(t_1), q(t_2)], q(t_3) \} \rangle_c, \\
\langle [q(t_1)q(t_2)_+q(t_3)_+] \rangle_c &\equiv \langle \{ \{ q(t_1), q(t_2) \}, q(t_3) \} \rangle_c.
\end{aligned} \tag{4.29}$$

The six correlators given above cover all possible time orderings with three operators. In the above, we have divided by a factor of  $\hbar$  for every commutator in LHS, so that the commutators smoothly go to Poisson brackets in the classical limit.

The reader should also note that apart from the non-linear Langevin/1-OTO couplings<sup>5</sup>, three new ‘out of time ordered’ 2-OTO couplings  $\bar{\kappa}_3$ ,  $\bar{\kappa}_{3\gamma}$  and  $\widehat{\kappa}_{3\gamma}$  are needed to fit the long-time behaviour of arbitrarily ordered cumulants.<sup>6</sup> On general grounds, we expect correlators with

<sup>5</sup>These labels characterise how much out of time ordered a particular correlator/coupling actually is. The numbers here represent the minimum number of time-folds required to define a particular correlator/coupling [34].

<sup>6</sup>Later, in equation (4.128) of section 4.5.3, we will relate these couplings to the couplings in the OTO effective theory introduced in chapter 2.

four out of the six time orderings to be computable via standard Schwinger-Keldysh/Feynman-Vernon influence functionals : these are the 1-OTO correlators in the classification of [34]. A basis of such correlators is provided by

$$\begin{aligned} &\langle [q(t_1)q(t_2)q(t_3)] \rangle_c, \quad \langle [q(t_1)q(t_2)q(t_3)_+] \rangle_c, \quad \langle [q(t_1)q(t_2)_+q(t_3)_+] \rangle_c, \\ &\langle [q(t_1)q(t_2)_+q(t_3)] \rangle_c = -\langle [q(t_3)q(t_2)q(t_1)_+] \rangle_c + \langle [q(t_1)q(t_3)q(t_2)_+] \rangle_c, \end{aligned} \quad (4.30)$$

all of which can be written down in terms of the standard non-linear Langevin/1-OTO couplings, as is evident from the expressions above. The two other remaining time-orderings are however genuinely out of time ordered which can neither be captured by the standard Schwinger-Keldysh/Feynman-Vernon influence functionals nor can they be written solely in terms of the standard non-linear Langevin couplings.

A historical aside may be in order : many authors have studied non-linear generalisation of Langevin equations in a variety of contexts (See, for example [129–132]). However, to our knowledge, there is no systematic discussion in the literature including all leading nonlinear corrections allowed on general grounds, nor a microscopic model within which Markovian approximation is justified and all couplings derived. Similarly, despite a long and rich literature on non-linear fluctuation-dissipation/Onsager relations [120, 126, 127, 133–140], the relations we derive here for non-linear Langevin theory are new, as far as we know.

In the rest of this section, we will give a detailed summary of our results listing the integrals that relate the couplings that appear in the above equation to the bath correlators in the microscopic theory. <sup>7</sup> The reader desirous of a briefer summary is encouraged to consult the subsection 4.3.6 at the end of this section.

### 4.3.1 Linear Langevin couplings

We will now summarise our results regarding how the above coefficients could be computed starting from a non-linear generalisation of Caldeira-Leggett like setup. Assume the Langevin degree of freedom  $q(t)$  is still linearly coupled to some bath operator  $O(t)$ .<sup>8</sup> As in the discussion above Eq.(4.11), take the bath to be in a general time-independent state and assume a Markovian description at long enough time scales.

---

<sup>7</sup>These relations are obtained by converting the time domain integrals given in subsection 2.3.3 to frequency space integrals, and then mapping the couplings discussed there to the couplings introduced in this chapter via equation (4.128).

<sup>8</sup>We assume that the thermal 1-point function of this bath operator is zero.

Under these assumptions, a general expression can be written for the Langevin couplings in leading order causal perturbation theory in particle-bath coupling (or equivalently by matching the local influence functional to MSRDPI action of the above stochastic equation to leading order in perturbation theory) :

$$\begin{aligned}
m_p \gamma &= \int_{C_2} \frac{\rho[12]}{i\omega_1^2}, \quad m_p \Delta \bar{\mu}^2 = - \int_{C_2} \frac{\rho[12]}{\omega_1}, \quad \Delta m_p = \int_{C_2} \frac{\rho[12]}{\omega_1^3}, \\
m_p^2 \langle f^2 \rangle &= \int_{C_2} \frac{\rho[12_+]}{i\omega_1} = \int_{C_2} \frac{\hbar}{i\omega_1} (1 + 2\tilde{f}_1) \rho[12], \\
m_p^2 Z_I &= - \int_{C_2} \frac{\rho[12_+]}{i\omega_1^3} = - \int_{C_2} \frac{\hbar}{i\omega_1^3} (1 + 2\tilde{f}_1) \rho[12],
\end{aligned} \tag{4.31}$$

where as before, we have an integral over the causal contour

$$\int_{C_2} \equiv \int_{-\infty-i\epsilon}^{\infty-i\epsilon} \frac{d\omega_1}{2\pi} \int_{-\infty+i\epsilon}^{\infty+i\epsilon} \frac{d\omega_2}{2\pi}. \tag{4.32}$$

Here  $\Delta m_p$  and  $\Delta \bar{\mu}^2$  denote the renormalisation of mass and frequency of the Brownian oscillators.

The spectral functions appearing in the integrand are defined via Fourier integrals

$$\begin{aligned}
\rho[12_+] &\equiv \int dt_1 \int dt_2 e^{i(\omega_1 t_1 + \omega_2 t_2)} \langle \{O(t_1), O(t_2)\} \rangle_B, \\
\rho[12] &\equiv \frac{1}{\hbar} \int dt_1 \int dt_2 e^{i(\omega_1 t_1 + \omega_2 t_2)} \langle [O(t_1), O(t_2)] \rangle_B.
\end{aligned} \tag{4.33}$$

Further, in writing the second equality for the couplings above, we have assumed that the bath state is thermal and consequently, we have used the Kubo-Martin-Schwinger (KMS) relation to convert the anti-commutator to commutator.

The complex contour  $C_2$  has the following *reality* property : it remains invariant under a simultaneous complex conjugation and the reversal of frequencies ;

$$C_2^*[\omega_i^c \rightarrow -\omega_i] = C_2[\omega_i], \tag{4.34}$$

where  $\omega_i^c$  denotes the complex conjugate of the frequency  $\omega_i$ . Further, the hermiticity of bath operator  $O(t)$  yields the result

$$(\rho[12])_{\omega_i^c \rightarrow -\omega_i}^* = -\rho[12], \quad (\rho[12_+])_{\omega_i^c \rightarrow -\omega_i}^* = \rho[12_+]. \tag{4.35}$$

Thus, integrating the conjugated, frequency-reversed spectral function over the conjugated, frequency-reversed contour gives the same answer as the original spectral function integrated over the original contour. Since the relabelling of the integration variables  $\omega_i^c \rightarrow -\omega_i$  should not change the value of the integral, the above assertion is equivalent to the statement of reality of the Langevin couplings.

The complex contour  $C_2$  also has the following *time-reversal property*<sup>9</sup>: it remains invariant under a simultaneous complex conjugation and the exchange of frequencies  $\omega_1$  and  $\omega_2$ . Say the spectral function has a specific time-reversal parity  $\eta_{12}$  inherited from the time parity of operators that define it. We then have

$$(\rho[12])_{\omega_1^c \rightarrow \omega_2, \omega_2^c \rightarrow \omega_1}^* = -\eta_{12} \rho[12], \quad (\rho[12_+])_{\omega_1^c \rightarrow \omega_2, \omega_2^c \rightarrow \omega_1}^* = \eta_{12} \rho[12_+], \quad (4.36)$$

thus guaranteeing that the couplings derived above obey Onsager reciprocal relations using a similar argument to the above argument for reality.

**A comment on the force term:** The force per unit mass  $F$  appearing in the particle's equation of motion (4.25) is determined at leading order in the particle-bath coupling by the 1-point function of the operator  $O(t)$ . For the  $qXY$  model introduced in section 4.4, this thermal 1-point function is zero. This, in turn, leads to the vanishing of the leading order term in  $F$ . At sub-leading order, it can receive contributions from the 3-point spectral functions of the bath. We will ignore such sub-leading corrections to the couplings in this chapter.

### 4.3.2 Anharmonicity parameters : time ordered and out of time ordered

A similar exercise can be carried out for 3-point functions : for the anharmonic couplings we have

$$m_p \bar{\lambda}_3 = 2 \int_{C_3} \frac{\rho[123]}{\omega_1 \omega_3}, \quad m_p \bar{\lambda}_{3\gamma} = \int_{C_3} \frac{1}{i\omega_1 \omega_3} \left( \frac{2}{\omega_1} - \frac{1}{\omega_3} \right) \rho[123] = \int_{C_3} \frac{(2\omega_3 - \omega_1)}{i(\omega_1 \omega_3)^2} \rho[123]. \quad (4.37)$$

---

<sup>9</sup>We refer the reader to section 4.6 for a detailed discussion of time-reversal invariance and its action on causal contours in the frequency domain.

As before, we have defined here the spectral function

$$\rho[123] \equiv \frac{1}{\hbar^2} \int dt_1 \int dt_2 \int dt_3 e^{i(\omega_1 t_1 + \omega_2 t_2 + \omega_3 t_3)} \langle [[\mathcal{O}(t_1), \mathcal{O}(t_2)], \mathcal{O}(t_3)] \rangle_B. \quad (4.38)$$

and the frequency domain contour which picks up the causal part of three point function :

$$\int_{C_3} \equiv \int_{-\infty - i\epsilon_1}^{\infty - i\epsilon_1} \frac{d\omega_1}{2\pi} \int_{-\infty + i\epsilon_1 - i\epsilon_3}^{\infty + i\epsilon_1 - i\epsilon_3} \frac{d\omega_2}{2\pi} \int_{-\infty + i\epsilon_3}^{\infty + i\epsilon_3} \frac{d\omega_3}{2\pi} \quad (4.39)$$

where  $\epsilon_1, \epsilon_3 > 0$ . We will find it convenient to not fix a particular ordering between  $\epsilon_1$  and  $\epsilon_3$  : the ordering will not matter, provided we take care that our integrands do not have poles/branch cuts in  $\omega_2$  near the real axis. For example, the above expression for the effective couplings is valid provided the spectral function has no discontinuities or branch cuts in the real axis :

$$\text{Disc}_{\omega_2} \rho[123] = 0. \quad (4.40)$$

In cases where there are discontinuities, they are known to lead to long time memory effects which, in turn, lead to a breakdown of Markovian approximation [128]. Markovian approximation also needs the following constraint on the spectral function :

$$\lim_{\omega_3 \rightarrow 0} \rho[123] = 0. \quad (4.41)$$

The complex contour  $C_3$  has the following *reality property* : it remains invariant under a simultaneous complex conjugation and the reversal of frequencies (similar to our discussion above for the two-point causal contour  $C_2$ ). It follows then that, if the spectral function  $\rho[123]$  is invariant under this operation, then the resultant answers for the anharmonic couplings are real.

The line of argument which establishes this invariance is identical to the argument outlined for two point functions : the hermiticity of bath operator  $\mathcal{O}(t)$  guarantees the reality of the double commutator  $\langle [[\mathcal{O}(t_1), \mathcal{O}(t_2)], \mathcal{O}(t_3)] \rangle_B$  and in turn, the invariance of  $\rho[123]$  under simultaneous complex conjugation and the reversal of frequencies, viz.,

$$(\rho[123])_{\omega_i^c \rightarrow -\omega_i}^* = \rho[123]. \quad (4.42)$$

This along with the invariance of the contour guarantees reality of the couplings.

The complex contour  $C_3$  also has the following *time-reversal property* : it remains invariant under a simultaneous complex conjugation and the exchange of frequencies  $\omega_1$  and  $\omega_3$  (with the concomitant exchange of their imaginary parts  $\epsilon_1$  and  $\epsilon_3$ ) . If there are no poles/branch cuts in  $\omega_2$  near the real axis, we can deform the contour back to  $C_3$  : it is in this sense that the frequency contour  $C_3$  is time-reversal invariant. This is similar to the time-reversal invariance of the two-point causal contour  $C_2$ . However, unlike the two point function case, the action on the *integrand* cannot be simply described : the spectral function  $\rho[123]$  gets mapped to a new function  $\rho[321]$

$$(\rho[123])_{\omega_1^c \rightarrow \omega_3, \omega_2^c \rightarrow \omega_2, \omega_3^c \rightarrow \omega_1}^* = \eta_{123} \rho[321], \quad (4.43)$$

where  $\eta_{123}$  is the time parity of the spectral function inherited from the time parities of the underlying operators. In the above, the function  $\rho[321]$  can be thought of as the time-reversed/out of time order (OTO) spectral function :

$$\rho[321] \equiv \frac{1}{\hbar^2} \int dt_1 \int dt_2 \int dt_3 e^{i(\omega_1 t_1 + \omega_2 t_2 + \omega_3 t_3)} \langle [[O(t_3), O(t_2)], O(t_1)] \rangle_B. \quad (4.44)$$

While the expression for  $\rho[321]$  looks formally similar to that of  $\rho[123]$ , note that these are two different functions on the  $C_3$  contour due to the different  $i\epsilon$  prescriptions. For a bath with no microscopic time-reversal invariance, these two spectral functions are a priori unrelated. On the other hand, in the presence of time-reversal invariance, the analogue of Onsager relations for cubic couplings relate the Langevin anharmonic couplings to anharmonic couplings in the time-reversed stochastic dynamics.

The above statement can be made precise by introducing the out of time order (or time-reversed) anharmonic couplings

$$m_p \bar{k}_3 \equiv 2 \int_{C_3} \frac{\rho[321]}{\omega_1 \omega_3}, \quad m_p \bar{k}_{3\gamma} \equiv \int_{C_3} \frac{1}{i\omega_1 \omega_3} \left( \frac{1}{\omega_1} - \frac{2}{\omega_3} \right) \rho[321] = \int_{C_3} \frac{(\omega_3 - 2\omega_1)}{i(\omega_1 \omega_3)^2} \rho[321]. \quad (4.45)$$

Say the bath operators  $O_k(t)$  with a definite time-reversal parity  $\eta_k$  couple to the single degree of freedom of the Brownian particle. For simplicity, assume that the relevant spectral function gets contribution only from the product of three operators  $O_{k=1,2,3}$ . We can then write down the

non-linear, OTO analogue of the Onsager reciprocal relations for the resultant couplings as

$$\boxed{\bar{\lambda}_3 = \eta_o \bar{\kappa}_3, \quad \bar{\lambda}_{3\gamma} = \eta_o \bar{\kappa}_{3\gamma},} \quad (4.46)$$

where  $\eta_o \equiv \eta_1 \eta_2 \eta_3$  is the total time-reversal parity of the given spectral function. Thus, rather than constraining the cubic couplings in the non-linear Langevin dynamics, the time-reversal invariance ends up relating the standard anharmonic couplings to the OTO anharmonic couplings.

### 4.3.3 Frequency Noise parameter $\zeta_\mu$

We now move on to quote the results for the other non-linear couplings that appear in the non-linear Langevin equation. We begin with the parameter  $\zeta_\mu$  that governs the thermal jitter in the frequency of the Brownian oscillator:

$$\begin{aligned} m_p^2 \zeta_\mu &= \int_{C_3} \frac{1}{2i\omega_1 \omega_3} (\rho[12_+3] + \rho[123_+]) \\ &= \int_{C_3} \frac{1}{2i\omega_1 \omega_3} (\rho[231_+] + \rho[132_+] + \rho[123_+]) \\ &= \int_{C_3} \frac{\hbar}{i\omega_1 \omega_3} \{ (1 + \tilde{f}_1 + \tilde{f}_2) \rho[321] - (1 + \tilde{f}_2 + \tilde{f}_3) \rho[123] \}. \end{aligned} \quad (4.47)$$

Here, the spectral functions are defined as before by Fourier transforming the appropriate nested commutators/anti-commutators.<sup>10</sup> For example, we have

$$\begin{aligned} \rho[12_+3] &\equiv \frac{1}{\hbar} \int dt_1 \int dt_2 \int dt_3 e^{i(\omega_1 t_1 + \omega_2 t_2 + \omega_3 t_3)} \langle \{ \{ \mathcal{O}(t_1), \mathcal{O}(t_2) \}, \mathcal{O}(t_3) \} \rangle_B, \\ \rho[123_+] &\equiv \frac{1}{\hbar} \int dt_1 \int dt_2 \int dt_3 e^{i(\omega_1 t_1 + \omega_2 t_2 + \omega_3 t_3)} \langle \{ [ \mathcal{O}(t_1), \mathcal{O}(t_2) ], \mathcal{O}(t_3) \} \rangle_B, \end{aligned} \quad (4.48)$$

where the subscript + indicates the anti-commutator. The integral is over the same causal contour  $C_3$  as before. The first line gives the appropriate causal Green function from which the effective coupling  $\zeta_\mu$  can be extracted.

The expression in the second line above arise from generalised Jacobi identities of the form

$$\rho[12_+3] = \rho[231_+] + \rho[132_+], \quad \rho[123] + \rho[231] + \rho[312] = 0 \quad (4.49)$$

<sup>10</sup>including a factor of inverse  $\hbar$  for every commutator to guarantee smooth classical limit.



and permutations thereof, and the last line which follows from Kubo-Martin-Schwinger (KMS) relation for three point functions :

$$\rho[123_+] = -\hbar(1 + 2\mathfrak{f}_3)\rho[123] \quad (4.50)$$

and permutations thereof. Here  $\mathfrak{f}_i \equiv \mathfrak{f}(\omega_i)$  are the Bose-Einstein functions of the respective frequencies. Thus, one can express the coupling as a causal contour integral over the spectral function  $\rho[123]$  and the out of time order spectral function  $\rho[321]$  multiplied by the appropriate Bose-Einstein factors.<sup>11</sup>

The discussion on the reality properties is similar to before : the causal contour  $C_3$  and the commutator spectral functions are invariant under simultaneous conjugation and frequency reversal (assuming no  $\omega_2$  discontinuities on the real axis). The anti-commutator spectral functions are odd under simultaneous conjugation and frequency reversal :

$$(\rho[123_+])_{\omega_i \rightarrow -\omega_i}^* = -\rho[123_+], \quad (\rho[12_+3])_{\omega_i \rightarrow -\omega_i}^* = -\rho[12_+3]. \quad (4.51)$$

This, then ensures the reality of  $\zeta_\mu$ . The reality can also be shown using the expression in terms of Bose-Einstein distributions, however the argument involved is slightly more subtle : the following property of Bose-Einstein functions

$$\mathfrak{f}(-\omega) = -\{1 + \mathfrak{f}(\omega)\}, \quad (4.52)$$

should be used along with the assumption that the potential discontinuity due to  $\mathfrak{f}_2$  near  $\omega_2 \rightarrow 0$  is cancelled among the two terms.<sup>12</sup>

As discussed in the last subsection, time-reversal acts on the causal contour  $C_3$  via a simultaneous complex conjugation and the exchange of frequencies  $\omega_1$  and  $\omega_3$ . If the bath operator  $\mathcal{O}(t)$  has a definite time-reversal parity  $\eta_o$ , we can then write down the non-linear Onsager reciprocal relation for  $\zeta_\mu$  as

$$\boxed{\zeta_\mu = \eta_o \zeta_\mu}, \quad (4.53)$$

i.e., one obtains a trivial relation for time-reversal even bath operators and for time-reversal odd

---

<sup>11</sup>Note that these are the spectral functions that appeared in the spectral representation of the 3-point Wightman array discussed in the previous chapter.

<sup>12</sup>One can explicitly prove that this indeed happens in the Markovian models of the bath we use.

bath operators,  $\zeta_\mu = 0$ .

At large temperatures (or small  $\beta$ ), one can approximate

$$\hbar\tilde{f}(\omega) \approx \frac{\hbar}{\beta\omega} = \frac{m_p v_{th}^2}{\omega}. \quad (4.54)$$

We then get a high temperature formula for  $\zeta_\mu$  of the form

$$\begin{aligned} m_p \zeta_\mu &= v_{th}^2 \int_{C_3} \frac{1}{i\omega_1\omega_3} \left\{ \left( \frac{1}{\omega_1} + \frac{1}{\omega_2} \right) \rho[321] - \left( \frac{1}{\omega_2} + \frac{1}{\omega_3} \right) \rho[123] \right\} \\ &= v_{th}^2 \int_{C_3} \frac{1}{i\omega_2} \left\{ \frac{\rho[123]}{\omega_3^2} - \frac{\rho[321]}{\omega_1^2} \right\}, \end{aligned} \quad (4.55)$$

where, in the last line, we have used the fact that the spectral functions are proportional to  $\delta(\omega_1 + \omega_2 + \omega_3)$  for time-independent state of the bath.

We now turn to possible fluctuation-dissipation type relation involving  $\zeta_\mu$ . While the integrand which appears in the first line above has structural similarities with the integrands in the sum rules of the couplings  $\bar{\lambda}_{3\gamma}$  and  $\bar{\kappa}_{3\gamma}$ , we have not succeeded in establishing any general fluctuation-dissipation type relation between these couplings. Nevertheless, in the qXY model with time-reversal invariance, we find the following relation :

$$\begin{aligned} &\int_{C_3} \frac{1}{i\omega_1\omega_3} \left\{ \left( \frac{1}{\omega_1} + \frac{1}{\omega_2} \right) \rho[321] - \left( \frac{1}{\omega_2} + \frac{1}{\omega_3} \right) \rho[123] \right\} \\ &= \int_{C_3} \frac{1}{i\omega_1\omega_3} \left( \frac{2}{\omega_1} - \frac{1}{\omega_3} \right) \rho[123] = \int_{C_3} \frac{1}{i\omega_1\omega_3} \left( \frac{1}{\omega_1} - \frac{2}{\omega_3} \right) \rho[321], \end{aligned} \quad (4.56)$$

where the last equality is the relation  $\bar{\lambda}_{3\gamma} = \bar{\kappa}_{3\gamma}$  which holds for even time-reversal bath operators. More generally, we find that the following integral vanishes in this model :

$$\begin{aligned} &v_{th}^2 (\bar{\lambda}_{3\gamma} + \bar{\kappa}_{3\gamma}) - 2\zeta_\mu \\ &= \frac{v_{th}^2}{m_p} \int_{C_3} \frac{1}{i\omega_1\omega_3} \left\{ \left( \frac{2}{\omega_1} + \frac{2}{\omega_2} + \frac{1}{\omega_3} \right) \rho[123] - \left( \frac{1}{\omega_1} + \frac{2}{\omega_2} + \frac{2}{\omega_3} \right) \rho[321] \right\} = 0, \end{aligned} \quad (4.57)$$

thus resulting in a relation of the form

$$\boxed{\zeta_\mu = \frac{1}{2} v_{th}^2 (\bar{\lambda}_{3\gamma} + \bar{\kappa}_{3\gamma})}. \quad (4.58)$$

### 4.3.4 Dissipative noise parameter $\zeta_\gamma$ and its OTO counterpart

We will now move on to the parameter  $\zeta_\gamma$  which describes the jitter in the dissipative constant  $\gamma$  of the Brownian particle. The sum rule(s) for computing  $\zeta_\gamma$  is given by

$$\begin{aligned}
m_p^2 \zeta_\gamma &= \int_{C_3} \frac{1}{(2\omega_1\omega_3)^2} \left( (\omega_3 - 2\omega_1) \rho[12_+3] - \omega_2 \rho[123_+] \right) \\
&= \int_{C_3} \frac{1}{(2\omega_1\omega_3)^2} \left( (2\omega_1 - \omega_3) \rho[321_+] + (\omega_3 - 2\omega_1) \rho[132_+] + (\omega_1 + \omega_3) \rho[123_+] \right) \\
&= \int_{C_3} \frac{\hbar}{(2\omega_1\omega_3)^2} \\
&\quad \times \left\{ 2(\omega_3 - 2\omega_1)(1 + \hat{f}_1 + \hat{f}_2) \rho[321] - (\omega_3 - 2\omega_1)(1 + 2\hat{f}_2) \rho[123] + \omega_2(1 + 2\hat{f}_3) \rho[123] \right\}.
\end{aligned} \tag{4.59}$$

In the first line, we have the representation in terms of the causal correlator. The second line comes from generalised Jacobi identities and the last line from Kubo-Martin-Schwinger (KMS) relations. Following arguments very similar to the ones sketched in the previous subsection, one can argue that  $\zeta_\gamma$  produced by the above integral is real.

Next we turn to examine the behaviour of the integrand under the exchange of frequencies  $\omega_1$  and  $\omega_3$  (which would be relevant for the action of time-reversal on this coupling). We have the following identity :

$$\begin{aligned}
&(2\omega_1 - \omega_3) \rho[321_+] + (\omega_3 - 2\omega_1) \rho[132_+] + (\omega_1 + \omega_3) \rho[123_+] \\
&\quad + (2\omega_3 - \omega_1) \rho[123_+] + (\omega_1 - 2\omega_3) \rho[312_+] + (\omega_3 + \omega_1) \rho[321_+] \\
&\quad = 3 \left( \omega_1 \rho[321_+] + (\omega_3 - \omega_1) \rho[132_+] + \omega_3 \rho[123_+] \right).
\end{aligned} \tag{4.60}$$

This implies that if the bath operator  $O(t)$  has a definite time-reversal parity  $\eta_o$ , then the generalised Onsager reciprocal relation for  $\zeta_\gamma$  becomes

$$\boxed{\zeta_\gamma = \eta_o (\widehat{\kappa}_{3\gamma} - \zeta_\gamma), \quad \widehat{\kappa}_{3\gamma} = \eta_o \widehat{\kappa}_{3\gamma},} \tag{4.61}$$

where we have defined a new OTO coupling  $\widehat{\kappa}_{3\gamma}$  via

$$\begin{aligned}
m_p^2 \widehat{\kappa}_{3\gamma} &\equiv 3 \int_{C_3} \frac{1}{(2\omega_1\omega_3)^2} (\omega_1 \rho[321_+] + (\omega_3 - \omega_1) \rho[132_+] + \omega_3 \rho[123_+]) \\
&= -3 \int_{C_3} \frac{1}{(2\omega_1\omega_3)^2} (\omega_1 \rho[12_+3] + \omega_3 \rho[32_+1]) \\
&= -3 \int_{C_3} \frac{\hbar}{(2\omega_1\omega_3)^2} (\{2\omega_1(1 + \check{f}_1 + \check{f}_2) - \omega_3(1 + 2\check{f}_2)\} \rho[321] \\
&\quad + \{2\omega_3(1 + \check{f}_2 + \check{f}_3) - \omega_1(1 + 2\check{f}_2)\} \rho[123]) .
\end{aligned} \tag{4.62}$$

We conclude that if  $\eta_o = 1$ , one has the constraint  $\widehat{\kappa}_{3\gamma} = 2\zeta_\gamma$  whereas for  $\eta_o = -1$ , one has the constraint  $\widehat{\kappa}_{3\gamma} = 0$ . Thus,  $\widehat{\kappa}_{3\gamma}$  can be thought of as the part of  $\zeta_\gamma$  even under time-reversal, whereas the part odd under time-reversal is given by

$$\begin{aligned}
m_p^2 (2\zeta_\gamma - \widehat{\kappa}_{3\gamma}) &\equiv \int_{C_3} \frac{1}{(2\omega_1\omega_3)^2} ((\omega_1 - 2\omega_3) \rho[321_+] + 3(\omega_3 - \omega_1) \rho[132_+] + (2\omega_1 - \omega_3) \rho[123_+]) \\
&= \int_{C_3} \frac{\hbar}{(2\omega_1\omega_3)^2} (\{2\omega_2(1 + \check{f}_1 + \check{f}_2) + 3\omega_3(1 + 2\check{f}_1)\} \rho[321] \\
&\quad - \{2\omega_2(1 + \check{f}_2 + \check{f}_3) + 3\omega_1(1 + 2\check{f}_3)\} \rho[123]) .
\end{aligned} \tag{4.63}$$

At high temperature, these expressions become

$$\begin{aligned}
m_p \zeta_\gamma &= v_{th}^2 \int_{C_3} \frac{1}{2\omega_1\omega_3} \\
&\quad \times \left\{ \left( \frac{1}{\omega_1} - \frac{2}{\omega_3} \right) \left( \frac{1}{\omega_1} + \frac{1}{\omega_2} \right) \rho[321] + \left( \frac{2}{\omega_2\omega_3} - \frac{1}{\omega_2\omega_1} + \frac{\omega_2}{\omega_1\omega_3^2} \right) \rho[123] \right\} \\
&= v_{th}^2 \int_{C_3} \frac{1}{\omega_1\omega_3} \left\{ \left( \frac{1}{\omega_1^2} + \frac{3}{\omega_1\omega_2} \right) \rho[321] + \left( \frac{3}{\omega_3\omega_2} - \frac{1}{\omega_3^2} \right) \rho[123] \right\} ,
\end{aligned} \tag{4.64}$$

or equivalently

$$m_p (2\zeta_\gamma - \widehat{\kappa}_{3\gamma}) = v_{th}^2 \int_{C_3} \frac{1}{\omega_1\omega_3} \left\{ \frac{1}{\omega_1^2} \rho[321] - \frac{1}{\omega_3^2} \rho[123] \right\} , \tag{4.65}$$

and

$$\begin{aligned}
m_p \widehat{\kappa}_{3\gamma} &= -3v_{th}^2 \int_{C_3} \frac{1}{2\omega_1\omega_3} \\
&\times \left\{ \left( \frac{1}{\omega_1\omega_3} + \frac{1}{\omega_3\omega_2} - \frac{1}{\omega_1\omega_2} \right) \rho[321] + \left( \frac{1}{\omega_1\omega_3} + \frac{1}{\omega_1\omega_2} - \frac{1}{\omega_3\omega_2} \right) \rho[123] \right\} \\
&= 3v_{th}^2 \int_{C_3} \frac{1}{\omega_1\omega_2\omega_3} \left\{ \frac{1}{\omega_1} \rho[321] + \frac{1}{\omega_3} \rho[123] \right\}.
\end{aligned} \tag{4.66}$$

In simplifying these expressions, we have used the identity

$$\frac{1}{\omega_1\omega_3} + \frac{1}{\omega_1\omega_2} + \frac{1}{\omega_3\omega_2} = 0, \tag{4.67}$$

which holds because of the  $\delta(\omega_1 + \omega_2 + \omega_3)$  inside the spectral functions.

### 4.3.5 Non-Gaussianity $\zeta_N$ and its fluctuation-dissipation relation

We finally turn our attention to the last parameter of the non-linear Langevin model which is the non-Gaussianity parameter  $\zeta_N$ . We find the sum rule(s) for computing  $\zeta_N$  as

$$m_p^3 \zeta_N = \int_{C_3} \frac{\rho[12_+3_+]}{4\omega_1\omega_3} = \int_{C_3} \frac{\hbar^2}{4\omega_1\omega_3} (1 + 2\mathfrak{f}_3) \left\{ (1 + 2\mathfrak{f}_2) \rho[123] - 2(1 + \mathfrak{f}_1 + \mathfrak{f}_2) \rho[321] \right\}, \tag{4.68}$$

where we have used the condition for the nested anti-commutator to write the second equality.

The relevant spectral function is

$$\rho[12_+3_+] \equiv \int dt_1 \int dt_2 \int dt_3 e^{i(\omega_1 t_1 + \omega_2 t_2 + \omega_3 t_3)} \langle \{ \{ \mathcal{O}(t_1), \mathcal{O}(t_2) \}, \mathcal{O}(t_3) \} \rangle_B. \tag{4.69}$$

It can be checked that the integral above does give a real coupling as an answer using methods described before. In order to study time-reversal, consider the following time-reversed/OTO counterpart of the spectral function appearing above :

$$\rho[32_+1_+] = \rho[12_+3_+] + \hbar^2 (\rho[123] - \rho[321]), \tag{4.70}$$

a relation which can be checked by a simple expansion of the nested commutators/anti-commutators.

It follows that the combination of spectral functions with good time-reversal properties is

$$\rho[12_+3_+] + \rho[32_+1_+] = 2\rho[12_+3_+] + \hbar^2(\rho[123] - \rho[321]) . \quad (4.71)$$

With this in mind, we examine the integral

$$\begin{aligned} \int_{C_3} \frac{\rho[12_+3_+] + \rho[32_+1_+]}{4\omega_1\omega_3} &= \int_{C_3} \frac{2\rho[12_+3_+] + \hbar^2(\rho[123] - \rho[321])}{4\omega_1\omega_3} \\ &= 2m_p^3\zeta_N + \frac{\hbar^2}{8}m_p(\bar{\lambda}_3 - \bar{\kappa}_3) . \end{aligned} \quad (4.72)$$

Here, we have used the sum rules quoted before to write a combination of couplings with good time-reversal properties. Microscopic time-reversal invariance thus implies

$$\boxed{2m_p^3\zeta_N + \frac{\hbar^2}{8}m_p(\bar{\lambda}_3 - \bar{\kappa}_3) = \eta_o \left\{ 2m_p^3\zeta_N + \frac{\hbar^2}{8}m_p(\bar{\lambda}_3 - \bar{\kappa}_3) \right\} ,} \quad (4.73)$$

which is trivially satisfied for  $\eta_o = +1$ . For  $\eta_o = -1$ , we get a generalised Onsager condition of the form

$$\zeta_N = -\frac{\hbar^2}{16m_p^2}(\bar{\lambda}_3 - \bar{\kappa}_3) . \quad (4.74)$$

Thus, the non-Gaussianity in thermal noise is quantum suppressed for time-reversal odd coupling to the bath.

At high temperature limit, we get

$$\begin{aligned} m_p\left\{\zeta_N + \frac{\hbar^2}{16m_p^2}(\bar{\lambda}_3 - \bar{\kappa}_3)\right\} &= v_{th}^4 \int_{C_3} \frac{1}{\omega_1\omega_3} \left\{ \frac{1}{\omega_3\omega_2} \rho[123] - \left( \frac{1}{\omega_1\omega_3} + \frac{1}{\omega_3\omega_2} \right) \rho[321] \right\} \\ &= v_{th}^4 \int_{C_3} \frac{1}{\omega_1\omega_3} \left\{ \frac{1}{\omega_1\omega_2} \rho[321] + \frac{1}{\omega_3\omega_2} \rho[123] \right\} . \end{aligned} \quad (4.75)$$

where we have used Eq.(4.67). Comparing this against the high temperature limit of  $\widehat{\kappa}_{3\gamma}$ , we obtain the fluctuation-dissipation relation :

$$\boxed{\zeta_N + \frac{\hbar^2}{16m_p^2}(\bar{\lambda}_3 - \bar{\kappa}_3) = \frac{1}{3}\widehat{\kappa}_{3\gamma}v_{th}^2 .} \quad (4.76)$$

We note that, in this way of writing both sides of these equations have the same time-reversal property.

### 4.3.6 Summary of relations in non-linear Langevin theory

We will now summarise all the Onsager type relations between the couplings of the non-linear Langevin theory :

$$\begin{aligned} \bar{\lambda}_3 &= \eta_o \bar{\kappa}_3, \quad \bar{\lambda}_{3\gamma} = \eta_o \bar{\kappa}_{3\gamma}, \quad \zeta_\mu = \eta_o \zeta_\mu, \quad \zeta_\gamma = \eta_o (\widehat{\kappa}_{3\gamma} - \zeta_\gamma), \quad \widehat{\kappa}_{3\gamma} = \eta_o \widehat{\kappa}_{3\gamma}, \\ 2m_p^3 \zeta_N + \frac{\hbar^2}{8} m_p (\bar{\lambda}_3 - \bar{\kappa}_3) &= \eta_o \left\{ 2m_p^3 \zeta_N + \frac{\hbar^2}{8} m_p (\bar{\lambda}_3 - \bar{\kappa}_3) \right\}. \end{aligned} \quad (4.77)$$

In addition, we have the consequence of KMS relations :

$$\zeta_\mu = \frac{1}{2} v_{th}^2 (\bar{\lambda}_{3\gamma} + \bar{\kappa}_{3\gamma}), \quad \zeta_N + \frac{\hbar^2}{16m_p^2} (\bar{\lambda}_3 - \bar{\kappa}_3) = \frac{1}{3} \widehat{\kappa}_{3\gamma} v_{th}^2. \quad (4.78)$$

Note that, in general, each of these conditions relate the time-ordered Langevin couplings to OTO Langevin couplings. These relations can be combined to solve for 5 of the non-linear Langevin couplings in terms of the 3 remaining couplings  $\{\bar{\lambda}_3, \bar{\lambda}_{3\gamma}, \zeta_\gamma\}$  :

$$\begin{aligned} \bar{\kappa}_3 &= \eta_o \bar{\lambda}_3, \quad \bar{\kappa}_{3\gamma} = \eta_o \bar{\lambda}_{3\gamma}, \quad \widehat{\kappa}_{3\gamma} = (1 + \eta_o) \zeta_\gamma, \\ \zeta_\mu &= \frac{1}{2} (1 + \eta_o) \bar{\lambda}_{3\gamma} v_{th}^2, \quad \zeta_N = \frac{1}{3} (1 + \eta_o) \zeta_\gamma v_{th}^2 - \frac{\hbar^2}{16m_p^2} (1 - \eta_o) \bar{\lambda}_3. \end{aligned} \quad (4.79)$$

These relations comprise one of the main results of this chapter. We collect in Table 4.4, the Onsager pairs related to each other by time-reversal.

The following tables summarise the integrands  $\mathcal{I}[g]$  associated with each coupling  $g$ . The tables 4.1, 4.2 and 4.3 summarise the integrals for quadratic couplings that are induced, in the leading order in perturbation theory, from a bath in a general time-independent state, by a general thermal bath and by a bath at high temperature respectively. The couplings are given by expressions of the form

$$g = \int_{C_2} \mathcal{I}[g]. \quad (4.80)$$

Similarly, the tables 4.4, 4.5 and 4.6 summarise the integrals for cubic couplings that are induced, in the leading order in perturbation theory, from a bath in a general time-independent state, by a general thermal bath and by a bath at high temperature respectively. In this case, the

couplings are given by

$$g = \int_{C_3} \mathcal{I}[g]. \quad (4.81)$$

Table 4.1: Quadratic Couplings (general environment)

$g$	$\mathcal{I}[g]$
$\Delta m_p$	$\frac{1}{\omega_1^3} \rho[12]$
$Z_I$	$-\frac{1}{im_p^2 \omega_1^3} \rho[12_+]$
$\Delta \bar{\mu}^2$	$-\frac{1}{m_p \omega_1} \rho[12]$
$\langle f^2 \rangle$	$\frac{1}{im_p^2 \omega_1} \rho[12_+]$
$\gamma$	$\frac{1}{im_p \omega_1^2} \rho[12]$

Table 4.2: Sum rules for Quadratic Couplings (Thermal environment)

$g$	$\mathcal{I}[g]$
$\Delta m_p$	$\frac{1}{\omega_1^3} \rho[12]$
$Z_I$	$-\frac{\hbar}{im_p^2 \omega_1^3} (1 + 2\bar{f}_1) \rho[12]$
$\Delta \bar{\mu}^2$	$-\frac{1}{m_p \omega_1} \rho[12]$
$\langle f^2 \rangle$	$\frac{\hbar}{im_p^2 \omega_1} (1 + 2\bar{f}_1) \rho[12]$
$\gamma$	$\frac{1}{im_p \omega_1^2} \rho[12]$

Table 4.3: Sum rules for quadratic Couplings (High Temperature limit)

$g$	$\mathcal{I}[g]$
$\Delta m_p$	$\frac{1}{\omega_1^3} \rho[12]$
$Z_I$	$-\frac{2v_{th}^2}{im_p} \frac{1}{\omega_1^3} \rho[12]$
$\Delta \bar{\mu}^2$	$-\frac{1}{m_p \omega_1} \rho[12]$
$\langle f^2 \rangle$	$\frac{2v_{th}^2}{im_p} \frac{1}{\omega_1^2} \rho[12]$
$\gamma$	$\frac{1}{im_p \omega_1^2} \rho[12]$



Table 4.4: Cubic couplings : doublets/singlets under microscopic time-reversal (general environment)

$g$	$\mathcal{I}[g]$
$\bar{\lambda}_3$	$\frac{2}{m_p \omega_1 \omega_3} \rho[123]$
$\bar{\kappa}_3$	$\frac{2}{m_p \omega_1 \omega_3} \rho[321]$
$\bar{\lambda}_{3\gamma}$	$\frac{1}{im_p \omega_1 \omega_3} \left( \frac{2}{\omega_1} - \frac{1}{\omega_3} \right) \rho[123]$
$\bar{\kappa}_{3\gamma}$	$\frac{1}{im_p \omega_1 \omega_3} \left( \frac{1}{\omega_1} - \frac{2}{\omega_3} \right) \rho[321]$
$\zeta_\gamma$	$\frac{1}{(2m_p \omega_1 \omega_3)^2} \left( (2\omega_1 - \omega_3) \rho[321_+] + (\omega_3 - 2\omega_1) \rho[132_+] + (\omega_1 + \omega_3) \rho[123_+] \right)$
$\widehat{\kappa}_{3\gamma} - \zeta_\gamma$	$\frac{1}{(2m_p \omega_1 \omega_3)^2} \left( (\omega_1 + \omega_3) \rho[321_+] + (2\omega_3 - \omega_1) \rho[132_+] + (2\omega_3 - \omega_1) \rho[123_+] \right)$
$\widehat{\kappa}_{3\gamma}$	$\frac{3}{(2m_p \omega_1 \omega_3)^2} \left( \omega_1 \rho[321_+] + (\omega_3 - \omega_1) \rho[132_+] + \omega_3 \rho[123_+] \right)$
$\zeta_\mu$	$\frac{1}{2im_p^2 \omega_1 \omega_3} \left( \rho[123_+] - \rho[321_+] + \rho[132_+] \right)$
$2\zeta_N + \frac{\hbar^2}{8m_p^2} (\bar{\lambda}_3 - \bar{\kappa}_3)$	$\frac{1}{8m_p^3 \omega_1 \omega_3} \left( \rho[12_+ 3_+] + \rho[32_+ 1_+] \right)$

## 4.4 Introduction to the qXY model

In this section, we will begin by describing a microscopic model of an oscillator coupled to bath oscillator degrees of freedom in a way that results in an effective non-linear Langevin equation for the original oscillator. Our motivation here is to construct a physical microscopic description in which one can check the Markovian assumption and the relation between the effective couplings that emerge therein.

### 4.4.1 Model of the bath

We will now begin with the Caldeira-Leggett model and then modify it to suit our requirements. As described before, the model is that of a single system oscillator (denoted by a degree of freedom  $q$ ) coupled to a bath of oscillators (denoted by degrees of freedom  $X$ ). One starts with a distribution of couplings and masses of bath oscillators specified by a characteristic distribution function, defined by

$$\left\langle \left\langle \frac{g_x^2}{m_x} \right\rangle \right\rangle \equiv \sum_i \frac{g_{x,i}^2}{m_{x,i}} 2\pi \delta(\mu_x - \mu_i). \quad (4.82)$$

Table 4.5: Sum rules for Coupling (Thermal environment)

$g$	$\mathcal{I}[g]$
$\bar{\lambda}_3$	$\frac{2}{m_p \omega_1 \omega_3} \rho[123]$
$\bar{\kappa}_3$	$\frac{2}{m_p \omega_1 \omega_3} \rho[321]$
$\bar{\lambda}_{3\gamma}$	$\frac{1}{im_p \omega_1 \omega_3} \left( \frac{2}{\omega_1} - \frac{1}{\omega_3} \right) \rho[123]$
$\bar{\kappa}_{3\gamma}$	$\frac{1}{im_p \omega_1 \omega_3} \left( \frac{1}{\omega_1} - \frac{2}{\omega_3} \right) \rho[321]$
$\zeta_\gamma$	$\frac{\hbar}{(2m_p \omega_1 \omega_3)^2} \left\{ 2(\omega_3 - 2\omega_1)(1 + \bar{f}_1 + \bar{f}_2) \rho[321] - (\omega_3 - 2\omega_1)(1 + 2\bar{f}_2) \rho[123] \right.$ $\left. + \omega_2(1 + 2\bar{f}_3) \rho[123] \right\}$
$\bar{\kappa}_{3\gamma}$	$-3 \frac{\hbar}{(2m_p \omega_1 \omega_3)^2} \left( \left\{ 2\omega_1(1 + \bar{f}_1 + \bar{f}_2) - \omega_3(1 + 2\bar{f}_2) \right\} \rho[321] \right.$ $\left. + \left\{ 2\omega_3(1 + \bar{f}_2 + \bar{f}_3) - \omega_1(1 + 2\bar{f}_2) \right\} \rho[123] \right)$
$\zeta_\mu$	$\frac{\hbar}{im_p^2 \omega_1 \omega_3} \left\{ (1 + \bar{f}_1 + \bar{f}_2) \rho[321] - (1 + \bar{f}_2 + \bar{f}_3) \rho[123] \right\}$
$\zeta_N$	$\frac{\hbar^2}{4m_p^3 \omega_1 \omega_3} (1 + 2\bar{f}_3) \left\{ (1 + 2\bar{f}_2) \rho[123] - 2(1 + \bar{f}_1 + \bar{f}_2) \rho[321] \right\}$

This distribution function multiplied by the spectral contribution of each bath oscillator can be summed to give the Caldeira-Leggett spectral function :

$$\rho[12]_{CL} \equiv \int_0^\infty \frac{d\mu_x}{2\pi} 2\pi \delta(\omega_1 + \omega_2) \times (2\pi) \operatorname{sgn}(\omega_1) \delta(\omega_1^2 - \mu_x^2) \left\langle \left\langle \frac{g_x^2}{m_x} \right\rangle \right\rangle. \quad (4.83)$$

To obtain a Lorentz-Drude spectral function, we consider a continuum of oscillators whose couplings add up to give a distribution of the form

$$\left\langle \left\langle \frac{g_x^2}{m_x} \right\rangle \right\rangle = m_p \gamma_x \frac{4\mu_x^2 \Omega^2}{\mu_x^2 + \Omega^2}, \quad (4.84)$$

where  $\gamma_x$  denotes the contribution of X oscillators to the damping constant  $\gamma$  of the particle.

The contribution to the noise is determined by fluctuation-dissipation relation

$$\langle f^2 \rangle = 2\gamma v_{th}^2.$$

To get a simple nonlinear generalisation, we will double the number of oscillators into two kinds of bath both at same temperature. We imagine them to be two different sets of bath oscillators distinguished by the letters X and Y. For simplicity, we will assume that the Y type

Table 4.6: Sum rules for Coupling (High Temperature limit)

$g$	$\mathcal{I}[g]$
$\bar{\lambda}_3$	$\frac{2}{m_p \omega_1 \omega_3} \rho[123]$
$\bar{\kappa}_3$	$\frac{2}{m_p \omega_1 \omega_3} \rho[321]$
$\bar{\lambda}_{3\gamma}$	$\frac{1}{im_p \omega_1 \omega_3} \left( \frac{2}{\omega_1} - \frac{1}{\omega_3} \right) \rho[123]$
$\bar{\kappa}_{3\gamma}$	$\frac{1}{im_p \omega_1 \omega_3} \left( \frac{1}{\omega_1} - \frac{2}{\omega_3} \right) \rho[321]$
$\zeta_\gamma$	$\frac{v_{th}^2}{m_p} \frac{1}{\omega_1 \omega_3} \left\{ \left( \frac{1}{\omega_1^2} + \frac{3}{\omega_1 \omega_2} \right) \rho[321] + \left( \frac{3}{\omega_3 \omega_2} - \frac{1}{\omega_3^2} \right) \rho[123] \right\}$
$\widehat{\kappa}_{3\gamma}$	$3 \frac{v_{th}^2}{m_p} \frac{1}{\omega_1 \omega_2 \omega_3} \left\{ \frac{1}{\omega_1} \rho[321] + \frac{1}{\omega_3} \rho[123] \right\}$
$\zeta_\mu$	$\frac{v_{th}^2}{m_p} \frac{1}{i\omega_2} \left\{ \frac{1}{\omega_3^2} \rho[123] - \frac{1}{\omega_1^2} \rho[321] \right\}$
$\zeta_N$	$\frac{v_{th}^4}{m_p} \frac{1}{\omega_1 \omega_2 \omega_3} \left\{ \frac{1}{\omega_1} \rho[321] + \frac{1}{\omega_3} \rho[123] \right\}$

oscillators also have similar coupling distribution as  $X$  type oscillators

$$\left\langle \left\langle \frac{g_y^2}{m_y} \right\rangle \right\rangle = m_p \gamma_y \frac{4\mu_y^2 \Omega^2}{\mu_y^2 + \Omega^2}, \quad (4.85)$$

and they add to the damping due to  $X$  type oscillators. Thus,  $\gamma = \gamma_x + \gamma_y$  and the noise contributions from the two sets of oscillators also add up. Till now, this is merely a relabelling of the original model, and the model is hence exactly solvable and yields linear Langevin theory.

We will now introduce non-linearity into this theory by introducing a very small 3-body interaction term of the form  $qXY$ . More precisely, one considers a system of oscillators with the Lagrangian

$$L[q, X, Y] = L_B[X, Y] + \frac{1}{2} m_{p0} (\dot{q}^2 - \bar{\mu}_0^2 q^2) + q \left( \sum_i g_{x,i} X_i + \sum_j g_{y,j} Y_j + \sum_{i,j} g_{xy,ij} X_i Y_j \right) \quad (4.86)$$

where we denote the oscillator's position by  $q$  and  $L_B[X, Y]$  is the free Lagrangian of the harmonic bath. The operator that acts on the Hilbert space of the bath and couples to  $q$  is

$$O \equiv \sum_i g_{x,i} X_i + \sum_j g_{y,j} Y_j + \sum_{i,j} g_{xy,ij} X_i Y_j. \quad (4.87)$$

When we integrate out the effects of the bath degrees of freedom, the effective couplings are now induced for the oscillator and there are corrections to the linear Langevin theory. These Langevin effective couplings have their microscopic origin in the thermal correlators/spectral

functions of the operator above.

One can think of the above as a toy model for say an atom coupled to photons whereby, apart from the standard, dominant linear dipole coupling responsible for single photon emission/absorption processes, one also has two photon processes involving two photons of two different frequencies. The physics here is familiar one say from Brillouin scattering of photons against phonons or the inelastic Raman scattering of photons against molecules. At the level of linear Langevin couplings, both the noise and the damping constant receive contributions from the inelastic 3-body scattering : first, there is an effect due to two ‘photon’ emission and absorption into/from the thermal bath which gives a contribution proportional to

$$\hbar(\mu_x + \mu_y) \left[ (1 + \bar{f}_x)(1 + \bar{f}_y) - \bar{f}_x \bar{f}_y \right] \quad (4.88)$$

in the spectral function. The second effect is due to inelastic scattering whose contribution is proportional to

$$\hbar(\mu_x - \mu_y) \left[ \bar{f}_x(1 + \bar{f}_y) - \bar{f}_y(1 + \bar{f}_x) \right]. \quad (4.89)$$

Putting these effects together, we get a spectral function<sup>13</sup>

$$\begin{aligned} \rho[12] = & (2\pi)\delta(\omega_1 + \omega_2) \int_0^\infty \frac{d\mu_x}{2\pi} \langle \langle \frac{g_x^2}{m_x} \rangle \rangle (2\pi) \text{sgn}(\omega_1) \delta(\omega_1^2 - \mu_x^2) \\ & + (2\pi)\delta(\omega_1 + \omega_2) \int_0^\infty \frac{d\mu_y}{2\pi} \langle \langle \frac{g_y^2}{m_y} \rangle \rangle (2\pi) \text{sgn}(\omega_1) \delta(\omega_1^2 - \mu_y^2) \\ & + (2\pi)\delta(\omega_1 + \omega_2) \int_0^\infty \frac{d\mu_x}{2\pi} \int_0^\infty \frac{d\mu_y}{2\pi} \langle \langle \frac{g_{xy}^2}{m_x m_y} \rangle \rangle \\ & \frac{1}{(2\mu_x)(2\mu_y)} \left\{ 2\hbar(\mu_x + \mu_y) \left[ (1 + \bar{f}_x)(1 + \bar{f}_y) - \bar{f}_x \bar{f}_y \right] (2\pi) \text{sgn}(\omega_1) \delta(\omega_1^2 - (\mu_x + \mu_y)^2) \right. \\ & \left. + 2\hbar(\mu_x - \mu_y) \left[ \bar{f}_x(1 + \bar{f}_y) - \bar{f}_y(1 + \bar{f}_x) \right] (2\pi) \text{sgn}(\omega_2) \delta(\omega_2^2 - (\mu_x - \mu_y)^2) \right\}. \end{aligned} \quad (4.91)$$

---

<sup>13</sup>The correction to the spectral function appearing in the last two lines comes from computing the Fourier transform of the thermal commutator

$$\langle [X(t_1)Y(t_1), X(t_2)Y(t_2)] \rangle. \quad (4.90)$$

Here we have introduced the cubic coupling distribution

$$\left\langle\left\langle\frac{g_{xy}^2}{m_x m_y}\right\rangle\right\rangle \equiv \sum_{ij} \frac{g_{xy,ij}^2}{m_{x,i} m_{y,j}} 2\pi\delta(\mu_x - \mu_i) 2\pi\delta(\mu_y - \mu_j). \quad (4.92)$$

This cubic coupling distribution should be judiciously chosen so that its dynamics does not destroy the Markovian approximation. We find it convenient to choose a distribution of couplings such that

$$\left\langle\left\langle\frac{g_{xy}^2}{m_x m_y}\right\rangle\right\rangle \sim \left\langle\left\langle\frac{g_x^2}{m_x}\right\rangle\right\rangle \left\langle\left\langle\frac{g_y^2}{m_y}\right\rangle\right\rangle. \quad (4.93)$$

More precisely, we take

$$\left\langle\left\langle\frac{g_{xy}^2}{m_x m_y}\right\rangle\right\rangle = \Gamma_{xy} \frac{4\mu_x^2 \Omega^2}{\mu_x^2 + \Omega^2} \frac{4\mu_y^2 \Omega^2}{\mu_y^2 + \Omega^2}. \quad (4.94)$$

As we will show later, this distribution function is sufficient to give a fast decay of correlator at timescales larger than  $\Omega^{-1}$ . In the large temperature limit i.e.  $\beta \rightarrow 0$ , this distribution function gives the following form of  $\rho[12]$  upto  $O(\beta^0)$  :

$$\rho[12] = 2m_p \left[ \frac{1}{2} \Gamma_{xy} \Omega v_{th}^2 \frac{4\Omega^2}{\omega_1^2 + 4\Omega^2} + (\gamma_x + \gamma_y) \frac{\Omega^2}{\omega_1^2 + \Omega^2} \right] \omega_1 (2\pi) \delta(\omega_1 + \omega_2). \quad (4.95)$$

Thus, the damping constant acquires a correction of the order  $\Gamma_{xy} \Omega v_{th}^2$ . This is a small correction provided we have

$$\Gamma_{xy} \ll \frac{\gamma}{\Omega v_{th}^2} = \frac{m_p \gamma}{\Omega k_B T},$$

a condition we will assume from now on.

We can now turn to the three point spectral functions obtained by Fourier transforming the nested commutators of the bath operator  $O$  defined in Eq.(4.87). This yields

$$\begin{aligned} \rho[123] = & (2\pi) \delta(\omega_1 + \omega_2 + \omega_3) \int_0^\infty \frac{d\mu_x}{2\pi} \int_0^\infty \frac{d\mu_y}{2\pi} \left\langle\left\langle\frac{g_x g_y g_{xy}}{m_x m_y}\right\rangle\right\rangle \\ & \left\{ \text{sgn}(\omega_3) (2\pi) \delta(\omega_3^2 - \mu_x^2) \left[ \text{sgn}(\omega_2) (2\pi) \delta(\omega_2^2 - \mu_y^2) - \text{sgn}(\omega_1) (2\pi) \delta(\omega_1^2 - \mu_y^2) \right] \right. \\ & \left. + \text{sgn}(\omega_3) (2\pi) \delta(\omega_3^2 - \mu_y^2) \left[ \text{sgn}(\omega_2) (2\pi) \delta(\omega_2^2 - \mu_x^2) - \text{sgn}(\omega_1) (2\pi) \delta(\omega_1^2 - \mu_x^2) \right] \right\}. \end{aligned} \quad (4.96)$$

and

$$\begin{aligned} \rho[321] = & (2\pi)\delta(\omega_1 + \omega_2 + \omega_3) \int_0^\infty \frac{d\mu_x}{2\pi} \int_0^\infty \frac{d\mu_y}{2\pi} \left\langle \left\langle \frac{g_x g_y g_{xy}}{m_x m_y} \right\rangle \right\rangle \\ & \left\{ \text{sgn}(\omega_1)(2\pi)\delta(\omega_1^2 - \mu_x^2) \left[ \text{sgn}(\omega_2)(2\pi)\delta(\omega_2^2 - \mu_y^2) - \text{sgn}(\omega_3)(2\pi)\delta(\omega_3^2 - \mu_y^2) \right] \right. \\ & \left. + \text{sgn}(\omega_1)(2\pi)\delta(\omega_1^2 - \mu_y^2) \left[ \text{sgn}(\omega_2)(2\pi)\delta(\omega_2^2 - \mu_x^2) - \text{sgn}(\omega_3)(2\pi)\delta(\omega_3^2 - \mu_x^2) \right] \right\}, \end{aligned} \quad (4.97)$$

where we have defined the distribution function

$$\left\langle \left\langle \frac{g_x g_y g_{xy}}{m_x m_y} \right\rangle \right\rangle \equiv \sum_{ij} \frac{g_{x,i} g_{y,j} g_{xy,ij}}{m_{x,i} m_{y,j}} 2\pi\delta(\mu_x - \mu_i) 2\pi\delta(\mu_y - \mu_j). \quad (4.98)$$

We will find it convenient to assume

$$\left| \left\langle \left\langle \frac{g_x g_y g_{xy}}{m_x m_y} \right\rangle \right\rangle \right|^2 \sim \left\langle \left\langle \frac{g_{xy}^2}{m_x m_y} \right\rangle \right\rangle \left\langle \left\langle \frac{g_x^2}{m_x} \right\rangle \right\rangle \left\langle \left\langle \frac{g_y^2}{m_y} \right\rangle \right\rangle. \quad (4.99)$$

More precisely, we take

$$\left\langle \left\langle \frac{g_x g_y g_{xy}}{m_x m_y} \right\rangle \right\rangle = \frac{m_p}{4} \Gamma_3 \frac{4\mu_x^2 \Omega^2}{\mu_x^2 + \Omega^2} \frac{4\mu_y^2 \Omega^2}{\mu_y^2 + \Omega^2}. \quad (4.100)$$

Here, the parameter  $\Gamma_3$  can roughly be thought of as an inverse penetration depth for the three body scattering. This induces a small correction to the usual Langevin dynamics if

$$\Gamma_3 \ll \frac{\gamma}{v_{th}} = \frac{m_p \gamma}{k_B T},$$

a condition we will assume from now on. In the next subsection, we will examine the correlation functions of the bath and to what extent they justify a Markovian approximation.

#### 4.4.2 KMS relations and decay of bath correlations

Consider the model described in the above section of a single oscillator coupled to two harmonic baths. In this subsection, we will be interested in the evolution starting from an initial time  $t_0$  and whether and how the bath correlators decay with time.

We will assume that the bath and the oscillator are unentangled at an initial time  $t_0$ . There-

fore, the initial density matrix of the oscillator and the bath is given by

$$\rho(t_0) = \frac{e^{-\frac{H_B}{k_B T}}}{Z_B} \otimes \rho_p, \quad (4.101)$$

where  $H_B$  is the Hamiltonian of the bath,  $Z_B$  is its partition function, and  $\rho_p$  is the initial density matrix of the oscillator at time  $t_0$ .

The effective theory of the Brownian particle is obtained after integrating out the degrees of freedom of the thermal bath. In the process, the bath correlation functions (in general out-of-time-order) imprint themselves on the effective couplings of the Brownian particle. In this section we are interested in studying the out-of-time-order bath correlators of the operator  $\mathcal{O}$ . We will use these correlators later to determine the effective couplings of the particle.

Since the bath is in a thermal state, not all the Wightman correlators of  $\mathcal{O}$  are independent. The bath correlators that are related to each other by cyclic permutations of insertions, satisfy the KMS (Kubo-Martin-Schwinger) conditions [41, 42, 54, 64, 69, 92, 95, 96, 98, 141, 142]. For a thermal  $n$ -point function of  $\mathcal{O}(t)$ , the KMS condition in time domain gives the following condition on the connected parts (cumulants) of the bath correlators :

$$\langle \mathcal{O}(t_1)\mathcal{O}(t_2)\dots\mathcal{O}(t_n) \rangle_c = \langle \mathcal{O}(t_n - i\beta)\mathcal{O}(t_1)\mathcal{O}(t_2)\dots\mathcal{O}(t_{n-1}) \rangle_c. \quad (4.102)$$

In frequency space the KMS condition simplifies to

$$\langle \mathcal{O}(\omega_1)\mathcal{O}(\omega_2)\dots\mathcal{O}(\omega_n) \rangle_c = e^{-\beta\omega_n} \langle \mathcal{O}(\omega_n)\mathcal{O}(\omega_1)\dots\mathcal{O}(\omega_{n-1}) \rangle_c. \quad (4.103)$$

This follows straightforwardly from the fact that the frequency domain analogue of  $\mathcal{O}(t_n - i\beta)$  is  $e^{-\beta\omega_n}\mathcal{O}(\omega_n)$ .

At the level of the two point function, the statement implies that there is only one independent two-point correlator of  $\mathcal{O}$ . We choose that to be  $\rho[12]$ . Then, using the KMS relations, the expectation value of the anticommutator is given by

$$\rho[12_+] = -\hbar(1 + 2\mathfrak{f}_2)\rho[12], \quad (4.104)$$

where  $\mathfrak{f}_1 = \frac{1}{e^{\beta\omega_1} - 1}$  and  $\mathfrak{f}_2 = \frac{1}{e^{\beta\omega_2} - 1}$  are the Bose-Einstein distribution functions.

Similarly all the three point functions of  $\mathcal{O}$  are determined by  $\rho[123]$  and  $\rho[321]$ . The other

3-point correlators are related to the two by the following KMS relations [64]

$$\begin{aligned}
\rho[123_+] &= -\hbar(1 + 2\tilde{f}_3)\rho[123] , \\
\rho[321_+] &= -\hbar(1 + 2\tilde{f}_1)\rho[321] , \\
\rho[12_+3] &= -\hbar(1 + 2\tilde{f}_2)\rho[123] + 2(1 + \tilde{f}_1 + \tilde{f}_2)\rho[321] , \\
\rho[12_+3_+] &= \hbar^2(1 + 2\tilde{f}_3)\left[(1 + 2\tilde{f}_2)\rho[123] - 2(1 + \tilde{f}_1 + \tilde{f}_2)\rho[321]\right].
\end{aligned}
\tag{4.105}$$

Hence the spectral functions  $\rho[12]$ ,  $\rho[123]$  and  $\rho[321]$  are sufficient to determine all two-point and three-point bath correlators.

For the two-point function, the correlator of the anticommutator in equation (4.104) provides a measure of the thermal noise arising from the thermal fluctuations in the bath whereas the correlation function of the commutator in that equation gives a measure of the dissipation/damping in the bath due to the motion of the Brownian particle [37]. We denote the connected part of nested commutators of operators in time domain by a tilde in the following <sup>14</sup>:

$$\langle [\widetilde{123}] \rangle \equiv \langle [[O(t_1), O(t_2)], O(t_3)] \rangle_c .
\tag{4.106}$$

For the cumulants of the nested anticommutators we use a similar notation with an extra ‘+’ sign inside the square bracket indicating the position of the anticommutator as follows

$$\begin{aligned}
\langle [\widetilde{12_+3}] \rangle &\equiv \langle [\{O(t_1), O(t_2)\}, O(t_3)] \rangle_c , \\
\langle [\widetilde{321_+}] \rangle &\equiv \langle [\{O(t_3), O(t_2)\}, O(t_1)] \rangle_c .
\end{aligned}
\tag{4.107}$$

We can use the forms of the spectral functions to get the bath correlators in time domain. The bath correlators decay with increase in separation between any two insertions. In the following, we provide the two-point and three-point cumulants for the slowest decaying modes with frequency  $\Omega$ .

---

<sup>14</sup>Here, we put a tilde on the bath’s cumulants just to distinguish it from those in chapter 2 as we have absorbed the weak particle-bath coupling strength while defining the operator  $O$  in this chapter.



For our model, the two point cumulants decay as

$$\begin{aligned}\frac{i}{\hbar}\langle[\widetilde{12}]_+\rangle &= \Omega^2\left[m_p(\gamma_x + \gamma_y)\exp(-\Omega t_{12}) + \hbar\Gamma_{xy}\Omega^2\exp(-2\Omega t_{12})\cot\left(\frac{\beta\Omega}{2}\right)\right], \\ \langle[\widetilde{12}_+]_+\rangle &= \frac{\Omega^2}{2}\left[(\gamma_x + \gamma_y)\hbar\csc\left(\frac{\beta\Omega}{2}\right)\exp(-\Omega t_{12}) + \hbar^2\Gamma_{xy}\Omega^2\left(\cot^2\left(\frac{\beta\Omega}{2}\right) - 1\right)\exp(-2\Omega t_{12})\right].\end{aligned}\quad (4.108)$$

In the high temperature limit, this yields

$$\begin{aligned}\frac{i}{\hbar}\langle[\widetilde{12}]_+\rangle &= m_p\Omega^2\left[(\gamma_x + \gamma_y)\exp(-\Omega t_{12}) + 2\Gamma_{xy}\Omega v_{th}^2\exp(-2\Omega t_{12})\right], \\ \langle[\widetilde{12}_+]_+\rangle &= m_p^2v_{th}^2\Omega\left[(\gamma_x + \gamma_y)\exp(-\Omega t_{12}) + 2\Gamma_{xy}\Omega v_{th}^2\exp(-2\Omega t_{12})\right].\end{aligned}\quad (4.109)$$

The three point nested cumulants are given by

$$\begin{aligned}\frac{i^2}{\hbar^2}\langle[\widetilde{321}]_+\rangle &= m_p\frac{\Gamma_3\Omega^4}{2}\exp(-\Omega t_{13})\left(1 + \exp(-\Omega t_{23})\right), \\ \frac{i^2}{\hbar^2}\langle[\widetilde{123}]_+\rangle &= m_p\frac{\Gamma_3\Omega^4}{2}\exp(-\Omega t_{13})\left(1 + \exp(-\Omega t_{12})\right).\end{aligned}\quad (4.110)$$

The other cumulants can also be computed to yield

$$\begin{aligned}\frac{i}{\hbar}\langle[\widetilde{321}_+]_+\rangle &= -m_p\Gamma_3\Omega^4\frac{\hbar}{2}\cot\left(\frac{\beta\Omega}{2}\right)\exp(-\Omega t_{13})\left(1 + \exp(-\Omega t_{23})\right), \\ \frac{i}{\hbar}\langle[\widetilde{123}_+]_+\rangle &= m_p\Gamma_3\Omega^4\frac{\hbar}{2}\cot\left(\frac{\beta\Omega}{2}\right)\exp(-\Omega t_{13})\left(1 + \exp(-\Omega t_{13})\right), \\ \frac{i}{\hbar}\langle[\widetilde{12}_+3]_+\rangle &= m_p\Gamma_3\Omega^4\frac{\hbar}{2}\cot\left(\frac{\beta\Omega}{2}\right)\exp(-\Omega t_{13})\left(1 + 2\exp(-\Omega t_{23}) + \exp(-\Omega t_{12})\right)\end{aligned}\quad (4.111)$$

and

$$\langle[\widetilde{12}_+3_+]_+\rangle = \hbar^2m_p\frac{\Gamma_3\Omega^4}{2}\exp(-\Omega t_{13})\left[\cot^2\left(\frac{\beta\Omega}{2}\right)\{1 + \exp(-\Omega t_{12}) + \exp(-\Omega t_{23})\} - \exp(-\Omega t_{23})\right].\quad (4.112)$$

In the high temperature limit, this yields

$$\begin{aligned}\frac{i}{\hbar}\langle[\widetilde{321}_+]_+\rangle &= -\Gamma_3m_p^2v_{th}^2\Omega^3\exp(-\Omega t_{13})\left(1 + \exp(-\Omega t_{23})\right), \\ \frac{i}{\hbar}\langle[\widetilde{123}_+]_+\rangle &= \Gamma_3m_p^2v_{th}^2\Omega^3\exp(-\Omega t_{13})\left(1 + \exp(-\Omega t_{13})\right), \\ \frac{i}{\hbar}\langle[\widetilde{12}_+3]_+\rangle &= \Gamma_3m_p^2v_{th}^2\Omega^3\exp(-\Omega t_{13})\left(1 + 2\exp(-\Omega t_{23}) + \exp(-\Omega t_{12})\right)\end{aligned}\quad (4.113)$$

and

$$\langle [\widetilde{12_+3_+}] \rangle = 2\Gamma_3 m_p^3 v_{th}^4 \Omega^4 \exp(-\Omega t_{13}) (1 + \exp(-\Omega t_{12}) + \exp(-\Omega t_{23})) . \quad (4.114)$$

Thus, given the decay of the memory in the bath at time-scales much larger than  $(\frac{1}{\Omega})$  we expect to obtain a local effective theory for the particle at long time-scales. In the next section, we will describe how such an effective theory can be obtained starting from the microscopic description.

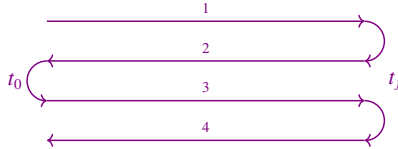
## 4.5 Effective theory of the Brownian particle

### 4.5.1 OTO Influence Phase

We will begin by describing the procedure we employ to derive the effective theory for the particle at long time-scales, closely following the discussion in chapter 2. Our aim is to obtain the couplings in the effective action of the Brownian particle (after systematically integrating out the degrees of freedom of the bath) in a way that keeps track of out-of-time order correlations. Thus, we are interested in an effective theory which has sufficient number of effective couplings that can compute along with the time-ordered correlators, also the out-of-time order correlators (OTOCs) of the particle.

We use the generalised Schwinger-Keldysh path integral formalism to arrive at an effective action/generalised influence phase for the Brownian particle. The path integral representation of 2-OTO correlators (correlators with two insertions whose immediate neighbours lie to their pasts)<sup>15</sup> is then defined on a contour with two time-folds as shown in figure 4.1. There are four

Figure 4.1: A contour with 2 time-folds



copies of the degrees of freedom of the particle and bath  $\{q_1, X_{i1}, Y_{j1}\}, \{q_2, X_{i2}, Y_{j2}\}, \{q_3, X_{i3}, Y_{j3}\}$  and  $\{q_4, X_{i4}, Y_{j4}\}$  living on the four legs of the contour. The action that enters in the path integral

<sup>15</sup>E.g. for  $t_1 > t_2 > t_3 > t_0$ ,  $\langle \mathcal{O}(t_1)\mathcal{O}(t_3)\mathcal{O}(t_2) \rangle = Tr(\rho(t_0)\mathcal{O}(t_1)\mathcal{O}(t_3)\mathcal{O}(t_2))$  has  $\mathcal{O}(t_1)$  and  $\mathcal{O}(t_2)$  whose immediate neighbours lie to their pasts. Hence this is an example of a 2-OTO correlator.

is

$$S_{\text{GSK}} = \int_{t_0}^{t_f} dt \{L[q_1, X_{i_1}, Y_{j_1}] - L[-q_2, X_{i_2}, Y_{j_2}] + L[q_3, X_{i_3}, Y_{j_3}] - L[-q_4, X_{i_4}, Y_{j_4}]\}. \quad (4.115)$$

The degrees of freedom of the particle are identified at the turning points of the contour while performing the path integral. After integrating out the degrees of freedom of the bath, one obtains an out-of-time-order generalised influence phase  $W_{\text{GSK}}$  for the particle which can be expanded in powers of the particle-bath coupling:

$$W_{\text{GSK}} = W_{\text{GSK}}^{(1)} + W_{\text{GSK}}^{(2)} + W_{\text{GSK}}^{(3)} + \dots \quad (4.116)$$

The  $n$ -th term in this perturbative expansion is given by

$$W_{\text{GSK}}^{(n)} = \frac{i^{n-1}}{\hbar^{n-1}} \int_{t_0}^{t_f} dt_1 \cdots \int_{t_0}^{t_{n-1}} dt_n \sum_{i_1, \dots, i_n=1}^4 \langle \mathcal{T}_C O_{i_1}(t_1) \cdots O_{i_n}(t_n) \rangle_c q_{i_1}(t_1) \cdots q_{i_n}(t_n) \quad (4.117)$$

Here the subscripts denote the contour legs and the expectation values are contour ordered cumulants computed in the initial state of the bath.

## 4.5.2 Markovian approximation and effective action

The correlators of the Brownian particle calculated from the generalised influence phase can be obtained from a 1-PI effective action. The 1-PI effective action is generally non-unitary and non-local. However since in our model the cumulants of  $O(t)$  decay sufficiently fast, with an increase in separation between the insertions compared to the natural time scale of the particle, we can work in a Markovian limit [49]. In this limit we get a local, non-unitary 1-PI effective action. In chapter 2 we discussed the form of this OTO effective action. We restate the Lagrangian corresponding to this effective action below for the convenience of the reader.

$$L_{1\text{-PI}} = L_{1\text{-PI}}^{(1)} + L_{1\text{-PI}}^{(2)} + L_{1\text{-PI}}^{(3)} + \dots \quad (4.118)$$

where the  $L_{1\text{PI}}^{(1)}$ ,  $L_{1\text{PI}}^{(2)}$  and  $L_{1\text{PI}}^{(3)}$  correspond to terms that are linear, quadratic and cubic in  $q$ 's respectively. The linear term is given by

$$L_{1\text{-PI}}^{(1)} = \widehat{F}(q_1 + q_2 + q_3 + q_4), \quad (4.119)$$

The quadratic term is given by

$$\begin{aligned}
L_{1\text{-PI}}^{(2)} &= \frac{1}{2}Z(\dot{q}_1^2 + \dot{q}_3^2) - \frac{1}{2}Z^*(\dot{q}_2^2 + \dot{q}_4^2) + i Z_\Delta \sum_{i<j} \dot{q}_i \dot{q}_j \\
&\quad - \frac{m^2}{2}(q_1^2 + q_3^2) + \frac{(m^2)^*}{2}(q_2^2 + q_4^2) \\
&\quad - im_\Delta^2 \sum_{i<j} q_i q_j + \frac{\widehat{\gamma}}{2} \sum_{i<j} (q_i \dot{q}_j - \dot{q}_i q_j),
\end{aligned} \tag{4.120}$$

The cubic term  $L_{1\text{PI}}^{(3)}$  can be split into 2 parts: One part, which reduces to the cubic terms in the Schwinger-Keldysh effective theory under identification of the degrees of freedom on any two successive legs, is given by

$$\begin{aligned}
L_{1\text{-PI,SK}}^{(3)} &= -\frac{\lambda_3}{3!}(q_1^3 + q_3^3) - \frac{\lambda_3^*}{3!}(q_2^3 + q_4^3) \\
&\quad + \frac{\sigma_3}{2!} \left[ q_1^2(q_2 + q_3 + q_4) - q_2^2(q_3 + q_4) + q_3^2 q_4 \right] \\
&\quad + \frac{\sigma_3^*}{2!} \left[ q_1(q_2^2 - q_3^2 + q_4^2) - q_2(q_3^2 - q_4^2) + q_3 q_4^2 \right] \\
&\quad + \frac{\sigma_{3\gamma}}{2!} \left[ q_1^2(\dot{q}_2 + \dot{q}_3 + \dot{q}_4) - q_2^2(\dot{q}_3 + \dot{q}_4) + q_3^2 \dot{q}_4 - (q_2^2 \dot{q}_2 + q_4^2 \dot{q}_4) \right] \\
&\quad + \frac{\sigma_{3\gamma}^*}{2!} \left[ \dot{q}_1(q_2^2 - q_3^2 + q_4^2) - \dot{q}_2(q_3^2 - q_4^2) + \dot{q}_3 q_4^2 - (q_1^2 \dot{q}_1 + q_3^2 \dot{q}_3) \right].
\end{aligned} \tag{4.121}$$

The other part, which vanishes under such identifications, is given by

$$\begin{aligned}
L_{1\text{-PI,OTO}}^{(3)} &= -\left(\kappa_3 + \frac{1}{2}\text{Re}[\lambda_3 - \sigma_3]\right)(q_1 + q_2)(q_2 + q_3)(q_3 + q_4) \\
&\quad - (q_2 + q_3) \left[ (\kappa_{3\gamma} - \text{Re}[\sigma_{3\gamma}]) (\dot{q}_1 + \dot{q}_2)(q_3 + q_4) \right. \\
&\quad \quad \left. + (\kappa_{3\gamma}^* - \text{Re}[\sigma_{3\gamma}]) (q_1 + q_2)(\dot{q}_3 + \dot{q}_4) \right].
\end{aligned} \tag{4.122}$$

As we had discussed in section 2.3.2, this effective Lagrangian is the most general Lagrangian (upto single time derivatives on the  $q$ 's in the cubic terms) that is consistent with the unitarity of the (particle+bath) combined system.

### 4.5.3 Comparison with the Nonlinear Langevin system

We will now relate the description in terms of generalised influence phase and generalised Schwinger Keldysh effective action to the classical stochastic description in terms of nonlinear Langevin equation. This relation, familiar in the stochastic quantisation literature, can

be studied at various levels : we can for example, study the correlators predicted by the two descriptions and match them against each other. We will instead derive the dictionary between the quantum and stochastic descriptions by deriving a path integral which generates the non-linear Langevin correlators and then matching its terms against the influence phase obtained by ignoring out of time ordered contributions.

We are interested in the non-linear Langevin theory described by the stochastic equation :

$$\mathcal{E}[q] \equiv \frac{d^2 q}{dt^2} + (\gamma + \zeta_\gamma \mathcal{N}) \frac{dq}{dt} + (\bar{\mu}^2 + \zeta_\mu \mathcal{N}) q + \left( \bar{\lambda}_3 - \bar{\lambda}_{3\gamma} \frac{d}{dt} \right) \frac{q^2}{2!} - F = \langle f^2 \rangle \mathcal{N} . \quad (4.123)$$

Here, we will take  $\mathcal{N}$  to be a random noise drawn from the non-Gaussian probability distribution

$$P[\mathcal{N}] \propto \exp \left\{ -\frac{1}{2\langle f^2 \rangle} \int dt (\langle f^2 \rangle \mathcal{N} - \zeta_N \mathcal{N}^2)^2 - \frac{1}{2} Z_I \int dt \dot{\mathcal{N}}^2 \right\} . \quad (4.124)$$

We will assume that the corrections to the Langevin equation are small : this is equivalent to assuming the parameters  $\{\zeta_\gamma, \zeta_\mu, \bar{\lambda}_3, \bar{\lambda}_{3\gamma}, \zeta_N, Z_I\}$  are small.

The equation above is a non-linear stochastic ODE with *multiplicative noise*, i.e., the noise variable  $\mathcal{N}$  appears in the equation multiplied by the functions of the fundamental stochastic variable  $q$  of the differential equation. In the theory of stochastic ODEs, such ODEs need a definite prescription for equal time stochastic products to be well-defined. In this chapter, we will adopt a time-symmetric (or Stratonovich) prescription for equal time stochastic products. But we will only need leading order corrections due to the multiplicative noise terms, where the subtleties regarding various prescriptions for stochastic products will not matter.

To study this non-linear Langevin theory in the context of path integrals, one can employ the following method (often attributed to Martin-Siggia-Rose [61]-De Dominicis-Peliti [62]-Janssen [63]) : We start by thinking about the functional integral<sup>16</sup> over noise realisations along with the imposition of the non-linear Langevin equation on a variable  $q_a(t)$ :

$$\begin{aligned} & \int [dq_a][d\mathcal{N}] P[\mathcal{N}] \delta[\langle f^2 \rangle \mathcal{N} - \mathcal{E}[q_a]] \\ &= \int [dq_a][dq_d][d\mathcal{N}] P[\mathcal{N}] \exp \left\{ i \frac{m_p}{\hbar} \int dt q_d [\langle f^2 \rangle \mathcal{N} - \mathcal{E}[q_a]] \right\} , \end{aligned} \quad (4.125)$$

<sup>16</sup>In this integral, we ignore the Jacobian  $\det \left[ \frac{\delta \mathcal{E}[q(t)]}{\delta q(t')} \right]$  as it does not correct the coefficients of the terms obtained in (4.126) up to leading order in the particle-bath coupling.

where we have given the standard functional integral representation of the delta function. We can now discretise the noise integral, add appropriate counterterms and perform the path integral perturbatively in the small parameters  $\{\zeta_\gamma, \zeta_\mu, \bar{\lambda}_3, \bar{\lambda}_{3\gamma}, \zeta_N, Z_I\}$ . This exercise yields

$$\begin{aligned} & \lim_{\delta t \rightarrow 0} \int [d\mathcal{N}] e^{-i\frac{m_p}{\hbar} \frac{3\zeta_N}{\langle f^2 \rangle_{\delta t}} \int dt q_d} P[\mathcal{N}] \exp \left\{ i\frac{m_p}{\hbar} \int dt q_d [\langle f^2 \rangle \mathcal{N} - \mathcal{E}[q_a]] \right\} \\ & \approx \exp \left\{ \frac{i}{\hbar} \int dt \left[ \frac{i}{2} \frac{m_p^2}{\hbar} \langle f^2 \rangle q_d^2 - \frac{i}{2} \frac{m_p^2}{\hbar} Z_I q_d^2 - \frac{m_p^3}{\hbar^2} \zeta_N q_d^3 - m_p q_d \mathcal{E}[q_a]_{\mathcal{N}=0} - i\frac{m_p^2}{\hbar} q_d^2 \frac{\partial \mathcal{E}[q_a]}{\partial \mathcal{N}} \right] \right\}. \end{aligned} \quad (4.126)$$

This MSRDPJ effective action can be connected to Schwinger Keldysh effective action by identifying  $q_d = q_1 + q_2$ ,  $q_a = \frac{1}{2}(q_1 - q_2)$ . We will refer the reader to [55] for a textbook level discussion of why this is the correct identification that maps the Schwinger Keldysh boundary conditions on the quantum side to the causal boundary conditions of the stochastic path integral. Using this map, we can write the above effective action in the form :

$$\begin{aligned} L_{\text{IPI,SK}}^{(1)} &= \widehat{F}(q_1 + q_2), \\ L_{\text{IPI,SK}}^{(2)} &= \frac{1}{2} Z \dot{q}_1^2 - \frac{1}{2} Z^* \dot{q}_2^2 + i Z_\Delta \dot{q}_1 \dot{q}_2 - \frac{m^2}{2} q_1^2 + \frac{(m^2)^*}{2} q_2^2 - i m_\Delta^2 q_1 q_2 + \frac{\widehat{\gamma}}{2} (q_1 \dot{q}_2 - \dot{q}_1 q_2), \\ L_{\text{IPI,SK}}^{(3)} &= -\frac{\lambda_3}{3!} q_1^3 - \frac{\lambda_3^*}{3!} q_2^3 + \frac{\sigma_3}{2!} q_1^2 q_2 + \frac{\sigma_3^*}{2!} q_1 q_2^2 + \frac{\sigma_{3\gamma}}{2!} q_1^2 \dot{q}_2 + \frac{\sigma_{3\gamma}^*}{2!} \dot{q}_1 q_2^2, \end{aligned} \quad (4.127)$$

where the Schwinger Keldysh effective couplings are given in terms of Langevin couplings via

$$\begin{aligned} \widehat{F} &\equiv m_p F, & \widehat{\gamma} &\equiv m_p \gamma, \\ Z &\equiv m_p - i\frac{m_p^2}{\hbar} Z_I, & Z_\Delta &\equiv -\frac{m_p^2}{\hbar} Z_I, \\ m^2 &\equiv m_p \bar{\mu}^2 - i\frac{m_p^2}{\hbar} \langle f^2 \rangle, & m_\Delta^2 &\equiv -\frac{m_p^2}{\hbar} \langle f^2 \rangle, \\ \lambda_3 &\equiv \frac{3}{4} m_p \bar{\lambda}_3 + 6\frac{m_p^3}{\hbar^2} \zeta_N + 3i\frac{m_p^2}{\hbar} \zeta_\mu, \\ \sigma_3 &\equiv \frac{1}{4} m_p \bar{\lambda}_3 - 6\frac{m_p^3}{\hbar^2} \zeta_N - i\frac{m_p^2}{\hbar} \zeta_\mu, \\ \sigma_{3\gamma} &\equiv -\frac{1}{2} m_p \bar{\lambda}_{3\gamma} + 2i\frac{m_p^2}{\hbar} \zeta_\gamma. \end{aligned} \quad (4.128)$$

We recognise the above form as the most general cubic Schwinger Keldysh effective action which was discussed in chapter 2. In section 2.3.2, we showed that this SK effective action can be obtained from the OTO effective action given in the previous subsection by identifying

the degrees of freedom on any two successive legs on the double-folded contour. As will be described elsewhere [119], one can extend the nonlinear Langevin theory to an ‘out of time order’ stochastic theory which can capture all the couplings of the generalised Schwinger Keldysh effective action. For now, we will content ourselves with matching the out of time-ordered couplings by looking at the OTOCs of the system. This yields a map

$$\begin{aligned}\kappa_3 &\equiv -\frac{1}{2}m_p\bar{\kappa}_3, \\ \kappa_{3\gamma} &\equiv -\frac{1}{2}m_p\bar{\kappa}_{3\gamma} + \frac{2}{3}i\frac{m_p^2}{\hbar}\widehat{\kappa}_{3\gamma}.\end{aligned}\tag{4.129}$$

The couplings in the OTO effective theory, and hence the non-linear Langevin couplings are then determined by the bath correlators which enter into the generalised influence phase Eq.(4.116). Such relations between the couplings and the correlators can be obtained by computing the particle’s correlators with generalised influence phase given in Eq.(4.116) and then comparing them with the results obtained from the effective theory. The expressions of the influence phase couplings in terms of correlators in the time domain were given in chapter 2 and in frequency domain, they take the forms summarised earlier in section 4.3. In the following subsection, we will use the expressions quoted in section 4.3 to compute explicitly the effective couplings for the qXY model.

#### 4.5.4 Influence couplings in the qXY model

We will now describe the computation of non-linear Langevin couplings starting from the spectral functions of the qXY model. In our model, quadratic spectral function is given at high temperatures by the expression

$$\rho[12] = 2m_p\left[(\gamma_x + \gamma_y)\frac{\Omega^2}{\omega_1^2 + \Omega^2} + \frac{1}{2}\Gamma_{xy}\Omega v_{in}^2\frac{4\Omega^2}{\omega_1^2 + 4\Omega^2}\right]\omega_1(2\pi)\delta(\omega_1 + \omega_2).\tag{4.130}$$

This two point spectral function obeys the following integral identities

$$\begin{aligned}
\int_{C_2} \frac{\rho[12]}{\omega_1} &= m_p \Omega (\gamma_x + \gamma_y + \Gamma_{xy} \Omega v_{th}^2), \\
\int_{C_2} \frac{\rho[12]}{i\omega_1^2} &= m_p (\gamma_x + \gamma_y + \Gamma_{xy} \Omega v_{th}^2), \\
\int_{C_2} \frac{\rho[12]}{\omega_1^3} &= -\frac{m_p}{\Omega} (\gamma_x + \gamma_y + \frac{1}{4} \Gamma_{xy} \Omega v_{th}^2), \\
-\int_{C_2} \frac{\rho[12]}{i\omega_1^4} &= \frac{m_p}{\Omega^2} (\gamma_x + \gamma_y + \frac{1}{8} \Gamma_{xy} \Omega v_{th}^2),
\end{aligned} \tag{4.131}$$

which yield the following quadratic couplings at high temperature :

$$\begin{aligned}
\Delta m_p &\equiv m_p - m_{p0} = -\frac{m_p}{\Omega} \left( \gamma_x + \gamma_y + \frac{1}{4} \Gamma_{xy} \Omega v_{th}^2 \right), \\
Z_I &= \frac{v_{th}^2}{\Omega^2} \left( 2\gamma_x + 2\gamma_y + \frac{1}{4} \Gamma_{xy} \Omega v_{th}^2 \right), \\
\Delta \bar{\mu}^2 &\equiv \bar{\mu}^2 - \bar{\mu}_0^2 = -\Omega \left( \gamma_x + \gamma_y + \Gamma_{xy} \Omega v_{th}^2 \right), \\
\langle f^2 \rangle &= 2v_{th}^2 \left( \gamma_x + \gamma_y + \frac{1}{2} \Gamma_{xy} \Omega v_{th}^2 \right), \\
\gamma &= \gamma_x + \gamma_y + \frac{1}{2} \Gamma_{xy} \Omega v_{th}^2.
\end{aligned} \tag{4.132}$$

Similarly, the cubic spectral functions are given by

$$\begin{aligned}
\rho[123] &= 2\pi\delta(\omega_1 + \omega_2 + \omega_3) \times 2m_p \Gamma_3 (\omega_1^2 - \omega_2^2) \left( 1 - \frac{\omega_1 \omega_2}{\Omega^2} \right) \times \prod_{k=1}^3 \frac{\Omega^2}{\omega_k^2 + \Omega^2}, \\
\rho[321] &= 2\pi\delta(\omega_1 + \omega_2 + \omega_3) \times 2m_p \Gamma_3 (\omega_3^2 - \omega_2^2) \left( 1 - \frac{\omega_3 \omega_2}{\Omega^2} \right) \times \prod_{k=1}^3 \frac{\Omega^2}{\omega_k^2 + \Omega^2}.
\end{aligned} \tag{4.133}$$

These three point spectral functions obey the following integral identities at high temperature :

$$\int_{C_3} \frac{\rho[123]}{\omega_1 \omega_3} = \int_{C_3} \frac{\rho[321]}{\omega_1 \omega_3} = -\frac{3}{4} m_p \Gamma_3 \Omega^2, \tag{4.134}$$

$$\begin{aligned}
\frac{2}{3} \int_{C_3} \frac{\rho[123]}{i\omega_1 \omega_3^2} &= \frac{4}{5} \int_{C_3} \frac{\rho[321]}{i\omega_1 \omega_3^2} = -\frac{4}{5} \int_{C_3} \frac{\rho[123]}{i\omega_1^2 \omega_3} = -\frac{2}{3} \int_{C_3} \frac{\rho[321]}{i\omega_1^2 \omega_3} = \int_{C_3} \frac{\rho[132]}{i\omega_1 \omega_2 \omega_3} \\
&= -\frac{1}{4} \int_{C_3} \frac{1}{i\omega_2} \left\{ \frac{\rho[123]}{\omega_3^2} - \frac{\rho[321]}{\omega_1^2} \right\} = \frac{1}{2} m_p \Gamma_3 \Omega,
\end{aligned} \tag{4.135}$$



$$\frac{4}{3} \int_{C_3} \frac{1}{\omega_1^3 \omega_3} \rho[321] = \frac{4}{3} \int_{C_3} \frac{1}{\omega_1 \omega_3^3} \rho[123] = \int_{C_3} \frac{1}{\omega_1 \omega_2 \omega_3} \left\{ \frac{1}{\omega_1} \rho[321] + \frac{1}{\omega_3} \rho[123] \right\} = m_p \Gamma_3 , \quad (4.136)$$

which yields the following values for cubic couplings

$$\begin{aligned} \bar{\lambda}_3 &= \bar{\kappa}_3 = -\frac{3}{2} \Gamma_3 \Omega^2 , \\ \bar{\lambda}_{3\gamma} &= \bar{\kappa}_{3\gamma} = -2 \Gamma_3 \Omega , \quad \zeta_\mu = -2 \Gamma_3 \Omega v_{th}^2 , \\ \zeta_\gamma &= \frac{1}{2} \widehat{\kappa}_{3\gamma} = \frac{3}{2} \Gamma_3 v_{th}^2 , \quad \zeta_N = \Gamma_3 v_{th}^4 . \end{aligned} \quad (4.137)$$

We provide more details about these integrals and the poles which contribute via their residues in appendix B.2.

It is evident from the expressions above that many of the couplings in the effective theory are related to each other by a series of relations. As we will elaborate in the next section, quite a few of these relations can be explained on general grounds using the fact that the bath correlators exhibit microscopic time-reversal invariance and obey KMS conditions.

## 4.6 Relations between effective couplings

In this section we discuss the origin of the relations between the cubic effective couplings given in Eq.(4.137). As we show in the following two subsections, most of these relations are based on the following two general features of our model:

1. Microscopic time-reversal invariance in the bath,
2. KMS relations between bath correlators.

While discussing the consequences of these features, we will first give a general proof of the relations between the couplings, and then describe why our particular model satisfies the conditions that go into the proof. The arguments in the following two subsections will show that most of the relations between the effective couplings in our model are not just particular features of our model alone. Rather, they are generally valid for a broad class of systems, whenever the two conditions mentioned above are satisfied.

### 4.6.1 Consequences of time-reversal invariance

First, let us discuss the consequence of microscopic time-reversal invariance in the bath. As we mentioned in the introduction, the implications of such microscopic time-reversal invariance for systems with multiple degrees of freedom were analysed by Onsager in [38, 39] where he showed that the quadratic effective couplings such as  $\gamma_{AB}$  and  $\langle f_{AB}^2 \rangle$  are symmetric under the exchange of the indices. The derivation of such reciprocal relations relied on the operators  $\{O_A\}$  being invariant under time-reversal. These relations were later generalised by Casimir [40] to the case where the operators  $\{O_A\}$  have the parities  $\{\eta_A\}$  under time-reversal. The corresponding generalisation of the Onsager relations is as follows:

$$\begin{aligned}\gamma_{AB} &= \eta_A \eta_B \gamma_{BA}, \\ \langle f_{AB}^2 \rangle &= \eta_A \eta_B \langle f_{BA}^2 \rangle.\end{aligned}\tag{4.138}$$

Here, we generalise the Onsager-Casimir reciprocal relations to cubic couplings in the OTO effective theory. We find that microscopic time-reversal invariance in the bath leads to certain relations between the 2-OTO couplings and the 1-OTO couplings which are derived below. We would like to point out that, unlike the scenario considered by Onsager and Casimir, our system (the Brownian particle) has a single degree of freedom. Nevertheless, the relations that we obtain between the couplings are based on principles similar to those for the reciprocal relations.

To keep the discussion precise, let us note that the operator  $\mathcal{O}(t)$  is defined with respect to some particular reference point in time when it coincides with  $\mathcal{O}$  (the Schrodinger-picture operator). While calculating the contribution of the correlators of this operator to the particle's dynamics, this reference point must be the instant  $t_0$  at which the particle starts interacting with the bath. However, if the bath's initial state (described by the density matrix  $\rho_B$ ) is time-translation invariant i.e

$$[\rho_B, H_B] = 0,\tag{4.139}$$

then such correlators are independent of the choice of the reference point and depend only on the intervals between the insertions. This is true, for instance, in our model where the bath is assumed to be in a thermal state.

For such an initial state of the bath, one can shift the reference point to  $t = 0$  which can be chosen well into the domain of validity of the particle's effective theory. With respect to this

new reference point, the bath's correlators with insertions at both positive and negative values of time are relevant for the particle's dynamics. In the following discussion we are going to assume time-translation invariance of the initial state of the bath and choose the reference point for the operators to be at the origin of time  $t = 0$ .

Let us now assume that the bath's dynamics has time-reversal invariance and the initial state of the bath respects this symmetry. Then, there exists an anti-linear and anti-unitary time-reversal operator  $\mathbf{T}$  such that<sup>17</sup>

$$[\mathbf{T}, H_B] = 0, \quad \mathbf{T}\rho_B\mathbf{T}^\dagger = \rho_B. \quad (4.140)$$

At the level of correlators, this symmetry implies

$$\text{Tr}[\mathbf{T}\rho_B\mathbf{T}^\dagger\mathbf{T}\mathcal{O}(t_1)\mathbf{T}^\dagger \cdots \mathbf{T}\mathcal{O}(t_n)\mathbf{T}^\dagger] = \text{Tr}[\rho_B\mathcal{O}(t_1) \cdots \mathcal{O}(t_n)]^*. \quad (4.141)$$

Now, say the operator  $\mathcal{O}$  has a definite time parity i.e.,

$$\mathbf{T}\mathcal{O}\mathbf{T}^\dagger = \eta_o\mathcal{O}, \quad (4.142)$$

where  $\eta_o = \pm 1$ . The fact that  $\mathbf{T}$  is an anti-linear operator which commutes with  $H_B$ , implies

$$\mathbf{T}\mathcal{O}(t)\mathbf{T}^\dagger = \eta_o\mathcal{O}(-t). \quad (4.143)$$

Inserting this transformation of  $\mathcal{O}(t)$  into the equation (4.141) and imposing the time-reversal invariance of the initial state, we get

$$\langle \mathcal{O}(-t_1) \cdots \mathcal{O}(-t_n) \rangle = \eta_o^n \langle \mathcal{O}(t_1) \cdots \mathcal{O}(t_n) \rangle^*. \quad (4.144)$$

As the operator  $\mathcal{O}$  is Hermitian, the complex conjugation in the RHS of the above equation implies reversing the order of the insertions. So we have

$$\langle \mathcal{O}(-t_1) \cdots \mathcal{O}(-t_n) \rangle = \eta_o^n \langle \mathcal{O}(t_n) \cdots \mathcal{O}(t_1) \rangle. \quad (4.145)$$

Such relations, in general, imply that correlators with different OTO numbers (i.e., the num-

---

<sup>17</sup>See [89] for a proof of the existence of such an operator.

ber of minimum time-folds required to compute the correlators [34]) get related to each other. In case of 3-point functions, as was mentioned earlier, we have at most 2-OTO correlators. For three time instants  $t_1 > t_2 > t_3$ , the 2-OTO correlators are:

$$\langle \mathcal{O}(t_1)\mathcal{O}(t_3)\mathcal{O}(t_2) \rangle \text{ and } \langle \mathcal{O}(t_2)\mathcal{O}(t_3)\mathcal{O}(t_1) \rangle. \quad (4.146)$$

In both these correlators, we have 2 future turning point insertions:  $\mathcal{O}(t_1)$  and  $\mathcal{O}(t_2)$ , and hence they are 2-OTO correlators. From (4.145) we can see that these correlators are related to their time-reversed counterparts as follows:

$$\begin{aligned} \langle \mathcal{O}(t_1)\mathcal{O}(t_3)\mathcal{O}(t_2) \rangle &= \eta_o \langle \mathcal{O}(-t_2)\mathcal{O}(-t_3)\mathcal{O}(-t_1) \rangle, \\ \langle \mathcal{O}(t_2)\mathcal{O}(t_3)\mathcal{O}(t_1) \rangle &= \eta_o \langle \mathcal{O}(-t_1)\mathcal{O}(-t_3)\mathcal{O}(-t_2) \rangle. \end{aligned} \quad (4.147)$$

The correlators in the RHS of the above equations are 1-OTO correlators. So we see that all 2-OTO 3-point correlators of the bath get related to 1-OTO correlators.

It is natural to ask whether such relations between the bath's correlators lead to any relation between the 2-OTO couplings and the 1-OTO couplings in the effective theory of the particle. To answer this question, first notice that the relation (4.144) implies that, when all the frequencies are real, correlators of  $\mathcal{O}$  in frequency space are either purely real or purely imaginary i.e.

$$\langle \mathcal{O}(\omega_1) \cdots \mathcal{O}(\omega_n) \rangle = \eta_o^n \langle \mathcal{O}(\omega_1) \cdots \mathcal{O}(\omega_n) \rangle^*. \quad (4.148)$$

This reality property gets carried over to the connected parts i.e. the cumulants of these correlators. Equivalently, the spectral functions satisfy relations of the form

$$\rho[1 \dots n] = \eta_o^n \rho[1 \dots n]^*. \quad (4.149)$$

We use this property of the cumulants in frequency space to derive relations between the 2-OTO and 1-OTO couplings.

From the expressions of the cubic couplings, we see that the couplings can be divided into doublets and singlets as shown in the table 4.7 . We will show that the pair of couplings in each doublet are related to each other due to time-reversal invariance. On the other hand, time-reversal maps the singlets to themselves upto a factor of  $\eta_o$ . So when  $\eta_o = 1$ , these relations are trivial. But when  $\eta_o = -1$ , these relations imply that these singlets vanish.

Table 4.7: Coupling doublets/singlets under microscopic time-reversal (general environment)

$g$	$\mathcal{I}[g]$
$\bar{\lambda}_3$	$\frac{2}{m_p \omega_1 \omega_3} \rho[123]$
$\bar{\kappa}_3$	$\frac{2}{m_p \omega_1 \omega_3} \rho[321]$
$\bar{\lambda}_{3\gamma}$	$\frac{1}{im_p \omega_1 \omega_3} \left( \frac{2}{\omega_1} - \frac{1}{\omega_3} \right) \rho[123]$
$\bar{\kappa}_{3\gamma}$	$\frac{1}{im_p \omega_1 \omega_3} \left( \frac{1}{\omega_1} - \frac{2}{\omega_3} \right) \rho[321]$
$\zeta_\gamma$	$\frac{1}{(2m_p \omega_1 \omega_3)^2} \left( (2\omega_1 - \omega_3) \rho[321_+] + (\omega_3 - 2\omega_1) \rho[132_+] + (\omega_1 + \omega_3) \rho[123_+] \right)$
$\widehat{\kappa}_{3\gamma} - \zeta_\gamma$	$\frac{1}{(2m_p \omega_1 \omega_3)^2} \left( (\omega_1 + \omega_3) \rho[321_+] + (2\omega_3 - \omega_1) \rho[132_+] + (2\omega_3 - \omega_1) \rho[123_+] \right)$
$\widehat{\kappa}_{3\gamma}$	$\frac{3}{(2m_p \omega_1 \omega_3)^2} \left( \omega_1 \rho[321_+] + (\omega_3 - \omega_1) \rho[132_+] + \omega_3 \rho[123_+] \right)$
$\zeta_\mu$	$\frac{1}{2im_p^2 \omega_1 \omega_3} \left( \rho[123_+] - \rho[321_+] + \rho[132_+] \right)$
$2\zeta_N + \frac{\hbar^2}{8m_p^2} (\bar{\lambda}_3 - \bar{\kappa}_3)$	$\frac{1}{8m_p^3 \omega_1 \omega_3} \left( \rho[12_+3_+] + \rho[32_+1_+] \right)$

As the couplings mentioned in table 4.7 are all real, their complex conjugates are equal to them. This can be used to obtain alternative expressions for these couplings by complex conjugating the integrals. Such a complex conjugation in the frequency space maps the contour of integration from  $C_3$  :

$$\int_{C_3} \equiv \int_{-\infty - i\epsilon_1}^{\infty - i\epsilon_1} \frac{d\omega_1}{2\pi} \int_{-\infty + i\epsilon_1 - i\epsilon_3}^{\infty + i\epsilon_1 - i\epsilon_3} \frac{d\omega_2}{2\pi} \int_{-\infty + i\epsilon_3}^{\infty + i\epsilon_3} \frac{d\omega_3}{2\pi} \quad (4.150)$$

to  $C_3^*$  where the frequencies run over the following values:

$$\int_{C_3^*} \equiv \int_{-\infty + i\epsilon_1}^{\infty + i\epsilon_1} \frac{d\omega_1^c}{2\pi} \int_{-\infty - i\epsilon_1 + i\epsilon_3}^{\infty - i\epsilon_1 + i\epsilon_3} \frac{d\omega_2^c}{2\pi} \int_{-\infty - i\epsilon_3}^{\infty - i\epsilon_3} \frac{d\omega_3^c}{2\pi} . \quad (4.151)$$

Note that the integration over  $\omega_1^c$  in the  $C_3^*$  contour runs just above the real axis, exactly like the integration over  $\omega_3$  in the  $C_3$  contour. Similarly, integration over  $\omega_3^c$  in the  $C_3^*$  contour runs just below the real axis exactly like the integration over  $\omega_1$  in the  $C_3$  contour. Therefore, under the following redefinitions:

$$\omega_1 \equiv \omega_3^c, \quad \omega_2 \equiv \omega_2^c, \quad \omega_3 \equiv \omega_1^c, \quad (4.152)$$

the contour of integration gets mapped back to  $C_3$  with  $\epsilon_1$  and  $\epsilon_3$  exchanged (and the imaginary part of  $\omega_2$  reversed). This exchange of  $\epsilon_1$  and  $\epsilon_3$  and the concomitant reversal of the imaginary

part of  $\omega_2$  can be undone by a contour deformation, provided our integrands have no  $\omega_2$  discontinuities near real axis (as required for the validity of Markovian approximation). To conclude, assuming appropriate analyticity in  $\omega_2$ , the complex conjugation and the above redefinition leave  $C_3$  contour invariant.

Now, let us turn to how the integrands are modified under the above operation. Notice that each term in the integrand has the following form : it is a product of a rational function of the frequencies and the bath cumulants. The modification of the rational functions is simple : the rational functions are modified by complex conjugating them and then performing the above frequency redefinition. This has the effect of replacing any explicit  $i$  by  $(-i)$  and exchanging  $\omega_1$  and  $\omega_3$ .

Turning to the cumulants, time-reversal invariance implies that, when the frequencies are real, these cumulants are either purely real or purely imaginary depending on their time-reversal parity  $\eta_o$ . Thus, the cumulants can be complex-conjugated by conjugating the frequencies in the argument of the cumulants followed by a multiplication by  $\eta_o$ . The frequency redefinition above then results in the exchange of  $\omega_1$  and  $\omega_3$  in the arguments. To summarise, the modified integrands are obtained from the original ones by the following rules:

- Replace  $i$  by  $-i$  in the coefficients,
- Exchange  $\omega_1$  and  $\omega_3$  in the rational functions and the cumulants,
- Multiply by  $\eta_o$ .

After re-expressing the couplings in terms of these modified integrals over the same contour  $C_3$ , one can compare them with the expression given in table 4.7 and find the following relations :

$$\begin{aligned} \bar{\kappa}_3 &= \eta_o \bar{\lambda}_3, & \bar{\kappa}_{3\gamma} &= \eta_o \bar{\lambda}_{3\gamma}, & \widehat{\kappa}_{3\gamma} - \zeta_\gamma &= \eta_o \zeta_\gamma, & \zeta_\mu &= \eta_o \zeta_\mu, \\ 2\zeta_N + \frac{\hbar^2}{8m_p}(\bar{\lambda}_3 - \bar{\kappa}_3) &= \eta_o \left( 2\zeta_N + \frac{\hbar^2}{8m_p}(\bar{\lambda}_3 - \bar{\kappa}_3) \right). \end{aligned} \quad (4.153)$$

This, in turn, implies

$$\begin{aligned} \bar{\kappa}_3 &= \eta_o \bar{\lambda}_3, & \bar{\kappa}_{3\gamma} &= \eta_o \bar{\lambda}_{3\gamma}, & \widehat{\kappa}_{3\gamma} &= (1 + \eta_o)\zeta_\gamma, & \widehat{\kappa}_{3\gamma} &= \eta_o \widehat{\kappa}_{3\gamma}, \\ \zeta_\mu &= \eta_o \zeta_\mu, & 2(1 - \eta_o)\zeta_N &= (\eta_o - 1) \frac{\hbar^2}{8m_p}(\bar{\lambda}_3 - \bar{\kappa}_3). \end{aligned} \quad (4.154)$$

When the operator  $O$  is even under time-reversal i.e. when  $\eta_o = 1$ , the last two relations are trivial. The other relations reduce to

$$\bar{\kappa}_3 = \bar{\lambda}_3, \quad \bar{\kappa}_{3\gamma} = \bar{\lambda}_{3\gamma}, \quad \widehat{\kappa}_{3\gamma} = 2\zeta_\gamma. \quad (4.155)$$

On the other hand, when the operator  $O$  is odd under time-reversal i.e. when  $\eta_o = -1$ , then the relations in (4.153) reduce to

$$\bar{\kappa}_3 = -\bar{\lambda}_3, \quad \bar{\kappa}_{3\gamma} = -\bar{\lambda}_{3\gamma}, \quad \widehat{\kappa}_{3\gamma} = 0, \quad \zeta_\mu = 0, \quad \zeta_N = -\frac{\hbar^2}{16m_p}(\bar{\lambda}_3 - \bar{\kappa}_3). \quad (4.156)$$

## 4.6.2 Time-reversal invariance of the bath in qXY model

We found in the preceding discussion that the bath needs to satisfy the following conditions for the relations given in equation (4.155) to hold true:

1. Time-translation invariance of the initial state,
2. Time-reversal invariance in the dynamics,
3. Time-reversal invariance of the initial state,
4. Time-reversal invariance of the operator that couples to the particle.

Let us check whether these conditions are satisfied in our model one by one.

As we have already mentioned, the initial state of the bath is a thermal state and hence it is invariant under time-translations.

To see the time-reversal invariance in the bath's dynamics, first note that the bath consists of two sets of harmonic oscillators. We can denote the lowering and raising operators of these oscillators by  $a_i$  and  $a_i^\dagger$  for the X-type oscillators and by  $b_j$  and  $b_j^\dagger$  for the Y-type oscillators. Therefore, the Hamiltonian of the bath is given by

$$H_B = \sum_i \hbar\mu_{x,i} \left( a_i^\dagger a_i + \frac{1}{2} \right) + \sum_j \hbar\mu_{y,j} \left( b_j^\dagger b_j + \frac{1}{2} \right). \quad (4.157)$$

Now, the action of the time-reversal operator on the raising and lowering operators is as follows:

$$\begin{aligned} \mathbf{T}a_i\mathbf{T}^\dagger &= a_i, \quad \mathbf{T}b_j\mathbf{T}^\dagger = b_j, \\ \mathbf{T}a_i^\dagger\mathbf{T}^\dagger &= a_i^\dagger, \quad \mathbf{T}b_j^\dagger\mathbf{T}^\dagger = b_j^\dagger. \end{aligned} \quad (4.158)$$

Using these transformations of the raising and lowering operators under time-reversal and the form of  $H_B$  given in (4.157) we see that

$$\mathbf{T}H_B\mathbf{T}^\dagger = H_B \implies [\mathbf{T}, H_B] = 0, \quad (4.159)$$

which means that time-reversal is a symmetry of the dynamics.

Now, the initial state is a thermal state i.e.

$$\rho_B = \frac{1}{Z_B} e^{-\frac{H_B}{k_B T}}. \quad (4.160)$$

Therefore, the commutation of the time-reversal operator with the Hamiltonian also implies

$$\mathbf{T}\rho_B\mathbf{T}^\dagger = \rho_B \quad (4.161)$$

i.e. the initial state is invariant under time-reversal.

Finally, the operator that couples to the particle is

$$O = \sum_i g_{x,i} X_i + \sum_j g_{y,j} Y_j + \sum_{i,j} g_{xy,ij} X_i Y_j. \quad (4.162)$$

Here the positions of the oscillators are given by

$$\begin{aligned} X_i &= \sqrt{\frac{\hbar}{2m_{x,i}\mu_{x,i}}} (a_i + a_i^\dagger), \\ Y_j &= \sqrt{\frac{\hbar}{2m_{y,j}\mu_{y,j}}} (b_j + b_j^\dagger). \end{aligned} \quad (4.163)$$

Therefore, using the transformations in (4.158) we have

$$\begin{aligned} \mathbf{T}X_i\mathbf{T}^\dagger &= X_i, \\ \mathbf{T}Y_j\mathbf{T}^\dagger &= Y_j. \end{aligned} \quad (4.164)$$

This implies that the operator  $O$  is invariant under time-reversal i.e.

$$\mathbf{T}O\mathbf{T}^\dagger = O. \quad (4.165)$$

So, all the conditions necessary for the relations (4.155) between the effective couplings are



satisfied in our model.

**Example of a time-reversal odd operator coupling to the particle:** We can slightly modify the qXY model to introduce a piece in the operator  $\mathcal{O}$  that is odd under time-reversal. For this, consider the following particle-bath interaction:

$$L_{\text{int}} = \left( \sum_i g_{x,i} X_i + \sum_i g_{y,j} Y_j \right) q - \sum_i \tilde{g}_{xy,ij} X_i Y_j \dot{q}. \quad (4.166)$$

Integrating by parts, we see that the operator that couples to the particle's position is

$$\mathcal{O} = \sum_i g_{x,i} X_i + \sum_i g_{y,j} Y_j + \sum_i \tilde{g}_{xy,ij} \dot{X}_i Y_j + \sum_i \tilde{g}_{xy,ij} X_i \dot{Y}_j. \quad (4.167)$$

Here, the operators  $\dot{X}_i$  and  $\dot{Y}_j$  are odd under time-reversal i.e.

$$\mathbf{T} \dot{X}_i \mathbf{T}^\dagger = -\dot{X}_i, \quad \mathbf{T} \dot{Y}_j \mathbf{T}^\dagger = -\dot{Y}_j. \quad (4.168)$$

The thermal correlators of 3 point functions  $\mathcal{O}$  receive contributions only from terms of the form:

$$\begin{aligned} \langle \mathcal{O}(t_1) \mathcal{O}(t_2) \mathcal{O}(t_3) \rangle &= \sum_{i,j} g_{x,i} g_{y,j} \tilde{g}_{xy,ij} \langle X_i(t_1) Y_j(t_2) \dot{X}_i(t_3) Y_j(t_3) \rangle \\ &+ \sum_{i,j} g_{x,i} g_{y,j} \tilde{g}_{xy,ij} \langle X_i(t_1) Y_j(t_2) X_i(t_3) \dot{Y}_j(t_3) \rangle + \dots \end{aligned} \quad (4.169)$$

All such terms are correlators with 3 position operators (which are time-reversal even) and one velocity operator (which is time-reversal odd). Therefore, the overall correlator satisfies the following relation:

$$\langle \mathcal{O}(t_1) \mathcal{O}(t_2) \mathcal{O}(t_3) \rangle = - \langle \mathcal{O}(-t_3) \mathcal{O}(-t_2) \mathcal{O}(-t_1) \rangle. \quad (4.170)$$

This, in turn, means that the relations in equation (4.156) are satisfied in this model.

### 4.6.3 Consequence of KMS relations: Generalised Fluctuation-Dissipation Relations

We have already seen that, at the high temperature limit, the KMS relations between thermal 2-point functions of the operator  $\mathcal{O}$  leads to a relation between the damping coefficient  $\gamma$  of the particle and the strength of the additive noise  $\langle f^2 \rangle$  that it experiences:

$$\langle f^2 \rangle = 2\gamma v_{th}^2. \quad (4.171)$$

This is the fluctuation-dissipation relation that was originally discovered through the studies of Brownian motion by Einstein, Smoluchowski and Sutherland. An analogous relation in electrical circuits was discovered by Johnson [44] and was theoretically derived by Nyquist [45]. A general proof of such relations was worked out by Callen and Welton in [46] which was further generalised by Stratonovich [126].

All these fluctuation-dissipation relations are relations between what we now understand to be 1-OTO couplings and are rooted in the KMS relations between the 1-OTO correlators of the bath. However, in [64] it was pointed out that the KMS relations can also relate 2-OTO correlators to 1-OTO correlators. For example, consider the following 2-OTO correlator:

$$\langle \mathcal{O}(t_1)\mathcal{O}(t_3)\mathcal{O}(t_2) \rangle \quad (4.172)$$

where  $t_1 > t_2 > t_3$ . By KMS relations, this 2-OTO correlator is related via analytic continuation to a 1-OTO correlator as follows:

$$\langle \mathcal{O}(t_1)\mathcal{O}(t_3)\mathcal{O}(t_2) \rangle = \langle \mathcal{O}(t_2 - i\beta)\mathcal{O}(t_1)\mathcal{O}(t_3) \rangle. \quad (4.173)$$

It is natural to wonder what imprint do such relations have on the effective dynamics of the particle. Do they lead to generalisations of the relation in (4.171)? If so, then do such relations connect 2-OTO couplings with the 1-OTO ones?

In section 4.3, we indeed saw such a relation between the 2-OTO coupling  $\widehat{\kappa}_{3\gamma}$  and the 1-OTO coupling  $\zeta_N$  at high temperature:

$$\zeta_N + \frac{\hbar^2}{16m_p^2}(\bar{\lambda}_3 - \bar{\kappa}_3) = \frac{1}{3}\widehat{\kappa}_{3\gamma}v_{th}^2. \quad (4.174)$$

As we mentioned there, this followed from using the KMS relations between the 3-point thermal correlators of the bath to express the couplings in terms of the spectral functions  $\rho[123]$  and  $\rho[321]$ , and keeping only the leading order term in  $\beta$ -expansion. Thus, this relation can be considered to be a generalisation of the fluctuation-dissipation relation between the quadratic couplings in (4.171).

Microscopic time-reversal invariance with  $\eta_o = 1$  implies  $\bar{\lambda}_3 = \bar{\kappa}_3$  and  $\widehat{\kappa}_{3\gamma} = 2\zeta_\gamma$ . In this case, the above relation reduces to

$$\zeta_N = \frac{1}{3}\widehat{\kappa}_{3\gamma}v_{th}^2 = \frac{2}{3}\zeta_\gamma v_{th}^2. \quad (4.175)$$

This is hence a relation between the coefficient  $\zeta_N$  of the cubic non-gaussian term in the probability distribution of the noise and the jitter  $\zeta_\gamma$  in the damping coefficient of the particle.

On the other hand, if  $\eta_o = -1$ , then  $\widehat{\kappa}_{3\gamma} = 0$  along with

$$\zeta_N = -\frac{\hbar^2}{16m_p^2}(\bar{\lambda}_3 - \bar{\kappa}_3). \quad (4.176)$$

This implies that the relation in (4.174) is trivially satisfied.

Apart from these relations, we also see another analogous fluctuation-dissipation relation in our model which is given by

$$\zeta_\mu = v_{th}^2\bar{\kappa}_{3\gamma} = v_{th}^2\bar{\lambda}_{3\gamma}. \quad (4.177)$$

As we discussed in the last subsection, the relation between  $\bar{\kappa}_{3\gamma}$  and  $\bar{\lambda}_{3\gamma}$  in the second half of the above equation is a consequence of time-reversal invariance in the bath. This equation relates the cubic 1-derivative anharmonicity in the particle's motion to the jitter in its frequency.

As yet, we do not know how generic this relation is. However, we suspect that, with some assumptions about the properties of the spectral functions, a general relation of the following form can be proven:

$$\zeta_\mu = \frac{v_{th}^2}{2}(\bar{\kappa}_{3\gamma} + \bar{\lambda}_{3\gamma}). \quad (4.178)$$

Such a relation is consistent with time-reversal invariance, since for the operator  $\mathcal{O}$  having a definite parity  $\eta_o$ , the two sides of the above equation transform similarly under time-reversal (see the relations in (4.153)). When  $\eta_o = -1$  both sides of the equation are equal to zero

and hence the relation (4.178) is trivially true. Moreover, we find it to be satisfied in the qXY model. Hence, we expect it to be true for a broad class of models than the one studied in this work. It will be interesting to check this expectation and determine the exact conditions which are required for this relation to hold.

## 4.7 Conclusion and discussion

In this chapter, we have constructed an effective theory of a Brownian particle which goes beyond the standard Langevin dynamics. We remind the reader that the standard Langevin theory describes a Brownian particle subject to linear damping and a Gaussian thermal noise. The effective theory described in this chapter includes in addition anharmonic couplings  $\bar{\lambda}_3$  and  $\bar{\lambda}_{3\gamma}$  along with a thermal jitter  $\zeta_\mu$  in the frequency and a jitter  $\zeta_\gamma$  in the damping constant. Apart from these parameters and the usual Langevin couplings, this theory also contains a parameter  $\zeta_N$  which is the strength of the non-Gaussianity in the thermal noise experienced by the particle.

When out of time ordered correlations (or more specifically, 2-OTO correlators) transmitted from the bath are kept track of, one has to add three more OTO couplings  $\bar{\kappa}_3, \bar{\kappa}_{3\gamma}$  and  $\widehat{\kappa}_{3\gamma}$  which are related by time-reversal to the standard (1-OTO) couplings  $\bar{\lambda}_3, \bar{\lambda}_{3\gamma}$  and  $\zeta_\gamma$  respectively. To demonstrate how these couplings affect the dynamics of the particle, we have expressed the classical limits of the particle's correlators in terms of these couplings. We find that the OTO couplings show up in the out of time ordered nested Poisson brackets of the particle. To develop a stochastic dynamics which can correctly reproduce these OTO Poisson brackets, one needs to extend the nonlinear Langevin equation introduced in this chapter. Such an extension would require introducing additional noise fields which capture OTO fluctuations in the system. We hope that a better understanding of this generalised Langevin dynamics would emerge in the future.

In this chapter, we have also explored the constraints imposed by microscopic time-reversal invariance of the (particle+bath) combined system on the effective theory of the particle. Such an invariance of the overall dynamics of the combined system under time-reversal holds when the interaction term between the particle and the bath is even under this transformation. This fixes the OTO cubic effective couplings in terms of the parameters in the nonlinear Langevin theory via the relations

$$\bar{\kappa}_3 = \bar{\lambda}_3, \quad \bar{\kappa}_{3\gamma} = \bar{\lambda}_{3\gamma}, \quad \widehat{\kappa}_{3\gamma} = 2\zeta_\gamma.$$

These relations between the cubic couplings are the generalisations of the well known Onsager-Casimir reciprocal relations that originate from the microscopic time-reversal invariance of the combined system.

Since the bath is in a thermal state, the bath correlators satisfy the KMS relations. In the high temperature limit, these further give rise to a generalised fluctuation-dissipation relation between the 2-OTO cubic derivative coupling  $\widehat{\kappa}_{3\gamma}$  and the 1-OTO cubic non-derivative coupling  $\zeta_N$ . Combining time-reversal invariance and the generalised fluctuation-dissipation relation, the coefficient of the thermal jitter  $\zeta_\gamma$  in the damping term of the non-linear Langevin equation gets related to the coefficient of non-Gaussianity  $\zeta_N$  of thermal noise.

To provide a concrete model where these general results are justified, we have constructed an OTO-effective theory of a Brownian particle interacting with a dissipative thermal bath composed of two sets of harmonic oscillators. To this, we add a small 3-body interaction coupling the particle to two other oscillators, one from each set. For this model, we show that all the bath correlators decay exponentially at late times, leading to a local non-unitary effective theory for the particle.

Working out the effective couplings of the particle in this model, we find that the above mentioned relations between these couplings are indeed satisfied. Furthermore, in this model, we find another fluctuation-dissipation type relation between the strength ( $\zeta_\mu$ ) of the thermal jitter in the frequency and the coefficient ( $\bar{\lambda}_{3\gamma}$ ) of the anharmonic term with a single time derivative.

Our techniques can potentially be extended to the context of quantum optics [140, 143]. As a toy model one can consider an atom that is interacting electromagnetically with a gas of photons [144–147]. One can write down an effective theory for the atom and calculate its OTOCs. Such predictions for the behaviour of OTOCs may be verified with development in experimental techniques to measure them [4, 15, 17–19, 52]. Moreover, our prediction of a generalised fluctuation-dissipation relation between the thermal jitter in the damping and the non-gaussianity in the noise may be testable in such a setup.

Another possible extension is to 1-D spin chains in a thermal environment [148–150]. It will be interesting to explore the possibility of writing a similar effective theory of the chain (or a part of it) which would aid in studying the thermalisation of its OTOCs and comparing them with those of time-ordered correlators. Such comparisons may be useful in classifying systems according to the behaviour of their OTOCs.

In this work, we saw that the OTO couplings are not just a feature of the quantum me-

chanical theory of the particle, but they show up in out of time ordered Poisson brackets in the classical limit as well (Similar classical limits of OTOCs have been discussed in [151–154]). A stochastic interpretation of this classical OTO behaviour would be useful in understanding the significance of such OTOCs in the quantum mechanical framework (where OTO dynamics has been mostly studied up till now) as well as devising experiments to measure them. In this context, it will also be interesting to extend the idea of decoherence of quantum systems to their out of time ordered dynamics.

# Chapter 5

## Quartic OTO effective theory

This chapter is based on the paper [32] written by the author in collaboration with Bidisha Chakrabarty.

### Comment on the conventions followed in this chapter:

In this chapter we go back to the convention of setting  $\hbar = 1$ . In addition, we work with units where the particle's renormalised mass  $m_p = 1$ . We also restore the small parameter  $\lambda$  in this chapter to represent the strength of the particle-bath coupling.

### 5.1 Introduction

In this chapter, we extend the analysis of the OTO effective theory of the Brownian particle by including the quartic terms in the effective action. There are three reasons for developing this extension. We enumerate them below.

1. Such an extension lays the ground for a convenient framework to compute 4-point OTO correlators in open quantum systems. This may lead to further insight into the role played by these OTOCs in physical phenomena.
2. The quartic couplings in this extended OTO effective theory receive contributions from the 4-point thermal OTOCs of the bath. Such thermal OTOCs have been the focus of most recent studies on chaos in quantum systems [2, 5–8, 12, 85]. Including the contributions of these 4-point OTOCs in the effective theory of the particle opens the possibility of probing the chaotic behaviour of the bath via the quartic effective couplings [29] (see the discussion in section 5.5).

3. The relations between the quartic effective couplings and the 4-point OTOCs of the bath allow one to extend the analysis of the constraints imposed on the effective dynamics of the particle due to the bath's thermality and microscopic reversibility.

To present the construction of the effective theory with a concrete example, we choose to work with the qXY model that we discussed in chapter 4. We simplify this model a bit by switching off the Caldeira-Legget-like bilinear interactions. This leads to a symmetry in the particle's dynamics under

$$q \rightarrow -q, \tag{5.1}$$

which results in the vanishing of all the odd degree terms in the effective action.

For this simplified qXY model, we first develop the Schwinger-Keldysh effective theory of the particle up to quartic terms. Working in a Markovian limit, we determine the dependence of the quartic couplings on the 4-point Schwinger-Keldysh correlators of the bath. Then we show that this quartic effective theory is dual to a non-linear Langevin dynamics with a non-Gaussian noise distribution. This stochastic dynamics has a structure quite similar to the one discussed in the previous chapter for the cubic effective theory.

We then extend the analysis to the OTO dynamics of the particle by determining its effective action on a contour with two time-folds. The form of this effective action is constrained by the microscopic unitarity in the dynamics of the (particle+bath) combined system. We figure out all the additional OTO couplings consistent with these constraints, and then determine their dependence on the 4-point OTO correlators of the bath. As in case of the 3-point correlators, these 4-point functions of the bath satisfy certain relations imposed by microscopic time-reversal invariance and thermality. We show that these relations between the bath's correlators lead to some constraints on the particle's effective couplings. These constraints can be interpreted as OTO generalisations of the Onsager reciprocal relations [38, 39] and the fluctuation-dissipation relation [46, 47]. Combining these constraints, one can obtain a generalised fluctuation-dissipation relation between two quartic couplings in the Schwinger-Keldysh effective theory (or equivalently, the dual non-linear Langevin dynamics). Just as in case of the cubic effective theory, we find that this generalised fluctuation-dissipation relation connects the thermal jitter in the damping coefficient of the particle and the non-Gaussianity in the noise distribution.

## Organisation of the chapter



The structure of this chapter is as follows:

In section 5.2, we briefly describe the  $qXY$  model which serves as a concrete example in our analysis.

In section 5.3, we develop the quartic Schwinger-Keldysh effective action for the particle in a Markovian regime. We determine the relations between the effective couplings and the Schwinger-Keldysh correlators of the bath. We also demonstrate a duality between the quartic Schwinger-Keldysh effective theory and a stochastic dynamics governed by a non-linear Langevin equation.

In section 5.4, we extend the effective theory framework to include 4-point OTOCs. We determine all the additional quartic OTO couplings appearing in this extension. Exploring the constraints imposed on the OTO effective theory by the thermality of the bath and its microscopic reversibility, we derive the generalised Onsager relations as well as a generalised fluctuation-dissipation relation between the quartic effective couplings. By computing the effective couplings for the  $qXY$  model, we verify that all these relations are indeed satisfied.

In section 5.5, we conclude with some discussion on future directions.

In appendix C.1, we show how the cumulants of the bath's correlators decay when the interval between any two insertions is increased. In appendix C.2, we provide an argument for the validity of Markov approximation in a certain parameter regime. In appendix C.3, we express the quartic OTO couplings in terms of the 4-point OTO cumulants of the bath. In appendix C.4, we provide the forms of the high-temperature limit of all the quartic couplings in terms of the thermal spectral functions of the bath.

## 5.2 Description of the $qXY$ model

In this section, we describe the  $qXY$  model which will serve as a concrete example for developing the particle's effective dynamics in the rest of the chapter. This is a minor modification of the  $qXY$  model introduced in the previous chapter.

In this model, a Brownian particle interacts with a thermal bath (at the temperature  $\frac{1}{\beta}$ )<sup>1</sup> comprising of two sets of harmonic oscillators. We represent the positions of the oscillators in these two sets by  $X^{(i)}$  and  $Y^{(j)}$ , and the position of the Brownian particle by  $q$ . The particle and the bath couple via cubic interactions involving two of the bath oscillators, one taken from each

---

<sup>1</sup>Here we are working in units where the Boltzmann constant  $k_B = 1$ .

set. These cubic interactions are switched on at an instant  $t_0$  before which the particle and the bath are unentangled. After the particle starts interacting with the bath, the Lagrangian of the (particle+bath) combined system is given by

$$L[q, X, Y] = \frac{m_{p0}}{2}(\dot{q}^2 - \bar{\mu}_0^2 q^2) + \sum_i \frac{m_{x,i}}{2}(\dot{X}^{(i)2} - \mu_{x,i}^2 X^{(i)2}) + \sum_j \frac{m_{y,j}}{2}(\dot{Y}^{(j)2} - \mu_{y,j}^2 Y^{(j)2}) + \lambda \sum_{i,j} g_{xy,ij} X^{(i)} Y^{(j)} q. \quad (5.2)$$

The bath operator that couples to the particle is

$$\lambda O \equiv \lambda \sum_{i,j} g_{xy,ij} X^{(i)} Y^{(j)}. \quad (5.3)$$

Notice that all odd point correlators of this operator vanish in the thermal state. We will see later that this leads to the vanishing of all odd degree terms in the effective action of the particle. Among the remaining terms, we would like to restrict our attention to only the quadratic and the quartic ones in this chapter. We will see that the couplings corresponding to these terms receive contributions from the connected parts of the 2-point and 4-point correlators of  $O$  at leading order in  $\lambda$ . So, we need to compute these correlators to obtain the leading order forms of the quadratic and the quartic couplings of the particle.

While computing the correlators, we assume that there is a large number of oscillators in the bath, and the frequencies of these oscillators are densely distributed. In such a situation, one can go to the continuum limit of this distribution, and replace the sum over the frequencies by integrals in the following way:

$$\sum_{i,j} \frac{g_{xy,ij}^2}{m_{x,i} m_{y,j}} \rightarrow \int_0^\infty \frac{d\mu_x}{2\pi} \int_0^\infty \frac{d\mu_y}{2\pi} \left\langle \left\langle \frac{g_{xy}^2(\mu_x, \mu_y)}{m_x m_y} \right\rangle \right\rangle, \quad (5.4)$$

$$\begin{aligned} & \sum_{i_1, j_1} \sum_{i_2, j_2} \frac{g_{xy, i_1 j_1} g_{xy, i_2 j_2} g_{xy, i_2 j_1} g_{xy, i_1 j_2}}{m_{x, i_1} m_{y, j_1} m_{x, i_2} m_{y, j_2}} \\ & \rightarrow \int_0^\infty \frac{d\mu_x}{2\pi} \int_0^\infty \frac{d\mu_y}{2\pi} \int_0^\infty \frac{d\mu'_x}{2\pi} \int_0^\infty \frac{d\mu'_y}{2\pi} \left\langle \left\langle \frac{g_{xy}(\mu_x, \mu_y) g_{xy}(\mu_x, \mu'_y) g_{xy}(\mu'_x, \mu_y) g_{xy}(\mu'_x, \mu'_y)}{m_x m_y m'_x m'_y} \right\rangle \right\rangle, \end{aligned} \quad (5.5)$$

where

$$\left\langle \left\langle \frac{g_{xy}^2(\mu_x, \mu_y)}{m_x m_y} \right\rangle \right\rangle \equiv \sum_{i,j} \frac{g_{xy,ij}^2}{m_{x,i} m_{y,j}} [2\pi\delta(\mu_x - \mu_{x,i}) 2\pi\delta(\mu_y - \mu_{y,j})], \quad (5.6)$$

$$\begin{aligned}
& \left\langle \left\langle \frac{g_{xy}(\mu_x, \mu_y) g_{xy}(\mu_x, \mu'_y) g_{xy}(\mu'_x, \mu_y) g_{xy}(\mu'_x, \mu'_y)}{m_x m_y m'_x m'_y} \right\rangle \right\rangle \\
& \equiv \sum_{i_1, j_1} \sum_{i_2, j_2} \frac{g_{xy, i_1 j_1} g_{xy, i_1 j_2} g_{xy, i_2 j_1} g_{xy, i_2 j_2}}{m_{x, i_1} m_{y, j_1} m_{x, i_2} m_{y, j_2}} \left[ 2\pi\delta(\mu_x - \mu_{x, i_1}) 2\pi\delta(\mu_y - \mu_{y, j_1}) \right] \\
& \quad \left[ 2\pi\delta(\mu'_x - \mu_{x, i_2}) 2\pi\delta(\mu'_y - \mu_{y, j_2}) \right].
\end{aligned} \tag{5.7}$$

We choose the functions  $\left\langle \left\langle \frac{g_{xy}^2(\mu_x, \mu_y)}{m_x m_y} \right\rangle \right\rangle$  and  $\left\langle \left\langle \frac{g_{xy}(\mu_x, \mu_y) g_{xy}(\mu_x, \mu'_y) g_{xy}(\mu'_x, \mu_y) g_{xy}(\mu'_x, \mu'_y)}{m_x m_y m'_x m'_y} \right\rangle \right\rangle$  in a manner which would give us an approximately local effective dynamics of the particle. As we will see, such a local dynamics can be obtained if the time-scales involved in the evolution of the particle are much larger than the time-scale in which cumulants of the operator  $O(t)$  decay. Keeping this in mind, we choose the distribution of the couplings to satisfy

$$\lambda^2 \left\langle \left\langle \frac{g_{xy}^2(\mu_x, \mu_y)}{m_x m_y} \right\rangle \right\rangle = \Gamma_2 \frac{4\mu_x^2 \Omega^2}{\mu_x^2 + \Omega^2} \frac{4\mu_y^2 \Omega^2}{\mu_y^2 + \Omega^2}, \tag{5.8}$$

$$\begin{aligned}
& \lambda^4 \left\langle \left\langle \frac{g_{xy}(\mu_x, \mu_y) g_{xy}(\mu_x, \mu'_y) g_{xy}(\mu'_x, \mu_y) g_{xy}(\mu'_x, \mu'_y)}{m_x m_y m'_x m'_y} \right\rangle \right\rangle \\
& = \Gamma_4 \left( \frac{4\mu_x^2 \Omega^2}{\mu_x^2 + \Omega^2} \right) \left( \frac{4\mu_y^2 \Omega^2}{\mu_y^2 + \Omega^2} \right) \left( \frac{4\mu_x'^2 \Omega^2}{\mu_x'^2 + \Omega^2} \right) \left( \frac{4\mu_y'^2 \Omega^2}{\mu_y'^2 + \Omega^2} \right),
\end{aligned} \tag{5.9}$$

where  $\Omega$  is a UV regulator.

For this distribution of the couplings, we study the high temperature limit of the 2-point and 4-point cumulants of  $O(t)$  in appendix C.1. There, we show that when the time intervals between the insertions are increased, these cumulants decay exponentially at rates which are of the order of  $\Omega$ . If the natural frequency ( $\bar{\mu}_0$ ) of the particle and the frequency scales associated with the parameters  $\Gamma_2$  and  $\Gamma_4$  are taken to be much smaller than  $\Omega$ , then the bath correlators decay much faster than the rate at which the particle evolves. This ensures that the effect (via the bath) of some earlier state of the particle on its later dynamics is heavily suppressed. Consequently, we get an approximately local effective dynamics of the particle. We discuss this effective dynamics in the next section.

### 5.3 Schwinger-Keldysh effective theory of the oscillator

In this section, we develop the quartic Schwinger-Keldysh effective theory for the dynamics of the particle. We also demonstrate a duality between this effective theory and a classical stochastic theory governed by a non-linear Langevin equation akin to the introduced in the

previous chapter.

### 5.3.1 Influence phase of the particle

In chapter 2, we discussed how one can integrate out the bath's degrees of freedom in a Schwinger-Keldysh path integral to get an influence phase for the particle. Here, we give the form of this influence phase again for the convenience of the reader:

$$W_{\text{SK}} = \sum_{n=1}^{\infty} \lambda^n W_{\text{SK}}^{(n)}, \quad (5.10)$$

where

$$W_{\text{SK}}^{(n)} = i^{n-1} \sum_{i_1, \dots, i_n=1}^2 \int_{t_0}^{t_f} dt_1 \cdots \int_{t_0}^{t_{n-1}} dt_n \langle \mathcal{T}_C O_{i_1}(t_1) \cdots O_{i_n}(t_n) \rangle_c q_{i_1}(t_1) \cdots q_{i_n}(t_n). \quad (5.11)$$

We remind the reader that, for the  $qXY$  model, all thermal correlator of  $O(t)$  with odd number of insertions are zero. This in turn means that all the odd degree terms in the perturbative expansion of the influence phase vanish. Among the remaining terms, we restrict our attention to those whose coefficients are up to  $O(\lambda^4)$ . This leaves us with only the quadratic and quartic terms whose expressions are given below:

$$W_{\text{SK}}^{(2)} = i \sum_{i_1, i_2=1}^2 \int_{t_0}^{t_f} dt_1 \int_{t_0}^{t_1} dt_2 \langle \mathcal{T}_C O_{i_1}(t_1) O_{i_2}(t_2) \rangle_c q_{i_1}(t_1) q_{i_2}(t_2), \quad (5.12)$$

$$W_{\text{SK}}^{(4)} = -i \sum_{i_1, \dots, i_4=1}^2 \int_{t_0}^{t_f} dt_1 \int_{t_0}^{t_1} dt_2 \int_{t_0}^{t_2} dt_3 \int_{t_0}^{t_3} dt_4 \langle \mathcal{T}_C O_{i_1}(t_1) O_{i_2}(t_2) O_{i_3}(t_3) O_{i_4}(t_4) \rangle_c q_{i_1}(t_1) q_{i_2}(t_2) q_{i_3}(t_3) q_{i_4}(t_4). \quad (5.13)$$

These expressions of the terms in the influence phase show that they are generally nonlocal in time. We will now discuss a regime where one can get an approximately local form for these terms.

#### Markovian limit:

In appendix C.1, we have shown that, in the high temperature limit ( $\beta\Omega \ll 1$ ), the cumulants of the operator  $O(t)$  appearing in (5.12) and (5.13) decay exponentially when the separation between any two insertions is increased. We have also shown that the decay rates of

these cumulants are of the order of the cut-off frequency  $\Omega$ . Then the values of the coefficient functions multiplying the  $q$ 's at different times in (5.12) and (5.13) become negligible when the interval between any two instants is  $O(\Omega^{-1})$ .

We choose to work in a regime where this time-scale ( $\Omega^{-1}$ ) is much smaller than all the time-scales involved in the evolution of the particle. To ensure this, we take the parameters in the qXY model to satisfy the following conditions:<sup>2</sup>

$$\beta\Omega \ll 1, \bar{\mu}_0 \ll \Omega, \Gamma_2 \ll \beta(\beta\Omega), \Gamma_4 \ll (\Gamma_2)^2. \quad (5.14)$$

In this regime, the bath's cumulants die out too fast to transmit any significant effect of the history of the particle on its dynamics at a later instant. Consequently, one can get an approximately local form for the influence phase by Taylor-expanding the  $q$ 's at different instants around  $t_1$ :

$$\begin{aligned} W_{\text{SK}}^{(2)} \approx i \sum_{i_1, i_2=1}^2 \int_{t_0}^{t_f} dt_1 & \left[ \left\{ \int_{t_0}^{t_1} dt_2 \langle \mathcal{T}_C O_{i_1}(t_1) O_{i_2}(t_2) \rangle_c \right\} q_{i_1}(t_1) q_{i_2}(t_1 - \epsilon) \right. \\ & + \left\{ \int_{t_0}^{t_1} dt_2 \langle \mathcal{T}_C O_{i_1}(t_1) O_{i_2}(t_2) \rangle_c t_{21} \right\} q_{i_1}(t_1) \dot{q}_{i_2}(t_1 - \epsilon) \\ & \left. + \left\{ \int_{t_0}^{t_1} dt_2 \langle \mathcal{T}_C O_{i_1}(t_1) O_{i_2}(t_2) \rangle_c \frac{t_{21}^2}{2} \right\} q_{i_1}(t_1) \ddot{q}_{i_2}(t_1 - \epsilon) \right], \end{aligned} \quad (5.15)$$

---

<sup>2</sup>In appendix C.2, we provide an argument for the validity of Markov approximation in this regime.

$$\begin{aligned}
W_{\text{SK}}^{(4)} \approx & -i \sum_{i_1, \dots, i_4=1}^2 \int_{t_0}^{t_f} dt_1 \left[ \left\{ \int_{t_0}^{t_1} dt_2 \int_{t_0}^{t_2} dt_3 \int_{t_0}^{t_3} dt_4 \langle \mathcal{T}_C O_{i_1}(t_1) O_{i_2}(t_2) O_{i_3}(t_3) O_{i_4}(t_4) \rangle_c \right\} \right. \\
& q_{i_1}(t_1) q_{i_2}(t_1 - \epsilon) q_{i_3}(t_1 - 2\epsilon) q_{i_4}(t_1 - 3\epsilon) \\
& + \left\{ \int_{t_0}^{t_1} dt_2 \int_{t_0}^{t_2} dt_3 \int_{t_0}^{t_3} dt_4 \langle \mathcal{T}_C O_{i_1}(t_1) O_{i_2}(t_2) O_{i_3}(t_3) O_{i_4}(t_4) \rangle_c t_{21} \right\} \\
& q_{i_1}(t_1) \dot{q}_{i_2}(t_1 - \epsilon) q_{i_3}(t_1 - 2\epsilon) q_{i_4}(t_1 - 3\epsilon) \\
& + \left\{ \int_{t_0}^{t_1} dt_2 \int_{t_0}^{t_2} dt_3 \int_{t_0}^{t_3} dt_4 \langle \mathcal{T}_C O_{i_1}(t_1) O_{i_2}(t_2) O_{i_3}(t_3) O_{i_4}(t_4) \rangle_c t_{31} \right\} \\
& q_{i_1}(t_1) q_{i_2}(t_1 - \epsilon) \dot{q}_{i_3}(t_1 - 2\epsilon) q_{i_4}(t_1 - 3\epsilon) \\
& + \left. \left\{ \int_{t_0}^{t_1} dt_2 \int_{t_0}^{t_2} dt_3 \int_{t_0}^{t_3} dt_4 \langle \mathcal{T}_C O_{i_1}(t_1) O_{i_2}(t_2) O_{i_3}(t_3) O_{i_4}(t_4) \rangle_c t_{41} \right\} \right. \\
& \left. q_{i_1}(t_1) q_{i_2}(t_1 - \epsilon) q_{i_3}(t_1 - 2\epsilon) \dot{q}_{i_4}(t_1 - 3\epsilon) \right].
\end{aligned} \tag{5.16}$$

Here, we have kept up to second order derivative terms in the quadratic piece to take into account the correction to the kinetic term in the particle's action. For the quartic piece, we have kept only terms with at most a single derivative. As in chapter 2, here also we have kept a small point-split regulator  $\epsilon > 0$ .

Using this approximate local form of the influence phase, one can determine the particle's correlators. As we discussed in chapter 2, the same correlators can be obtained from a local 1-PI effective action. The only difference of this 1-PI effective action from the one discussed earlier in chapter 2 is that now, the cubic terms will vanish and we will include the quartic terms in our analysis. Let us discuss the form of this 1-PI effective action in the following subsection.

### 5.3.2 The Schwinger-Keldysh 1-PI effective action

Let us remind the reader that the form of the Schwinger-Keldysh 1-PI effective action is constrained by some general principles which were discussed in section 5.3.2. We restate these conditions below for the convenience of the reader.

- Collapse rule:

The effective action should vanish under the following identification:

$$q_1 = -q_2 = \tilde{q}. \quad (5.17)$$

- **Reality condition:**

The effective action should become its own negative under complex conjugation along with the following exchange:

$$q_1 \leftrightarrow -q_2. \quad (5.18)$$

In addition to the above conditions, the effective action now has an additional symmetry which is given below.

- **Symmetry under  $q_1 \rightarrow -q_1, q_2 \rightarrow -q_2$ :**

The Lagrangian of the qXY model given in (5.2) is symmetric under the following two transformations:

$$\begin{aligned} q &\rightarrow -q, X \rightarrow -X, Y \rightarrow Y, \\ q &\rightarrow -q, X \rightarrow X, Y \rightarrow -Y. \end{aligned} \quad (5.19)$$

Moreover, the bath is in a thermal state which is also invariant under the above transformations. Now, if the initial state of the particle obeys the same symmetry, then all correlators of the particle with odd number of insertions would vanish. This vanishing of the odd point functions of the particle for a class of initial conditions can be ensured by demanding that the 1-PI effective action is symmetric under the following transformation:

$$q_1 \rightarrow -q_1, q_2 \rightarrow -q_2. \quad (5.20)$$

The most general 1-PI effective Lagrangian that is consistent with these conditions can be written as a sum of terms with even number of q's as follows:

$$L_{\text{SK},1\text{-PI}} = L_{\text{SK},1\text{-PI}}^{(2)} + L_{\text{SK},1\text{-PI}}^{(4)} + \dots \quad (5.21)$$

In this chapter, we will focus only on the quadratic and the quartic terms in this effective action. We give the forms of these terms below:

**Quadratic terms:**

$$L_{\text{SK},1\text{-PI}}^{(2)} = \frac{1}{2}(\dot{q}_1^2 - \dot{q}_2^2) - \frac{i}{2} Z_I(\dot{q}_1 + \dot{q}_2)^2 - \frac{1}{2}\bar{\mu}^2(q_1^2 - q_2^2) + \frac{i}{2} \langle f^2 \rangle (q_1 + q_2)^2 - \frac{1}{2}\gamma(q_1 + q_2)(\dot{q}_1 - \dot{q}_2). \quad (5.22)$$

Here we consider all quadratic terms up to two derivatives acting on the  $q$ 's.<sup>3</sup> We have included the double derivative terms to take into account the renormalisation of the kinetic term in the action. Such a renormalisation introduces a correction to the effective mass of the particle on top of the bare mass  $m_{p0}$ . After taking into account this correction, we choose to work in units where the renormalised mass of the particle is unity.

**Quartic terms:**

$$L_{\text{SK},1\text{-PI}}^{(4)} = \frac{i\zeta_N^{(4)}}{4!} (q_1 + q_2)^4 + \frac{\zeta_\mu^{(2)}}{2} (q_1 + q_2)^2 (q_1^2 - q_2^2) - \frac{i\bar{\zeta}_3}{8} (q_1^2 - q_2^2)^2 - \frac{\bar{\lambda}_4}{48} (q_1^2 - q_2^2)(q_1 - q_2)^2 + \frac{\zeta_\gamma^{(2)}}{2} (q_1 + q_2)^3 (\dot{q}_1 - \dot{q}_2) - \frac{\bar{\lambda}_{4\gamma}}{48} (\dot{q}_1 + \dot{q}_2)(q_1 - q_2)^3 + \frac{i\bar{\zeta}_{3\gamma}}{4} (q_1 + q_2)^2 (q_1 - q_2)(\dot{q}_1 - \dot{q}_2). \quad (5.23)$$

Among the quartic terms, we keep those with at most a single derivative acting on the  $q$ 's.<sup>4</sup> This is consistent with the order at which we truncated the Taylor series expansion of the terms in the influence phase. The reality conditions imply that all the couplings introduced in (5.22) and (5.23) are real.

Now, using this form of the 1-PI effective action, one can calculate the particle's correlators and match them with the same correlators obtained from the approximately local form of the influence phase. The computation of the correlators from both the influence phase and the 1-PI effective action would require specifying the corresponding initial conditions of the particle at some time after the local dynamics has set in. We assume that these initial conditions are the same in the two approaches up to perturbative corrections in  $\lambda$ . This allows us to compare the leading order forms of the connected parts of 2-point and 4-point correlators of  $q$  obtained from the two approaches. Just as we saw in chapter 2, such a comparison would yield relations between the effective couplings and the cumulants of the bath's correlators up to leading order

<sup>3</sup>We are using the convention introduced in chapter 4 for the quadratic couplings.

<sup>4</sup>The terms without any derivative were identified for a scalar field theory in [57].



in  $\lambda$ . We enumerate these relations in (5.26), (5.27) and table 5.1 below.<sup>5</sup>

While expressing these relations, we adopt the following notational conventions:

1. We denote the time interval between two instants  $t_i$  and  $t_j$  by

$$t_{ij} \equiv t_i - t_j. \quad (5.24)$$

2. For connected parts of correlators with nested commutators/ anti-commutators, we put all the insertions within square brackets enclosed by angular brackets. The inner-most operator in the nested structure is positioned left-most in the expression within the brackets. The operators that one encounters as one moves outwards through the nested structure are placed progressively rightwards in the expression. The position of each anti-commutator is indicated by a + sign. For example,

$$\begin{aligned} \langle [12] \rangle &\equiv \langle [O(t_1), O(t_2)] \rangle_c, \quad \langle [12_+] \rangle \equiv \langle \{O(t_1), O(t_2)\} \rangle_c, \\ \langle [1234] \rangle &\equiv \langle [[[O(t_1), O(t_2)], O(t_3)], O(t_4)] \rangle_c, \\ \langle [12_+34] \rangle &\equiv \langle [[\{O(t_1), O(t_2)\}, O(t_3)], O(t_4)] \rangle_c, \\ \langle [12_+3_+4] \rangle &\equiv \langle [\{\{O(t_1), O(t_2)\}, O(t_3)\}, O(t_4)] \rangle_c, \\ \langle [12_+3_+4_+] \rangle &\equiv \langle \{\{\{O(t_1), O(t_2)\}, O(t_3)\}, O(t_4)\} \rangle_c, \text{ etc.} \end{aligned} \quad (5.25)$$

**Quadratic couplings at leading order in  $\lambda$ :** The dependence of all the quadratic couplings on the bath's correlators were obtained in [29]. We provide these expressions below:

$$\begin{aligned} Z_I &= \frac{\lambda^2}{2} \lim_{t_1-t_0 \rightarrow \infty} \left[ \int_{t_0}^{t_1} dt_2 \langle [12_+] t_{12}^2 \rangle + \mathcal{O}(\lambda^4), \right. \\ \langle f^2 \rangle &= \lambda^2 \lim_{t_1-t_0 \rightarrow \infty} \left[ \int_{t_0}^{t_1} dt_2 \langle [12_+] \rangle + \mathcal{O}(\lambda^4), \right. \\ \Delta \bar{\mu}^2 \equiv \bar{\mu}^2 - \bar{\mu}_0^2 &= -i \lambda^2 \lim_{t_1-t_0 \rightarrow \infty} \left[ \int_{t_0}^{t_1} dt_2 \langle [12] \rangle + \mathcal{O}(\lambda^4), \right. \\ \gamma &= i \lambda^2 \lim_{t_1-t_0 \rightarrow \infty} \left[ \int_{t_0}^{t_1} dt_2 \langle [12] \rangle t_{12} + \mathcal{O}(\lambda^4). \right. \end{aligned} \quad (5.26)$$

---

<sup>5</sup>The expressions for the quadratic couplings are the same as those given in (2.36). To convert those expressions in chapter 2 to the expressions in the present chapter, one needs to use the relations between the two sets of couplings given in (4.128), and then set  $\hbar$  and  $m_p$  to unity in those relations.

**Quartic couplings at leading order in  $\lambda$ :** The leading order form of any quartic coupling  $g$  can be expressed as follows:

$$g = \lambda^4 \lim_{t_1 - t_0 \rightarrow \infty} \int_{t_0}^{t_1} dt_2 \int_{t_0}^{t_2} dt_3 \int_{t_0}^{t_3} dt_4 \mathcal{I}[g] + O(\lambda^6). \quad (5.27)$$

We provide the forms of the integrand  $\mathcal{I}[g]$  for the quartic couplings in table 5.1.

Table 5.1: Relations between the SK 1-PI effective couplings and the correlators of  $O(t)$

$g$	$\mathcal{I}[g]$
$\zeta_N^{(4)}$	$-3\langle[12_+3_+4_+]\rangle$
$\lambda_4$	$6i\langle[1234]\rangle$
$\bar{\lambda}_{4\gamma}$	$2i(t_{12} + t_{13} + t_{14})\langle[1234]\rangle$
$\zeta_{5\mu}^{(2)}$	$-\frac{i}{4}(\langle[123_+4_+]\rangle + \langle[12_+34_+]\rangle + \langle[12_+3_+4]\rangle)$
$\zeta_{\gamma}^{(2)}$	$\frac{i}{12}((3t_{12} - t_{13} - t_{14})\langle[123_+4_+]\rangle + (-t_{12} + 3t_{13} - t_{14})\langle[12_+34_+]\rangle + (-t_{12} - t_{13} + 3t_{14})\langle[12_+3_+4]\rangle)$
$\bar{\zeta}_3$	$(\langle[12_+34]\rangle + \langle[123_+4]\rangle + \langle[1234_+]\rangle)$
$\bar{\zeta}_{3\gamma}$	$\frac{1}{2}((-t_{12} + t_{13} + t_{14})\langle[12_+34]\rangle + (t_{12} - t_{13} + t_{14})\langle[123_+4]\rangle + (t_{12} + t_{13} - t_{14})\langle[1234_+]\rangle)$

From the expressions of the couplings given in table 5.1, one can easily check that these couplings are real. For this, first note that the operator  $O$  given in (5.3) is Hermitian. This implies that its correlators should satisfy relations of the following form:

$$\langle\langle O(t_1)O(t_2)O(t_3)O(t_4) \rangle\rangle^* = \langle\langle O(t_4)O(t_3)O(t_2)O(t_1) \rangle\rangle. \quad (5.28)$$

Such relations between the bath's correlators lead to the following conditions on the corresponding cumulants:

$$\begin{aligned} \langle[1234]\rangle^* &= -\langle[1234]\rangle, \langle[12_+3_+4_+]\rangle^* = \langle[12_+3_+4_+]\rangle, \\ \langle[12_+34]\rangle^* &= \langle[12_+34]\rangle, \langle[123_+4]\rangle^* = \langle[123_+4]\rangle, \langle[1234_+]\rangle^* = \langle[1234_+]\rangle, \\ \langle[12_+3_+4]\rangle^* &= -\langle[12_+3_+4]\rangle, \langle[12_+34_+]\rangle^* = -\langle[12_+34_+]\rangle, \langle[123_+4_+]\rangle^* = -\langle[123_+4_+]\rangle. \end{aligned} \quad (5.29)$$

From these conditions, the reality of the couplings (see table 5.1) is manifest.

In section 5.4.5, we will evaluate these couplings (along with the additional OTO couplings) for the qXY model at the high temperature limit of the bath. For now, we would like the reader to just note that the leading order terms in the quadratic and the quartic couplings are  $O(\lambda^2)$  and  $O(\lambda^4)$  respectively. In the following subsection, we will show that these leading order forms of the couplings enter as parameters in a dual stochastic dynamics.

### 5.3.3 Duality with a non-linear Langevin dynamics

In this subsection, we show that the quartic Schwinger-Keldysh effective theory of the particle is dual to a classical stochastic theory governed by a non-linear Langevin equation. This stochastic dynamics has a structure similar to the one obtained for the cubic effective theory in chapter 4. We will first propose the form of the dual non-linear Langevin dynamics and then demonstrate its equivalence to the quartic effective theory discussed in the previous subsection.

#### The dual non-linear Langevin dynamics:

Consider a non-linear Langevin equation of the following form:

$$\mathcal{E}[q, \mathcal{N}] \equiv \ddot{q} + \left(\gamma + \zeta_\gamma^{(2)} \mathcal{N}^2\right) \dot{q} + \left(\bar{\mu}^2 + \zeta_\mu^{(2)} \mathcal{N}^2\right) q + \mathcal{N} \left(\bar{\zeta}_3 - \bar{\zeta}_{3\gamma} \frac{d}{dt}\right) \frac{q^2}{2!} + \left(\bar{\lambda}_4 - \bar{\lambda}_{4\gamma} \frac{d}{dt}\right) \frac{q^3}{3!} - \langle f^2 \rangle \mathcal{N} = 0, \quad (5.30)$$

where  $\mathcal{N}$  is a noise drawn from a non-Gaussian probability distribution given below

$$P[\mathcal{N}] \propto \exp \left[ - \int dt \left( \frac{\langle f^2 \rangle}{2} \mathcal{N}^2 + \frac{Z_I}{2} \dot{\mathcal{N}}^2 + \frac{\zeta_N^{(4)}}{4!} \mathcal{N}^4 \right) \right]. \quad (5.31)$$

The non-linearities in this dynamics as well as the non-Gaussianity in the noise are fixed by the following parameters:  $\zeta_N^{(4)}, \zeta_\gamma^{(2)}, \zeta_\mu^{(2)}, \bar{\zeta}_3, \bar{\zeta}_{3\gamma}, \bar{\lambda}_4, \bar{\lambda}_{4\gamma}$ . From equation (5.27) and table 5.1, we can see that all these parameters are  $O(\lambda^4)$ . If we ignore these  $O(\lambda^4)$  contributions, then the dynamics satisfies a linear Langevin equation of the following form:

$$\ddot{q} + \gamma \dot{q} + \bar{\mu}^2 q = \langle f^2 \rangle \mathcal{N}, \quad (5.32)$$

where the noise is drawn from the Gaussian probability distribution given below

$$P[\mathcal{N}] \propto \exp \left[ - \int dt \left( \frac{\langle f^2 \rangle}{2} \mathcal{N}^2 + \frac{Z_I}{2} \dot{\mathcal{N}}^2 \right) \right]. \quad (5.33)$$

- Parameters in the linear Langevin dynamics

The parameters appearing in the linear Langevin dynamics given in (5.32) and (5.33) are the same as those discussed in chapter 4. They can be interpreted in the following manner:

1.  $\langle f^2 \rangle$  is the strength of an additive noise in the dynamics.
2.  $Z_I$  introduces nonzero correlations between the noise at two different times.
3.  $\bar{\mu}$  is the renormalised frequency.
4.  $\gamma$  is the coefficient of damping.

• **Additional parameters in the non-linear dynamics**

If we include the contribution of the  $O(\lambda^4)$  parameters in the dynamics, then these additional parameters can be interpreted as follows:

1.  $\zeta_\mu^{(2)}$  is a jitter in the renormalised frequency due to the thermal noise.
2.  $\zeta_\gamma^{(2)}$  is a jitter in the damping coefficient due to the thermal noise.
3.  $\zeta_N^{(4)}$  is the strength of non-Gaussianity in the noise distribution.
4.  $\bar{\lambda}_4$  and  $\bar{\lambda}_{4\gamma}$  are the strengths of anharmonic terms in the equation of motion.
5.  $\bar{\zeta}_3$  and  $\bar{\zeta}_{3\gamma}$  are the strengths of anharmonic terms which couple to the noise.

Now, let us demonstrate the duality between this non-linear Langevin dynamics and the quartic effective theory that we introduced earlier.

**Argument for the duality:**

Consider the following stochastic path integral<sup>6</sup> for the non-linear Langevin dynamics given in (5.30) and (5.31):

$$\mathcal{Z} = \int [D\mathcal{N}][Dq] e^{\int dt \left( \frac{\zeta_\mu^{(2)} N q}{\langle f^2 \rangle \delta t} + \frac{\zeta_\gamma^{(2)} N \dot{q}}{\langle f^2 \rangle \delta t} + \frac{\zeta_N^{(4)} N^2}{4 \langle f^2 \rangle \delta t} \right)} \delta(\mathcal{E}[q, \mathcal{N}]) P[\mathcal{N}]. \quad (5.34)$$

Here,  $\delta t$  is a UV-regulator for 2-point functions of  $\mathcal{N}$ , and  $\left[ \int dt \left( \frac{\zeta_\mu^{(2)} N q}{\langle f^2 \rangle \delta t} + \frac{\zeta_\gamma^{(2)} N \dot{q}}{\langle f^2 \rangle \delta t} + \frac{\zeta_N^{(4)} N^2}{4 \langle f^2 \rangle \delta t} \right) \right]$  is a counter-term introduced to cancel the regulator-dependent contributions arising from loop integrals of  $\mathcal{N}$ .

Notice that  $q$  is a dummy variable in the above path integral. We choose to relabel this variable as  $q_a$ . In addition, we introduce an auxiliary variable  $q_d$  which replaces the delta

---

<sup>6</sup>We ignore the Jacobian  $\det \left[ \frac{\delta \mathcal{E}[q(t), \mathcal{N}(t)]}{\delta q(t')} \right]$  in the path integral as it does not contribute to the quadratic and quartic terms that we eventually get in (5.41) upto leading orders in  $\lambda$ .

function for the equation of motion by an integral as shown below

$$\begin{aligned}
\mathcal{Z} &= \int [DN][Dq_a][Dq_d] e^{\int dt \left( \frac{\zeta_\mu^{(2)} N q_a}{\langle f^2 \rangle \delta t} + \frac{\zeta_\gamma^{(2)} N \dot{q}_a}{\langle f^2 \rangle \delta t} + \frac{\zeta_N^{(4)} N^2}{4 \langle f^2 \rangle \delta t} \right)} e^{-i \int dt \mathcal{E}[q_a, N] q_d} P[\mathcal{N}] \\
&= \int [DN][Dq_a][Dq_d] \exp \left[ i \int dt \left\{ -i \frac{\zeta_\mu^{(2)} N q_a}{\langle f^2 \rangle \delta t} - i \frac{\zeta_\gamma^{(2)} N \dot{q}_a}{\langle f^2 \rangle \delta t} - i \frac{\zeta_N^{(4)} N^2}{4 \langle f^2 \rangle \delta t} - q_d \ddot{q}_a \right. \right. \\
&\quad - q_d (\gamma + \zeta_\gamma^{(2)} N^2) \dot{q}_a - q_d (\bar{\mu}^2 + \zeta_\mu^{(2)} N^2) q_a \\
&\quad - \mathcal{N} q_d \left( \bar{\zeta}_3 - \bar{\zeta}_{3\gamma} \frac{d}{dt} \right) \frac{q_a^2}{2!} - q_d \left( \bar{\lambda}_4 - \bar{\lambda}_{4\gamma} \frac{d}{dt} \right) \frac{q_a^3}{3!} \\
&\quad \left. \left. + \langle f^2 \rangle \mathcal{N} q_d + i \frac{\langle f^2 \rangle}{2} \mathcal{N}^2 + i \frac{Z_I}{2} \mathcal{N}^2 + i \frac{\zeta_N^{(4)}}{4!} \mathcal{N}^4 \right\} \right]. \tag{5.35}
\end{aligned}$$

Now, let us introduce the following shift in the noise variable appearing in the above path integral:

$$\mathcal{N} \rightarrow \mathcal{N} + i q_d. \tag{5.36}$$

Integrating out this shifted noise variable leads to a residual path integral over  $q_a$  and  $q_d$ . In the action of this residual path integral, we retain all the quadratic terms up to  $O(\lambda^2)$ , and all the quartic terms up to  $O(\lambda^4)$ .<sup>7</sup> Up to this approximation, the residual path integral has the following form:

$$\begin{aligned}
\mathcal{Z} &= C \int [Dq_a][Dq_d] \exp \left[ i \int dt \left\{ -q_d \ddot{q}_a - \gamma q_d \dot{q}_a - \bar{\mu}^2 q_d q_a - i \frac{Z_I}{2} \dot{q}_d^2 + i \frac{\langle f^2 \rangle}{2} q_d^2 \right. \right. \\
&\quad + i \frac{\zeta_N^{(4)}}{4!} q_d^4 + \zeta_\mu^{(2)} q_d^3 q_a + \zeta_\gamma^{(2)} q_d^3 \dot{q}_a - i \bar{\zeta}_3 \frac{q_d^2 q_a^2}{2!} \\
&\quad \left. \left. + i \bar{\zeta}_{3\gamma} q_d^2 q_a \dot{q}_a - \bar{\lambda}_4 \frac{q_d q_a^3}{3!} + \bar{\lambda}_{4\gamma} \frac{q_d q_a^2 \dot{q}_a}{2!} \right\} \right], \tag{5.39}
\end{aligned}$$

<sup>7</sup>While integrating out the noise, we consider the terms associated with  $Z_I$  and all the  $O(\lambda^4)$  parameters in the action to be small corrections over the term associated with  $\langle f^2 \rangle$ . Then the 2-point function of the noise reduces to

$$\langle \mathcal{N}(t_1) \mathcal{N}(t_2) \rangle = \frac{1}{\langle f^2 \rangle} \delta(t_1 - t_2) + (\text{perturbative corrections}). \tag{5.37}$$

We ignore the perturbative corrections and regulate the delta function by the UV regulator  $\delta t$  that we introduced earlier. Then the equal-time 2-point correlator of  $\mathcal{N}$  reduces to

$$\langle \mathcal{N}^2 \rangle = \frac{1}{\langle f^2 \rangle \delta t}, \tag{5.38}$$

The contribution of  $\langle \mathcal{N}^2 \rangle$  to the action of the residual path integral exactly cancels the contribution from the counter-term.

where  $C$  is a constant given by

$$C = \int [DN] e^{\int dt \frac{\zeta_N^{(4)} N^2}{4 \langle f^2 \rangle \delta t}} e^{-\int dt \left( \frac{\langle f^2 \rangle}{2} N^2 + \frac{Z_I}{2} \dot{N}^2 + \frac{\zeta_N^{(4)}}{4!} N^4 \right)}. \quad (5.40)$$

Integrating by parts the first term and the last term in the action of the above path integral, we get

$$\begin{aligned} \mathcal{Z} = C \int [Dq_a][Dq_d] \exp \left[ i \int dt \left\{ \dot{q}_d \dot{q}_a - i \frac{Z_I}{2} \dot{q}_d^2 - \gamma q_d \dot{q}_a + i \frac{\langle f^2 \rangle}{2} q_d^2 - \bar{\mu}^2 q_d q_a \right. \right. \\ \left. \left. + i \frac{\zeta_N^{(4)}}{4!} q_d^4 + \zeta_\mu^{(2)} q_d^3 q_a + \zeta_\gamma^{(2)} q_d^3 \dot{q}_a - i \bar{\zeta}_3 \frac{q_d^2 q_a^2}{2!} \right. \right. \\ \left. \left. + i \bar{\zeta}_{3\gamma} q_d^2 q_a \dot{q}_a - \bar{\lambda}_4 \frac{q_d q_a^3}{3!} - \bar{\lambda}_{4\gamma} \frac{\dot{q}_d q_a^3}{3!} \right\} \right]. \quad (5.41) \end{aligned}$$

Now, notice that the action in the above expression is exactly the Schwinger-Keldysh effective action given in (5.22) and (5.23) under the following identification:

$$q_a \equiv \frac{q_1 - q_2}{2}, \quad q_d \equiv q_1 + q_2. \quad (5.42)$$

This basis  $\{q_a, q_d\}$  is the Keldysh basis [36] that we encountered in chapter 4. The Schwinger-Keldysh effective Lagrangian of the particle in this basis is given by

$$\begin{aligned} L_{\text{SK,1-PI}} = \dot{q}_d \dot{q}_a - \frac{i}{2} Z_I \dot{q}_d^2 - \bar{\mu}^2 q_d q_a + \frac{i}{2} \langle f^2 \rangle q_d^2 - \gamma q_d \dot{q}_a \\ + \frac{i \zeta_N^{(4)}}{4!} q_d^4 + \zeta_\mu^{(2)} q_d^3 q_a - \frac{i \bar{\zeta}_3}{2!} q_d^2 q_a^2 - \frac{\bar{\lambda}_4}{3!} q_d q_a^3 \\ + \zeta_\gamma^{(2)} q_d^3 \dot{q}_a - \frac{\bar{\lambda}_{4\gamma}}{3!} \dot{q}_d q_a^3 + i \bar{\zeta}_{3\gamma} q_d^2 q_a \dot{q}_a. \quad (5.43) \end{aligned}$$

Therefore, one can express the stochastic path integral in terms of the Schwinger-Keldysh effective action as shown below

$$\mathcal{Z} = C \int [Dq_a][Dq_d] e^{i \int dt L_{\text{SK,1-PI}}}. \quad (5.44)$$

This concludes our argument for the duality between the quartic effective theory and the non-linear Langevin dynamics. We refer the reader to [55] for a more detailed discussion on such dualities between stochastic and Schwinger-Keldysh path integrals.

**A brief comment on the sign of  $\zeta_N^{(4)}$ :**

In section 5.4.5, we will see that, for the  $qXY$  model, the value of  $\zeta_N^{(4)}$  is negative. This may raise concern about the validity of the probability distribution given in (5.31) since it diverges when  $|\mathcal{N}| \rightarrow \infty$ . However, we would like to remind the reader that we have done a perturbative analysis here and ignored all possible corrections to the probability distribution beyond the quartic order. Such a perturbative analysis is insufficient to determine the behaviour of the probability density at large values of  $\mathcal{N}$ .

## 5.4 Extension to the effective theory for OTO correlators

In this section, we will move on to the OTO extension of the quartic effective dynamics of the Brownian particle. We will see that the quartic effective couplings in this extended framework receive contributions from the 4-point OTOCs of the operator  $O$  that couples to the particle. We will show that some of these OTO correlators of the bath are related to Schwinger-Keldysh correlators due to the following two reasons:

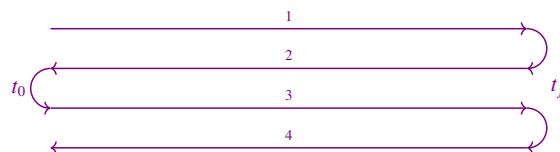
1. microscopic reversibility in the bath's dynamics,
2. thermality of the bath.

These relations between the bath's correlators, in turn, impose certain constraints on the quartic effective couplings of the particle. Following the methods developed in chapter 4, we will derive these constraints, and show that they lead to generalisations of the Onsager reciprocal relations [38, 39] and the fluctuation-dissipation relation [46, 47]. Finally, we will provide the values of the effective couplings for the  $qXY$  model introduced in section 5.2 and check that they satisfy all the constraints.

### 5.4.1 Generalised influence phase of the particle

In chapter 2, we had discussed that to get a path integral representation of the particle's OTOCs, one needs to consider a contour with two time-folds as shown in figure 5.1.

Figure 5.1: OTO contour



There, we had shown how one can get a generalisation of the influence phase by integrating out the bath's degrees of freedom on this double-folded contour. We had also shown that the OTOCs of the bath enter in a perturbative expansion of this generalised influence. For the convenience of the reader, we restate the form of this perturbative expansion below:

$$W_{\text{GSK}} = \sum_{n=1}^{\infty} \lambda^n W_{\text{GSK}}^{(n)} \quad (5.45)$$

where

$$W_{\text{GSK}}^{(n)} = i^{n-1} \sum_{i_1, \dots, i_n=1}^4 \int_{t_0}^{t_f} dt_1 \int_{t_0}^{t_1} dt_2 \cdots \int_{t_0}^{t_{n-1}} dt_n \langle \mathcal{T}_C O_{i_1}(t_1) \cdots O_{i_n}(t_n) \rangle_c q_{i_1}(t_1) \cdots q_{i_n}(t_n). \quad (5.46)$$

As in case of the influence phase, one can expand the  $q$ 's in (5.46) at the times  $t_2, \dots, t_n$  about  $t_1$  to get an approximately local form for the generalised influence phase. The quadratic and the quartic terms in this approximately local form are given in appendix C.3.

Following the method introduced in chapter 2, we will next construct a OTO 1-PI effective action which correctly reproduces the OTOCs of the particle. As we will see next, this OTO 1-PI effective action is a straightforward extension of the Schwinger-Keldysh effective action discussed in the previous section.

## 5.4.2 Out of time ordered 1-PI effective action of the particle

In chapter 2, we had introduced an OTO 1-PI effective action of the particle. There, we had mentioned that the form of this effective action is constrained by microscopic unitarity of the (particle+bath) combined system and the Hermiticity of the operator representing the position of the particle. We restate these constraints on the OTO effective action below for the convenience of the reader.

- **Collapse rules:**

The 1-PI effective action should become independent of  $\tilde{q}$  under any of the following identifications:

1.  $q_1 = -q_2 = \tilde{q}$ ,



$$2. q_2 = -q_3 = \tilde{q},$$

$$3. q_3 = -q_4 = \tilde{q}.$$

Moreover, under any of these collapses, the OTO effective action should reduce to the Schwinger-Keldysh effective action introduced earlier.

• **Reality conditions:**

The effective action should become its own negative under complex conjugation along with the following exchanges:

$$q_1 \leftrightarrow -q_4, q_2 \leftrightarrow -q_3. \quad (5.47)$$

In addition, the 1-PI effective action on the 2-fold contour should be invariant under

$$q_1 \rightarrow -q_1, q_2 \rightarrow -q_2, q_3 \rightarrow -q_3, q_4 \rightarrow -q_4 \quad (5.48)$$

to respect the symmetries given in (5.19).

The most general 1-PI effective action which is consistent with these conditions can be expanded as

$$L_{1\text{-PI}} = L_{1\text{-PI}}^{(2)} + L_{1\text{-PI}}^{(4)} + \dots, \quad (5.49)$$

where  $L_{1\text{-PI}}^{(2)}$  and  $L_{1\text{-PI}}^{(4)}$  are the quadratic and the quartic terms in the action respectively.

**Quadratic terms:** The quadratic terms can be obtained by extending their Schwinger-Keldysh(SK) counterparts given in (5.22) just as we discussed in 2.3.2. We provide the form of these terms below:

$$\begin{aligned} L_{1\text{-PI}}^{(2)} = & \frac{1}{2}(\dot{q}_1^2 - \dot{q}_2^2 + \dot{q}_3^2 - \dot{q}_4^2) - \frac{\bar{\mu}^2}{2}(q_1^2 - q_2^2 + q_3^2 - q_4^2) \\ & - \frac{\gamma}{2}[(q_1 + q_2)(\dot{q}_1 - \dot{q}_2 - \dot{q}_3 - \dot{q}_4) + (q_3 + q_4)(\dot{q}_1 + \dot{q}_2 + \dot{q}_3 - \dot{q}_4)] \\ & + \frac{i\langle f^2 \rangle}{2}(q_1 + q_2 + q_3 + q_4)^2 - \frac{iZ_I}{2}(\dot{q}_1 + \dot{q}_2 + \dot{q}_3 + \dot{q}_4)^2 \end{aligned} \quad (5.50)$$

One can easily check that these quadratic terms reduce to the corresponding terms in the SK effective action under any of the collapses mentioned above.

**Quartic terms:** The quartic terms can be split into two parts <sup>8</sup>:

1. terms which reduce to their SK counterparts given in (5.23) under any of the collapses,
2. terms which go to zero under these collapses.

Accordingly, the quartic effective action can be written as

$$L_{1-PI}^{(4)} = L_{1-PI,SK}^{(4)} + L_{1-PI,OTO}^{(4)} \quad (5.51)$$

where  $L_{1-PI,SK}^{(4)}$  and  $L_{1-PI,OTO}^{(4)}$  are the two sets of terms mentioned above.

**Extension of quartic terms in Schwinger-Keldysh effective theory:** The extension of the quartic terms in the SK effective theory can be further divided into different sets according to the number of time derivatives in them. Here, we keep terms with up to a single derivative acting on the  $q$ 's. Then  $L_{1-PI,SK}^{(4)}$  can be decomposed as

$$L_{1-PI,SK}^{(4)} = L_{1-PI,SK}^{(4,0)} + L_{1-PI,SK}^{(4,1)} + \dots, \quad (5.52)$$

where  $L_{1-PI,SK}^{(4,0)}$  and  $L_{1-PI,SK}^{(4,1)}$  are terms without any derivative and terms with a single derivative respectively. We give the forms of these terms below:

$$\begin{aligned} & L_{1-PI,SK}^{(4,0)} \\ &= -\frac{\bar{\lambda}_4}{48} \left[ (q_1 + q_2)(q_1 - q_2 - q_3 - q_4)^3 + (q_3 + q_4)(q_1 + q_2 + q_3 - q_4)^3 \right] \\ &+ \frac{\zeta_\mu^{(2)}}{2} (q_1 + q_2 + q_3 + q_4)^2 (q_1^2 - q_2^2 + q_3^2 - q_4^2) - \frac{i\bar{\zeta}_3}{8} (q_1^2 - q_2^2 + q_3^2 - q_4^2)^2 \\ &+ \frac{i\zeta_N^{(4)}}{24} (q_1 + q_2 + q_3 + q_4)^4, \end{aligned} \quad (5.53)$$

---

<sup>8</sup>This is analogous to the way we split the cubic terms of the OTO effective theory in chapter 2.

$$\begin{aligned}
& L_{1\text{-PI,SK}}^{(4,1)} \\
&= -\frac{\bar{\lambda}_{4\gamma}}{48} \left[ (\dot{q}_1 + \dot{q}_2)(q_1 - q_2 - q_3 - q_4)^3 + (\dot{q}_3 + \dot{q}_4)(q_1 + q_2 + q_3 - q_4)^3 \right] \\
&+ \frac{\bar{\zeta}_{3\gamma}^{(2)}}{2} (q_1 + q_2 + q_3 + q_4)^2 \left[ (q_1 + q_2)(\dot{q}_1 - \dot{q}_2 - \dot{q}_3 - \dot{q}_4) + (q_3 + q_4)(\dot{q}_1 + \dot{q}_2 + \dot{q}_3 - \dot{q}_4) \right] \\
&+ \frac{i\bar{\zeta}_{3\gamma}}{4} (q_1 + q_2 + q_3 + q_4) \left[ (q_1 + q_2)(q_1 - q_2 - q_3 - q_4)(\dot{q}_1 - \dot{q}_2 - \dot{q}_3 - \dot{q}_4) \right. \\
&\quad \left. + (q_3 + q_4)(q_1 + q_2 + q_3 - q_4)(\dot{q}_1 + \dot{q}_2 + \dot{q}_3 - \dot{q}_4) \right].
\end{aligned} \tag{5.54}$$

**Additional OTO quartic terms:** The additional OTO quartic terms which vanish under any of the collapses can also be split into terms with different number of derivatives acting on the  $q$ 's. As in case of the extension of the SK effective action terms,  $L_{1\text{-PI,OTO}}^{(4)}$  can be decomposed as

$$L_{1\text{-PI,OTO}}^{(4)} = L_{1\text{-PI,OTO}}^{(4,0)} + L_{1\text{-PI,OTO}}^{(4,1)} + \dots, \tag{5.55}$$

where  $L_{1\text{-PI,OTO}}^{(4,0)}$  and  $L_{1\text{-PI,OTO}}^{(4,1)}$  are terms without any derivative and terms with a single derivative respectively. The forms of these terms are given below:

$$\begin{aligned}
& L_{1\text{-PI,OTO}}^{(4,0)} \\
&= (q_1 + q_2)(q_2 + q_3)(q_3 + q_4) \left[ A_1(q_1 + q_2) + A_2(q_3 + q_4) + A_3(q_1 - q_4) + A_4(q_2 + q_3) \right],
\end{aligned} \tag{5.56}$$

$$\begin{aligned}
L_{1\text{-PI,OTO}}^{(4,1)} &= (q_1 + q_2)(q_2 + q_3)(\dot{q}_3 + \dot{q}_4) \left[ B_1(q_1 - q_4) + B_2(q_1 + q_2) + B_3(q_2 + q_3) \right] \\
&+ (q_1 + q_2)(\dot{q}_2 + \dot{q}_3)(q_3 + q_4) \left[ B_4(q_1 - q_4) + B_5(q_1 + q_2) + B_6(q_3 + q_4) \right] \\
&+ (\dot{q}_1 + \dot{q}_2)(q_2 + q_3)(q_3 + q_4) \left[ B_7(q_1 - q_4) + B_8(q_3 + q_4) + B_9(q_2 + q_3) \right].
\end{aligned} \tag{5.57}$$

The reality conditions impose the following constraints on the quartic OTO couplings:

$$\begin{aligned}
& A_1 = -A_2^*, \quad A_3 = A_3^*, \quad A_4 = -A_4^*, \\
& B_1 = B_7^*, \quad B_2 = -B_8^*, \quad B_3 = -B_9^*, \quad B_4 = B_4^*, \quad B_5 = -B_6^*.
\end{aligned} \tag{5.58}$$

These additional OTO terms will not contribute to any correlator on the 2-fold contour that can also be obtained from the Schwinger-Keldysh contour. This is ensured by the collapse rules mentioned above. However, they are essential for computing OTOCs of the particle. The couplings appearing in these OTO terms, in turn, receive contributions from the OTOCs of the bath. As we will discuss next, some of these OTOCs of the bath are related to Schwinger-Keldysh correlators due to the microscopic reversibility in the dynamics of the bath. We will show that such relations impose constraints on the quartic couplings in the effective action which can be interpreted as generalisations of the Onsager reciprocal relations [38, 39].

### 5.4.3 Generalised Onsager relations

In the qXY model, the bath's dynamics (excluding the perturbation by the particle) has a symmetry under time-reversal:

$$\mathbf{T}X^{(i)}(t)\mathbf{T}^\dagger = X^{(i)}(-t), \quad \mathbf{T}Y^{(j)}(t)\mathbf{T}^\dagger = Y^{(j)}(-t). \quad (5.59)$$

Here,  $\mathbf{T}$  is an anti-linear and anti-unitary operator which commutes with the bath's Hamiltonian i.e.

$$[\mathbf{T}, H_B] = 0. \quad (5.60)$$

Moreover, the bath operator  $O \equiv \sum_{i,j} g_{xy,ij} X^{(i)} Y^{(j)}$  that couples to the particle has an even parity under time-reversal which implies

$$\mathbf{T}O(t)\mathbf{T}^\dagger = O(-t). \quad (5.61)$$

In chapter 4, we showed that such a microscopic reversibility in the bath leads to some generalisations of the Onsager reciprocal relations [38, 39] which connect all the cubic OTO couplings to the certain Schwinger-Keldysh couplings (see equation (4.155)). There, we discussed how these generalised Onsager relations arise from certain relations between the 3-point correlators of the bath which are rooted in its microscopic reversibility. Here, we will first show that similar relations exist between the 4-point correlators of the bath. Then we will discuss the constraints imposed on the quartic effective couplings of the particle due to these relations between the 4-point functions of the bath.

**Relations between the bath's correlators due to microscopic reversibility:**

The microscopic reversibility in the bath leads to the following kind of relations between the 4-point correlators of  $O$ :

$$\langle O(t_1)O(t_2)O(t_3)O(t_4) \rangle = \left( \langle \mathbf{T}O(t_1)\mathbf{T}^\dagger\mathbf{T}O(t_2)\mathbf{T}^\dagger\mathbf{T}O(t_3)\mathbf{T}^\dagger\mathbf{T}O(t_4)\mathbf{T}^\dagger \rangle \right)^* . \quad (5.62)$$

Using the transformation of  $O(t)$  under time-reversal (see equation (5.61)), we get

$$\langle O(t_1)O(t_2)O(t_3)O(t_4) \rangle = \left( \langle O(-t_1)O(-t_2)O(-t_3)O(-t_4) \rangle \right)^* . \quad (5.63)$$

Now, due to the Hermiticity of the operator  $O$ , the above relation reduces to

$$\langle O(t_1)O(t_2)O(t_3)O(t_4) \rangle = \langle O(-t_4)O(-t_3)O(-t_2)O(-t_1) \rangle . \quad (5.64)$$

Note that such relations can connect two OTO correlators as in the following example:

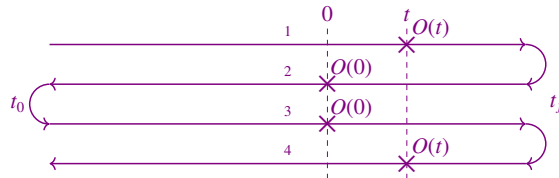
$$\langle O(t)O(0)O(t)O(0) \rangle = \langle O(0)O(-t)O(0)O(-t) \rangle . \quad (5.65)$$

Moreover, they can also connect an OTO correlator to a Schwinger-Keldysh correlator. For example, consider the relation

$$\langle O(t)O(0)O(0)O(t) \rangle = \langle O(-t)O(0)O(0)O(-t) \rangle , \quad (5.66)$$

where  $t > 0$ . The correlator on the left hand side of the above equation is an OTOC which can be obtained by putting insertions on a 2-fold contour as shown in figure 5.2. The correlator on

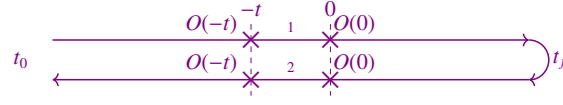
Figure 5.2: Contour-ordered correlator for  $\langle O(t)O(0)O(0)O(t) \rangle$  where  $t > 0$



the right-hand side of (5.66), however, can be obtained from a path integral on the Schwinger-Keldysh contour as shown in figure 5.3.

Such relations between the bath's 4-point correlators can introduce two kinds of constraints

Figure 5.3: Contour-ordered correlator for  $\langle O(-t)O(0)O(0)O(-t) \rangle$  where  $t > 0$



on the quartic effective couplings of the particle:

1. They can lead to a relation between two different OTO couplings.
2. They can also relate an OTO coupling to a Schwinger-Keldysh coupling.

We will now derive these constraints on the effective couplings of the particle. Our derivation of these constraints would closely follow the derivation of similar relations between the cubic couplings given in chapter 4

### Constraints on the quartic effective couplings:

To analyse the constraints on the effective couplings, we find it convenient to re-express the quartic OTO couplings in terms of some new real parameters as shown below:

$$\begin{aligned}
 A_1 = -A_2^* &= \frac{1}{12} \left[ (-\bar{\lambda}_4 + \bar{\kappa}_4) - 6i(\varrho_4 - \bar{\varrho}_4) \right], \\
 A_3 = A_3^* &= \kappa_4, \\
 A_4 = -A_4^* &= \frac{i}{2}(\varrho_4 + \bar{\varrho}_4).
 \end{aligned}
 \tag{5.67}$$

$$\begin{aligned}
 B_1 = B_7^* &= \frac{1}{4} \left[ (2\kappa_{4\gamma}^{II} + 4\kappa_{4\gamma}^{III} + \bar{\kappa}_{4\gamma}^{II}) + i(\varrho_{4\gamma}^{II} + \bar{\varrho}_{4\gamma}^I - \bar{\varrho}_{4\gamma}^{II}) \right], \\
 B_2 = -B_8^* &= \frac{1}{16} \left[ (-\bar{\lambda}_{4\gamma} + 24\zeta_{5\gamma}^{(2)} + 12\kappa_{4\gamma}^I - 4\bar{\kappa}_{4\gamma}^I - 6\bar{\kappa}_{4\gamma}^{II}) \right. \\
 &\quad \left. + i(4\bar{\zeta}_{3\gamma} - 2\varrho_{4\gamma}^I + 2\varrho_{4\gamma}^{II} - 6\bar{\varrho}_{4\gamma}^I + 2\bar{\varrho}_{4\gamma}^{II}) \right], \\
 B_3 = -B_9^* &= \frac{1}{4} \left[ (-2\kappa_{4\gamma}^{II} + \bar{\kappa}_{4\gamma}^{II}) + i\varrho_{4\gamma}^I \right], \\
 B_4 = B_4^* &= \frac{1}{2} (2\kappa_{4\gamma}^{II} + \bar{\kappa}_{4\gamma}^{II}), \\
 B_5 = -B_6^* &= \frac{1}{16} \left[ (\bar{\lambda}_{4\gamma} + 8\zeta_{5\gamma}^{(2)} + 4\kappa_{4\gamma}^I + 4\bar{\kappa}_{4\gamma}^I - 2\bar{\kappa}_{4\gamma}^{II}) \right. \\
 &\quad \left. + i(-4\bar{\zeta}_{3\gamma} + 2\varrho_{4\gamma}^I + 6\varrho_{4\gamma}^{II} - 2\bar{\varrho}_{4\gamma}^I + 6\bar{\varrho}_{4\gamma}^{II}) \right].
 \end{aligned}
 \tag{5.68}$$

These new parameters are chosen so that they have definite parities under time-reversal (see the discussion below). The presence or absence of tilde over any coupling indicates whether it has

odd or even parity respectively. The symbols  $\kappa$  and  $\varrho$  are used to represent the couplings which get multiplied to real and imaginary terms in the effective action respectively. The subscript  $\gamma$  is introduced to distinguish the couplings corresponding to the single derivative terms in the action.

One can determine the dependence of these OTO couplings on the cumulants of the operator  $O$  by comparing the particle's 4-point OTOCs obtained from the generalised influence phase with those computed using the OTO 1-PI effective action. We provide the expressions of these couplings in terms of the bath's OTO cumulants in appendix C.3.

For the purpose of analysing the constraints on the effective couplings, we find it convenient to convert their expressions (see (5.27),(C.12) , and tables 5.1 and C.3) into integrals over a frequency domain where the integrands are determined by some spectral functions of the bath. These spectral functions are the Fourier transforms of the 4-point cumulants of  $O(t)$  as defined by the relations given in (5.70), (5.71) and (5.72). In these relations, we define the measure for the integral over the frequencies as

$$\int \frac{d^4\omega}{(2\pi)^4} \equiv \int_{-\infty}^{\infty} \frac{d\omega_1}{2\pi} \int_{-\infty}^{\infty} \frac{d\omega_2}{2\pi} \int_{-\infty}^{\infty} \frac{d\omega_3}{2\pi} \int_{-\infty}^{\infty} \frac{d\omega_4}{2\pi}. \quad (5.69)$$

- **Spectral functions for Wightman correlators:**

$$\begin{aligned} \int \frac{d^4\omega}{(2\pi)^4} \rho\langle 1234 \rangle e^{-i(\omega_1 t_1 + \omega_2 t_2 + \omega_3 t_3 + \omega_4 t_4)} &\equiv \lambda^4 \langle O(t_1)O(t_2)O(t_3)O(t_4) \rangle_c, \\ \int \frac{d^4\omega}{(2\pi)^4} \rho\langle 4321 \rangle e^{-i(\omega_1 t_1 + \omega_2 t_2 + \omega_3 t_3 + \omega_4 t_4)} &\equiv \lambda^4 \langle O(t_4)O(t_3)O(t_2)O(t_1) \rangle_c, \text{ etc.} \end{aligned} \quad (5.70)$$

- **Spectral functions for single-nested (anti-)commutators:**

$$\begin{aligned} \int \frac{d^4\omega}{(2\pi)^4} \rho[1234] e^{-i(\omega_1 t_1 + \omega_2 t_2 + \omega_3 t_3 + \omega_4 t_4)} &\equiv \lambda^4 \langle [[[O(t_1), O(t_2)], O(t_3)], O(t_4)] \rangle_c, \\ \int \frac{d^4\omega}{(2\pi)^4} \rho[12_+3_+4_+] e^{-i(\omega_1 t_1 + \omega_2 t_2 + \omega_3 t_3 + \omega_4 t_4)} &\equiv \lambda^4 \langle \{ \{ O(t_1), O(t_2) \}, O(t_3) \}, O(t_4) \rangle_c, \\ \int \frac{d^4\omega}{(2\pi)^4} \rho[1234_+] e^{-i(\omega_1 t_1 + \omega_2 t_2 + \omega_3 t_3 + \omega_4 t_4)} &\equiv \lambda^4 \langle \{ [ [ O(t_1), O(t_2) ], O(t_3) ], O(t_4) \} \rangle_c, \\ \int \frac{d^4\omega}{(2\pi)^4} \rho[123_+4] e^{-i(\omega_1 t_1 + \omega_2 t_2 + \omega_3 t_3 + \omega_4 t_4)} &\equiv \lambda^4 \langle [ \{ [ O(t_1), O(t_2) ], O(t_3) \}, O(t_4) ] \rangle_c, \\ \int \frac{d^4\omega}{(2\pi)^4} \rho[12_+34] e^{-i(\omega_1 t_1 + \omega_2 t_2 + \omega_3 t_3 + \omega_4 t_4)} &\equiv \lambda^4 \langle [ [ \{ O(t_1), O(t_2) \}, O(t_3) ], O(t_4) ] \rangle_c, \text{ etc.} \end{aligned} \quad (5.71)$$

- **Spectral functions for double (anti-)commutators:**

$$\begin{aligned}
& \int \frac{d^4\omega}{(2\pi)^4} \rho[12][34] e^{-i(\omega_1 t_1 + \omega_2 t_2 + \omega_3 t_3 + \omega_4 t_4)} \equiv \lambda^4 \langle [O(t_1), O(t_2)][O(t_3), O(t_4)] \rangle_c \\
& \int \frac{d^4\omega}{(2\pi)^4} \rho[12_+][34_+] e^{-i(\omega_1 t_1 + \omega_2 t_2 + \omega_3 t_3 + \omega_4 t_4)} \equiv \lambda^4 \langle \{O(t_1), O(t_2)\}\{O(t_3), O(t_4)\} \rangle_c, \\
& \int \frac{d^4\omega}{(2\pi)^4} \rho[12_+][34] e^{-i(\omega_1 t_1 + \omega_2 t_2 + \omega_3 t_3 + \omega_4 t_4)} \equiv \lambda^4 \langle \{O(t_1), O(t_2)\}[O(t_3), O(t_4)] \rangle_c \\
& \int \frac{d^4\omega}{(2\pi)^4} \rho[12][34_+] e^{-i(\omega_1 t_1 + \omega_2 t_2 + \omega_3 t_3 + \omega_4 t_4)} \equiv \lambda^4 \langle [O(t_1), O(t_2)]\{O(t_3), O(t_4)\} \rangle_c, \text{ etc.}
\end{aligned} \tag{5.72}$$

Any quartic coupling  $g$  can be expressed as an integral of these spectral functions in the following manner:

$$g = \int_{C_4} \tilde{\mathcal{I}}[g] + \mathcal{O}(\lambda^6). \tag{5.73}$$

The domain of integration  $C_4$  is given by<sup>9</sup>

$$\int_{C_4} \equiv \int_{-\infty-i\epsilon_1}^{\infty-i\epsilon_1} \frac{d\omega_1}{2\pi} \int_{-\infty-i\epsilon_2}^{\infty-i\epsilon_2} \frac{d\omega_2}{2\pi} \int_{-\infty+i\epsilon_2}^{\infty+i\epsilon_2} \frac{d\omega_3}{2\pi} \int_{-\infty+i\epsilon_1}^{\infty+i\epsilon_1} \frac{d\omega_4}{2\pi} \tag{5.74}$$

where  $\epsilon_1$  and  $\epsilon_2$  are infinitesimally small positive numbers. We provide the dependence of the integrand  $\tilde{\mathcal{I}}[g]$  on the spectral functions for all the quartic couplings in tables 5.2 and 5.3.

---

<sup>9</sup>The domain  $C_4$  in frequency space is determined by the time domain over which the integrals in (5.27) and (C.12) are defined.



Table 5.2: Couplings with even parity under time-reversal

$g$	$\widetilde{I}[g]$
$\bar{\lambda}_4 - \frac{1}{2}\bar{\kappa}_4$	$\frac{3}{\omega_1\omega_4(\omega_3+\omega_4)}(-\rho[1234] + \rho[4321])$
$\bar{\zeta}_\mu^{(2)} - \frac{1}{24}\bar{\lambda}_4$	$\frac{1}{\omega_1\omega_4(\omega_3+\omega_4)}(\rho[1234] - \rho[4321])$
$\zeta_N^{(4)} + 3\bar{\mathcal{Q}}_4$	$-\frac{3i}{2\omega_1\omega_4(\omega_3+\omega_4)}(\rho[12_+3_+4_+] + \rho[43_+2_+1_+])$
$\bar{\zeta}_3 - \frac{1}{3}\zeta_N^{(4)}$	$\frac{4i}{\omega_1\omega_4(\omega_3+\omega_4)}(\rho[1234] + \rho[4321])$
$\kappa_4$	$-\frac{1}{2\omega_1\omega_4(\omega_3+\omega_4)}\left[(\rho[1234] - \rho[4321]) - \frac{1}{2}(\rho[1423] - \rho[4132] + \rho[2314] - \rho[3241])\right]$
$\mathcal{Q}_4$	$\frac{i}{2\omega_1\omega_4(\omega_3+\omega_4)}(-\rho[12_+3_+4_+] - \rho[4_+3_+2_+1_+] + \rho[14_+2_+3_+] + \rho[41_+3_+2_+] + \rho[2314_+] + \rho[3241_+])$
$\bar{\lambda}_{4\gamma} + 2\bar{\kappa}_{4\gamma}^I$	$\frac{i}{\omega_1^2\omega_4^2(\omega_3+\omega_4)^2}\left[(\omega_1(\omega_2 + \omega_1) - \omega_4(3\omega_2 + 5\omega_1))\rho[1234] - (\omega_4(\omega_3 + \omega_4) - \omega_1(3\omega_3 + 5\omega_4))\rho[4321]\right]$
$\bar{\zeta}_{3\gamma} - \frac{1}{2}\bar{\mathcal{Q}}_{4\gamma}^I$	$\frac{1}{4\omega_1^2\omega_4^2(\omega_3+\omega_4)^2}\left[(\omega_3 + \omega_4)(\omega_4 - \omega_1) - 2\omega_1\omega_4\right](\rho[12_+34] + \rho[43_+21]) + (\omega_3 + \omega_4)(\omega_4 - \omega_1)(\rho[123_+4] + \rho[432_+1]) + (\omega_3 + \omega_4)(\omega_4 + \omega_1)(\rho[1234_+] - \rho[4321_+])$
$\kappa_{4\gamma}^I$	$\frac{i}{4\omega_1^2\omega_4^2(\omega_3+\omega_4)^2}\left[(\omega_3 + \omega_4)(\omega_1 - \omega_4) + 2\omega_1\omega_4\right](\rho[12_+][34_+] - \rho[43_+][21_+]) + (\omega_3 + \omega_4)(\omega_1 - \omega_4)(\rho[13_+][24_+] - \rho[42_+][31_+]) - (\omega_3 + \omega_4)(\omega_4 + \omega_1)(\rho[14_+][23_+] - \rho[32_+][41_+])$
$\kappa_{4\gamma}^{II}$	$\frac{i}{4\omega_1^2\omega_4^2(\omega_3+\omega_4)^2}\left[(\omega_3 + \omega_4)(\omega_1 - \omega_4) + 2\omega_1\omega_4\right](\rho[12][34] - \rho[43][21]) + (\omega_3 + \omega_4)(\omega_1 - \omega_4)(\rho[13][24] - \rho[42][31]) - (\omega_3 + \omega_4)(\omega_4 + \omega_1)(\rho[14][23] - \rho[32][41])$
$\kappa_{4\gamma}^{III}$	$\frac{i}{8\omega_1^2\omega_4^2(\omega_3+\omega_4)^2}\left[(\omega_3 + \omega_4)(\omega_1 - \omega_4) + 2\omega_1\omega_4\right](\rho[4321] - \rho[1234] + \rho[2314] - \rho[3241] + \rho[2413] - \rho[3142]) + (\omega_3 + \omega_4)(\omega_1 - \omega_4)(\rho[4231] - \rho[1324] + \rho[2341] - \rho[3214] + \rho[3412] - \rho[2143])$
$\mathcal{Q}_{4\gamma}^I$	$\frac{1}{\omega_1^2\omega_4^2(\omega_3+\omega_4)^2}\left[-(\omega_3 + \omega_4)(\omega_1 - \omega_4) + 2\omega_1\omega_4\right](\rho[13][24] + \rho[42][31] + \rho[14][23] + \rho[32][41]) - (\omega_3 + \omega_4)(\omega_1 - \omega_4)(\rho[12][34] + \rho[43][21])$
$\mathcal{Q}_{4\gamma}^{II}$	$\frac{1}{4\omega_1^2\omega_4^2(\omega_3+\omega_4)^2}\left[(\omega_3 + \omega_4)(\omega_1 - \omega_4) + 2\omega_1\omega_4\right](\rho[12_+][34] + \rho[43_+][21] + \rho[12][34_+] + \rho[43][21_+]) + (\omega_3 + \omega_4)(\omega_1 - \omega_4)(\rho[13_+][24] + \rho[42_+][31] + \rho[13][24_+] + \rho[42][31_+]) - (\omega_3 + \omega_4)(\omega_1 + \omega_4)(\rho[14_+][23] + \rho[32_+][41] + \rho[14][23_+] + \rho[32][41_+])$

Table 5.3: Couplings with odd parity under time-reversal

$g$	$\widetilde{I}[g]$
$\bar{\kappa}_4$	$-\frac{6}{\omega_1\omega_4(\omega_3+\omega_4)}(\rho[1234] + \rho[4321])$
$\bar{\mathcal{Q}}_4$	$-\frac{2\omega_1\omega_4(\omega_3+\omega_4)}{\omega_1^2\omega_4^2(\omega_3+\omega_4)^2}\left[(\rho[12_+34] + \rho[123_+4] + \rho[1234_+]) - (\rho[43_+21] + \rho[432_+1] + \rho[4321_+])\right]$
$\bar{\lambda}_{4\gamma} - 24\zeta_{5\gamma}^{(2)}$ $-8(\kappa_{4\gamma}^I - \kappa_{4\gamma}^{II})$	$-\frac{2i}{\omega_1^2\omega_4^2(\omega_3+\omega_4)^2}\left[(\omega_3 + \omega_4)(\omega_1 - \omega_4) + 2\omega_1\omega_4\right](\rho[12][34_+] + \rho[43][21_+] - \rho[12_+][34] - \rho[43_+][21]) + (\omega_3 + \omega_4)(\omega_1 - \omega_4)(\rho[13][24_+] + \rho[42][31_+] - \rho[13_+][24] - \rho[42_+][31]) - (\omega_3 + \omega_4)(\omega_1 + \omega_4)(\rho[14][23_+] + \rho[32][41_+] - \rho[14_+][23] - \rho[32_+][41])$
$\bar{\kappa}_{4\gamma}^I$	$-\frac{i}{2\omega_1^2\omega_4^2(\omega_3+\omega_4)^2}\left[(\omega_1(\omega_2 + \omega_1) - \omega_4(3\omega_2 + 5\omega_1))\rho[1234] + (\omega_4(\omega_3 + \omega_4) - \omega_1(3\omega_3 + 5\omega_4))\rho[4321]\right]$
$\bar{\kappa}_{4\gamma}^{II}$	$\frac{i}{2\omega_1^2\omega_4^2(\omega_3+\omega_4)^2}(\omega_1 - \omega_4)(\rho[23][14] - \rho[14][23]) + (\omega_1 + \omega_4)(\rho[12][34] - \rho[43][21] + \rho[13][24] - \rho[42][31])$
$\bar{\mathcal{Q}}_{4\gamma}^I$	$-\frac{1}{2\omega_1^2\omega_4^2(\omega_3+\omega_4)^2}\left[(\omega_1 - \omega_4)(\omega_3 + \omega_4) + 2\omega_1\omega_4\right](\rho[12_+34] - \rho[43_+21]) + (\omega_1 - \omega_4)(\omega_3 + \omega_4)(\rho[123_+4] - \rho[432_+1]) - (\omega_1 + \omega_4)(\omega_3 + \omega_4)(\rho[1234_+] + \rho[4321_+])$
$\bar{\mathcal{Q}}_{4\gamma}^{II}$	$\frac{1}{2\omega_1^2\omega_4^2(\omega_3+\omega_4)^2}\left[-(\omega_1 - \omega_4)(\omega_3 + \omega_4) + \omega_1\omega_4\right](\rho[14][23_+] + \rho[32_+][41]) + \omega_1\omega_4(\rho[14_+][23] + \rho[32][41_+]) + \omega_1(\omega_3 + 2\omega_4)(\rho[13_+][24] + \rho[42][31_+]) - \omega_4(\omega_2 + 2\omega_1)(\rho[42_+][31] + \rho[13][24_+]) + \omega_1(\omega_3 + \omega_4)(\rho[12_+][34] + \rho[43][21_+]) - \omega_4(\omega_2 + \omega_1)(\rho[43_+][21] + \rho[12][34_+])$

Now, since all the couplings in tables 5.2 and 5.3 are real <sup>10</sup>, one can obtain alternative

<sup>10</sup>To see the reality of the OTO couplings, one can substitute relations like (5.28) in the expressions of these

expressions for them by taking complex conjugates of the corresponding integrals. Such a complex conjugation results in the following transformations in the integral:

1. All explicit factors of  $i$  go to  $(-i)$ .
2. In all factors involving the frequencies explicitly,  $\omega_i$  goes to  $\omega_i^*$  for  $i \in \{1, 2, 3, 4\}$ .
3. The spectral functions go to their complex conjugates.

Now, using the relation (5.63) which is based on the microscopic reversibility in the bath, one can obtain the following relations between the spectral functions:

$$\begin{aligned}
 (\rho\langle 1234 \rangle)^* &= \rho\langle 1^*2^*3^*4^* \rangle, \\
 (\rho[1234])^* &= \rho[1^*2^*3^*4^*], \\
 (\rho[12][34])^* &= \rho[1^*2^*][3^*4^*], \text{ etc.}
 \end{aligned} \tag{5.75}$$

On the right hand sides of these equations,  $i^*$  stands for  $\omega_i^*$ .

Hence, the net effect of the complex conjugation of the couplings is the replacement of all  $\omega_i$ 's by  $\omega_i^*$ 's and all explicit factors of  $i$  by  $(-i)$  in the corresponding frequency integrals. The complex conjugation of the frequencies takes the domain of integration to  $C_4^*$ , the integral over which is defined as

$$\int_{C_4^*} \equiv \int_{-\infty+i\epsilon_1}^{\infty+i\epsilon_1} \frac{d\omega_1^*}{2\pi} \int_{-\infty+i\epsilon_2}^{\infty+i\epsilon_2} \frac{d\omega_2^*}{2\pi} \int_{-\infty-i\epsilon_2}^{\infty-i\epsilon_2} \frac{d\omega_3^*}{2\pi} \int_{-\infty-i\epsilon_1}^{\infty-i\epsilon_1} \frac{d\omega_4^*}{2\pi}. \tag{5.76}$$

Now, notice that the domain  $C_4^*$  gets mapped exactly back to  $C_4$  under the following relabeling of the frequencies:

$$\omega_1^* \rightarrow \omega_4, \omega_2^* \rightarrow \omega_3, \omega_3^* \rightarrow \omega_2, \omega_4^* \rightarrow \omega_1. \tag{5.77}$$

Therefore, to summarise, the alternative expressions for the couplings can be obtained by integrating over the same domain  $C_4$ , but performing the following transformations on the integrands in the original expressions:

1.  $i \rightarrow -i$  for all explicit factors of  $i$ ,
2.  $\omega_1 \leftrightarrow \omega_4, \omega_2 \leftrightarrow \omega_3$ .

---

couplings given in table C.3.

We define the action of time-reversal on the couplings to be the above transformations on the integrands in their expressions. As we saw, the equality between the couplings and their time-reversed counterparts crucially relies on the relations given in (5.75) which are based on the microscopic reversibility in the bath's dynamics.

Now, one can compare the expressions of the couplings given in tables 5.2 and 5.3 with the expressions of their time-reversed counterparts. While making these comparisons, it is important to bear in mind that the spectral functions include a delta function corresponding to energy conservation in the unperturbed dynamics of the bath. This allows one to impose conditions such as

$$(\omega_1 + \omega_2) = -(\omega_3 + \omega_4) \quad (5.78)$$

within the expressions of the integrands. Taking this into account one can easily see, that the expressions for the couplings in table 5.2 remain unchanged under time-reversal. On the other hand, the expressions for the couplings in table 5.3 pick up a minus sign under time-reversal. Thus, all the couplings mentioned in table 5.2 have even parity under time-reversal, whereas the couplings in table 5.3 have odd parity under the same. All the couplings with odd parity must go to zero due to the microscopic reversibility in the bath's dynamics. This imposes the following constraints on the effective couplings:

$$\boxed{\bar{\kappa}_4 = \bar{\varrho}_4 = \bar{\kappa}_{4\gamma}^I = \bar{\kappa}_{4\gamma}^{II} = \bar{\varrho}_{4\gamma}^I = \bar{\varrho}_{4\gamma}^{II} = 0,} \quad (5.79)$$

$$\boxed{\bar{\lambda}_{4\gamma} - 24\zeta_\gamma^{(2)} - 8(\kappa_{4\gamma}^I - \kappa_{4\gamma}^{II}) = 0.} \quad (5.80)$$

Since these constraints are based on the microscopic reversibility in the bath, one can think of them as generalisations of the Onsager reciprocal relations [38,39]. These generalised Onsager relations are extensions of similar relations obtained between the cubic effective couplings in chapter 4.

As we mentioned earlier, apart from the microscopic reversibility in the bath's dynamics, there is another source of relations between the effective couplings of the particle, viz. the thermality of the bath. In the next subsection, we will discuss how the KMS relations [41,42,64] between the thermal correlators of the bath lead to constraints on the quartic effective couplings. We will see that these constraints, when combined with the relation given in (5.80), give rise to a generalised fluctuation-dissipation relation between the thermal jitter in the particle's damping

and the non-Gaussianity in the distribution of the noise.

#### 5.4.4 Generalised fluctuation-dissipation relation

In section 5.3.3, we saw that if we ignore the quartic couplings in the Schwinger-Keldysh effective theory, the corresponding stochastic dual reduces to a linear Langevin dynamics (see (5.32) and (5.33)). Under this dynamics, the particle experiences a damping as well as a random force drawn from a Gaussian distribution. These two forces are related to each other since both of them arise from the interaction with the bath. More precisely, in the high temperature limit of the bath, the relation between these forces is given by

$$\langle f^2 \rangle = \frac{2}{\beta} \gamma, \quad (5.81)$$

where  $\langle f^2 \rangle$  is the strength of the thermal noise experienced by the particle and  $\gamma$  is its damping coefficient. This relation is commonly known as the ‘fluctuation-dissipation relation’.

As discussed in [41, 47], the fluctuation-dissipation relation is a consequence of certain relations between the 2-point thermal correlators of the bath, which are now commonly known as the Kubo-Martin-Schwinger (KMS) relations [41, 42]. These relations were studied for higher point thermal correlators in [64]. There, it was observed that such KMS relations can connect the thermal OTOCs of a bath to its Schwinger-Keldysh correlators. This indicated the need for including the effects of the bath’s OTOCs while exploring the possibility of finding generalisations of the fluctuation-dissipation relation.

To include the effects of the OTOCs of the bath, we developed an OTO effective theory of the particle up to cubic terms in chapter 2. The cubic couplings in this effective theory receive contributions from the 3-point correlators of the bath. In chapter 3, we obtained a spectral representation of such 3-point thermal OTOCs by exploiting the microscopic unitarity of the bath as well as the KMS relations. This spectral representation showed that the KMS relations imply that all the 3-point OTOCs of the bath can be expressed in terms of two spectral functions of the bath. By expressing the cubic couplings in the particle’s OTO effective dynamics in terms of these spectral functions we derived an OTO generalisation of the fluctuation-dissipation relation (FDR) in 4. There we saw that, when combined with the constraints imposed by microscopic reversibility in the bath, this relation leads to a generalised FDR between a non-Gaussianity in the noise distribution and a jitter in the particle’s damping coefficient.

Now, we will see that a similar generalised fluctuation-dissipation relation holds between the quartic effective couplings as well. Before discussing this relation, we will first briefly review the KMS relations between thermal correlators and the derivation of the fluctuation-dissipation relation for the convenience of the reader.

### Kubo-Martin-Schwinger relations:

The KMS relations [41, 42, 64] connect all thermal correlators of the bath which can be obtained from each other by cyclic permutations of insertions. For example, consider the following  $n$ -point correlator

$$\langle O(t_1)O(t_2)\cdots O(t_n)\rangle = \text{Tr}\left[\frac{e^{-\beta H_B}}{Z_B}O(t_1)O(t_2)\cdots O(t_n)\right]. \quad (5.82)$$

In the above expression, if we bring the insertion  $O(t_n)$  from the right-most position to the left-most position across the thermal density matrix, the argument of the insertion picks up an extra term  $(-i\beta)$  i.e.

$$\langle O(t_1)O(t_2)\cdots O(t_n)\rangle = \langle O(t_n - i\beta)O(t_1)\cdots O(t_{n-1})\rangle. \quad (5.83)$$

In frequency space, these relations lead to the following kind of relations between the spectral functions:

$$\rho\langle 12\cdots n\rangle = e^{-\beta\omega_n}\rho\langle n\ 1\cdots(n-1)\rangle. \quad (5.84)$$

Here  $\rho\langle 12\cdots n\rangle$  and  $\rho\langle n\ 1\cdots(n-1)\rangle$  are defined in terms of the  $n$ -point cumulants of  $O$  in the time domain as follows:

$$\begin{aligned} \int_{-\infty}^{\infty} \frac{d\omega_1}{2\pi} \cdots \int_{-\infty}^{\infty} \frac{d\omega_n}{2\pi} \rho\langle 12\cdots n\rangle e^{-i(\omega_1 t_1 + \cdots + \omega_n t_n)} &\equiv \lambda^n \langle O(t_1)O(t_2)\cdots O(t_n)\rangle_c, \\ \int_{-\infty}^{\infty} \frac{d\omega_1}{2\pi} \cdots \int_{-\infty}^{\infty} \frac{d\omega_n}{2\pi} \rho\langle n\ 1\cdots(n-1)\rangle e^{-i(\omega_1 t_1 + \cdots + \omega_n t_n)} &\equiv \lambda^n \langle O(t_n)O(t_1)\cdots O(t_{n-1})\rangle_c. \end{aligned} \quad (5.85)$$

In general, there are  $n!$  such spectral functions corresponding to all the  $n$ -point Wightman correlators of  $O$ . However, KMS relations like (5.84) reduce the number of independent  $n$ -point spectral functions to  $(n-1)!$ .

Let us now review how such KMS relations between the bath's correlators lead to the fluctuation-dissipation relation given in (5.81).

### Fluctuation-dissipation relation between quadratic couplings:

The couplings in the quadratic terms of the effective action receive contributions from the 2-point cumulants of the operator  $O$  as shown in (5.26). These quadratic couplings up to leading order in  $\lambda$  can be re-expressed in terms of two spectral functions  $\rho[12]$  and  $\rho[12_+]$  which are defined as

$$\begin{aligned} \int_{-\infty}^{\infty} \frac{d\omega_1}{2\pi} \int_{-\infty}^{\infty} \frac{d\omega_2}{2\pi} \rho[12] e^{-i(\omega_1 t_1 + \omega_2 t_2)} &\equiv \lambda^2 \langle [O(t_1), O(t_2)] \rangle_c, \\ \int_{-\infty}^{\infty} \frac{d\omega_1}{2\pi} \int_{-\infty}^{\infty} \frac{d\omega_2}{2\pi} \rho[12_+] e^{-i(\omega_1 t_1 + \omega_2 t_2)} &\equiv \lambda^2 \langle \{O(t_1), O(t_2)\} \rangle_c. \end{aligned} \quad (5.86)$$

We provide the expressions for these leading order forms of the quadratic couplings below:

$$Z_I = - \int_{C_2} \frac{\rho[12_+]}{i\omega_1^3}, \quad \Delta\bar{\mu}^2 = - \int_{C_2} \frac{\rho[12]}{\omega_1}, \quad \langle f^2 \rangle = \int_{C_2} \frac{\rho[12_+]}{i\omega_1}, \quad \gamma = \int_{C_2} \frac{\rho[12]}{i\omega_1^2}. \quad (5.87)$$

Here, the integrals are performed over the following domain

$$\int_{C_2} \equiv \int_{-\infty-i\epsilon}^{\infty-i\epsilon} \frac{d\omega_1}{2\pi} \int_{-\infty+i\epsilon}^{\infty+i\epsilon} \frac{d\omega_2}{2\pi}, \quad (5.88)$$

where  $\epsilon$  is a small positive number.

Now, the KMS relations connect the two spectral functions as follows

$$\rho[12_+] = \coth\left(\frac{\beta\omega_1}{2}\right) \rho[12]. \quad (5.89)$$

Then, in the high temperature limit of the bath i.e. the small  $\beta$  limit, the above relation reduces to

$$\rho[12_+] = \left(\frac{2}{\beta\omega_1}\right) \rho[12], \quad (5.90)$$

where we take the leading order (in  $\beta$ ) forms of the two spectral functions. Plugging this relation into the expressions of the couplings given in (5.87), we get

$$Z_I = -\frac{2}{\beta} \int_{C_2} \frac{\rho[12]}{i\omega_1^4}, \quad \Delta\bar{\mu}^2 = - \int_{C_2} \frac{\rho[12]}{\omega_1}, \quad \langle f^2 \rangle = \frac{2}{\beta} \int_{C_2} \frac{\rho[12]}{i\omega_1^2}, \quad \gamma = \int_{C_2} \frac{\rho[12]}{i\omega_1^2}. \quad (5.91)$$

From these expressions, one can clearly see that at this high temperature limit,

$$\boxed{\langle f^2 \rangle = \frac{2}{\beta} \gamma}, \quad (5.92)$$

which is the fluctuation-dissipation relation that we mentioned earlier.

Let us now discuss how one can obtain a generalisation of this fluctuation-dissipation relation for the quartic couplings.

### Generalised fluctuation-dissipation relation between quartic couplings:

As pointed out in [64], the KMS relations between the 4-point functions of the bath can connect OTOCs to Schwinger-Keldysh correlators. For example, consider the correlator

$$\langle O(t_1)O(t_3)O(0)O(t_2) \rangle \equiv \text{Tr} \left[ \frac{e^{-\beta H_B}}{Z_B} O(t_1)O(t_3)O(0)O(t_2) \right], \quad (5.93)$$

where  $t_1 > t_2 > t_3 > 0$ . Notice that this correlator satisfies the following KMS relation:

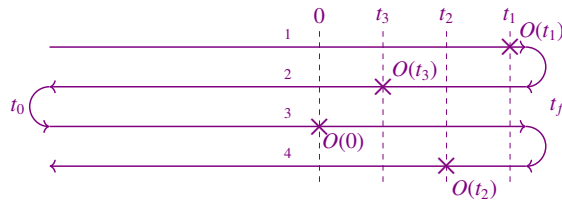
$$\langle O(t_1)O(t_3)O(0)O(t_2) \rangle = \langle O(t_2 - i\beta)O(t_1)O(t_3)O(0) \rangle. \quad (5.94)$$

This KMS relation connects the correlator given in (5.93) to the following correlator by analytic continuation:

$$\langle O(t_2)O(t_1)O(t_3)O(0) \rangle \equiv \text{Tr} \left[ \frac{e^{-\beta H_B}}{Z_B} O(t_2)O(t_1)O(t_3)O(0) \right]. \quad (5.95)$$

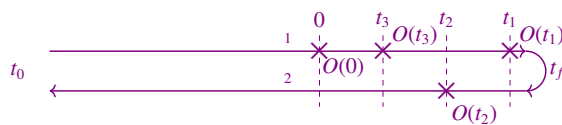
The correlator given in (5.93) is an OTOC which can be obtained by putting insertions on the 2-fold contour as shown in figure 5.4. On the other hand, the correlator given in (5.95) is a

Figure 5.4: Contour-ordered correlator for  $\langle O(t_1)O(t_3)O(0)O(t_2) \rangle$  where  $t_1 > t_2 > t_3 > 0$



Schwinger-Keldysh correlator as demonstrated in figure 5.5.

Figure 5.5: Contour-ordered correlator for  $\langle O(t_2)O(t_1)O(t_3)O(0) \rangle$  where  $t_1 > t_2 > t_3 > 0$



We will see that KMS relations like (5.94) which connect OTO correlators of the bath to Schwinger-Keldysh correlators result in a relation between a quartic OTO coupling and a Schwinger-Keldysh coupling of the particle. To derive this relation, we need to go back to the expressions of the particle's effective couplings in terms of the bath's spectral functions given in tables 5.2 and 5.3. As discussed earlier, the KMS relations reduce the number of independent 4-point spectral functions to  $(4 - 1)! = 6$ . We choose these 6 independent spectral functions to be the following<sup>11</sup>:

$$\rho[1234], \rho[4321], \rho[2314], \rho[3241], \rho[2143], \rho[3142]. \quad (5.96)$$

We provide the expressions of the quartic effective couplings in terms of these 6 spectral functions at the high temperature limit of the bath in appendix C.4. Among these expressions, we will focus on the forms of two particular couplings here:  $\kappa_{4\gamma}^I$  and  $\zeta_N^{(4)}$ . From the expressions of these couplings given in tables C.4 and C.5, we can see that the corresponding integrands satisfy the following relation:

$$\begin{aligned} \widetilde{\mathcal{I}}[\kappa_{4\gamma}^I] &= \frac{\beta}{4} \widetilde{\mathcal{I}}[\zeta_N^{(4)}] \\ &= \frac{6i}{\beta^2 \omega_1^2 \omega_2 \omega_3 \omega_4^2 (\omega_1 + \omega_3)(\omega_1 + \omega_4)(\omega_3 + \omega_4)^2} \\ &\quad \left[ \omega_1(\omega_1 + \omega_4)(\omega_4^2 - \omega_2 \omega_3) \rho[1234] + \omega_4(\omega_1 + \omega_3)(\omega_1 + \omega_4)(\omega_3 + \omega_4) \rho[4321] \right. \\ &\quad \left. - \omega_1 \omega_4 (\omega_1 + \omega_3)(\omega_1 + \omega_4) \rho[2143] + \omega_1 \omega_2 (\omega_3^2 - \omega_4^2) \rho[2314] \right. \\ &\quad \left. + \omega_1 \omega_4 (\omega_1 + \omega_4)(\omega_3 + \omega_4) \rho[3142] - \omega_4 \omega_2 (\omega_1 + \omega_3)(\omega_3 + \omega_4) \rho[3241] \right], \end{aligned} \quad (5.97)$$

where we take only the leading order (in  $\beta$ ) forms for the spectral functions. From this relation between the integrands, we conclude that at leading order in  $\lambda$  and  $\beta$ , these two couplings satisfy the following relation:

$$\boxed{\kappa_{4\gamma}^I = \frac{\beta}{4} \zeta_N^{(4)}}. \quad (5.98)$$

This is an example of a generalisation of the fluctuation-dissipation relation which connects an OTO coupling to a Schwinger-Keldysh coupling. From this analysis, one can see that this relation is purely a consequence of KMS relations between the bath's correlators and holds even when the bath's dynamics lacks microscopic reversibility.

<sup>11</sup>See appendix C.4 for the relation between this basis of the 4-point spectral functions and the basis introduced in chapter 3.



In the presence of microscopic reversibility in the bath, there is an additional relation which involves the coupling  $\kappa_{4\gamma}^I$ . This is one of the generalised Onsager relations given in (5.80) which we quote here once more for convenience:

$$\bar{\lambda}_{4\gamma} - 24\zeta_{5\gamma}^{(2)} - 8(\kappa_{4\gamma}^I - \kappa_{4\gamma}^{II}) = 0. \quad (5.99)$$

Now, referring to the expressions of the leading order forms of the couplings  $\bar{\lambda}_{4\gamma}$  and  $\kappa_{4\gamma}^{II}$  given in tables C.4 and C.5, we see that the corresponding integrands are as follows:

$$\begin{aligned} \tilde{\mathcal{I}}[\bar{\lambda}_{4\gamma}] &= \frac{2i}{\omega_1^2 \omega_4^2 (\omega_3 + \omega_4)^2} \{3(\omega_4 - \omega_1)(\omega_3 + \omega_4) + 2\omega_1 \omega_3\} \rho[1234], \\ \tilde{\mathcal{I}}[\kappa_{4\gamma}^{II}] &= \frac{i}{4\omega_1^2 \omega_4^2 (\omega_3 + \omega_4)^2} \left[ (\omega_1 - \omega_4)(\omega_3 + \omega_4) (\rho[1234] + \rho[2314] + \rho[3142]) \right. \\ &\quad \left. + (\omega_1 + \omega_4)(\omega_3 + \omega_4) (\rho[2314] + \rho[3241]) \right. \\ &\quad \left. + ((\omega_1 - \omega_4)(\omega_3 + \omega_4) + 2\omega_1 \omega_4) (\rho[1234] + \rho[2143]) \right]. \end{aligned} \quad (5.100)$$

Notice that these integrands are suppressed by a factor of  $\beta^2$  compared to the integrand for  $\kappa_{4\gamma}^I$  given in (5.97). Therefore, in the high temperature limit, we can ignore the couplings  $\bar{\lambda}_{4\gamma}$  and  $\kappa_{4\gamma}^{II}$  in (5.80) to get

$$\boxed{\kappa_{4\gamma}^I = -3\zeta_{5\gamma}^{(2)}}. \quad (5.101)$$

Combining the equations (5.101) and (5.98), we get the following relation in the high temperature limit:

$$\boxed{\zeta_N^{(4)} = -\frac{12}{\beta} \zeta_{5\gamma}^{(2)}}. \quad (5.102)$$

This is a generalised fluctuation-dissipation relation which connects the non-Gaussianity in the noise experienced by the particle to the thermal jitter in its damping coefficient. It is a combined effect of microscopic reversibility in the bath and its thermality. In the following subsection, we will compute the effective couplings in the  $qXY$  model and verify the validity of this relation.

### 5.4.5 Values of the effective couplings

In this subsection, we will enumerate the values of the effective couplings of the Brownian particle in the  $qXY$  model.

The forms of the quadratic couplings at leading order in  $\lambda$  and  $\beta$  are given in (5.91) in terms of the 2-point function  $\rho[12]$ . Similar forms for the quartic couplings are given in tables C.4

and C.5 in terms of the 4-point spectral functions enumerated in (5.96).

We provide the leading order (in  $\beta$ ) forms of the 2-point spectral function  $\rho[12]$  and the 4-point spectral function  $\rho[1234]$  for the  $qXY$  model in (5.103) and (5.104) respectively.

$$\rho[12] = 2\pi\delta(\omega_1 + \omega_2) \frac{\Gamma_2}{\beta} \frac{4\omega_1\Omega^3}{\omega_1^2 + 4\Omega^2}. \quad (5.103)$$

$$\begin{aligned} \rho[1234] = & 2\pi\delta(\omega_1 + \omega_2 + \omega_3 + \omega_4) \left( 16i \frac{\Gamma_4 \Omega^7}{\beta} \right) \\ & \left[ \left\{ \frac{(\Omega - i\omega_3)(\Omega - i(\omega_1 + \omega_3))}{\omega_3(\omega_1 + \omega_3)(2\Omega - i\omega_3)(2\Omega + i\omega_4)(2\Omega - i(\omega_1 + \omega_3))} \right. \right. \\ & - \frac{(\Omega + i\omega_2)(\Omega + i(\omega_1 + \omega_2))}{\omega_2(\omega_1 + \omega_2)(2\Omega + i\omega_2)(2\Omega - i\omega_4)(2\Omega + i(\omega_1 + \omega_2))} \\ & + \frac{\omega_4\Omega(\Omega - i\omega_1)}{\omega_1\omega_3(\omega_1 + \omega_2)(2\Omega - i\omega_1)(2\Omega + i\omega_3)(2\Omega - i(\omega_1 + \omega_2))} \\ & \left. \left. - \frac{\omega_4\Omega(\Omega + i\omega_1)}{\omega_1\omega_2(\omega_1 + \omega_3)(2\Omega + i\omega_1)(2\Omega - i\omega_2)(2\Omega + i(\omega_1 + \omega_3))} \right\} \right. \\ & \left. - \left\{ (\omega_1 \leftrightarrow \omega_2) \right\} \right]. \quad (5.104) \end{aligned}$$

The other five 4-point spectral functions can be obtained from (5.104) by appropriate permutations of the frequencies.

Substituting these spectral functions in the integrals for the couplings, one can calculate the values of these couplings in the high temperature limit. We provide the values of the quadratic couplings in (5.105), the Schwinger-Keldysh quartic couplings in (5.106), and the OTO quartic couplings in (5.107) and (5.108).

### Quadratic couplings:

$$\boxed{Z_I = \frac{\Gamma_2}{4\beta^2\Omega}, \Delta\bar{\mu}^2 = -\frac{\Gamma_2\Omega^2}{\beta}, \langle f^2 \rangle = \frac{\Gamma_2\Omega}{\beta^2}, \gamma = \frac{\Gamma_2\Omega}{2\beta}.} \quad (5.105)$$

### Quartic couplings:

A) **Schwinger-Keldysh couplings:**

$$\boxed{\begin{aligned} \zeta_N^{(4)} &= -\frac{15\Gamma_4\Omega}{\beta^4}, \quad \bar{\lambda}_4 = -\frac{6\Gamma_4\Omega^4}{\beta}, \quad \bar{\zeta}_3 = -\frac{6\Gamma_4\Omega^3}{\beta^2}, \quad \zeta_\mu^{(2)} = -\frac{5\Gamma_4\Omega^2}{2\beta^3}, \\ \bar{\lambda}_{4\gamma} &= -\frac{6\Gamma_4\Omega^3}{\beta}, \quad \bar{\zeta}_{3\gamma} = -\frac{15\Gamma_4\Omega^2}{4\beta^2}, \quad \zeta_\gamma^{(2)} = \frac{5\Gamma_4\Omega}{4\beta^3}. \end{aligned}} \quad (5.106)$$

B) **OTO couplings:**

$$\boxed{\tilde{\kappa}_4 = \tilde{\varrho}_4 = \tilde{\kappa}_{4\gamma}^I = \tilde{\kappa}_{4\gamma}^{II} = \tilde{\varrho}_{4\gamma}^I = \tilde{\varrho}_{4\gamma}^{II} = 0.} \quad (5.107)$$

$$\boxed{\begin{aligned} \kappa_4 &= -\frac{3\Gamma_4\Omega^4}{2\beta}, \quad \varrho_4 = \frac{7\Gamma_4\Omega^3}{2\beta^2}, \quad \kappa_{4\gamma}^I = -\frac{15\Gamma_4\Omega}{4\beta^3}, \quad \kappa_{4\gamma}^{II} = \frac{5\Gamma_4\Omega^3}{8\beta}, \\ \kappa_{4\gamma}^{III} &= -\frac{19\Gamma_4\Omega^3}{16\beta}, \quad \varrho_{4\gamma}^I = -\frac{15\Gamma_4\Omega^2}{4\beta^2}, \quad \varrho_{4\gamma}^{II} = \frac{5\Gamma_4\Omega^2}{2\beta^2}. \end{aligned}} \quad (5.108)$$

From the values of these couplings, one can easily verify the validity of the fluctuation dissipation relation (5.92), the generalised fluctuation dissipation relation (5.102), and the generalised Onsager relations (5.79) and (5.101) in the  $qXY$  model.

## 5.5 Conclusion and discussion

In this chapter, we have developed the quartic effective dynamics of a Brownian particle weakly interacting with a thermal bath. To illustrate the features of this effective dynamics, we have introduced a simple toy model (the  $qXY$  model described in section 5.2) where the bath comprises of two sets of harmonic oscillators coupled to the particle through cubic interactions.

For this model, we have identified a Markovian regime, where the particle's effective dynamics is approximately local in time. Working in this regime, we have constructed a quartic effective action of the particle in the Schwinger-Keldysh (SK) formalism. Using the techniques developed in [61–63], we have demonstrated a duality between this quantum effective theory and a classical stochastic dynamics governed by a non-linear Langevin equation.

The SK effective theory and the dual non-linear Langevin dynamics suffer from the limitation that they provide no information about the 4-point out of time order correlators (OTOCs) of the particle. To transcend this limitation, we have extended the SK effective action to an out of time ordered effective action defined on a generalised Schwinger-Keldysh contour (see

figure 2.3). In this extended framework, we have determined the additional quartic couplings which encode the effects of the bath's 4-point OTOCs on the particle's dynamics. We have worked out the dependence of these OTO couplings (as well as the SK effective couplings) on the correlators of the bath up to leading order in the particle-bath interaction. As in case of the cubic effective theory, a stochastic dynamics which is dual to the quartic OTO effective theory is still lacking. Working out such a dual stochastic dynamics would shed more light on the significance of the different couplings appearing in the OTO dynamics of the particle.

The relations between the particle's effective couplings and the bath's correlators provide a way to analyse the constraints imposed on the effective dynamics due to thermality and microscopic reversibility of the bath. These constraints manifest in the form of certain relations between the quartic couplings which can be interpreted as OTO generalisations of the well-known Onsager reciprocal relations and fluctuation-dissipation relation (FDR). By combining these relations, we have obtained a generalised FDR which connects two of the Schwinger-Keldysh effective couplings. In the dual stochastic dynamics, these two couplings correspond to a thermal jitter in the damping coefficient and a non-Gaussianity in the noise distribution. The generalised FDR between these two quartic couplings is an extension of a similar relation obtained for the cubic effective dynamics in chapter 4.

The generalised FDRs and Onsager relations in both the cubic and the quartic effective theories of the particle suggest that such relations probably hold for even higher degree terms in the effective action when the bath's microscopic dynamics is reversible. It would be interesting to identify the general form of these relations.

Although the construction of the quartic effective theory in this chapter is demonstrated with the  $qXY$  model, the analysis mostly relies on the validity of the Markov approximation for the particle's dynamics. Hence, it may be employed to study the effective theory of the particle when it interacts with more complicated baths. For instance, the bath may even be a strongly coupled system<sup>12</sup> in which case a microscopic analysis of the particle's dynamics is very difficult. In such a scenario, the quartic effective theory of the particle would allow one to determine the particle's 4-point correlators (including its OTOCs) in terms of the effective couplings.

For the  $qXY$  model studied in this chapter, the bath's 4-point cumulants decay exponentially when the time interval between any two insertions is increased. This allowed us to work in a

---

<sup>12</sup>Notice that we have assumed a weak coupling only between the particle and the bath. The couplings between the internal degrees of freedom of the bath may be strong.

Markovian regime by tuning the parameters in the model such that the particle's evolution is much slower than the decay of the bath's cumulants. However, as pointed out in section 2.4, such an exponential damping of the bath's cumulants is not strictly necessary in all time regimes for obtaining a nearly local dynamics of the particle. In fact, the Markov approximation for the particle's dynamics may be valid even for a chaotic bath <sup>13</sup> [65–68] as long as the bath's OTO cumulants saturate to sufficiently small values much faster than the particle's evolution [29]. This opens up the possibility of probing the Lyapunov exponents [5] in such chaotic baths by measuring the OTO effective couplings of the particle [29] (See the relations between the particle's OTO effective couplings and the bath's OTOCs given in (C.12) and table C.3).

The applicability of our effective theory framework to the scenario where the bath is chaotic and strongly coupled indicate that it is possible to construct a holographic dual description [155–163] of the particle's non-linear dynamics. Recently, such a holographic dual description was constructed in [164] for the nonlinear Langevin dynamics discussed in this chapter. The generalised FDR between the non-Gaussianity in the noise and the thermal jitter in the damping coefficient was verified to hold in this holographic setting. It would be interesting to extend this holographic prescription to the quartic OTO effective theory discussed in this chapter.

The non-linear Langevin equation that we discussed in section 5.3.3 has a structural similarity with the equations of motion of damped anharmonic oscillators like the Van der Pol oscillator [165] and the Duffing oscillator [166] <sup>14</sup>. Such oscillators, under periodic driving, are known to exhibit chaos in appropriate parameter regimes [166–168]. It would be interesting to see whether one can find a similar regime in the non-linear Langevin dynamics where the particle undergoes a chaotic motion.

It will be useful to formulate a Wilsonian counterpart of the out of time ordered 1-PI effective action developed in this chapter. Such a Wilsonian effective theory can be extended to open quantum field theories [57, 70, 169–175] which show up in the study of quantum cosmology and heavy ion physics. It will be interesting to determine the RG flow [57] of the OTO couplings in this Wilsonian framework to estimate their relative importance at different energy scales.

Finally, we would like to emphasise that the OTO effective dynamics discussed in this chapter, as well as in chapters 2 and 4, are steps towards constructing similar effective the-

---

<sup>13</sup>The OTO cumulants in such chaotic baths show an exponentially fast fall-off initially (in the Lyapunov regime) before saturating to some constant values.

<sup>14</sup>The major difference is the presence of a thermal noise in the Langevin dynamics.

ories for more general open quantum systems. When the microscopic details of the (system+environment) is too complicated to be solved exactly, such an effective theory can immensely simplify the study of scrambling, thermalisation and build-up of entanglement in such systems. The OTO couplings that enter in such effective theories would be generalisations of the transport coefficients that appear in the SK effective dynamics. They would determine the spread of entanglement between the system and the environment, as well as the same between the different components of the system. We hope that such an interpretation of the effective OTO couplings would emerge in future studies on the subject.

# Chapter 6

## Conclusion

### 6.1 Summary of the thesis

In this thesis, we introduced an effective theory framework for computing out of time ordered correlators of a Brownian particle weakly coupled to an environment. In chapter 1, we discussed the basic motivations for developing such an OTO effective theory framework.

In chapter 2, we started the analysis of this OTO effective theory by first reviewing the simpler effective dynamics governing the evolution of the particle's reduced density matrix. We saw that in a Markovian limit, this effective theory can be formulated in terms of an action in the Schwinger-Keldysh formalism [35–37, 54, 55]. We discussed how the form of this effective action is constrained by the microscopic unitarity of the (particle+environment) combined system. By using these constraints, we identified all the possible cubic terms in the effective action which have at most a single time derivative acting on the position of the particle. We showed how the coefficients of these cubic terms are determined upto the leading order in the particle-environment coupling by the Schwinger-Keldysh 3-point correlators of the environment. We argued that these cubic SK effective couplings fail to capture the contributions of the environment's 3-point OTOCs to the particle's dynamics. Moreover, they are also inadequate for computing OTOCs of the particle. To overcome these limitations we extended the particle's effective dynamics to an OTO contour (a contour with two time folds). We saw that in this extended framework, one needs to introduce some additional couplings which encode the contributions of the environment's OTOCS. We also determined how these OTO couplings enter in the expressions for the particle's 3-point OTO correlators.

In chapter 3, we started discussing the special case where the environment is in a thermal

state. We saw that correlators of such a thermal environment (with insertions ordered along an OTO contour) are constrained to satisfy some relations due to unitarity and thermality. We showed that these relations can be exploited to come up with convenient spectral representations of these contour-ordered thermal correlators. In these representations, the thermal correlators are expressed in terms of a minimal set of independent objects called ‘spectral functions’. These spectral functions when multiplied to appropriate tensor structures generate the Fourier transforms of the array of contour-ordered thermal correlators. We showed that these tensor structures can be neatly expressed as linear combinations of tensor products of some column vectors which are independent of the particular theory governing the thermal bath. We discussed how these column vectors can provide an OTO generalisation of the familiar retarded-advanced basis in the Schwinger-Keldysh formalism [95]. This generalised retarded-advanced basis can immensely simplify the diagrammatic analysis of thermal OTOCs in interacting theories. This simplification is possible due to a drastic reduction in the number of non-zero propagators in this basis compared to the original basis of fields on the different legs of the multi-folded contour. Another utility of these spectral representations, which is more relevant to this thesis, is that they clearly show the relations satisfied by the bath’s OTOCs and express these OTOCs in terms of a smaller number of spectral functions. We used these spectral functions to study the constraints imposed on the particle’s dynamics by the bath’s thermality in chapters 4 and 5.

In chapter 4, we returned to our analysis of the cubic effective theory of the Brownian particle, but now with the additional condition that the environment is a thermal bath governed by a reversible dynamics. To develop the main ideas of this chapter, we introduced a simple toy model which is a simple extension of the well-known Caldeira-Leggett model [58]. In this model, the particle is coupled to two harmonic baths (at the same temperature) via interactions which are bilinear in the positions of the particle and the bath oscillators. On top of such bilinear interactions, we introduced small cubic interactions involving the particle and two of the bath oscillators (one from each set). For this simple model, we determined a Markovian regime where the cubic effective theory introduced in chapter 2 is valid. Following the methods developed in [61–63], we showed that the Schwinger-Keldysh version of this effective theory is dual to a nonlinear Langevin dynamics with a non-Gaussian noise distribution. Apart from the non-Gaussianity in the noise, this Langevin dynamics also included thermal jitters to the frequency and the damping of the particle. We carefully analysed the high-temperature limit of the cou-



plings in this nonlinear dynamics (as well as its OTO extension) for our toy model. We observed that there were certain relations between the couplings in the Langevin theory and its OTO extension. We demonstrated that these relations stem from the microscopic reversibility and the thermality of the bath. Hence, they provide OTO generalisations of the Onsager-Casimir reciprocal relations [38–40] and the fluctuation-dissipation relation [44–46, 176]. Combining these relations, we obtained a generalised FDR which related two of the cubic Schwinger-Keldysh couplings. At the level of the Langevin theory this connected the non-Gaussianity in the noise distribution to the thermal jitter in the particle’s damping coefficient.

In chapter 5, we extended the analysis of the OTO effective dynamics by including the quartic terms in the effective action. To simplify this analysis, we slightly modified the microscopic model of the particle-bath interaction described in the chapter 4 by turning off the Caldeira-Leggett-like bilinear interactions. We saw that this resulted in the vanishing of the cubic terms in the effective action allowing us to focus on the quartic terms as the leading order correction to the quadratic theory. Again working in a Markovian regime, we identified all the quartic terms in the Schwinger-Keldysh (SK) effective action (upto a single time derivative acting on the position of the particle). We demonstrated that, just like the cubic case, this SK effective theory was also dual to a non-linear Langevin dynamics. The form of this Langevin dynamics was slightly different from the one that was dual to the cubic effective theory. However, it shared the following two features with the cubic dynamics:

1. There was a non-Gaussianity in the noise distribution.
2. There were thermal jitters in the particle’s frequency and damping coefficient.

We argued that, as before, this Langevin theory or the dual SK effective theory is inadequate for computing the particle’s 4-point OTOCs. We went on to overcome this limitation by extending the effective theory of the particle to the double-folded contour. We identified the additional quartic couplings in this extended OTO framework and established the relations between these couplings and the bath’s 4-point OTOCs in the high temperature limit. These relations allowed us to study the constraints imposed on the particle’s OTO dynamics by microscopic reversibility and the thermality of the bath. We found that, just like the cubic case, these constraints manifest in the form of some OTO generalisations of the Onsager relations and the fluctuation-dissipation relation between the quartic couplings. By combining these relations, we verified that a generalised FDR held between two Schwinger-Keldysh quartic couplings. We demon-

strated that, analogous to the cubic case, this generalised FDR connected the non-Gaussianity in the noise with the thermal jitter in the damping coefficient of the dual Langevin theory.

## 6.2 Future directions

The analysis presented in this thesis clearly demonstrates that a complete information about the evolution of the reduced density matrix of an open quantum system, encoded in its Schwinger-Keldysh effective action, is inadequate for computing its OTOCs. We overcame this limitation by constructing an OTO extension of this effective dynamics. However, it would be useful to come up with an equivalent Schrodinger picture for computing the OTOCs of the system. Such a picture would require an OTO extension of the notion of reduced density matrix, which can be then treated as an ‘OTO effective state’ of the system. Such a construction would be useful for at least the following two reasons:

1. The path integral formalism for computing OTOCs is hard to implement numerically. On the other hand, if one can come up with a quantum master equation for the ‘OTO effective state’, it may be numerically solvable in simple systems with finite dimensional Hilbert spaces. This may lead to a better understanding of OTOCs for diverse open quantum systems.
2. The reduced density matrix of open quantum systems plays an important role in defining entanglement entropy and similar information-theoretic quantities [177]. These quantities have turned out to be very useful in understanding the evolution of quantum systems. It is possible that similar insights can be obtained for the OTOCs by coming up with a proper notion of an ‘OTO effective state’ and constructing similar information-theoretic quantities out of it.

The existence of such additional information in the OTO effective dynamics of an open quantum system also raises the question of what it might mean for a system with a holographic dual. Over the last decade and a half, several results have come to fore which connect the entanglement in a boundary CFT to the geometry of an asymptotically AdS bulk spacetime [178]. Such a relation is encapsulated in the famous Ryu-Takayanagi formula [179, 180] which relates the entanglement entropy of a region in the boundary to the area of the extremal surface in the bulk which is anchored on the edge of this region. It would be interesting to find some analogous relation for the OTO effective state of a region in the boundary theory.

As we saw in this thesis, the OTO extension of the effective dynamics of an open quantum system is crucial to gain insights on some old questions such as the following:

- What are the constraints imposed on the effective dynamics of the system by the microscopic reversibility in the dynamics of the (system+environment) combined setup?
- When the environment is in a thermal state, are there additional constraints on the system's effective dynamics?

As we discussed in chapter 4, these questions were studied and partially answered in [38–40, 44–46, 126, 127]. In this thesis, we extended these analyses by considering the cubic and quartic OTO effective theories of a Brownian particle and demonstrating how the OTO couplings enter in such constraints. However, we are far from a full understanding of the general structure of such constraints in open quantum systems. It would be useful to extend our work to more diverse quantum systems and come up with a general  $k$ -OTO version of the generalised Onsager-Casimir reciprocal relations and the fluctuation-dissipation relations. For this one would have to extend our analysis to a broader class of systems and look at more general OTOCs of the system.

In a considerable part of this thesis, we discussed the OTO effective dynamics of a Brownian particle interacting with a thermal bath. For such a setup, one may wonder whether this effective theory can be used to study the thermalisation of the particle's OTOCs. To address this issue of thermalisation of the particle's OTOCs, one needs to look at their behaviour when the separation between any two insertions is much larger than the time-scales set by the parameters in the effective dynamics. This requires going beyond the perturbative analysis employed here by re-summing the perturbation series expansions of the correlators.

Studying the question of thermalisation of the particle's OTOCs can provide useful insight into similar questions for more general open quantum systems. In particular, it can shed light on the circumstances in which a system with a large number of degrees of freedom can be brought to thermal equilibrium with an environment of even larger size. Experimentally, this may lead to a specification of the conditions in which a thermal bath can be prepared by making a quantum system interact with an environment at thermal equilibrium. Hence, the OTO effective theory developed here can be seen as a step towards understanding when quantum mechanical systems can serve as ideal thermal baths.

# Appendix A

## Appendices to Chapter 3

In the series of appendices that follow, we will sketch the computations behind the spectral representations quoted in the main text. For simplicity, we will suppress the spatial dependence and the dependence on the spatial momenta in all the correlators that appear in these appendices. We will only retain the time/frequency dependencies.

### A.1 Basis of column vectors

We will begin by describing the basis vectors that we use on the  $k$ -fold time contour. We expand the array  $\tilde{\mathbf{M}}(\omega_1, \dots, \omega_n)$  in the basis of tensor products of the following (generalised RA basis) column vectors:

$$\begin{aligned}\bar{e}_P^{(j)}(\omega) &\equiv \underbrace{\{\tilde{f}(\omega), \tilde{f}(\omega), \dots, \tilde{f}(\omega)\}}_{2j-2 \text{ times}} \underbrace{\{1 + \tilde{f}(\omega), 1 + \tilde{f}(\omega), \dots, 1 + \tilde{f}(\omega)\}}_{2k-2j+2 \text{ times}}^T, \\ \bar{e}_F^{(j)}(\omega) &\equiv \underbrace{\{\tilde{f}(\omega), \tilde{f}(\omega), \dots, \tilde{f}(\omega)\}}_{2j-1 \text{ times}} \underbrace{\{1 + \tilde{f}(\omega), 1 + \tilde{f}(\omega), \dots, 1 + \tilde{f}(\omega)\}}_{2k-2j+1 \text{ times}}^T,\end{aligned}\tag{A.1}$$

where  $\tilde{f}(\omega) \equiv \frac{1}{e^{\beta\omega} - 1}$  is the Bose-Einstein distribution and  $j = 1, 2, \dots, k$ .

The dual basis of row vectors consists of the following vectors:

$$\begin{aligned}
e_p^{(1)}(\omega) &\equiv (1, 0, 0, 0, \dots, 0, -e^{-\beta\omega}), \\
e_p^{(2)}(\omega) &\equiv (0, -1, 1, 0, \dots, 0), \\
e_p^{(3)}(\omega) &\equiv (0, 0, 0, -1, 1, 0, \dots), \\
&\dots, \\
e_p^{(j)}(\omega) &\equiv (0, 0, 0, \dots, -1_{2j-2}, 1_{2j-1}, 0, \dots, 0), \\
&\dots, \\
e_p^{(k)}(\omega) &\equiv (0, 0, \dots, 0, -1, 1, 0),
\end{aligned} \tag{A.2}$$

$$\begin{aligned}
e_F^{(1)}(\omega) &\equiv (-1, 1, 0, \dots, 0), \\
e_F^{(2)}(\omega) &\equiv (0, 0, -1, 1, 0, \dots, 0), \\
&\dots, \\
e_F^{(j)}(\omega) &\equiv (0, 0, 0, \dots, -1_{2j-1}, 1_{2j}, 0, \dots, 0), \\
&\dots, \\
e_F^{(k)}(\omega) &\equiv (0, 0, \dots, -1, 1).
\end{aligned}$$

We then have

$$\begin{aligned}
e_p^{(i)}(\omega) \cdot \bar{e}_p^{(j)}(\omega) &= e_F^{(i)}(\omega) \cdot \bar{e}_F^{(j)}(\omega) = \delta^{ij}, \\
e_p^{(i)}(\omega) \cdot \bar{e}_F^{(j)}(\omega) &= e_F^{(i)}(\omega) \cdot \bar{e}_p^{(j)}(\omega) = 0.
\end{aligned} \tag{A.3}$$

Here  $e_p^{(j)}$  corresponds to the difference field across  $j^{\text{th}}$  past turning point (with density matrix being counted as the first past turning point) counted from the ket to the bra, whereas  $e_F^{(j)}$  corresponds to the difference field across  $j^{\text{th}}$  future turning point counted from the ket to the bra. For notational convenience, we will extend the definition of these vectors to all integers via Bloch-Floquet periodicity :

$$\begin{aligned}
e_p^{(j+k)}(\omega) &\equiv e^{\beta\omega} e_p^{(j)}(\omega), & \bar{e}_p^{(j+k)}(\omega) &\equiv e^{-\beta\omega} \bar{e}_p^{(j)}(\omega), \\
e_F^{(j+k)}(\omega) &\equiv e^{\beta\omega} e_F^{(j)}(\omega), & \bar{e}_F^{(j+k)}(\omega) &\equiv e^{-\beta\omega} \bar{e}_F^{(j)}(\omega),
\end{aligned} \tag{A.4}$$

with

$$\begin{aligned}
e_p^{(i)}(\omega) \cdot \bar{e}_p^{(j)}(\omega) &= e_F^{(i)}(\omega) \cdot \bar{e}_F^{(j)}(\omega) = e^{\beta\omega(i-j)} \delta^{i-j \bmod k, 0}, \\
e_p^{(i)}(\omega) \cdot \bar{e}_F^{(j)}(\omega) &= e_F^{(i)}(\omega) \cdot \bar{e}_p^{(j)}(\omega) = 0.
\end{aligned} \tag{A.5}$$

In particular, we have

$$\begin{aligned}
e_p^{(k+1)}(\omega) &\equiv (e^{\beta\omega}, 0, 0, 0, \dots, 0, -1) = e^{\beta\omega} e_p^{(1)}(\omega), \\
\bar{e}_p^{(k+1)}(\omega) &\equiv \{\check{f}(\omega), \check{f}(\omega), \dots, \check{f}(\omega)\}^T = e^{-\beta\omega} \bar{e}_p^{(1)}(\omega), \\
e_F^{(0)}(\omega) &\equiv \{0, 0, \dots, 0, -e^{-\beta\omega}, e^{-\beta\omega}\}^T = e^{-\beta\omega} e_F^{(k)}(\omega), \\
\bar{e}_F^{(0)}(\omega) &\equiv \{1 + \check{f}(\omega), 1 + \check{f}(\omega), \dots, \check{f}(\omega), e^{\beta\omega}(1 + \check{f}(\omega))\}^T = e^{\beta\omega} \bar{e}_F^{(k)}(\omega).
\end{aligned} \tag{A.6}$$

## A.2 Rules of contraction for general $k$

### A.2.1 Summary of the rules

The contractions of the array  $\tilde{\mathbf{M}}(\omega_1, \dots, \omega_n)$  with the tensor products of the row vectors introduced above give the components of the array in the basis of tensor products of the dual column vectors. For instance,

$$\tilde{\mathbf{M}}_{PPF}^{rsu} = \sum_{a=1}^4 \sum_{b=1}^4 \sum_{c=1}^4 e_p^{(r)}(\omega_1)_a e_p^{(s)}(\omega_2)_b e_F^{(u)}(\omega_3)_c \tilde{\mathbf{M}}(3\text{-Pt})_{abc}. \tag{A.7}$$

In this example the indices of  $e_F^{(u)}(\omega_3)$  and  $e_p^{(s)}(\omega_2)$  contract with the third and the second indices of  $\tilde{\mathbf{M}}(3\text{-Pt})$  respectively. These 2 indices correspond to the positions of past-most insertion and the next insertion to its future in the array  $\mathbf{M}(t_1, t_2, t_3)$  which is obtained by taking the inverse Fourier transform of  $\tilde{\mathbf{M}}(3\text{-Pt})$  and multiplying by a theta function  $\Theta_{123}$ . In what follows, for such a contraction, we would loosely say that  $e_F^{(u)}(\omega_3)$  lies to the past of  $e_p^{(s)}(\omega_2)$ . In a similar sense, we would say that  $e_p^{(r)}(\omega_1)$  lies to the future of  $e_p^{(s)}(\omega_2)$ .

As we noted in the main text, the components obtained from these contractions with tensor products of the row vectors are not all independent. Here, we enumerate a set of rules that such contractions satisfy:

1. **F-collapse(Largest time Eqn)** : The contraction is zero if there is an  $e_F^{(r)}$  and if there is no  $e_p^{(s)}$  to its future such that  $s \in \{r, r + 1\}$ .

2. **P-collapse(Smallest time Eqn)** : The contraction is zero if there is an  $e_p^{(r)}$  and if there is no  $e_F^{(s)}$  to its past such that  $s \in \{r, r-1\}$ .
3. **F-sliding** : One can replace  $e_F^{(r-1)}$  by  $-e_F^{(r)}$  without changing the value of the contraction,
  - (a) if there is an  $e_p^{(r)}$  to its future (Anchor condition) and
  - (b) if there is no other  $e_F^{(r)}$  or  $e_F^{(r-1)}$  to the past of  $e_p^{(r)}$  (Eclipse condition).
4. **P-sliding** : One can replace  $e_p^{(r+1)}$  by  $-e_p^{(r)}$  without changing the value of the contraction,
  - (a) if there is an  $e_F^{(r)}$  to its past (Anchor condition) and
  - (b) if there is no other  $e_p^{(r)}$  or  $e_p^{(r+1)}$  to the future of  $e_F^{(j)}$  (Eclipse condition).
5. **C-shift** : One can do a global contour translation, viz., shift all the indices by a given number i.e. do the following replacement :

$$\begin{aligned}
 e_F^{(r)} &\mapsto e_F^{(r+m)}, \\
 e_p^{(s)} &\mapsto e_p^{(s+m)}
 \end{aligned}
 \tag{A.8}$$

for all  $e_F^{(r)}$  and  $e_p^{(s)}$  in the contraction and any integer  $m$ , without changing the value contraction.

6. **F-fragmentation** : For a given  $r$ , one can do the following replacements together without changing the value of the contraction:

$$\begin{aligned}
 e_F^{(r)} &\mapsto e_F^{(r)} + e_F^{(r+1)}, \\
 e_F^{(r+m)} &\mapsto e_F^{(r+1+m)} \quad \forall m > 0, \\
 e_p^{(r+m)} &\mapsto e_p^{(r+1+m)} \quad \forall m > 0.
 \end{aligned}$$

7. **P-fragmentation** : For a given  $r$ , one can do the following replacements together without changing the value of the contraction:

$$\begin{aligned}
 e_p^{(r)} &\mapsto e_p^{(r)} + e_p^{(r+1)}, \\
 e_p^{(r+m)} &\mapsto e_p^{(r+1+m)} \quad \forall m > 0, \\
 e_F^{(r-1+m)} &\mapsto e_F^{(r+m)} \quad \forall m > 0.
 \end{aligned}$$







### A.2.3 Some examples demonstrating the rules of contraction

#### F-collapse :

Consider the contraction of  $\tilde{\mathbf{M}}(3\text{-Pt})$  with the tensor  $(e_F^{(2)}(\omega_1) \otimes e_P^{(2)}(\omega_2) \otimes e_F^{(2)}(\omega_3))$ . The corresponding diagram is

$$\tilde{\mathbf{M}}(3\text{-Pt}) \cdot (e_F^{(2)}(\omega_1) \otimes e_P^{(2)}(\omega_2) \otimes e_F^{(2)}(\omega_3))$$

$$=$$

$$(A.12)$$

Notice that  $e_F^{(2)}(\omega_1)$  is the future-most insertion and there is no  $e_P^{(2)}$  or  $e_P^{(1)}$  to block it from collapsing. One can slide down the future-most insertion on the third leg down to the fourth leg without changing the value of the contraction as there is no other insertion to obstruct this sliding. But this leads to the pair of future-most insertions with opposite signs lying on exactly the same position. Consequently they cancel each other's contribution and the value of the contraction is 0.

#### P-collapse :

Consider the contraction of  $\tilde{\mathbf{M}}(3\text{-Pt})$  with the tensor  $(e_P^{(2)}(\omega_1) \otimes e_F^{(1)}(\omega_2) \otimes e_P^{(2)}(\omega_3))$ . The corresponding diagram is

$$\tilde{\mathbf{M}}(3\text{-Pt}) \cdot (e_P^{(2)}(\omega_1) \otimes e_F^{(1)}(\omega_2) \otimes e_P^{(2)}(\omega_3))$$

$$=$$

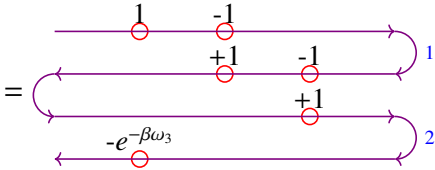
$$(A.13)$$

Notice that  $e_P^{(2)}(\omega_3)$  is the past-most insertion and there is no  $e_F^{(2)}$  or  $e_F^{(1)}$  to block it from collapsing. One can slide down the past-most insertion on the second leg down to the third leg without changing the value of the contraction as there is no other insertion to obstruct this sliding. But this leads to the pair of past-most insertions with opposite signs lying on exactly the same position. Consequently they cancel each other's contribution and the value of the

contraction is 0.

Similarly, consider the contraction of  $\widetilde{\mathbf{M}}(3\text{-Pt})$  with the tensor  $(e_p^{(2)}(\omega_1) \otimes e_F^{(1)}(\omega_2) \otimes e_p^{(1)}(\omega_3))$ .

The corresponding diagram is

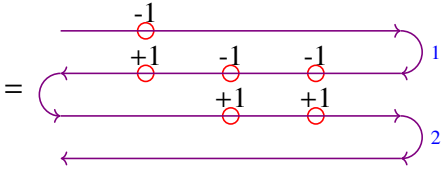
$$\widetilde{\mathbf{M}}(3\text{-Pt}) \cdot (e_p^{(2)}(\omega_1) \otimes e_F^{(1)}(\omega_2) \otimes e_p^{(1)}(\omega_3))$$


$$= \text{Diagram (A.14)} \tag{A.14}$$

Again, notice that  $e_p^{(1)}(\omega_3)$  is the past-most insertion and there is no  $e_F^{(1)}$  or  $e_F^{(2)}$  to block it from collapsing. One can slide the past-most insertion on the fourth leg up to the first leg picking up a factor  $e^{\beta\omega_3}$  because of the KMS relations. Again, this leads to the pair of past-most insertions with opposite signs lying on exactly the same position. Consequently, as before, they cancel each other's contribution and the value of the contraction is 0.

### F-sliding :

Consider the contraction of  $\widetilde{\mathbf{M}}(3\text{-Pt})$  with the tensor  $(e_p^{(2)}(\omega_1) \otimes e_p^{(2)}(\omega_2) \otimes e_F^{(1)}(\omega_3))$ . The corresponding diagram is

$$\widetilde{\mathbf{M}}(3\text{-Pt}) \cdot (e_p^{(2)}(\omega_1) \otimes e_p^{(2)}(\omega_2) \otimes e_F^{(1)}(\omega_3))$$


$$= \text{Diagram (A.15)} \tag{A.15}$$

Notice that  $e_F^{(1)}(\omega_3)$  is the past-most insertion. There is an  $e_p^{(2)}(\omega_2)$  to its future. But, apart from  $e_F^{(1)}(\omega_3)$ , there is no other  $e_F^{(1)}$  or  $e_F^{(2)}$  to the past of  $e_p^{(2)}(\omega_2)$ . If we choose the past-most insertion with the factor (-1) on the first leg, then there is no insertion to block the 2 insertions corresponding to  $e_p^{(2)}(\omega_2)$  from collapsing on to each other i.e. one can slide either of those insertions to the position of the other and their contributions would exactly cancel each other.



### P-sliding :

Consider the contraction of  $\widetilde{\mathbf{M}}(3\text{-Pt})$  with the tensor  $(e_p^{(2)}(\omega_1) \otimes e_F^{(1)}(\omega_2) \otimes e_F^{(1)}(\omega_3))$ . The corresponding diagram is

$$\widetilde{\mathbf{M}}(3\text{-Pt}) \cdot (e_p^{(2)}(\omega_1) \otimes e_F^{(1)}(\omega_2) \otimes e_F^{(1)}(\omega_3))$$

$$=$$

$$(A.19)$$

Notice that  $e_p^{(2)}(\omega_1)$  is the future-most insertion. There is an  $e_F^{(1)}(\omega_2)$  to its past. But, apart from  $e_p^{(2)}(\omega_1)$ , there is no other  $e_p^{(1)}$  or  $e_p^{(2)}$  to the future of  $e_F^{(1)}(\omega_2)$ . If we choose, the future-most insertion with the factor (+1) on the third leg, then there is no insertion to block the 2 insertions corresponding to  $e_F^{(1)}(\omega_2)$  from collapsing on to each other i.e. one can slide either of those insertions to the position of the other and their contributions would exactly cancel each other. Therefore, we have

$$\widetilde{\mathbf{M}}(3\text{-Pt}) \cdot (e_p^{(2)}(\omega_1) \otimes e_F^{(1)}(\omega_2) \otimes e_F^{(1)}(\omega_3))$$

$$=$$

$$(A.20)$$

One can slide the future-most insertion on the second leg up to the first leg without changing the value of the contraction and obtain

$$\widetilde{\mathbf{M}}(3\text{-Pt}) \cdot (e_p^{(2)}(\omega_1) \otimes e_F^{(1)}(\omega_2) \otimes e_F^{(1)}(\omega_3))$$

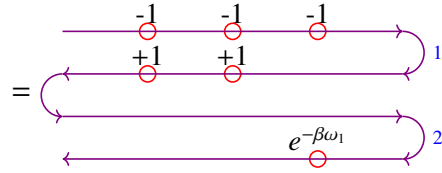
$$=$$

$$(A.21)$$

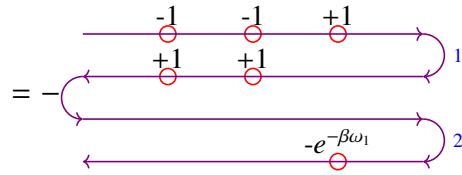
Now, one can add another future-most insertion with a factor  $(e^{-\beta\omega_1})$  on the fourth leg without changing the value of the contraction because if we choose this new insertion, then again there is no insertion to block the pair of points of  $e_F^{(1)}(\omega_2)$  from collapsing onto each other. Therefore,

we have

$$\tilde{\mathbf{M}}(3\text{-Pt}) \cdot \left( e_p^{(2)}(\omega_1) \otimes e_p^{(2)}(\omega_2) \otimes e_F^{(1)}(\omega_3) \right)$$



(A.22)



$$= -\tilde{\mathbf{M}}(3\text{-Pt}) \cdot \left( e_p^{(1)}(\omega_1) \otimes e_F^{(1)}(\omega_2) \otimes e_F^{(1)}(\omega_3) \right).$$

So, we see that, in this case the transformation  $e_p^{(2)}(\omega_1) \mapsto -e_p^{(1)}(\omega_1)$  keeps the value of the contraction unchanged.

### C-shift:

Consider the contraction of  $\tilde{\mathbf{M}}(2\text{-Pt})$  with the tensor  $\left( e_p^{(1)}(\omega_1) \otimes e_F^{(1)}(\omega_2) \right)$ . The corresponding diagram is

$$\tilde{\mathbf{M}}(2\text{-Pt}) \cdot \left( e_p^{(1)}(\omega_1) \otimes e_F^{(1)}(\omega_2) \right) =$$
(A.23)

One can slide the insertions one after the other without changing the value of the contraction as shown below:

$$\begin{aligned}
\widetilde{\mathbf{M}}(2\text{-Pt}) \cdot (e_P^{(1)}(\omega_1) \otimes e_F^{(1)}(\omega_2)) &= \begin{array}{c} \begin{array}{c} \xrightarrow{-1} \xrightarrow{+1} \\ \xleftarrow{+1} \end{array} \xrightarrow{1} \\ \xleftarrow{-e^{-\beta\omega_1}} \xrightarrow{2} \end{array} \\
= & \begin{array}{c} \begin{array}{c} \xrightarrow{-1} \xrightarrow{+1} \\ \xleftarrow{+1} \end{array} \xrightarrow{1} \\ \xleftarrow{-e^{-\beta\omega_1}} \xrightarrow{2} \end{array} + \begin{array}{c} \xrightarrow{+1} \xrightarrow{+1} \\ \xleftarrow{+1} \end{array} \xrightarrow{1} \\ & \xleftarrow{-e^{-\beta\omega_1}} \xrightarrow{2} \\
+ & \begin{array}{c} \xrightarrow{-1} \\ \xleftarrow{-1} \end{array} \xrightarrow{1} \\ & \begin{array}{c} \xrightarrow{+1} \xrightarrow{+1} \\ \xleftarrow{+1} \end{array} \xrightarrow{1} \\ & \xleftarrow{-e^{-\beta\omega_1}} \xrightarrow{2} \\
= & \begin{array}{c} \xrightarrow{-1} \xrightarrow{+1} \\ \xleftarrow{+1} \end{array} \xrightarrow{1} \\ & \begin{array}{c} \xrightarrow{+1} \xrightarrow{+1} \\ \xleftarrow{+1} \end{array} \xrightarrow{1} \\ & \xleftarrow{-e^{-\beta\omega_1}} \xrightarrow{2} \\
+ & \begin{array}{c} \xrightarrow{-1} \xrightarrow{-1} \\ \xleftarrow{-1} \end{array} \xrightarrow{1} \\ & \begin{array}{c} \xrightarrow{-1} \xrightarrow{-1} \\ \xleftarrow{-1} \end{array} \xrightarrow{1} \\ & \xleftarrow{-e^{-\beta\omega_1}} \xrightarrow{2} \\
= & \begin{array}{c} \xrightarrow{-1} \xrightarrow{+1} \\ \xleftarrow{+1} \end{array} \xrightarrow{1} \\ & \begin{array}{c} \xrightarrow{-1} \xrightarrow{+1} \\ \xleftarrow{+1} \end{array} \xrightarrow{1} \\ & \xleftarrow{-e^{-\beta\omega_1}} \xrightarrow{2} \\ & = \widetilde{\mathbf{M}}(2\text{-Pt}) \cdot (e_P^{(2)}(\omega_1) \otimes e_F^{(2)}(\omega_2)).
\end{aligned} \tag{A.24}$$

So, we see that, in this case the transformation  $e_P^{(1)}(\omega_1) \mapsto e_P^{(2)}(\omega_1), e_F^{(1)}(\omega_2) \mapsto e_F^{(2)}(\omega_2)$  keeps the value of the contraction unchanged.

### F-fragmentation :

Consider the contraction of  $\widetilde{\mathbf{M}}(4\text{-Pt})$  with the tensor  $(e_P^{(2)}(\omega_1) \otimes e_P^{(3)}(\omega_2) \otimes e_F^{(2)}(\omega_3) \otimes e_F^{(2)}(\omega_4))$ . The corresponding diagram is

$$\tilde{\mathbf{M}}(4\text{-Pt}) \cdot \left( e_P^{(2)}(\omega_1) \otimes e_P^{(3)}(\omega_2) \otimes e_F^{(2)}(\omega_3) \otimes e_F^{(2)}(\omega_4) \right)$$
(A.25)

One can slide all the insertions that lie on the 4<sup>th</sup> leg or below down by two legs to obtain the following diagram:

$$\tilde{\mathbf{M}}(4\text{-Pt}) \cdot \left( e_P^{(2)}(\omega_1) \otimes e_P^{(3)}(\omega_2) \otimes e_F^{(2)}(\omega_3) \otimes e_F^{(2)}(\omega_4) \right)$$
(A.26)

We can add a pair of points with opposite signs on the 4<sup>th</sup> and the 5<sup>th</sup> legs at positions corresponding to the frequency  $\omega_3$  without changing the value of the contraction as shown below:

$$\tilde{\mathbf{M}}(4\text{-Pt}) \cdot \left( e_P^{(2)}(\omega_1) \otimes e_P^{(3)}(\omega_2) \otimes e_F^{(2)}(\omega_3) \otimes e_F^{(2)}(\omega_4) \right)$$
(A.27)

There is no insertion to the past of these new insertions which can block them from collapsing



onto one another. Now, one can add another pair of insertions with opposite signs on the 4<sup>th</sup> and the 5<sup>th</sup> legs at positions corresponding to the frequency  $\omega_4$  without changing the value of the contraction as shown below:

$$\widetilde{\mathbf{M}}(4\text{-Pt}) \cdot \left( e_P^{(2)}(\omega_1) \otimes e_P^{(3)}(\omega_2) \otimes e_F^{(2)}(\omega_3) \otimes e_F^{(2)}(\omega_4) \right)$$

$$=$$

$$(A.28)$$

As before, there is no insertion to the past of these new insertions which can block them from collapsing onto one another. But this is exactly the diagram for the contraction of  $\widetilde{\mathbf{M}}(4\text{-Pt})$  with

$$\left( e_P^{(2)}(\omega_1) \otimes e_P^{(4)}(\omega_2) \otimes (e_F^{(2)}(\omega_3) + e_F^{(3)}(\omega_3)) \otimes (e_F^{(2)}(\omega_4) + e_F^{(3)}(\omega_4)) \right).$$

Therefore, we have

$$\begin{aligned} & \widetilde{\mathbf{M}}(4\text{-Pt}) \cdot \left( e_P^{(2)}(\omega_1) \otimes e_P^{(3)}(\omega_2) \otimes e_F^{(2)}(\omega_3) \otimes e_F^{(2)}(\omega_4) \right) \\ &= \widetilde{\mathbf{M}}(4\text{-Pt}) \cdot \left( e_P^{(2)}(\omega_1) \otimes e_P^{(4)}(\omega_2) \otimes (e_F^{(2)}(\omega_3) + e_F^{(3)}(\omega_3)) \right. \\ & \quad \left. \otimes (e_F^{(2)}(\omega_4) + e_F^{(3)}(\omega_4)) \right). \end{aligned} \quad (A.29)$$

### **P-fragmentation :**

Consider the contraction of  $\widetilde{\mathbf{M}}(4\text{-Pt})$  with the tensor  $\left( e_P^{(2)}(\omega_1) \otimes e_P^{(2)}(\omega_2) \otimes e_F^{(1)}(\omega_3) \otimes e_F^{(2)}(\omega_4) \right)$ . The corresponding diagram is

$$\tilde{\mathbf{M}}(4\text{-Pt}) \cdot \left( e_P^{(2)}(\omega_1) \otimes e_P^{(2)}(\omega_2) \otimes e_F^{(1)}(\omega_3) \otimes e_F^{(2)}(\omega_4) \right)$$
(A.30)

One can slide all the insertions that lie on the 3<sup>rd</sup> leg or below down by two legs to obtain the following diagram:

$$\tilde{\mathbf{M}}(4\text{-Pt}) \cdot \left( e_P^{(2)}(\omega_1) \otimes e_P^{(2)}(\omega_2) \otimes e_F^{(1)}(\omega_3) \otimes e_F^{(2)}(\omega_4) \right)$$
(A.31)

We can add a pair of points with opposite signs on the 3<sup>rd</sup> and the 4<sup>th</sup> legs at positions corresponding to the frequency  $\omega_2$  without changing the value of the contraction as shown below:

$$\tilde{\mathbf{M}}(4\text{-Pt}) \cdot \left( e_P^{(2)}(\omega_1) \otimes e_P^{(2)}(\omega_2) \otimes e_F^{(1)}(\omega_3) \otimes e_F^{(2)}(\omega_4) \right)$$
(A.32)



## Orthogonal tensors for two pt. functions

The expression in (A.35) can be proved by demonstrating that the array of two pt. functions should be orthogonal to the following tensors :

$$\begin{aligned}
 & 3k^2 \text{ orthogonal tensors : } e_{PP}^{rs}, e_{FP}^{rs}, e_{FF}^{rs}, \\
 & k(k-2) \text{ orthogonal tensors : } e_{PF}^{rs} \text{ for } r \neq s, s+1, \\
 & k \text{ orthogonal tensors : } e_{PF}^{rr} + e_{PF}^{(r+1)r}, \\
 & k-1 \text{ orthogonal tensors : } e_{PF}^{rr} - e_{PF}^{11}.
 \end{aligned} \tag{A.36}$$

Here we have used a short-hand notation for the tensor products of the row vectors. For example, we have written  $e_p^{(r)}(\omega_1) \otimes e_F^{(s)}(\omega_2)$  as  $e_{PF}^{rs}$  and so on.

The total number of elements in this array is  $2k \times 2k = 4k^2$ . The total number of tensors that are orthogonal to the array  $\widetilde{\mathbf{M}}(2\text{-Pt})$  is  $(4k^2 - 1)$ . These are enumerated in (A.36). Therefore, the orthogonal tensors completely fix the array upto a single function which has to be determined.

The arguments for the tensors mentioned in (A.36) being orthogonal to the array of contour correlators are based on rules of contraction enumerated in appendix A.2.1. These arguments are given in table A.1.

Orthogonal tensor	Total no. of tensors	Argument
$e_{PP}^{rs}$	$k^2$	$e_{PP}^{rs} \xrightarrow{\text{P-collapse}} 0$
$e_{FP}^{rs}$	$k^2$	$e_{FP}^{rs} \xrightarrow{\text{F-collapse}} 0$
$e_{FF}^{rs}$	$k^2$	$e_{FF}^{rs} \xrightarrow{\text{F-collapse}} 0$
$e_{PF}^{rs}$ for $r \neq s, s+1$	$k(k-2)$	$e_{PF}^{rs} \xrightarrow{\text{F-collapse}} 0$
$e_{PF}^{rr} + e_{PF}^{(r+1)r}$	$k$	$e_{PF}^{(r+1)r} \xrightarrow{\text{P-sliding}} -e_{PF}^{rr}$
$e_{PF}^{rr} - e_{PF}^{11}$	$k-1$	$e_{PF}^{rr} \xrightarrow{\text{C-shift}} e_{PF}^{11}$

Table A.1: Arguments for the tensors orthogonal to the array of 2 point contour correlators

In this table, we have indicated the  $e_p(e_F)$  which leads to a P(F)-collapse by red colour, and in case of a P/F-sliding we have indicated the  $e_p/e_F$  that slides by blue colour and the

corresponding  $e_F/e_p$  that acts as the anchor by brown colour. The array that is orthogonal to all the tensors mentioned above must have the form

$$\tilde{\mathbf{M}}(2\text{-Pt}) = \alpha^{(2)} \sum_{r=1}^k (\bar{e}_p^{(r+1)}(\omega_1) - \bar{e}_p^{(r)}(\omega_1)) \otimes \bar{e}_F^{(r)}(\omega_2) . \quad (\text{A.37})$$

Now, the coefficient  $\alpha^{(2)}$  is given by the contraction with the tensor  $e_{pF}^{(r+1)r}$ , an example of which is the case  $r = 1$ . Then this coefficient is given by

$$\alpha^{(2)} = \tilde{\mathbf{M}}(2\text{-Pt}) \cdot e_{pF}^{21} = \rho[12] . \quad (\text{A.38})$$

Substituting the value of  $\alpha^{(2)}$  that was obtained in (A.38) into the equation (A.37) we get the expansion that was mentioned in (A.35).

### A.3.2 Column Vector Representation for 3 pt. functions

Now, let us discuss the column vector representation of the array of 3-point correlators on a  $k$ -fold contour. We take  $\tilde{\mathbf{M}}(3\text{-Pt})$  to be the Wightman array in the Fourier domain. Its components in column vector basis satisfy the rules mentioned in A.2.1. Using these rules, one can show that

$$\begin{aligned} \tilde{\mathbf{M}}(3\text{-Pt}) = & \rho[321] \sum_{r=1}^k (\bar{e}_p^{(r+1)} \otimes \bar{e}_p^{(r+1)} - \bar{e}_p^{(r)} \otimes \bar{e}_p^{(r)}) \otimes \bar{e}_F^{(r)} \\ & - \rho[123] \sum_{r=1}^k (\bar{e}_p^{(r+1)} - \bar{e}_p^{(r)}) \otimes \bar{e}_F^{(r)} \otimes \bar{e}_F^{(r)} . \end{aligned} \quad (\text{A.39})$$

Orthogonal tensor	Total no. of tensors	Argument
$e_{PPP}^{rsu}$	$k^3$	$e_{PPP}^{rsu} \xrightarrow{\text{P-collapse}} 0$
$e_{PPF}^{rsu}$	$k^3$	$e_{PPF}^{rsu} \xrightarrow{\text{P-collapse}} 0$
$e_{FPP}^{rsu}$	$k^3$	$e_{FPP}^{rsu} \xrightarrow{\text{F-collapse}} 0$
$e_{FPF}^{rsu}$	$k^3$	$e_{FPF}^{rsu} \xrightarrow{\text{F-collapse}} 0$
$e_{FFP}^{rsu}$	$k^3$	$e_{FFP}^{rsu} \xrightarrow{\text{F-collapse}} 0$
$e_{FFF}^{rsu}$	$k^3$	$e_{FFF}^{rsu} \xrightarrow{\text{F-collapse}} 0$

Table A.2: Arguments for the tensors trivially orthogonal to the array of 3 point contour correlators

### Orthogonal tensors for three pt. functions

The expression in (A.39) can be proved by demonstrating that the three pt. function should be orthogonal to the following tensors :

$$\begin{aligned}
& 6k^3 \text{ orthogonal tensors : } e_{PPP}^{rsu}, e_{FPP}^{rsu}, e_{PPF}^{rsu}, e_{FPF}^{rsu}, e_{FPP}^{rsu}, e_{FFF}^{rsu}, \\
& k^2(k-1) \text{ orthogonal tensors : } e_{PPF}^{rsu} \text{ for } r \neq s, \\
& k(k-2) \text{ orthogonal tensors : } e_{PPF}^{rrs} \text{ for } s \neq r, r-1, \\
& k \text{ orthogonal tensors : } e_{PPF}^{rrr} + e_{PPF}^{(r+1)(r+1)r}, \\
& k-1 \text{ orthogonal tensors : } e_{PPF}^{rrr} - e_{PPF}^{111}, \tag{A.40} \\
& k^2(k-1) \text{ orthogonal tensors : } e_{PPF}^{rsu} \text{ for } s \neq u, \\
& k(k-2) \text{ orthogonal tensors : } e_{PPF}^{rss} \text{ for } r \neq s, s+1, \\
& k \text{ orthogonal tensors : } e_{PPF}^{rrr} + e_{PPF}^{(r+1)rr}, \\
& k-1 \text{ orthogonal tensors : } e_{PPF}^{rrr} - e_{PPF}^{111}.
\end{aligned}$$

This gives in total  $8k^3 - 2$  orthogonal tensors.

The arguments for the tensors mentioned in (A.40) being orthogonal to the array of contour correlators are given in tables A.2, A.3 and A.4.

As before, in tables A.2, A.3 and A.4 we have indicated the  $e_p(e_f)$  which leads to a P(F)-

Orthogonal tensor	Total no. of tensors	Argument
$e_{PPF}^{rsu}$ for $r \neq s$	$k^2(k-1)$	W.L.O.G let us consider $r > s$ . <u>Case 1 : <math>r &gt; (s+1)</math></u> If $u \neq s, s-1$ , then $e_{PPF}^{rsu} \xrightarrow{\text{P-collapse}} 0$ , otherwise $e_{PPF}^{rsu} \xrightarrow{\text{P-collapse}} 0$ . <u>Case 2 : <math>r = (s+1)</math></u> If $u = s$ , then $e_{PPF}^{(s+1)s} \xrightarrow{\text{F-sliding}} -e_{PPF}^{(s+1)s(s+1)} \xrightarrow{\text{P-collapse}} 0$ , if $u > s$ , then $e_{PPF}^{(s+1)su} \xrightarrow{\text{P-collapse}} 0$ , and if $u < s$ , then $e_{PPF}^{(s+1)su} \xrightarrow{\text{P-collapse}} 0$ .
$e_{PPF}^{rrs}$ for $s \neq r, r-1$	$k(k-2)$	$e_{PPF}^{rrs} \xrightarrow{\text{F-collapse}} 0$
$e_{PPF}^{rrr} + e_{PPF}^{(r+1)(r+1)r}$	$k$	$e_{PPF}^{(r+1)(r+1)r} \xrightarrow{\text{C-shift}} e_{PPF}^{rr(r-1)} \xrightarrow{\text{F-sliding}} -e_{PPF}^{rrr}$
$e_{PPF}^{rrr} - e_{PPF}^{111}$	$k-1$	$e_{PPF}^{rrr} \xrightarrow{\text{C-shift}} e_{PPF}^{111}$

Table A.3: Arguments for the tensors in the PPF sector orthogonal to the array of 3 point contour correlators

Orthogonal tensor	Total no. of tensors	Argument
$e_{PPF}^{rsu}$ for $s \neq u$	$k^2(k-1)$	W.L.O.G let us consider $s > u$ . <u>Case 1 : <math>s &gt; (u+1)</math></u> If $r \neq s, s+1$ , then $e_{PPF}^{rsu} \xrightarrow{\text{F-collapse}} 0$ , otherwise $e_{PPF}^{rsu} \xrightarrow{\text{F-collapse}} 0$ . <u>Case 2 : <math>s = (u+1)</math></u> If $r = u+1$ , then $e_{PPF}^{(u+1)(u+1)u} \xrightarrow{\text{P-sliding}} -e_{PPF}^{(u+2)(u+1)u} \xrightarrow{\text{F-collapse}} 0$ , if $r > (u+1)$ , then $e_{PPF}^{r(u+1)u} \xrightarrow{\text{F-collapse}} 0$ , and if $r < (u+1)$ , then $e_{PPF}^{r(u+1)u} \xrightarrow{\text{F-collapse}} 0$ .
$e_{PPF}^{rss}$ for $r \neq s, s+1$	$k(k-2)$	$e_{PPF}^{rss} \xrightarrow{\text{F-collapse}} 0$
$e_{PPF}^{rrr} + e_{PPF}^{(r+1)rr}$	$k$	$e_{PPF}^{(r+1)rr} \xrightarrow{\text{P-sliding}} -e_{PPF}^{rrr}$
$e_{PPF}^{rrr} - e_{PPF}^{111}$	$k-1$	$e_{PPF}^{rrr} \xrightarrow{\text{C-shift}} e_{PPF}^{111}$

Table A.4: Arguments for the tensors in the PPF sector orthogonal to the array of 3 point contour correlators

collapse by red colour, and in case of a P/F-sliding we have indicated the  $e_p/e_f$  that slides by blue colour and the corresponding  $e_f/e_p$  that acts as the anchor by brown colour.

The array that is orthogonal to all the tensors mentioned above must have the form

$$\begin{aligned} & \widetilde{\mathbf{M}}(3\text{-Pt}) \\ &= \alpha_1^{(3)} \left( \sum_{r=1}^k (\bar{e}_p^{(r+1)}(\omega_1) \otimes \bar{e}_p^{(r+1)}(\omega_2) \otimes \bar{e}_f^{(r)}(\omega_3) - \bar{e}_p^{(r)}(\omega_1) \otimes \bar{e}_p^{(r)}(\omega_2) \otimes \bar{e}_f^{(r)}(\omega_3)) \right) \\ &+ \alpha_2^{(3)} \left( \sum_{r=1}^k (\bar{e}_p^{(r+1)}(\omega_1) - \bar{e}_p^{(r)}(\omega_1)) \otimes \bar{e}_f^{(r)}(\omega_2) \otimes \bar{e}_f^{(r)}(\omega_3) \right). \end{aligned} \quad (\text{A.41})$$

Now, the coefficient  $\alpha_1^{(3)}$  is given by the contraction with the tensor  $e_{PPF}^{(r+1)(r+1)r}$ , an example of which is the case  $r = 1$ . Then this coefficient is given by

$$\alpha_1^{(3)} = \widetilde{\mathbf{M}}(3\text{-Pt}) \cdot e_{PPF}^{221} = \rho[321]. \quad (\text{A.42})$$

The coefficient  $\alpha_2^{(3)}$  is given by the contraction with the tensor  $e_{PPF}^{(r+1)rr}$ , an example of which is the case  $r = 1$ . Then this coefficient is given by

$$\alpha_2^{(3)} = \widetilde{\mathbf{M}}(3\text{-Pt}) \cdot e_{PPF}^{211} = -\rho[123]. \quad (\text{A.43})$$

Substituting the values of  $\alpha_1^{(3)}$  and  $\alpha_2^{(3)}$  that were obtained in (A.42) and (A.43) into the equation (A.41) we get the expansion that was mentioned in (A.39).

### A.3.3 Column Vector Representation for 4 pt. functions

Finally, let us discuss the column vector representation of the array of 4-point correlators on a  $k$ -fold contour. We take  $\widetilde{\mathbf{M}}(4\text{-Pt})$  to be the Wightman array in the Fourier domain. Its components in column vector basis satisfy the rules mentioned in A.2.1. Using these rules, one can show that

$$\widetilde{\mathbf{M}}(4\text{-Pt}) = \widetilde{\mathbf{M}}_{PPPF} + \widetilde{\mathbf{M}}_{PFFF} + \widetilde{\mathbf{M}}_{FPFF} + \widetilde{\mathbf{M}}_{FFPF} \quad (\text{A.44})$$

where

$$\widetilde{\mathbf{M}}_{PPPF} = -\rho[4321] \sum_{r=1}^k (\bar{e}_p^{(r+1)} \otimes \bar{e}_p^{(r+1)} \otimes \bar{e}_p^{(r+1)} \otimes \bar{e}_f^{(r)} - \bar{e}_p^{(r)} \otimes \bar{e}_p^{(r)} \otimes \bar{e}_p^{(r)} \otimes \bar{e}_f^{(r)}), \quad (\text{A.45})$$



$$\tilde{\mathbf{M}}_{PPFF} = \rho[1234] \sum_{r=1}^k \left( \bar{e}_p^{(r+1)} - \bar{e}_p^{(r)} \right) \otimes \bar{e}_F^{(r)} \otimes \bar{e}_F^{(r)} \otimes \bar{e}_F^{(r)}, \quad (\text{A.46})$$

$$\begin{aligned} \tilde{\mathbf{M}}_{PPFF} &= \sum_{r,s=1}^k \left( \theta_{r>s} \rho[12][34] + \theta_{r\leq s} \rho[34][12] \right) \left( \bar{e}_p^{(r+1)} - \bar{e}_p^{(r)} \right) \otimes \bar{e}_F^{(r)} \otimes \bar{e}_p^{(s+1)} \otimes \bar{e}_F^{(s)} \\ &\quad - \sum_{r,s=1}^k \left( \theta_{r\geq s} \rho[12][34] + \theta_{r<s} \rho[34][12] \right) \left( \bar{e}_p^{(r+1)} - \bar{e}_p^{(r)} \right) \otimes \bar{e}_F^{(r)} \otimes \bar{e}_p^{(s)} \otimes \bar{e}_F^{(s)}, \end{aligned} \quad (\text{A.47})$$

$$\begin{aligned} \tilde{\mathbf{M}}_{PPFF} &= \sum_{r,s=1}^k \left( \theta_{r>s} \rho[13][24] + \theta_{r\leq s} \rho[24][13] \right) \left( \bar{e}_p^{(r+1)} - \bar{e}_p^{(r)} \right) \otimes \bar{e}_p^{(s+1)} \otimes \bar{e}_F^{(r)} \otimes \bar{e}_F^{(s)} \\ &\quad - \sum_{r,s=1}^k \left( \theta_{r\geq s} \rho[13][24] + \theta_{r<s} \rho[24][13] \right) \left( \bar{e}_p^{(r+1)} - \bar{e}_p^{(r)} \right) \otimes \bar{e}_p^{(s)} \otimes \bar{e}_F^{(r)} \otimes \bar{e}_F^{(s)} \\ &\quad + \sum_{r,s=1}^k \left( \theta_{r\geq s} \rho[14][23] + \theta_{r<s} \rho[23][14] \right) \bar{e}_p^{(r+1)} \otimes \left( \bar{e}_p^{(s+1)} - \bar{e}_p^{(s)} \right) \otimes \bar{e}_F^{(s)} \otimes \bar{e}_F^{(r)} \\ &\quad - \sum_{r,s=1}^k \left( \theta_{r>s} \rho[14][23] + \theta_{r\leq s} \rho[23][14] \right) \bar{e}_p^{(r)} \otimes \left( \bar{e}_p^{(s+1)} - \bar{e}_p^{(s)} \right) \otimes \bar{e}_F^{(s)} \otimes \bar{e}_F^{(r)} \\ &\quad + \rho[2314] \sum_{r=1}^k \left( \bar{e}_p^{(r+1)} \otimes \bar{e}_p^{(r+1)} - \bar{e}_p^{(r)} \otimes \bar{e}_p^{(r)} \right) \otimes \bar{e}_F^{(r)} \otimes \bar{e}_F^{(r)}. \end{aligned} \quad (\text{A.48})$$

### Orthogonal tensors for four pt. functions:

The results in (A.44),(A.45),(A.46),(A.47) and (A.48) can be proved by demonstrating that the four pt. function should be orthogonal to the following tensors. The arguments for the orthogonality of these tensors to the array of 4 point functions are given in tables A.5–A.12.

### Trivial orthogonal tensors:

$$\begin{aligned} 12k^4 \text{ orthogonal tensors : } & e_{PPPP}^{rSUV}, e_{PPFP}^{rSUV}, e_{PFPP}^{rSUV}, e_{PFFP}^{rSUV}, e_{FPPP}^{rSUV}, e_{FFPF}^{rSUV}, \\ & e_{FPFP}^{rSUV}, e_{FFFF}^{rSUV}, e_{FFPP}^{rSUV}, e_{FFPF}^{rSUV}, e_{FFFP}^{rSUV}, e_{FFFF}^{rSUV} \end{aligned} \quad (\text{A.49})$$

Orthogonal tensor	Total no. of tensors	Argument
$e_{PPPP}^{rsuv}$	$k^4$	$e_{PPPP}^{rsuv} \xrightarrow{\text{P-collapse}} 0$
$e_{PPFP}^{rsuv}$	$k^4$	$e_{PPFP}^{rsuv} \xrightarrow{\text{P-collapse}} 0$
$e_{PFPP}^{rsuv}$	$k^4$	$e_{PFPP}^{rsuv} \xrightarrow{\text{P-collapse}} 0$
$e_{FFPP}^{rsuv}$	$k^4$	$e_{FFPP}^{rsuv} \xrightarrow{\text{P-collapse}} 0$
$e_{FPPF}^{rsuv}$	$k^4$	$e_{FPPF}^{rsuv} \xrightarrow{\text{F-collapse}} 0$
$e_{FFPF}^{rsuv}$	$k^4$	$e_{FFPF}^{rsuv} \xrightarrow{\text{F-collapse}} 0$
$e_{FPFF}^{rsuv}$	$k^4$	$e_{FPFF}^{rsuv} \xrightarrow{\text{F-collapse}} 0$
$e_{FFPF}^{rsuv}$	$k^4$	$e_{FFPF}^{rsuv} \xrightarrow{\text{F-collapse}} 0$
$e_{FFFP}^{rsuv}$	$k^4$	$e_{FFFP}^{rsuv} \xrightarrow{\text{F-collapse}} 0$
$e_{FFPF}^{rsuv}$	$k^4$	$e_{FFPF}^{rsuv} \xrightarrow{\text{F-collapse}} 0$
$e_{FFFP}^{rsuv}$	$k^4$	$e_{FFFP}^{rsuv} \xrightarrow{\text{F-collapse}} 0$
$e_{FFFF}^{rsuv}$	$k^4$	$e_{FFFF}^{rsuv} \xrightarrow{\text{F-collapse}} 0$

Table A.5: Arguments for the tensors trivially orthogonal to the array of 4 point contour correlators

**Orthogonal tensors in the PPPF sector:**

$$\begin{aligned}
&k(k^3 - k) \text{ orthogonal tensors : } e_{PPPF}^{rsuv} \text{ when } r, s \text{ and } u \text{ are not all equal ,} \\
&k(k - 2) \text{ orthogonal tensors : } e_{PPPF}^{rrrs} \text{ for } r \neq s, s + 1 , \\
&2k - 1 \text{ orthogonal tensors : } e_{PPPF}^{(r+1)(r+1)(r+1)r} + e_{PPPF}^{rrrr} .
\end{aligned} \tag{A.50}$$

Total number of orthogonal tensors in this sector =  $k^4 - 1$ .

These orthogonal tensors fix  $\tilde{\mathbf{M}}_{PPPF}$  to be of the following form:

$$\begin{aligned}
&\tilde{\mathbf{M}}_{PPPF} \\
&= \alpha_1^{(4)} \sum_{r=1}^k \left( \bar{e}_p^{(r+1)}(\omega_1) \otimes \bar{e}_p^{(r+1)}(\omega_2) \otimes \bar{e}_p^{(r+1)}(\omega_3) \otimes \bar{e}_F^{(r)}(\omega_4) \right. \\
&\quad \left. - \bar{e}_p^{(r)}(\omega_1) \otimes \bar{e}_p^{(r)}(\omega_2) \otimes \bar{e}_p^{(r)}(\omega_3) \otimes \bar{e}_F^{(r)}(\omega_4) \right) .
\end{aligned} \tag{A.51}$$

The coefficient  $\alpha_1^{(4)}$  is given by the contraction with the tensor  $e_{PPPF}^{(r+1)(r+1)(r+1)r}$ , an example of which is the case  $r = 1$ . Then this coefficient is given by

$$\alpha_1^{(4)} = \tilde{\mathbf{M}}(4\text{-Pt}) \cdot e_{PPPF}^{2221} = \rho[4321] . \tag{A.52}$$

Orthogonal tensor	Total no. of tensors	Argument
$e_{PPPF}^{rsuv}$ when $r, s$ and $u$ are not all equal	$k(k^3 - k)$	<p style="text-align: center;"><u>Case 1: <math>s \neq u</math></u></p> <p style="text-align: center;">W.L.O.G let us consider <math>s &gt; u</math>.</p> <p style="text-align: center;"><u>Subcase 1 : <math>s &gt; (u + 1)</math></u></p> $e_{PPPF}^{rsuv} \xrightarrow{\text{P-collapse}} 0, \text{ otherwise } e_{PPPF}^{rsuv} \xrightarrow{\text{P-collapse}} 0.$ <p style="text-align: center;"><u>Subcase 2 : <math>s = (u + 1)</math></u></p> <p style="text-align: center;">If <math>v = u</math>, then</p> $e_{PPPF}^{r(u+1)uu} \xrightarrow{\text{F-sliding}} -e_{PPPF}^{r(u+1)u(u+1)} \xrightarrow{\text{P-collapse}} 0,$ <p style="text-align: center;">if <math>v &gt; u</math>, then</p> $e_{PPPF}^{r(u+1)uv} \xrightarrow{\text{P-collapse}} 0,$ <p style="text-align: center;">if <math>v &lt; u</math>, then</p> $e_{PPPF}^{r(u+1)uv} \xrightarrow{\text{P-collapse}} 0,$ <p style="text-align: center;"><u>Case 2: <math>s = u \neq r</math></u></p> <p style="text-align: center;">W.L.O.G let us consider <math>r &gt; s</math>.</p> <p style="text-align: center;"><u>Subcase 1 : <math>r &gt; (s + 1)</math></u></p> <p style="text-align: center;">If <math>v \neq s, s - 1</math>, then</p> $e_{PPPF}^{rsvv} \xrightarrow{\text{P-collapse}} 0,$ <p style="text-align: center;">otherwise <math>e_{PPPF}^{rsvv} \xrightarrow{\text{P-collapse}} 0.</math></p> <p style="text-align: center;"><u>Subcase 2 : <math>r = (s + 1)</math></u></p> <p style="text-align: center;">If <math>v = s</math>, then</p> $e_{PPPF}^{(s+1)sss} \xrightarrow{\text{F-sliding}} -e_{PPPF}^{(s+1)ss(s-1)} \xrightarrow{\text{P-collapse}} 0,$ <p style="text-align: center;">if <math>v &gt; s</math>, then <math>e_{PPPF}^{(s+1)ssv} \xrightarrow{\text{P-collapse}} 0,</math></p> <p style="text-align: center;">and if <math>v &lt; s</math>, then <math>e_{PPPF}^{(s+1)ssv} \xrightarrow{\text{P-collapse}} 0.</math></p>
$e_{PPPF}^{rrrs}$ for $s \neq r, r - 1$	$k(k - 2)$	$e_{PPPF}^{rrrs} \xrightarrow{\text{F-collapse}} 0$
$e_{PPPF}^{rrrr} + e_{PPPF}^{(r+1)(r+1)(r+1)r}$	$2k - 1$	$e_{PPPF}^{(r+1)(r+1)(r+1)r} \xrightarrow{\text{C-shift}} e_{PPPF}^{rrr(r-1)} \xrightarrow{\text{F-sliding}} -e_{PPPF}^{rrrr}$

Table A.6: Arguments for the tensors in the PPPF sector orthogonal to the array of 4 point contour correlators

### Orthogonal tensors in the PFFF sector:

$$\begin{aligned}
&k(k^3 - k) \text{ orthogonal tensors : } e_{PFFF}^{rsuv} \text{ when } s, u \text{ and } v \text{ are not all equal ,} \\
&k(k - 2) \text{ orthogonal tensors : } e_{PFFF}^{rsss} \text{ for } r \neq s, s + 1 , \\
&2k - 1 \text{ orthogonal tensors : } e_{PFFF}^{(r+1)rrr} + e_{PFFF}^{rrrr} .
\end{aligned} \tag{A.53}$$

Total number of orthogonal tensors in this sector =  $k^4 - 1$ .

Orthogonal tensor	Total no. of tensors	Argument
$e_{PFFF}^{rsuv}$ when $s, u$ and $v$ are not all equal	$k(k^3 - k)$	<p>Case 1 : <math>s \neq u</math> W.L.O.G, let us consider <math>s &gt; u</math> Subcase 1 : <math>s &gt; (u + 1)</math> <math>e_{PFFF}^{rsuv} \xrightarrow{\text{F-collapse}} 0</math>, otherwise <math>e_{PFFF}^{rsuv} \xrightarrow{\text{F-collapse}} 0</math>.</p> <p>Subcase 2 : <math>s = (u + 1)</math> If <math>r = u + 1</math>, then <math>e_{PFFF}^{(u+1)(u+1)uv} \xrightarrow{\text{P-sliding}} -e_{PFFF}^{u(u+1)uv} \xrightarrow{\text{F-collapse}} 0</math>, if <math>r &gt; u + 1</math>, then <math>e_{PFFF}^{r(u+1)uv} \xrightarrow{\text{F-collapse}} 0</math>, if <math>r &lt; u + 1</math>, then <math>e_{PFFF}^{r(u+1)uv} \xrightarrow{\text{F-collapse}} 0</math>.</p> <p>Case 2 : <math>s = u \neq v</math> W.L.O.G, let us consider <math>s &gt; v</math> Subcase 1 : <math>s &gt; (v + 1)</math> If <math>r \neq s, s + 1</math>, then <math>e_{PFFF}^{rssv} \xrightarrow{\text{F-collapse}} 0</math>, otherwise <math>e_{PFFF}^{rssv} \xrightarrow{\text{F-collapse}} 0</math>.</p> <p>Subcase 2 : <math>s = (v + 1)</math> If <math>r = v + 1</math>, then <math>e_{PFFF}^{(v+1)(v+1)(v+1)v} \xrightarrow{\text{P-sliding}} -e_{PFFF}^{(v+2)(v+1)(v+1)v} \xrightarrow{\text{F-collapse}} 0</math>, if <math>r &gt; (v + 1)</math>, then <math>e_{PFFF}^{r(v+1)(v+1)v} \xrightarrow{\text{F-collapse}} 0</math>, and if <math>r &lt; (v + 1)</math>, then <math>e_{PFFF}^{r(v+1)(v+1)v} \xrightarrow{\text{F-collapse}} 0</math></p>
$e_{PFFF}^{rsss}$ for $r \neq s, s + 1$	$k(k - 2)$	$e_{PFFF}^{rsss} \xrightarrow{\text{F-collapse}} 0$
$e_{PFFF}^{rrrr} + e_{PFFF}^{(r+1)rrr}$	$2k - 1$	$e_{PFFF}^{(r+1)rrr} \xrightarrow{\text{P-sliding}} -e_{PFFF}^{rrrr}$

Table A.7: Arguments for the tensors in the PFFF sector orthogonal to the array of 4 point contour correlators

These orthogonal tensors fix  $\tilde{\mathbf{M}}_{PFFF}$  to be of the following form:

$$\begin{aligned} \tilde{\mathbf{M}}_{PFFF} &= \alpha_2^{(4)} \sum_{r=1}^k \left( \bar{e}_p^{(r+1)}(\omega_1) - \bar{e}_p^{(r)}(\omega_1) \right) \otimes \bar{e}_p^{(r)}(\omega_2) \otimes \bar{e}_p^{(r)}(\omega_3) \otimes \bar{e}_p^{(r)}(\omega_4). \end{aligned} \quad (\text{A.54})$$

The coefficient  $\alpha_2^{(4)}$  is given by the contraction with the tensor  $e_{PFFF}^{(r+1)rrr}$ , an example of which is the case  $r = 1$ . Then this coefficient is given by

$$\alpha_2^{(4)} = \widetilde{\mathbf{M}}(4\text{-Pt}) \cdot e_{PFFF}^{2111} = \rho[1234]. \quad (\text{A.55})$$

**Orthogonal tensors in the PFPF sector:**

$$\begin{aligned}
& k^3(k-2) \text{ orthogonal tensors : } e_{PFFF}^{rsuv} \text{ for } r \neq s, s+1, \\
& k^2(k-2) \text{ orthogonal tensors : } e_{PFFF}^{(r+1)ruv} \text{ for } v \neq u, u-1, \\
& k^2(k-2) \text{ orthogonal tensors : } e_{PFFF}^{rruv} \text{ for } v \neq u, u-1, \\
& k^2 \text{ orthogonal tensors : } e_{PFFF}^{(r+1)ruu} + e_{PFFF}^{rruu}, \\
& k^2 \text{ orthogonal tensors : } e_{PFFF}^{rr(u+1)u} + e_{PFFF}^{rr(u+1)(u+1)}, \\
& k^2 \text{ orthogonal tensors : } e_{PFFF}^{(r+1)r(u+1)u} - e_{PFFF}^{rr(u+1)(u+1)}, \\
& \frac{1}{2}(k^2 - k) \text{ orthogonal tensors : } e_{PFFF}^{(r+1+l)(r+1+l)rr} - e_{PFFF}^{(r+1)(r+1)rr} \text{ for } 1 \leq l \leq (k-r), \\
& \frac{1}{2}(k^2 - k) \text{ orthogonal tensors : } e_{PFFF}^{(r-l)(r-l)(r+1)(r+1)} - e_{PFFF}^{rr(r+1)(r+1)} \text{ for } 1 \leq l \leq (r-1), \\
& k-1 \text{ orthogonal tensors : } e_{PFFF}^{rrrr} - e_{PFFF}^{1111}.
\end{aligned} \quad (\text{A.56})$$

Total number of orthogonal tensors in this sector =  $k^4 - 1$ .

These orthogonal tensors fix  $\widetilde{\mathbf{M}}_{PFPF}$  to be of the following form:

$$\begin{aligned}
& \widetilde{\mathbf{M}}_{PFPF} \\
& = \alpha_3^{(4)} \sum_{r,s=1}^k \left( \theta_{r>s} + \theta_{r \leq s} e^{\beta(\omega_3 + \omega_4)} \right) \\
& \quad \left( \bar{e}_p^{(r+1)}(\omega_1) - \bar{e}_p^{(r)}(\omega_1) \right) \otimes \bar{e}_f^{(r)}(\omega_2) \otimes \bar{e}_p^{(s+1)}(\omega_3) \otimes \bar{e}_f^{(s)}(\omega_4) \\
& - \alpha_3^{(4)} \sum_{r,s=1}^k \left( \theta_{r \geq s} + \theta_{r < s} e^{\beta(\omega_3 + \omega_4)} \right) \\
& \quad \left( \bar{e}_p^{(r+1)}(\omega_1) - \bar{e}_p^{(r)}(\omega_1) \right) \otimes \bar{e}_f^{(r)}(\omega_2) \otimes \bar{e}_p^{(s)}(\omega_3) \otimes \bar{e}_f^{(s)}(\omega_4).
\end{aligned} \quad (\text{A.57})$$

The coefficient  $\alpha_3^{(4)}$  is given by the contraction with the tensor  $e_{PFFF}^{(r+1)r(s+1)s}$  for  $r>s$ , an example of which is the case  $r=2, s=1$ . Then this coefficient is given by

$$\alpha_3^{(4)} = \widetilde{\mathbf{M}}(4\text{-Pt}) \cdot e_{PFFF}^{3221} = \rho[12][34]. \quad (\text{A.58})$$

Orthogonal tensor	Total no. of tensors	Argument
$e_{PPFF}^{r,suv}$ for $r \neq s, s+1$	$k^3(k-2)$	$e_{PPFF}^{r,suv} \xrightarrow{\text{F-collapse}} 0$
$e_{PPFF}^{(s+1)suv}$ for $v \neq u, u-1$	$k^2(k-2)$	$e_{PPFF}^{(s+1)suv} \xrightarrow{\text{P-collapse}} 0$
$e_{PPFF}^{ssuv}$ for $v \neq u, u-1$	$k^2(k-2)$	$e_{PPFF}^{ssuv} \xrightarrow{\text{P-collapse}} 0$
$e_{PPFF}^{(s+1)suu} + e_{PPFF}^{ssuu}$	$k^2$	$e_{PPFF}^{(s+1)suu} \xrightarrow{\text{P-sliding}} -e_{PPFF}^{ssuu}$
$e_{PPFF}^{ss(u+1)u} + e_{PPFF}^{ss(u+1)(u+1)}$	$k^2$	$e_{PPFF}^{ss(u+1)u} \xrightarrow{\text{F-sliding}} -e_{PPFF}^{ss(u+1)(u+1)}$
$e_{PPFF}^{(s+1)s(u+1)u} - e_{PPFF}^{ss(u+1)(u+1)}$	$k^2$	$e_{PPFF}^{(s+1)s(u+1)u} \xrightarrow{\text{F-sliding}} -e_{PPFF}^{(s+1)s(u+1)(u+1)}$ $\xrightarrow{\text{P-sliding}} e_{PPFF}^{ss(u+1)(u+1)}$
$e_{PPFF}^{(s+1)l(s+1+l)ss} - e_{PPFF}^{(s+1)(s+1)ss}$ for $1 \leq l \leq (k-s)$	$\frac{1}{2}(k^2 - k)$	$e_{PPFF}^{(s+1)(s+1)ss} \xrightarrow{\text{P-sliding}} -e_{PPFF}^{(s+2)(s+1)ss}$ $\xrightarrow{\text{F-sliding}} e_{PPFF}^{(s+2)(s+2)ss}$ $\xrightarrow{\text{P-sliding}} -e_{PPFF}^{(s+3)(s+2)ss}$ $\xrightarrow{\text{F-sliding}} e_{PPFF}^{(s+3)(s+3)ss}$ $\xrightarrow{\text{P-sliding}} \dots \xrightarrow{\text{F-sliding}} e_{PPFF}^{(s+1+l)(s+1+l)ss}$
$\left( e_{PPFF}^{(s-l)(s-l)(s+1)(s+1)} - e_{PPFF}^{ss(s+1)(s+1)} \right)$ for $1 \leq l \leq (s-1)$	$\frac{1}{2}(k^2 - k)$	$e_{PPFF}^{ss(s+1)(s+1)} \xrightarrow{\text{F-sliding}} -e_{PPFF}^{s(s-1)(s+1)(s+1)}$ $\xrightarrow{\text{P-sliding}} e_{PPFF}^{(s-1)(s-1)(s+1)(s+1)}$ $\xrightarrow{\text{F-sliding}} -e_{PPFF}^{(s-1)(s-2)(s+1)(s+1)}$ $\xrightarrow{\text{P-sliding}} e_{PPFF}^{(s-2)(s-2)(s+1)(s+1)}$ $\xrightarrow{\text{F-sliding}} \dots \xrightarrow{\text{P-sliding}} e_{PPFF}^{(s-l)(s-l)(s+1)(s+1)}$
$e_{PPFF}^{ssss} - e_{PPFF}^{1111}$	$k-1$	$e_{PPFF}^{ssss} \xrightarrow{\text{C-shift}} e_{PPFF}^{1111}$

Table A.8: Arguments for the tensors in the PFPF sector orthogonal to the array of 4 point contour correlators

**Orthogonal tensors in the PPF sector:**

$k(k-3)(k^2-8)$  orthogonal tensors :  $e_{PPFF}^{rsuv}$  for  $|u-v| > 1$  and

$$(r, s) \notin \{(u, v), (u, v+1), (u+1, v), (u+1, v+1), \\ (v, u), (v+1, u), (v, u+1), (v+1, u+1)\},$$

$k(k-3)$  orthogonal tensors :  $e_{PPFF}^{(u+1)vu} + e_{PPFF}^{uvuv}$  for  $|u-v| > 1$ ,

$k(k-3)$  orthogonal tensors :  $e_{PPFF}^{u(v+1)uv} + e_{PPFF}^{uvuv}$  for  $|u-v| > 1$ ,

$k(k-3)$  orthogonal tensors :  $e_{PPFF}^{(u+1)(v+1)uv} - e_{PPFF}^{uvuv}$  for  $|u-v| > 1$ ,

$k(k-3)$  orthogonal tensors :  $e_{PPFF}^{v(u+1)uv} + e_{PPFF}^{vuuv}$  for  $|u-v| > 1$ ,

$k(k-3)$  orthogonal tensors :  $e_{PPFF}^{(v+1)uv} + e_{PPFF}^{vuuv}$  for  $|u-v| > 1$ ,

$k(k-3)$  orthogonal tensors :  $e_{PPFF}^{(v+1)(u+1)uv} - e_{PPFF}^{vuuv}$  for  $|u-v| > 1$ .

(A.59)



$k(k^2 - 7)$  orthogonal tensors :  $e_{PPFF}^{rsu(u+1)}$

for  $(r, s) \notin \{(u, u + 1), (u, u + 2), (u + 1, u + 1),$

$(u + 1, u + 2), (u + 1, u), (u + 2, u),$

$(u + 2, u + 1)\}$ ,

$k(k^2 - 7)$  orthogonal tensors :  $e_{PPFF}^{rs(v+1)v}$

for  $(r, s) \notin \{(v + 1, v), (v + 2, v), (v + 1, v + 1),$

$(v + 2, v + 1), (v, v + 1), (v, v + 2),$

$(v + 1, v + 2)\}$ ,

$k$  orthogonal tensors :  $e_{PPFF}^{u(u+2)u(u+1)} + e_{PPFF}^{u(u+1)u(u+1)}$ ,

(A.60)

$k$  orthogonal tensors :  $e_{PPFF}^{(u+1)(u+2)u(u+1)} - e_{PPFF}^{u(u+1)u(u+1)}$ ,

$k$  orthogonal tensors :  $e_{PPFF}^{(u+2)uu(u+1)} + e_{PPFF}^{(u+1)uu(u+1)}$ ,

$k$  orthogonal tensors :  $e_{PPFF}^{(u+2)(u+1)u(u+1)} - e_{PPFF}^{(u+1)uu(u+1)}$ ,

$k$  orthogonal tensors :  $e_{PPFF}^{v(v+2)(v+1)v} + e_{PPFF}^{v(v+1)(v+1)v}$ ,

$k$  orthogonal tensors :  $e_{PPFF}^{(v+1)(v+2)(v+1)v} - e_{PPFF}^{v(v+1)(v+1)v}$ ,

$k$  orthogonal tensors :  $e_{PPFF}^{(v+2)v(v+1)v} + e_{PPFF}^{(v+1)v(v+1)v}$ ,

$k$  orthogonal tensors :  $e_{PPFF}^{(v+2)(v+1)(v+1)v} - e_{PPFF}^{(v+1)v(v+1)v}$ ,

$k - 1$  orthogonal tensors :  $e_{PPFF}^{(u+1)(u+1)u(u+1)} - e_{PPFF}^{2212}$ ,

$k - 1$  orthogonal tensors :  $e_{PPFF}^{(v+1)(v+1)(v+1)v} - e_{PPFF}^{2221}$ .

$\frac{1}{2}k(k - 1) - 1$  orthogonal tensors :  $e_{PPFF}^{uvuv} - e_{PPFF}^{2121}$  for  $u > v$ ,

$\frac{1}{2}k(k - 1) - 1$  orthogonal tensors :  $e_{PPFF}^{uvuv} - e_{PPFF}^{1212}$  for  $u < v$ ,

$\frac{1}{2}k(k - 1) - 1$  orthogonal tensors :  $e_{PPFF}^{vuuv} - e_{PPFF}^{1221}$  for  $u > v$ ,

$\frac{1}{2}k(k - 1) - 1$  orthogonal tensors :  $e_{PPFF}^{vuuv} - e_{PPFF}^{2112}$  for  $u < v$ ,

(A.61)

1 orthogonal tensor :  $e_{PPFF}^{1212} - e^{\beta(\omega_2 + \omega_4)} e_{PPFF}^{2121}$ ,

1 orthogonal tensor :  $e_{PPFF}^{2112} - e^{\beta(\omega_1 + \omega_4)} e_{PPFF}^{1221}$ .

$k(k^2 - 4)$  orthogonal tensors :  $e_{PPFF}^{rsuu}$  for  $(r, s) \notin \{(u, u), (u + 1, u), (u, u + 1), (u + 1, u + 1)\}$  ,

$k - 1$  orthogonal tensors :  $e_{PPFF}^{uuuu} - e_{PPFF}^{1111}$  ,

$k - 1$  orthogonal tensors :  $e_{PPFF}^{(u+1)(u+1)uu} - e_{PPFF}^{2211}$  ,

$k - 1$  orthogonal tensors :  $e_{PPFF}^{(u+1)uuu} - e_{PPFF}^{2111}$  ,

$k - 1$  orthogonal tensors :  $e_{PPFF}^{u(u+1)uu} - e_{PPFF}^{1211}$  ,

1 orthogonal tensor :  $e_{PPFF}^{2111} - e_{PPFF}^{3121} - e_{PPFF}^{3112}$  ,

1 orthogonal tensor :  $e_{PPFF}^{1211} - e_{PPFF}^{1321} - e_{PPFF}^{1312}$  ,

1 orthogonal tensor :  $e_{PPFF}^{2221} - e_{PPFF}^{2331} - e_{PPFF}^{3231}$  ,

1 orthogonal tensor :  $e_{PPFF}^{2212} - e_{PPFF}^{2313} - e_{PPFF}^{3213}$  ,

1 orthogonal tensor :  $e_{PPFF}^{1111} + e_{PPFF}^{2111} + e_{PPFF}^{1211} + e_{PPFF}^{2211}$  .

(A.62)

Total number of orthogonal tensors in this sector =  $k^4 - 3$ .

Orthogonal tensor	Total no. of tensors	Argument
$e_{PPFF}^{rsuv}$ for $ u - v  > 1$ and $(r, s) \notin \{(u, v), (u, v + 1), (u + 1, v), (u + 1, v + 1), (v, u), (v + 1, u), (v, u + 1), (v + 1, u + 1)\}$	$k(k - 3)$ $(k^2 - 8)$	If $r \neq u, u + 1$ and $s \neq u, u + 1$ , then $e_{PPFF}^{rsuv} \xrightarrow{\text{F-collapse}} 0$ If $r \neq v, v + 1$ and $s \neq v, v + 1$ then $e_{PPFF}^{rsuv} \xrightarrow{\text{F-collapse}} 0$
$e_{PPFF}^{(u+1)vuv} + e_{PPFF}^{uvuv}$ for $ u - v  > 1$	$k(k - 3)$	$e_{PPFF}^{(u+1)vuv} \xrightarrow{\text{P-sliding}} -e_{PPFF}^{uvuv}$
$e_{PPFF}^{u(v+1)uv} + e_{PPFF}^{uvuv}$ for $ u - v  > 1$	$k(k - 3)$	$e_{PPFF}^{u(v+1)uv} \xrightarrow{\text{P-sliding}} -e_{PPFF}^{uvuv}$
$e_{PPFF}^{(u+1)(v+1)uv} - e_{PPFF}^{uvuv}$ for $ u - v  > 1$	$k(k - 3)$	$e_{PPFF}^{(u+1)(v+1)uv} \xrightarrow{\text{P-sliding}} -e_{PPFF}^{(u+1)vuv}$ $\xrightarrow{\text{P-sliding}} e_{PPFF}^{uvuv}$
$e_{PPFF}^{v(u+1)uv} + e_{PPFF}^{vuvv}$ for $ u - v  > 1$	$k(k - 3)$	$e_{PPFF}^{v(u+1)uv} \xrightarrow{\text{P-sliding}} -e_{PPFF}^{vuvv}$
$e_{PPFF}^{(v+1)uvv} + e_{PPFF}^{vuvv}$ for $ u - v  > 1$	$k(k - 3)$	$e_{PPFF}^{(v+1)uvv} \xrightarrow{\text{P-sliding}} -e_{PPFF}^{vuvv}$
$e_{PPFF}^{(v+1)(u+1)uv} - e_{PPFF}^{uvuv}$ for $ u - v  > 1$	$k(k - 3)$	$e_{PPFF}^{(v+1)(u+1)uv} \xrightarrow{\text{P-sliding}} -e_{PPFF}^{v(u+1)uv}$ $\xrightarrow{\text{P-sliding}} e_{PPFF}^{vuvv}$

Table A.9: Arguments for the tensors in the PPF sector orthogonal to the array of 4 point contour correlators

Orthogonal tensor	Total no. of tensors	Argument
$e_{PPFF}^{rsu(u+1)}$ <p>for <math>(r, s) \notin \{(u, u+1), (u, u+2), (u+1, u+1), (u+1, u+2), (u+1, u), (u+2, u), (u+2, u+1)\}</math></p>	$k(k^2 - 7)$	<p>If <math>r \neq u, u+1</math> and <math>s \neq u, u+1</math>,</p> <p>then <math>e_{PPFF}^{rsu(u+1)} \xrightarrow{\text{F-collapse}} 0</math>.</p> <p>If <math>r \neq u+1, u+2</math> and <math>s \neq u+1, u+2</math>,</p> <p>then <math>e_{PPFF}^{rsu(u+1)} \xrightarrow{\text{F-collapse}} 0</math>.</p>
$e_{PPFF}^{rs(v+1)v}$ <p>for <math>(r, s) \notin \{(v+1, v), (v+2, v), (v+1, v+1), (v+2, v+1), (v, v+1), (v, v+2), (v+1, v+2)\}</math></p>	$k(k^2 - 7)$	<p>If <math>r \neq v, v+1</math> and <math>s \neq v, v+1</math>,</p> <p>then <math>e_{PPFF}^{rs(v+1)v} \xrightarrow{\text{F-collapse}} 0</math>.</p> <p>If <math>r \neq v+1, v+2</math> and <math>s \neq v+1, v+2</math>,</p> <p>then <math>e_{PPFF}^{rs(v+1)v} \xrightarrow{\text{F-collapse}} 0</math>.</p>
$e_{PPFF}^{u(u+2)u(u+1)} + e_{PPFF}^{u(u+1)u(u+1)}$	$k$	$e_{PPFF}^{u(u+2)u(u+1)} \xrightarrow{\text{P-sliding}} -e_{PPFF}^{u(u+1)u(u+1)}$
$e_{PPFF}^{(u+1)(u+2)u(u+1)} - e_{PPFF}^{u(u+1)u(u+1)}$	$k$	$e_{PPFF}^{(u+1)(u+2)u(u+1)} \xrightarrow{\text{P-sliding}} -e_{PPFF}^{u(u+2)u(u+1)}$ $\xrightarrow{\text{P-sliding}} e_{PPFF}^{u(u+1)u(u+1)}$
$e_{PPFF}^{(u+2)uu(u+1)} + e_{PPFF}^{(u+1)uu(u+1)}$	$k$	$e_{PPFF}^{(u+2)uu(u+1)} \xrightarrow{\text{P-sliding}} -e_{PPFF}^{(u+1)uu(u+1)}$
$e_{PPFF}^{(u+2)(u+1)u(u+1)} - e_{PPFF}^{(u+1)uu(u+1)}$	$k$	$e_{PPFF}^{(u+2)(u+1)u(u+1)} \xrightarrow{\text{P-sliding}} -e_{PPFF}^{(u+2)uu(u+1)}$ $\xrightarrow{\text{P-sliding}} e_{PPFF}^{(u+1)uu(u+1)}$
$e_{PPFF}^{v(v+2)(v+1)v} + e_{PPFF}^{v(v+1)(v+1)v}$	$k$	$e_{PPFF}^{v(v+2)(v+1)v} \xrightarrow{\text{P-sliding}} -e_{PPFF}^{v(v+1)(v+1)v}$
$e_{PPFF}^{(v+1)(v+2)(v+1)v} - e_{PPFF}^{v(v+1)(v+1)v}$	$k$	$e_{PPFF}^{(v+1)(v+2)(v+1)v} \xrightarrow{\text{P-sliding}} -e_{PPFF}^{v(v+2)(v+1)v}$ $\xrightarrow{\text{P-sliding}} e_{PPFF}^{v(v+1)(v+1)v}$
$e_{PPFF}^{(v+2)v(v+1)v} + e_{PPFF}^{(v+1)v(v+1)v}$	$k$	$e_{PPFF}^{(v+2)v(v+1)v} \xrightarrow{\text{P-sliding}} -e_{PPFF}^{(v+1)v(v+1)v}$
$e_{PPFF}^{(v+2)(v+1)(v+1)v} - e_{PPFF}^{(v+1)v(v+1)v}$	$k$	$e_{PPFF}^{(v+2)(v+1)(v+1)v} \xrightarrow{\text{P-sliding}} -e_{PPFF}^{(v+2)v(v+1)v}$ $\xrightarrow{\text{P-sliding}} e_{PPFF}^{(v+1)v(v+1)v}$
$e_{PPFF}^{(u+1)(u+1)u(u+1)} - e_{PPFF}^{2212}$	$k - 1$	$e_{PPFF}^{2212} \xrightarrow{\text{C-shift}} e_{PPFF}^{(u+1)(u+1)u(u+1)}$
$e_{PPFF}^{(v+1)(v+1)(v+1)v} - e_{PPFF}^{2221}$	$k - 1$	$e_{PPFF}^{2221} \xrightarrow{\text{C-shift}} e_{PPFF}^{(v+1)(v+1)(v+1)v}$

Table A.10: Arguments for the tensors in the PPF sector orthogonal to the array of 4 point contour correlators

Orthogonal tensor	Total no. of tensors	Argument
$e_{PPFF}^{uvuv} - e_{PPFF}^{2121}$ for $u > v$	$\frac{1}{2}k(k-1) - 1$	<p><u>Case 1: <math>u=v+1</math></u>  <math>e_{PPFF}^{2121} \xrightarrow{\text{C-shift}} e_{PPFF}^{(v+1)v(v+1)v}</math></p> <p><u>Case 2: <math>u=(v+m)</math> where <math>m &gt; 1</math></u>  <math>e_{PPFF}^{2121} \xrightarrow{\text{P-sliding}} e_{PPFF}^{3121} \xrightarrow{\text{F-sliding}} e_{PPFF}^{3131}</math>  <math>\xrightarrow{\text{P-sliding}} \dots \xrightarrow{\text{F-sliding}} e_{PPFF}^{(1+m)1(1+m)1}</math>  <math>\xrightarrow{\text{C-shift}} e_{PPFF}^{(v+m)v(v+m)v}</math></p>
$e_{PPFF}^{uvuv} - e_{PPFF}^{1212}$ for $u < v$	$\frac{1}{2}k(k-1) - 1$	<p><u>Case 1: <math>v=u+1</math></u>  <math>e_{PPFF}^{1212} \xrightarrow{\text{C-shift}} e_{PPFF}^{u(u+1)u(u+1)}</math></p> <p><u>Case 2: <math>v=(u+m)</math> where <math>m &gt; 1</math></u>  <math>e_{PPFF}^{1212} \xrightarrow{\text{P-sliding}} e_{PPFF}^{1312} \xrightarrow{\text{F-sliding}} e_{PPFF}^{1313}</math>  <math>\xrightarrow{\text{P-sliding}} \dots \xrightarrow{\text{F-sliding}} e_{PPFF}^{1(1+m)1(1+m)}</math>  <math>\xrightarrow{\text{C-shift}} e_{PPFF}^{u(u+m)u(u+m)}</math></p>
$e_{PPFF}^{vuuv} - e_{PPFF}^{1221}$ for $u > v$	$\frac{1}{2}k(k-1) - 1$	<p><u>Case 1: <math>u=v+1</math></u>  <math>e_{PPFF}^{1221} \xrightarrow{\text{C-shift}} e_{PPFF}^{v(v+1)(v+1)v}</math></p> <p><u>Case 2: <math>u=(v+m)</math> where <math>m &gt; 1</math></u>  <math>e_{PPFF}^{1221} \xrightarrow{\text{P-sliding}} e_{PPFF}^{1321} \xrightarrow{\text{F-sliding}} e_{PPFF}^{1331}</math>  <math>\xrightarrow{\text{P-sliding}} \dots \xrightarrow{\text{F-sliding}} e_{PPFF}^{1(1+m)(1+m)1}</math>  <math>\xrightarrow{\text{C-shift}} e_{PPFF}^{v(v+m)(v+m)v}</math></p>
$e_{PPFF}^{vuuv} - e_{PPFF}^{2112}$ for $u < v$	$\frac{1}{2}k(k-1) - 1$	<p><u>Case 1: <math>v=u+1</math></u>  <math>e_{PPFF}^{2112} \xrightarrow{\text{C-shift}} e_{PPFF}^{(u+1)uu(u+1)}</math></p> <p><u>Case 2: <math>v=(u+m)</math> where <math>m &gt; 1</math></u>  <math>e_{PPFF}^{2112} \xrightarrow{\text{P-sliding}} e_{PPFF}^{3112} \xrightarrow{\text{F-sliding}} e_{PPFF}^{3113}</math>  <math>\xrightarrow{\text{P-sliding}} \dots \xrightarrow{\text{F-sliding}} e_{PPFF}^{(1+m)11(1+m)}</math>  <math>\xrightarrow{\text{C-shift}} e_{PPFF}^{(u+m)uu(u+m)}</math></p>
$e_{PPFF}^{1212} - e^{\beta(\omega_2+\omega_4)} e_{PPFF}^{2121}$	1	$e_{PPFF}^{1212} \xrightarrow{\text{C-shift}} e_{PPFF}^{k(k+1)k(k+1)} \rightarrow e^{\beta(\omega_2+\omega_4)} e_{PPFF}^{k1k1}$ We have already shown that $e_{PPFF}^{k1k1} \rightarrow e_{PPFF}^{2121}$ . Therefore, $e_{PPFF}^{1212} \rightarrow e^{\beta(\omega_2+\omega_4)} e_{PPFF}^{2121}$ .
$e_{PPFF}^{2112} - e^{\beta(\omega_1+\omega_4)} e_{PPFF}^{1221}$	1	$e_{PPFF}^{2112} \xrightarrow{\text{C-shift}} e_{PPFF}^{(k+1)kk(k+1)} \rightarrow e^{\beta(\omega_1+\omega_4)} e_{PPFF}^{1kk1}$ We have already shown that $e_{PPFF}^{1kk1} \rightarrow e_{PPFF}^{1221}$ . Therefore, $e_{PPFF}^{2112} \rightarrow e^{\beta(\omega_1+\omega_4)} e_{PPFF}^{1221}$ .

Table A.11: Arguments for the tensors in the PPF sector orthogonal to the array of 4 point contour correlators

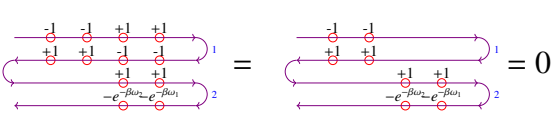
Orthogonal tensor	Total no. of tensors	Argument
$e_{PPFF}^{rsuu}$ for $(r, s) \notin \{(u, u), (u + 1, u), (u, u + 1), (u + 1, u + 1)\}$	$k(k^2 - 4)$	If $r \neq u, u + 1$ then, $e_{PPFF}^{rsuu} \xrightarrow{\text{P-collapse}} 0$ . If $s \neq u, u + 1$ then, $e_{PPFF}^{rsuu} \xrightarrow{\text{P-collapse}} 0$ .
$e_{PPFF}^{uuuu} - e_{PPFF}^{1111}$	$k - 1$	$e_{PPFF}^{1111} \xrightarrow{\text{C-shift}} e_{PPFF}^{uuuu}$
$e_{PPFF}^{(u+1)(u+1)uu} - e_{PPFF}^{2211}$	$k - 1$	$e_{PPFF}^{2211} \xrightarrow{\text{C-shift}} e_{PPFF}^{(u+1)(u+1)uu}$
$e_{PPFF}^{(u+1)uuu} - e_{PPFF}^{2111}$	$k - 1$	$e_{PPFF}^{2111} \xrightarrow{\text{C-shift}} e_{PPFF}^{(u+1)uuu}$
$e_{PPFF}^{u(u+1)uu} - e_{PPFF}^{1211}$	$k - 1$	$e_{PPFF}^{1211} \xrightarrow{\text{C-shift}} e_{PPFF}^{u(u+1)uu}$
$e_{PPFF}^{2111} - e_{PPFF}^{3121} - e_{PPFF}^{3112}$	1	$e_{PPFF}^{2111} \xrightarrow{\text{F-fragmentation}} e_{PPFF}^{3111} + e_{PPFF}^{3121} + e_{PPFF}^{3112} + e_{PPFF}^{3122}$ $\xrightarrow{\text{P-collapse}} e_{PPFF}^{3121} + e_{PPFF}^{3112}$
$e_{PPFF}^{1211} - e_{PPFF}^{1321} - e_{PPFF}^{1312}$	1	$e_{PPFF}^{1211} \xrightarrow{\text{F-fragmentation}} e_{PPFF}^{1311} + e_{PPFF}^{1321} + e_{PPFF}^{1312} + e_{PPFF}^{1322}$ $\xrightarrow{\text{P-collapse}} e_{PPFF}^{1321} + e_{PPFF}^{1312}$
$e_{PPFF}^{2221} - e_{PPFF}^{2331} - e_{PPFF}^{3231}$	1	$e_{PPFF}^{2221} \xrightarrow{\text{P-fragmentation}} e_{PPFF}^{2231} + e_{PPFF}^{2331} + e_{PPFF}^{3231} + e_{PPFF}^{3331}$ $\xrightarrow{\text{F-collapse}} e_{PPFF}^{2331} + e_{PPFF}^{3231}$
$e_{PPFF}^{2212} - e_{PPFF}^{2313} - e_{PPFF}^{3213}$	1	$e_{PPFF}^{2212} \xrightarrow{\text{P-fragmentation}} e_{PPFF}^{2213} + e_{PPFF}^{2313} + e_{PPFF}^{3213} + e_{PPFF}^{3313}$ $\xrightarrow{\text{F-collapse}} e_{PPFF}^{2313} + e_{PPFF}^{3213}$
$e_{PPFF}^{1111} + e_{PPFF}^{2111} + e_{PPFF}^{1211} + e_{PPFF}^{2211}$	1	

Table A.12: Arguments for the tensors in the PPF sector orthogonal to the array of 4 point contour correlators

In table A.12, when there is a P/F or fragmentation we indicate the  $e_P/e_F$  that fragments by green colour. Let us explain the argument given for the last orthogonal tensor in table A.12. We successively remove the pair of future-most insertions on the first 2 legs whose contributions cancel each other, thus resulting in zero. These orthogonal tensors fix  $\widetilde{\mathbf{M}}_{PPFF}$  to be of the following form:

$$\begin{aligned}
& \tilde{\mathbf{M}}_{PPFF} \\
&= \alpha_4^{(4)} \sum_{r,s=1}^k \left( \theta_{r>s} + \theta_{r\leq s} e^{\beta(\omega_2+\omega_4)} \right) \\
&\quad \left( \bar{e}_p^{(r+1)}(\omega_1) - \bar{e}_p^{(r)}(\omega_1) \right) \otimes \bar{e}_p^{(s+1)}(\omega_2) \otimes \bar{e}_F^{(r)}(\omega_3) \otimes \bar{e}_F^{(s)}(\omega_4) \\
&- \alpha_4^{(4)} \sum_{r,s=1}^k \left( \theta_{r\geq s} + \theta_{r<s} e^{\beta(\omega_2+\omega_4)} \right) \\
&\quad \left( \bar{e}_p^{(r+1)}(\omega_1) - \bar{e}_p^{(r)}(\omega_1) \right) \otimes \bar{e}_p^{(s)}(\omega_2) \otimes \bar{e}_F^{(r)}(\omega_3) \otimes \bar{e}_F^{(s)}(\omega_4) \\
&+ \alpha_5^{(4)} \sum_{r,s=1}^k \left( \theta_{r\geq s} e^{\beta(\omega_1+\omega_4)} + \theta_{r<s} \right) \\
&\quad \bar{e}_p^{(r+1)}(\omega_1) \otimes \left( \bar{e}_p^{(s+1)}(\omega_2) - \bar{e}_p^{(s)}(\omega_2) \right) \otimes \bar{e}_F^{(s)}(\omega_3) \otimes \bar{e}_F^{(r)}(\omega_4) \\
&- \alpha_5^{(4)} \sum_{r,s=1}^k \left( \theta_{r>s} e^{\beta(\omega_1+\omega_4)} + \theta_{r\leq s} \right) \\
&\quad \bar{e}_p^{(r)}(\omega_1) \otimes \left( \bar{e}_p^{(s+1)}(\omega_2) - \bar{e}_p^{(s)}(\omega_2) \right) \otimes \bar{e}_F^{(s)}(\omega_3) \otimes \bar{e}_F^{(r)}(\omega_4) \\
&+ \alpha_6^{(4)} \sum_{r=1}^k \left( \bar{e}_p^{(r+1)}(\omega_1) \otimes \bar{e}_p^{(r+1)}(\omega_2) \otimes \bar{e}_F^{(r)}(\omega_3) \otimes \bar{e}_F^{(r)}(\omega_4) \right. \\
&\quad \left. - \bar{e}_p^{(r)}(\omega_1) \otimes \bar{e}_p^{(r)}(\omega_2) \otimes \bar{e}_F^{(r)}(\omega_3) \otimes \bar{e}_F^{(r)}(\omega_4) \right).
\end{aligned} \tag{A.63}$$

The coefficient  $\alpha_4^{(4)}$  is given by the contraction with the tensor  $e_{PPFF}^{(r+1)(s+1)rs}$  for  $r > s$ , an example of which is the case  $r = 2, s = 1$ . Then this coefficient is given by

$$\alpha_4^{(4)} = \tilde{\mathbf{M}}(4\text{-Pt}) \cdot e_{PPFF}^{3221} = \rho[13][24]. \tag{A.64}$$

The coefficient  $\alpha_5^{(4)}$  is given by the contraction with the tensor  $e_{PPFF}^{(r+1)(s+1)sr}$  for  $r < s$ , an example of which is the case  $r = 1, s = 2$ . Then this coefficient is given by

$$\alpha_5^{(4)} = \tilde{\mathbf{M}}(4\text{-Pt}) \cdot e_{PPFF}^{2321} = \rho[23][14]. \tag{A.65}$$

Finally, the contraction with the tensor  $e_{PPFF}^{(r+1)(r+1)rr}$  for any  $r \in \{1, \dots, k\}$  gives

$$\alpha_4^{(4)} e^{\beta(\omega_2+\omega_4)} + \alpha_5^{(4)} e^{\beta(\omega_1+\omega_4)} + \alpha_6^{(4)}.$$

Let us look at this contraction for  $r = 1$  which gives

$$\begin{aligned} \alpha_4^{(4)} e^{\beta(\omega_2+\omega_4)} + \alpha_5^{(4)} e^{\beta(\omega_1+\omega_4)} + \alpha_6^{(4)} &= \widetilde{\mathbf{M}}(4\text{-Pt}) \cdot e_{PPFF}^{2211} \\ &= \rho[2314] + \rho[24][13] + \rho[14][23] . \end{aligned} \quad (\text{A.66})$$

Now, using equations (A.64) , (A.65) and the KMS relations, we have

$$\begin{aligned} \alpha_4^{(4)} e^{\beta(\omega_2+\omega_4)} &= e^{\beta(\omega_2+\omega_4)} \rho[13][24] = \rho[24][13] , \\ \alpha_5^{(4)} e^{\beta(\omega_1+\omega_4)} &= e^{\beta(\omega_1+\omega_4)} \rho[23][14] = \rho[14][23] . \end{aligned} \quad (\text{A.67})$$

Replacing the expressions of  $\alpha_4^{(4)} e^{\beta(\omega_2+\omega_4)}$  and  $\alpha_5^{(4)} e^{\beta(\omega_1+\omega_4)}$  obtained in (A.67) into (A.66) we get

$$\alpha_6^{(4)} = \rho[2314] . \quad (\text{A.68})$$

Next using the values of  $\alpha_i^{(4)}$ 's obtained in (A.52), (A.55), (A.58), (A.64), (A.65) and (A.68) respectively, and the following KMS relations:

$$\begin{aligned} \rho[34][12] &= e^{\beta(\omega_3+\omega_4)} \rho[12][34] , \\ \rho[24][13] &= e^{\beta(\omega_2+\omega_4)} \rho[13][24] , \\ \rho[14][23] &= e^{\beta(\omega_1+\omega_4)} \rho[23][14] , \end{aligned} \quad (\text{A.69})$$

we get the expressions in (A.45),(A.46),(A.47) and (A.48).



# Appendix B

## Appendices to Chapter 4

### B.1 Dimensional analysis

In this appendix, we list the dimensions of various couplings etc. that appear in chapter 4.

- Dimensions of position and noise variables :

$$[q] = L, \quad [N] = L^{-1}T. \quad (\text{B.1})$$

- Dimensions of couplings :

$$\begin{aligned} [m_p] &= M, \quad [F] = LT^{-2}, \quad [\gamma] = T^{-1}, \quad [\bar{\mu}^2] = T^{-2}, \\ [\zeta_\gamma] &= [\widehat{\kappa}_{3\gamma}] = LT^{-2}, \quad [\zeta_\mu] = LT^{-3}, \\ [\bar{\lambda}_3] &= [\bar{\kappa}_3] = L^{-1}T^{-2}, \quad [\bar{\lambda}_{3\gamma}] = [\bar{\kappa}_{3\gamma}] = L^{-1}T^{-1}. \end{aligned} \quad (\text{B.2})$$

- Dimensions of Noise parameters :

$$[\langle f^2 \rangle] = L^2T^{-3}, \quad [\zeta_N] = L^3T^{-4}, \quad [Z_l] = L^2T^{-1}. \quad (\text{B.3})$$

- Dimensions of Spectral functions :

$$[\rho[12]] = MT^{-1}, \quad [\rho[12_+]] = M^2L^2T^{-2}, \quad (\text{B.4})$$

$$[\rho[123]] = ML^{-1}T^{-1}, \quad [\rho[123_+]] = [\rho[12_+3]] = M^2LT^{-2}, \quad [\rho[12_+3_+]] = M^3L^3T^{-3}. \quad (\text{B.5})$$

- Dimensions of System Bath couplings

$$[g_x] = [g_y] = MT^{-2}, \quad [g_{xy}] = ML^{-1}T^{-2}. \quad (\text{B.6})$$

- Dimensions of System Bath coupling distribution functions

$$\begin{aligned} [\langle\langle \frac{g_x^2}{m_x} \rangle\rangle] = [\langle\langle \frac{g_y^2}{m_y} \rangle\rangle] &= MT^{-3}, \quad [\langle\langle \frac{g_{xy}^2}{m_x m_y} \rangle\rangle] = L^{-2}T^{-2}, \\ [\langle\langle \frac{g_x g_y g_{xy}}{m_x m_y} \rangle\rangle] &= ML^{-1}T^{-4}. \end{aligned} \quad (\text{B.7})$$

- Dimensions of Spectral function parameters

$$[\gamma_x] = [\gamma_y] = [\Omega] = T^{-1}, \quad [\Gamma_{xy}] = L^{-2}T^2, \quad [\Gamma_3] = L^{-1}. \quad (\text{B.8})$$

- Dimensions of Thermal parameters

$$[\beta] = T, \quad [v_{th}^2] = L^2T^{-2}. \quad (\text{B.9})$$

## B.2 Contour integrals and Poles for the Effective Couplings

In this appendix, we will present some more details about the contour integrals that have to be evaluated to obtain the effective couplings in our model.

For each coupling, we write down the explicit integrals over which double contour integra-

tion <sup>1</sup> needs to be performed. In table 8, we tabulate the poles in each integrand whose residues add to give the final coupling as we perform the contour integral first over  $\omega_1$  and then over  $\omega_3$ . We will write our integrands performing an integral over the frequency delta function:

$$\int_{C'_3} \equiv \int_{C_3} 2\pi\delta(\omega_1 + \omega_2 + \omega_3) . \quad (\text{B.10})$$

The explicit integrals for the cubic couplings are given by the following expressions :

$$\begin{aligned} \bar{\lambda}_3 &= -4\Gamma_3 \int_{C'_3} \frac{(\omega_1 - \omega_2)}{\omega_1} \left(1 - \frac{\omega_1\omega_2}{\Omega^2}\right) \times \prod_{k=1}^3 \frac{\Omega^2}{\omega_k^2 + \Omega^2} = -\frac{3\Gamma_3\Omega^2}{2} , \\ \bar{\kappa}_3 &= -4\Gamma_3 \int_{C'_3} \frac{(\omega_3 - \omega_2)}{\omega_3} \left(1 - \frac{\omega_2\omega_3}{\Omega^2}\right) \times \prod_{k=1}^3 \frac{\Omega^2}{\omega_k^2 + \Omega^2} = -\frac{3\Gamma_3\Omega^2}{2} , \\ \bar{\lambda}_{3\gamma} &= 2i\Gamma_3 \int_{C'_3} \frac{(2\omega_3 - \omega_1)(\omega_1 - \omega_2)}{\omega_1^2\omega_3} \left(1 - \frac{\omega_1\omega_2}{\Omega^2}\right) \times \prod_{k=1}^3 \frac{\Omega^2}{\omega_k^2 + \Omega^2} = -2\Gamma_3\Omega , \\ \bar{\kappa}_{3\gamma} &= 2i\Gamma_3 \int_{C'_3} \frac{(\omega_3 - 2\omega_1)(\omega_3 - \omega_2)}{\omega_1\omega_3^2} \left(1 - \frac{\omega_2\omega_3}{\Omega^2}\right) \times \prod_{k=1}^3 \frac{\Omega^2}{\omega_k^2 + \Omega^2} = -2\Gamma_3\Omega , \end{aligned} \quad (\text{B.11})$$

$$\begin{aligned} \zeta_\gamma &= -\Gamma_3 v_{th}^2 \int_{C'_3} \left[ \left( \frac{2}{\omega_1^2} + \frac{3}{\omega_1\omega_3} \right) \left( 1 + \frac{\omega_3^2}{\Omega^2} \right) - \left( \frac{2}{\omega_3^2} + \frac{3}{\omega_1\omega_3} \right) \left( 1 + \frac{\omega_1^2}{\Omega^2} \right) \right. \\ &\quad \left. - \frac{3}{\omega_1\omega_3} \left( 3 + 2 \frac{\omega_3^2 + \omega_1\omega_3 + \omega_1^2}{\Omega^2} \right) \right] \times \prod_{k=1}^3 \frac{\Omega^2}{\omega_k^2 + \Omega^2} = \frac{3}{2}\Gamma_3 v_{th}^2 , \end{aligned} \quad (\text{B.12})$$

$$\widehat{\kappa}_{3\gamma} = 6\Gamma_3 v_{th}^2 \int_{C'_3} \frac{1}{\omega_1\omega_3} \left( 3 + 2 \frac{\omega_3^2 + \omega_1\omega_3 + \omega_1^2}{\Omega^2} \right) \times \prod_{k=1}^3 \frac{\Omega^2}{\omega_k^2 + \Omega^2} = 3\Gamma_3 v_{th}^2 ,$$

$$\zeta_N = 2\Gamma_3 v_{th}^4 \int_{C'_3} \frac{1}{\omega_1\omega_3} \left( 3 + 2 \frac{\omega_3^2 + \omega_1\omega_3 + \omega_1^2}{\Omega^2} \right) \times \prod_{k=1}^3 \frac{\Omega^2}{\omega_k^2 + \Omega^2} = \Gamma_3 v_{th}^4 ,$$

$$\begin{aligned} \zeta_\mu &= \frac{2\Gamma_3 v_{th}^2}{im_p \Omega^2} \int_{C'_3} \frac{(\omega_1 - \omega_3)}{\omega_1\omega_3} \left( 2\Omega^2 + \omega_1\omega_3 + 2(\omega_1^2 + \omega_1\omega_3 + \omega_3^2) \right) \times \prod_{k=1}^3 \frac{\Omega^2}{\omega_k^2 + \Omega^2} \\ &= -2\Gamma_3 \Omega v_{th}^2 . \end{aligned} \quad (\text{B.13})$$

<sup>1</sup>The integral over  $\omega_2$  is trivial due to the presence of a delta function coming from energy conservation. So, one has to integrate over the frequencies  $\omega_1$  and  $\omega_3$ .

	<b>Poles in <math>\omega_1</math></b>	<b>Poles in <math>\omega_3</math></b>		<b>Poles in <math>\omega_1</math></b>	<b>Poles in <math>\omega_3</math></b>
$\bar{\kappa}_3$	$i\Omega + i\epsilon_1$	$i\Omega - i\epsilon_2$	$\bar{\lambda}_3$	$i\Omega + i\epsilon_1$	$i\Omega - i\epsilon_2$
	$-\omega_3 + i\Omega + i\epsilon_1 - i\epsilon_2$	$2i\Omega - i\epsilon_2$		$-\omega_3 + i\Omega + i\epsilon_1 - i\epsilon_2$	$i\Omega - i\epsilon_2$
$\bar{\kappa}_{3\gamma}$	$i\epsilon_1$	$i\Omega - i\epsilon_2$	$\widehat{\kappa}_{3\gamma}$	$i\epsilon_1$	$i\Omega - i\epsilon_2$
	$i\Omega + i\epsilon_1$	$i\Omega - i\epsilon_2$		$i\Omega + i\epsilon_1$	$i\Omega - i\epsilon_2$
	$-\omega_3 + i\Omega + i\epsilon_1 - i\epsilon_2$	$i\Omega - i\epsilon_2$		$-\omega_3 + i\Omega + i\epsilon_1 - i\epsilon_2$	$i\Omega - i\epsilon_2$
	$-\omega_3 + i\Omega + i\epsilon_1 - i\epsilon_2$	$2i\Omega - i\epsilon_2$		$-\omega_3 + i\Omega + i\epsilon_1 - i\epsilon_2$	$2i\Omega - i\epsilon_2$
$\bar{\lambda}_{3\gamma}$	$i\epsilon_1$	$i\Omega - i\epsilon_2$	$\zeta_\mu$	$i\epsilon_1$	$i\Omega - i\epsilon_2$
	$i\Omega + i\epsilon_1$	$i\Omega - i\epsilon_2$		$-\omega_3 + i\Omega + i\epsilon_1 - i\epsilon_2$	$i\Omega - i\epsilon_2$
	$-\omega_3 + i\Omega + i\epsilon_1 - i\epsilon_2$	$i\Omega - i\epsilon_2$		$-\omega_3 + i\Omega + i\epsilon_1 - i\epsilon_2$	$2i\Omega - i\epsilon_2$
$\zeta_N$	$i\epsilon_1$	$i\Omega - i\epsilon_2$	$\zeta_\gamma$	$i\epsilon_1$	$i\Omega - i\epsilon_2$
	$i\Omega + i\epsilon_1$	$i\Omega - i\epsilon_2$		$i\Omega + i\epsilon_1$	$i\Omega - i\epsilon_2$
	$-\omega_3 + i\Omega + i\epsilon_1 - i\epsilon_2$	$i\Omega - i\epsilon_2$		$-\omega_3 + i\Omega + i\epsilon_1 - i\epsilon_2$	$i\Omega - i\epsilon_2$
	$-\omega_3 + i\Omega + i\epsilon_1 - i\epsilon_2$	$2i\Omega - i\epsilon_2$		$-\omega_3 + i\Omega + i\epsilon_1 - i\epsilon_2$	$2i\Omega - i\epsilon_2$

Table B.1: Poles for determining cubic couplings

# Appendix C

## Appendices to Chapter 5

### C.1 Cumulants of the bath operator that couples to the particle

In this appendix, we provide the forms of the 2-point and 4-point cumulants of the bath operator  $\lambda O(t) \equiv \lambda \sum_{i,j} g_{xy,ij} X^{(i)}(t) Y^{(j)}(t)$  that couples to the particle. These cumulants are calculated in the high temperature limit where

$$\beta\Omega \ll 1. \quad (\text{C.1})$$

We will see that, in this limit, the cumulants decay exponentially when the separations between insertions are increased. To show the form of this decay we follow the notational conventions given below:

- The interval between two time instants  $t_i$  and  $t_j$  is expressed as

$$t_{ij} \equiv t_i - t_j. \quad (\text{C.2})$$

- The cumulant of any Wightman correlator  $\langle O(t_{i_1}) O(t_{i_2}) \cdots O(t_{i_n}) \rangle$  is expressed as

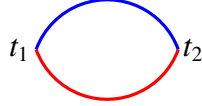
$$\langle i_1 i_2 \cdots i_n \rangle \equiv \langle O(t_{i_1}) O(t_{i_2}) \cdots O(t_{i_n}) \rangle_c. \quad (\text{C.3})$$

Keeping these notational conventions in mind, let us now discuss the decaying behaviour of the cumulants.

### C.1.1 2-point cumulants

From the form of the operator  $O(t)$  given in (5.3), we can see that the 2 point cumulants receive contributions from the Feynman diagram shown in figure C.1. Here the blue and red lines

Figure C.1: Feynman diagram contributing to the 2-point cumulants



represent  $X^{(i)}-X^{(i)}$  and  $Y^{(j)}-Y^{(j)}$  propagators respectively. To get the 2-point cumulants, one has to sum over all the oscillator frequencies in the bath. In the continuum limit, these sums reduce to integrals with the appropriate distribution of the couplings given in (5.8). Performing these integrals over the oscillator frequencies, we find that the cumulants decay exponentially when the time interval between the insertions is increased. In table C.1, we provide the forms of the slowest decaying modes in these cumulants. The decay rates of these modes are of the order of  $\Omega$ . All the other modes which we have not mentioned in table C.1 decay at much faster rates which are of the order of  $\beta^{-1}$ .

Table C.1: Decay of 2-point cumulants for  $t_1 > t_2$

Cumulant	Slowest decaying mode
$\lambda^2\langle 12 \rangle$	$-\frac{\Gamma_2 \Omega^4}{(e^{\beta \Omega} - 1)^2} e^{-2\Omega t_{12}}$
$\lambda^2\langle 21 \rangle$	$-\frac{\Gamma_2 \Omega^4}{(-1 + e^{-\beta \Omega})^2} e^{-2\Omega t_{12}}$

### C.1.2 4-point cumulants

The Feynman diagrams that contribute to the 4-point cumulants of  $O(t)$  are given in figure C.2. Again, integrating over all the oscillator frequencies with the corresponding couplings following the distribution given in (5.9), one can obtain the forms of these cumulants. As in case of the 2-point cumulants, these 4-point cumulants also decay exponentially when the separation between any two insertions is increased. We provide the forms of the slowest decaying modes of these cumulants in table C.2. By looking at these forms, one can see that the decay rates of these modes are of the order of  $\Omega$  as well.

Figure C.2: Feynman diagrams contributing to the 4-point cumulants

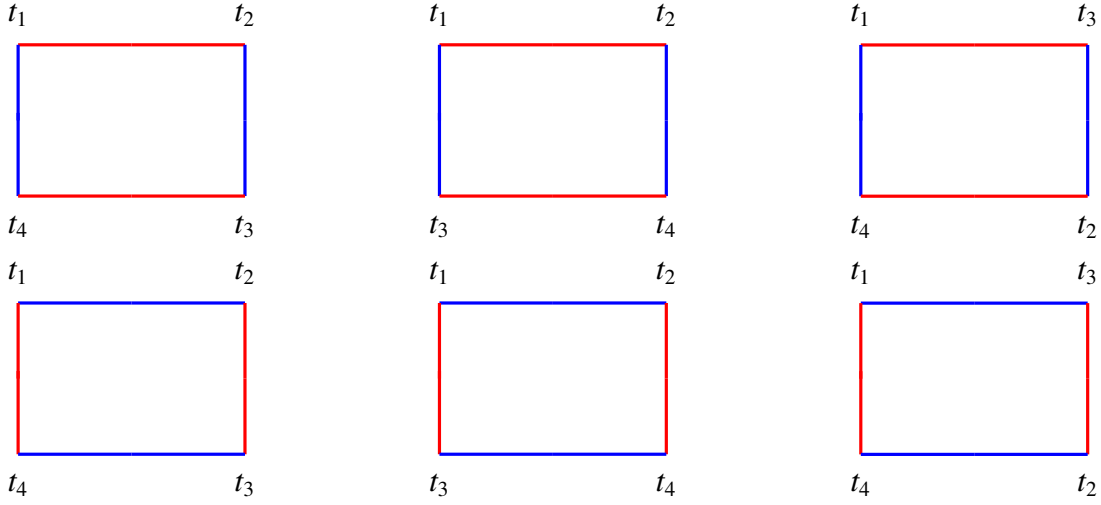


Table C.2: Decay of 4-point cumulants for  $t_1 > t_2 > t_3 > t_4$

Cumulant	Slowest decaying mode
$\lambda^4 \langle 1234 \rangle$	$\frac{2\Gamma_4 \Omega^8}{(e^{i\beta\Omega} - 1)^4} e^{-2t_{14}\Omega} (e^{-2t_{23}\Omega} + 2)$
$\lambda^4 \langle 1243 \rangle$	$\frac{2\Gamma_4 \Omega^8}{(e^{i\beta\Omega} - 1)^4} e^{-2t_{14}\Omega} (e^{-2t_{23}\Omega} + 2e^{i\beta\Omega})$
$\lambda^4 \langle 1324 \rangle$	$\frac{2\Gamma_4 \Omega^8}{(e^{i\beta\Omega} - 1)^4} e^{-2t_{14}\Omega} (e^{-2t_{23}\Omega + i\beta\Omega} + e^{i\beta\Omega} + 1)$
$\lambda^4 \langle 1342 \rangle$	$\frac{2\Gamma_4 \Omega^8}{(e^{i\beta\Omega} - 1)^4} e^{-2t_{14}\Omega + 2i\beta\Omega} (e^{-2t_{23}\Omega} + 2e^{-i\beta\Omega})$
$\lambda^4 \langle 1423 \rangle$	$\frac{2\Gamma_4 \Omega^8}{(e^{i\beta\Omega} - 1)^4} e^{-2t_{14}\Omega + i\beta\Omega} (1 + e^{-2t_{23}\Omega} + e^{i\beta\Omega})$
$\lambda^4 \langle 1432 \rangle$	$\frac{2\Gamma_4 \Omega^8}{(e^{i\beta\Omega} - 1)^4} e^{-2t_{14}\Omega + 2i\beta\Omega} (2 + e^{-2t_{23}\Omega})$
$\lambda^4 \langle 2134 \rangle$	$\frac{2\Gamma_4 \Omega^8}{(e^{i\beta\Omega} - 1)^4} e^{-2t_{14}\Omega} (e^{-2t_{23}\Omega} + 2e^{i\beta\Omega})$
$\lambda^4 \langle 2143 \rangle$	$\frac{2\Gamma_4 \Omega^8}{(e^{i\beta\Omega} - 1)^4} e^{-2t_{14}\Omega} (e^{-2t_{23}\Omega} + 2e^{2i\beta\Omega})$
$\lambda^4 \langle 2314 \rangle$	$\frac{2\Gamma_4 \Omega^8}{(e^{i\beta\Omega} - 1)^4} e^{-2t_{14}\Omega + i\beta\Omega} (1 + e^{-2t_{23}\Omega} + e^{i\beta\Omega})$
$\lambda^4 \langle 2341 \rangle$	$\frac{2\Gamma_4 \Omega^8}{(e^{i\beta\Omega} - 1)^4} e^{-2t_{14}\Omega + 2i\beta\Omega} (e^{-2t_{23}\Omega} + 2)$
$\lambda^4 \langle 2413 \rangle$	$\frac{2\Gamma_4 \Omega^8}{(e^{i\beta\Omega} - 1)^4} e^{-2t_{14}\Omega + i\beta\Omega} (e^{-2t_{23}\Omega} + e^{i\beta\Omega} + e^{2i\beta\Omega})$
$\lambda^4 \langle 2431 \rangle$	$\frac{2\Gamma_4 \Omega^8}{(e^{i\beta\Omega} - 1)^4} e^{-2t_{14}\Omega + 2i\beta\Omega} (e^{-2t_{23}\Omega} + 2e^{i\beta\Omega})$
$\lambda^4 \langle 3124 \rangle$	$\frac{2\Gamma_4 \Omega^8}{(e^{i\beta\Omega} - 1)^4} e^{-2t_{14}\Omega + 2i\beta\Omega} (e^{-2t_{23}\Omega} + 2e^{-i\beta\Omega})$
$\lambda^4 \langle 3142 \rangle$	$\frac{2\Gamma_4 \Omega^8}{(e^{i\beta\Omega} - 1)^4} e^{-2t_{14}\Omega + i\beta\Omega} (1 + e^{i\beta\Omega} + e^{-2t_{23}\Omega + 2i\beta\Omega})$
$\lambda^4 \langle 3214 \rangle$	$\frac{2\Gamma_4 \Omega^8}{(e^{i\beta\Omega} - 1)^4} e^{-2t_{14}\Omega + 2i\beta\Omega} (2 + e^{-2t_{23}\Omega})$
$\lambda^4 \langle 3241 \rangle$	$\frac{2\Gamma_4 \Omega^8}{(e^{i\beta\Omega} - 1)^4} e^{-2t_{14}\Omega + 2i\beta\Omega} (1 + e^{i\beta\Omega} + e^{-2t_{23}\Omega + i\beta\Omega})$
$\lambda^4 \langle 3412 \rangle$	$\frac{2\Gamma_4 \Omega^8}{(e^{i\beta\Omega} - 1)^4} e^{-2t_{14}\Omega + 2i\beta\Omega} (2 + e^{-2t_{23}\Omega + 2i\beta\Omega})$
$\lambda^4 \langle 3421 \rangle$	$\frac{2\Gamma_4 \Omega^8}{(e^{i\beta\Omega} - 1)^4} e^{-2t_{14}\Omega + 3i\beta\Omega} (2 + e^{-2t_{23}\Omega + i\beta\Omega})$
$\lambda^4 \langle 4123 \rangle$	$\frac{2\Gamma_4 \Omega^8}{(e^{i\beta\Omega} - 1)^4} e^{-2t_{14}\Omega + 2i\beta\Omega} (2 + e^{-2t_{23}\Omega})$
$\lambda^4 \langle 4132 \rangle$	$\frac{2\Gamma_4 \Omega^8}{(e^{i\beta\Omega} - 1)^4} e^{-2t_{14}\Omega + 2i\beta\Omega} (1 + e^{i\beta\Omega} + e^{-2t_{23}\Omega + i\beta\Omega})$
$\lambda^4 \langle 4213 \rangle$	$\frac{2\Gamma_4 \Omega^8}{(e^{i\beta\Omega} - 1)^4} e^{-2t_{14}\Omega + 2i\beta\Omega} (2e^{i\beta\Omega} + e^{-2t_{23}\Omega})$
$\lambda^4 \langle 4231 \rangle$	$\frac{2\Gamma_4 \Omega^8}{(e^{i\beta\Omega} - 1)^4} e^{-2t_{14}\Omega + 3i\beta\Omega} (1 + e^{i\beta\Omega} + e^{-2t_{23}\Omega})$
$\lambda^4 \langle 4312 \rangle$	$\frac{2\Gamma_4 \Omega^8}{(e^{i\beta\Omega} - 1)^4} e^{-2t_{14}\Omega + 3i\beta\Omega} (2 + e^{-2t_{23}\Omega + i\beta\Omega})$
$\lambda^4 \langle 4321 \rangle$	$\frac{2\Gamma_4 \Omega^8}{(e^{i\beta\Omega} - 1)^4} e^{-2t_{14}\Omega + 4i\beta\Omega} (2 + e^{-2t_{23}\Omega})$

## C.2 Argument for the validity of the Markovian limit

In this appendix, we provide an argument for the validity of the Markov approximation for the parameter regime given in (5.14). This argument will mainly involve dimensional analysis.

In the units where  $\hbar$  and the renormalised mass of the particle are unity, the dimension of each effective coupling can be expressed as some power of time. We provide these dimensions below.

### Dimensions of quadratic couplings:

$$[Z_I] = T^0, [\gamma] = T^{-1}, [\bar{\mu}^2] = [\langle f^2 \rangle] = T^{-2}. \quad (\text{C.4})$$

### Dimensions of SK quartic couplings:

$$\begin{aligned} [\zeta_N^{(4)}] = [\bar{\lambda}_4] = [\bar{\zeta}_3] = [\zeta_\mu^{(2)}] &= T^{-3}, \\ [\bar{\lambda}_{4\gamma}] = [\bar{\zeta}_{3\gamma}] = [\zeta_\gamma^{(2)}] &= T^{-2}. \end{aligned} \quad (\text{C.5})$$

### Dimensions of OTO quartic couplings:

$$\begin{aligned} [\kappa_4] = [\tilde{\kappa}_4] = [\varrho_4] = [\tilde{\varrho}_4] &= T^{-3}, \\ [\kappa_{4\gamma}^I] = [\kappa_{4\gamma}^{II}] = [\kappa_{4\gamma}^{III}] = [\tilde{\kappa}_{4\gamma}^I] = [\tilde{\kappa}_{4\gamma}^{II}] = [\varrho_{4\gamma}^I] = [\varrho_{4\gamma}^{II}] = [\tilde{\varrho}_{4\gamma}^I] = [\tilde{\varrho}_{4\gamma}^{II}] &= T^{-2}. \end{aligned} \quad (\text{C.6})$$

Now, from the value of each of these couplings given in section 5.4.5, one can obtain a time-scale. For the Markov approximation to be valid, we need all these time-scales to be much larger than  $\Omega^{-1}$ . This fixes the following Markovian regime for the parameters:

$$\bar{\mu}_0 \ll \Omega, \Gamma_2 \ll \beta(\beta\Omega), \Gamma_4 \ll \beta^2(\beta\Omega). \quad (\text{C.7})$$

Since, the values of the parameters in section 5.4.5 are computed in the higher temperature limit, we need to impose the following condition as well:

$$\beta\Omega \ll 1. \quad (\text{C.8})$$

In addition to the above hierarchy, we need the following condition for the validity of the



perturbative analysis <sup>1</sup>:

$$\Gamma_4 \ll (\Gamma_2)^2. \quad (\text{C.9})$$

Note that imposing this condition along with the high temperature limit in (C.8) and the inequality for  $\Gamma_2$  in (C.7) automatically ensures that  $\Gamma_4$  falls in the domain given in (C.7).

Combining all these conditions, we get the Markovian regime mentioned in (5.14).

### C.3 Relations between the OTO effective couplings and the bath's OTOCs

In section 5.4.1, we obtained the form of the non-local generalised influence phase of the particle by integrating out the bath's degrees of freedom on the 2-fold contour. When the bath's cumulants decay sufficiently fast compared to the time-scales involved in the particle's evolution, one can get an approximately local form for this generalised influence phase. This approximately local form is similar to its Schwinger-Keldysh counterpart (see (5.15) and (5.16)). The quadratic and quartic terms in this approximately local generalised influence phase are as follows:

$$\begin{aligned} W_{\text{GSK}}^{(2)} \approx i \sum_{i_1, i_2=1}^4 \int_{t_0}^{t_f} dt_1 \left[ \left\{ \int_{t_0}^{t_1} dt_2 \langle \mathcal{T}_C O_{i_1}(t_1) O_{i_2}(t_2) \rangle_c \right\} q_{i_1}(t_1) q_{i_2}(t_1 - \epsilon) \right. \\ \left. + \left\{ \int_{t_0}^{t_1} dt_2 \langle \mathcal{T}_C O_{i_1}(t_1) O_{i_2}(t_2) \rangle_c t_{21} \right\} q_{i_1}(t_1) \dot{q}_{i_2}(t_1 - \epsilon) \right. \\ \left. + \left\{ \int_{t_0}^{t_1} dt_2 \langle \mathcal{T}_C O_{i_1}(t_1) O_{i_2}(t_2) \rangle_c \frac{t_{21}^2}{2} \right\} q_{i_1}(t_1) \ddot{q}_{i_2}(t_1 - \epsilon) \right], \end{aligned} \quad (\text{C.10})$$

---

<sup>1</sup>In this perturbative analysis, we assume that the contributions of the quartic terms to the particle's dynamics are small compared to those of the quadratic terms.

$$\begin{aligned}
W_{\text{GSK}}^{(4)} \approx & -i \sum_{i_1, \dots, i_4=1}^4 \int_{t_0}^{t_f} dt_1 \left[ \left\{ \int_{t_0}^{t_1} dt_2 \int_{t_0}^{t_2} dt_3 \int_{t_0}^{t_3} dt_4 \langle \mathcal{T}_C O_{i_1}(t_1) O_{i_2}(t_2) O_{i_3}(t_3) O_{i_4}(t_4) \rangle_c \right\} \right. \\
& q_{i_1}(t_1) q_{i_2}(t_1 - \epsilon) q_{i_3}(t_1 - 2\epsilon) q_{i_4}(t_1 - 3\epsilon) \\
& + \left\{ \int_{t_0}^{t_1} dt_2 \int_{t_0}^{t_2} dt_3 \int_{t_0}^{t_3} dt_4 \langle \mathcal{T}_C O_{i_1}(t_1) O_{i_2}(t_2) O_{i_3}(t_3) O_{i_4}(t_4) \rangle_c t_{21} \right\} \\
& q_{i_1}(t_1) \dot{q}_{i_2}(t_1 - \epsilon) q_{i_3}(t_1 - 2\epsilon) q_{i_4}(t_1 - 3\epsilon) \\
& + \left\{ \int_{t_0}^{t_1} dt_2 \int_{t_0}^{t_2} dt_3 \int_{t_0}^{t_3} dt_4 \langle \mathcal{T}_C O_{i_1}(t_1) O_{i_2}(t_2) O_{i_3}(t_3) O_{i_4}(t_4) \rangle_c t_{31} \right\} \\
& q_{i_1}(t_1) q_{i_2}(t_1 - \epsilon) \dot{q}_{i_3}(t_1 - 2\epsilon) q_{i_4}(t_1 - 3\epsilon) \\
& + \left\{ \int_{t_0}^{t_1} dt_2 \int_{t_0}^{t_2} dt_3 \int_{t_0}^{t_3} dt_4 \langle \mathcal{T}_C O_{i_1}(t_1) O_{i_2}(t_2) O_{i_3}(t_3) O_{i_4}(t_4) \rangle_c t_{41} \right\} \\
& \left. q_{i_1}(t_1) q_{i_2}(t_1 - \epsilon) q_{i_3}(t_1 - 2\epsilon) \dot{q}_{i_4}(t_1 - 3\epsilon) \right]. \tag{C.11}
\end{aligned}$$

One can compare the leading order forms of the 4-point OTO cumulants of the particle obtained from this approximately local generalised influence phase, and the similar forms obtained from the out of time ordered 1-PI effective action given in section 5.4.2. This comparison yields the leading order form of any quartic OTO coupling  $g$  in terms of an integral of the 4-point OTO cumulants of  $O(t)$  as follows

$$g = \lambda^4 \lim_{t_1 - t_0 \rightarrow \infty} \int_{t_0}^{t_1} dt_2 \int_{t_0}^{t_2} dt_3 \int_{t_0}^{t_3} dt_4 \mathcal{I}[g] + \mathcal{O}(\lambda^6), \tag{C.12}$$

where the dependence of  $\mathcal{I}[g]$  on cumulants of the bath are given in table C.3 for all the OTO couplings. In expressing these cumulants, we follow the conventions introduced in section 5.3.2. In addition, we represent the cumulants corresponding to double (anti-)commutators of  $O(t)$  as follows:

$$\begin{aligned}
\langle [12][34] \rangle & \equiv \langle [O(t_1), O(t_2)][O(t_3), O(t_4)] \rangle_c, \\
\langle [12_+][34] \rangle & \equiv \langle \{O(t_1), O(t_2)\}[O(t_3), O(t_4)] \rangle_c, \\
\langle [12][34_+] \rangle & \equiv \langle [O(t_1), O(t_2)]\{O(t_3), O(t_4)\} \rangle_c, \\
\langle [12_+][34_+] \rangle & \equiv \langle \{O(t_1), O(t_2)\}\{O(t_3), O(t_4)\} \rangle_c, \text{ etc.}
\end{aligned} \tag{C.13}$$

Table C.3: Relations between the OTO couplings and the 4-point OTO cumulants of  $O(t)$ 

$g$	$\mathcal{I}[g]$
$\kappa_4$	$\frac{i}{4} [2(\langle[1234]\rangle - \langle[4321]\rangle) - (\langle[2314]\rangle - \langle[3241]\rangle + \langle[1423]\rangle - \langle[4132]\rangle)]$
$\bar{\kappa}_4$	$6i(\langle[1234]\rangle + \langle[4321]\rangle)$
$\varrho_4$	$\frac{1}{2} [-\langle[12_+3_+4_+]\rangle - \langle[43_+2_+1_+]\rangle + \langle[14_+2_+3_+]\rangle + \langle[41_+3_+2_+]\rangle + \langle[2314_+]\rangle + \langle[3241_+]\rangle]$
$\bar{\varrho}_4$	$\frac{1}{2} [(\langle[43_+21]\rangle + \langle[432_+1]\rangle + \langle[4321_+]\rangle) - (\langle[12_+,34]\rangle + \langle[123_+,4]\rangle + \langle[1234_+]\rangle)]$
$\kappa_{4\gamma}^I$	$\frac{i}{4} [(-t_{12} + t_{13} + t_{14})(\langle[34_+][12_+]\rangle - \langle[12_+][34_+]\rangle) + (t_{12} - t_{13} + t_{14})(\langle[24_+][13_+]\rangle - \langle[13_+][24_+]\rangle) + (t_{12} + t_{13} - t_{14})(\langle[23_+][14_+]\rangle - \langle[14_+][23_+]\rangle)]$
$\kappa_{4\gamma}^{II}$	$\frac{i}{4} [(-t_{12} + t_{13} + t_{14})(\langle[34][12]\rangle - \langle[12][34]\rangle) + (t_{12} - t_{13} + t_{14})(\langle[24][13]\rangle - \langle[13][24]\rangle) + (t_{12} + t_{13} - t_{14})(\langle[23][14]\rangle - \langle[14][23]\rangle)]$
$\kappa_{4\gamma}^{III}$	$-\frac{i}{4} [(-t_{12} + t_{13} + t_{14})(\langle[4321]\rangle + \langle[2314]\rangle + \langle[2413]\rangle) + (t_{12} - t_{13} + t_{14})(\langle[4231]\rangle + \langle[2341]\rangle + \langle[3412]\rangle)]$
$\bar{\kappa}_{4\gamma}^I$	$-\frac{i}{2} [(t_{12} + t_{13} + t_{14})(\langle[1234]\rangle) + (-t_{12} - t_{13} + 3t_{14})(\langle[4321]\rangle)]$
$\bar{\kappa}_{4\gamma}^{II}$	$\frac{i}{2} [(t_{12} - t_{13} + t_{14})(\langle[14][23]\rangle - \langle[32][41]\rangle) + (t_{12} + t_{13} - t_{14})(\langle[12][34]\rangle - \langle[43][21]\rangle + \langle[13][24]\rangle - \langle[42][31]\rangle)]$
$\varrho_{4\gamma}^I$	$[ (t_{12} - t_{13} + t_{14})(\langle[12][34]\rangle + \langle[43][21]\rangle) + (-t_{12} + t_{13} + t_{14})(\langle[13][24]\rangle + \langle[42][31]\rangle + \langle[14][23]\rangle - \langle[32][41]\rangle)]$
$\varrho_{4\gamma}^{II}$	$(-t_{12} + t_{13} + t_{14})(\langle[12_+][34]\rangle + \langle[43_+][21]\rangle + \langle[12][34_+]\rangle + \langle[43][21_+]\rangle) + (t_{12} - t_{13} + t_{14})(\langle[13_+][24]\rangle + \langle[42_+][31]\rangle + \langle[13][24_+]\rangle - \langle[42][31_+]\rangle) + (t_{12} + t_{13} - t_{14})(\langle[14_+][23]\rangle + \langle[32_+][41]\rangle + \langle[14][23_+]\rangle - \langle[32][41_+]\rangle)$
$\bar{\varrho}_{4\gamma}^I$	$\frac{1}{2} [(-t_{12} + t_{13} + t_{14})(\langle[12_+,34]\rangle - \langle[43_+,21]\rangle) + (t_{12} - t_{13} + t_{14})(\langle[123_+,4]\rangle - \langle[432_+,1]\rangle) + (t_{12} + t_{13} - t_{14})(\langle[1234_+]\rangle + \langle[4321_+]\rangle)]$
$\bar{\varrho}_{4\gamma}^{II}$	$\frac{1}{2} [t_{12}(\langle[12][34_+]\rangle + \langle[43_+][21]\rangle) + t_{43}(\langle[43][21_+]\rangle + \langle[12_+][34]\rangle) + t_{13}(\langle[13][24_+]\rangle + \langle[42_+][31]\rangle) + t_{42}(\langle[42][31_+]\rangle + \langle[13_+][24]\rangle) + t_{14}(\langle[14][23_+]\rangle + \langle[32_+][41]\rangle) + t_{32}(\langle[32][41_+]\rangle + \langle[14_+][23]\rangle)]$

## C.4 Quartic couplings in the high temperature limit

In this appendix, we provide the expressions of all the quartic effective couplings at the high temperature limit in terms of the 6 spectral functions given in (5.96). These expressions are obtained from the forms given in tables 5.2 and 5.3 by imposing the KMS relations between the spectral functions. We studied such KMS relations between the bath's correlators in chapter 3 to express the Fourier transforms of all contour-ordered correlators in terms of a different basis of spectral functions which is given below:

$$\rho[1234], \rho[4321], \rho[2314], \rho[12][34], \rho[13][24], \rho[14][23]. \quad (\text{C.14})$$

Notice that the spectral functions corresponding to the nested commutators in this basis are identical to three of the spectral functions given in (5.96). The remaining three spectral func-

tions corresponding to double commutators can be expressed in terms of the spectral functions in our basis as follows:

$$\begin{aligned}
\rho[12][34] &= \frac{(1 + \mathfrak{f}(\omega_1))(1 + \mathfrak{f}(\omega_2))}{(1 + \mathfrak{f}(\omega_1) + \mathfrak{f}(\omega_2))} (\rho[1234] + \rho[2143]), \\
\rho[13][24] &= \frac{(1 + \mathfrak{f}(\omega_1))(1 + \mathfrak{f}(\omega_3))}{(1 + \mathfrak{f}(\omega_1) + \mathfrak{f}(\omega_3))} (\rho[1234] + \rho[2314] + \rho[3142]), \\
\rho[14][23] &= \frac{(1 + \mathfrak{f}(\omega_1))(1 + \mathfrak{f}(\omega_4))}{(1 + \mathfrak{f}(\omega_1) + \mathfrak{f}(\omega_4))} (\rho[2314] + \rho[3241]),
\end{aligned} \tag{C.15}$$

where  $\mathfrak{f}(\omega)$  is the Bose-Einstein distribution function given by

$$\mathfrak{f}(\omega) \equiv \frac{1}{e^{\beta\omega} - 1}. \tag{C.16}$$

This demonstrates that the spectral functions given in (5.96) indeed form a basis. We choose to work with this basis rather than the one given in (C.14) because, in the high temperature limit, the  $\beta$ -expansions of all the spectral functions in this basis begin at the same power of  $\beta$ . This simplifies comparisons between the leading order forms of the different couplings.

Now, let us provide the expressions of the quartic couplings in terms of this basis. In the high temperature limit, any quartic coupling can be expressed as

$$g = \int_{C_4} \tilde{\mathcal{I}}[g] + \mathcal{O}(\lambda^6), \tag{C.17}$$

where the integrand  $\tilde{\mathcal{I}}[g]$  for the Schwinger-Keldysh couplings and the OTO couplings are given in tables C.4 and C.5 respectively. In these integrands, the spectral functions are truncated at their leading order in  $\beta$ -expansion.

Table C.4: SK couplings upto leading order in  $\beta$ 

$\bar{g}$	$\bar{I}[g]$
$\bar{\lambda}_4$	$-\frac{6}{\omega_1\omega_4(\omega_3+\omega_4)}\rho[1234]$
$\zeta_N^{(4)}$	$\frac{24i}{\beta^3\omega_1^2\omega_2\omega_3\omega_4^2(\omega_1+\omega_3)(\omega_1+\omega_4)(\omega_3+\omega_4)^2}\left[\omega_1(\omega_1+\omega_4)(\omega_4^2-\omega_2\omega_3)\rho[1234]\right.$ $+ \omega_4(\omega_1+\omega_3)(\omega_1+\omega_4)(\omega_3+\omega_4)\rho[4321]$ $- \omega_1\omega_4(\omega_1+\omega_3)(\omega_1+\omega_4)\rho[2143] + \omega_1\omega_2(\omega_3^2-\omega_4^2)\rho[2314]$ $\left. - \omega_2\omega_4(\omega_1+\omega_3)(\omega_3+\omega_4)\rho[3241] + \omega_1\omega_4(\omega_1+\omega_4)(\omega_3+\omega_4)\rho[3142]\right]$
$\bar{\zeta}_3$	$\frac{2i}{\beta\omega_1^2\omega_2\omega_3\omega_4^2(\omega_1+\omega_3)(\omega_1+\omega_4)(\omega_3+\omega_4)^2}\left[-\omega_1\omega_2\omega_3(\omega_1+\omega_4)((\omega_3+\omega_4)(\omega_1+\omega_3)+\omega_4(\omega_1-\omega_4))\rho[1234]\right.$ $+ \omega_1\omega_2\omega_4^2(\omega_1+\omega_3)(\omega_1+\omega_4)\rho[2143]$ $- \omega_1\omega_2\omega_3\omega_4(\omega_3^2-\omega_4^2)\rho[2314] + \omega_2\omega_3\omega_4^2(\omega_1+\omega_3)(\omega_3+\omega_4)\rho[3241]$ $\left. - \omega_1\omega_3\omega_4^2(\omega_1+\omega_4)(\omega_3+\omega_4)\rho[3142]\right]$
$\zeta_\mu^{(2)}$	$\frac{1}{\beta^2\omega_1^2\omega_2\omega_3\omega_4^2(\omega_1+\omega_3)(\omega_1+\omega_4)(\omega_3+\omega_4)^2}\left[\omega_1(\omega_1+\omega_4)(\omega_3(\omega_4-\omega_1)(\omega_1+\omega_3)+\omega_4(\omega_3+\omega_4)^2)\rho[1234]\right.$ $+ \omega_4^2(\omega_1+\omega_3)(\omega_1+\omega_4)(\omega_3+\omega_4)\rho[4321]$ $+ \omega_1\omega_4(\omega_1+\omega_4)(\omega_1+\omega_3)^2\rho[2143] + \omega_1\omega_2(\omega_3+\omega_4)(\omega_3^2-\omega_4^2)\rho[2314]$ $\left. - \omega_2\omega_4(\omega_1+\omega_3)(\omega_3+\omega_4)^2\rho[3241] + \omega_1\omega_4(\omega_1+\omega_4)(\omega_3+\omega_4)^2\rho[3142]\right]$
$\bar{\lambda}_{4\gamma}$	$\frac{2i}{\omega_1^2\omega_4^2(\omega_3+\omega_4)^2}\left[3(\omega_4-\omega_1)(\omega_3+\omega_4)+2\omega_1\omega_3\right]\rho[1234]$
$\bar{\zeta}_{3\gamma}$	$\frac{1}{\beta\omega_1^3\omega_2\omega_3\omega_4^3(\omega_1+\omega_3)(\omega_1+\omega_4)(\omega_3+\omega_4)^2}\left[-\omega_1\omega_2\omega_3(\omega_1+\omega_4)(\omega_2\omega_3(\omega_2+\omega_3)+5\omega_1\omega_4^2-\omega_4^3)\rho[1234]\right.$ $- \omega_1\omega_2\omega_4^2(\omega_1+\omega_3)(\omega_1^2-\omega_4^2)\rho[2143]$ $+ \omega_1\omega_2\omega_3\omega_4(\omega_3-\omega_4)((\omega_1-\omega_4)(\omega_3+\omega_4)+2\omega_1\omega_4)\rho[2314]$ $- \omega_2\omega_3\omega_4^2(\omega_1+\omega_3)((\omega_1-\omega_4)(\omega_3+\omega_4)+2\omega_1\omega_4)\rho[3241]$ $\left. + \omega_1\omega_3\omega_4^2(\omega_1+\omega_4)((\omega_1-\omega_4)(\omega_3+\omega_4)+2\omega_1\omega_4)\rho[3142]\right]$
$\zeta_\gamma^{(2)}$	$\frac{i}{3\beta^2\omega_1^3\omega_2\omega_3\omega_4^3(\omega_1+\omega_3)(\omega_1+\omega_4)(\omega_3+\omega_4)^2}\left[-\omega_1(\omega_1+\omega_4)(\omega_1^3\omega_3(\omega_3+3\omega_4)+\omega_1^2\omega_3(\omega_3^2+11\omega_3\omega_4+10\omega_4^2)\right.$ $- \omega_4^2(2\omega_3^3+4\omega_3^2\omega_4+3\omega_3\omega_4^2+\omega_4^3)+\omega_1\omega_4(7\omega_3^3+12\omega_3^2\omega_4+8\omega_3\omega_4^2+5\omega_4^3))\rho[1234]$ $- \omega_4^2(\omega_1+\omega_3)(\omega_1+\omega_4)(\omega_3+\omega_4)(-\omega_4(\omega_3+\omega_4)+\omega_1(3\omega_3+5\omega_4))\rho[4321]$ $+ \omega_1\omega_4(\omega_1+\omega_3)(\omega_1+\omega_4)(\omega_3\omega_4(\omega_3+\omega_4)+\omega_1^2(\omega_3+3\omega_4)+\omega_1(\omega_3^2+8\omega_3\omega_4+9\omega_4^2))\rho[2143]$ $+ \omega_1\omega_2(\omega_3-\omega_4)(\omega_3+\omega_4)^2(\omega_1(\omega_3-5\omega_4)+\omega_4(\omega_3+\omega_4))\rho[2314]$ $- \omega_2\omega_4(\omega_1+\omega_3)(\omega_3+\omega_4)^2(\omega_1(\omega_3-5\omega_4)+\omega_4(\omega_3+\omega_4))\rho[3241]$ $\left. + \omega_1\omega_4(\omega_1+\omega_4)(\omega_3+\omega_4)^2(\omega_1(\omega_3-5\omega_4)+\omega_4(\omega_3+\omega_4))\rho[3142]\right]$

Table C.5: OTO couplings upto leading order in  $\beta$ 

$g$	$\tilde{I}[g]$
$\kappa_4$	$-\frac{1}{2\omega_1\omega_4(\omega_3+\omega_4)}[2\rho[1234] + \rho[2143] + \rho[3142] + \rho[3241]]$
$\tilde{\kappa}_4$	$-\frac{6}{\omega_1\omega_4(\omega_3+\omega_4)}[\rho[1234] + \rho[4321]]$
$\mathcal{Q}_4$	$\frac{i}{\beta\omega_1^2\omega_2\omega_3\omega_4^2(\omega_3+\omega_4)}[-\omega_1(\omega_4^2 + (\omega_1 + \omega_3)(\omega_3 + \omega_4))\rho[1234]$ $-\omega_4(\omega_1^2 + (\omega_1 + \omega_3)(\omega_3 + \omega_4))\rho[4321]$ $+ \omega_1\omega_4(\omega_3 - \omega_2)(\rho[2143] - \rho[3142]) - \omega_1\omega_2(\omega_3 - \omega_4)\rho[2314] + \omega_4\omega_2(\omega_1 - \omega_3)\rho[3241]]$
$\tilde{\mathcal{Q}}_4$	$-\frac{i}{\beta\omega_1^2\omega_2\omega_3\omega_4^2(\omega_3+\omega_4)}[-\omega_1(\omega_4^2 + \omega_1\omega_4 + \omega_2\omega_3)\rho[1234] - \omega_4(\omega_1^2 + \omega_1\omega_4 - \omega_2\omega_3)\rho[4321]$ $-\omega_1\omega_4(\omega_1 + \omega_4)(\rho[2143] + \rho[3142]) - \omega_1\omega_2(\omega_3 - \omega_4)\rho[2314] + \omega_4\omega_2(\omega_1 + \omega_3)\rho[3241]]$
$\kappa_{4\gamma}^I$	$\frac{6i}{\beta^2\omega_1^2\omega_2\omega_3\omega_4^2(\omega_1+\omega_3)(\omega_1+\omega_4)(\omega_3+\omega_4)^2}[\omega_1(\omega_1 + \omega_4)(\omega_4^2 - \omega_2\omega_3)\rho[1234]$ $+ \omega_4(\omega_1 + \omega_3)(\omega_1 + \omega_4)(\omega_3 + \omega_4)\rho[4321]$ $- \omega_1\omega_4(\omega_1 + \omega_3)(\omega_1 + \omega_4)\rho[2143] + \omega_1\omega_2(\omega_3^2 - \omega_4^2)\rho[2314]$ $+ \omega_1\omega_4(\omega_1 + \omega_4)(\omega_3 + \omega_4)\rho[3142] - \omega_4\omega_2(\omega_1 + \omega_3)(\omega_3 + \omega_4)\rho[3241]]$
$\kappa_{4\gamma}^{II}$	$\frac{i}{4\omega_1^2\omega_4^2(\omega_3+\omega_4)^2}[(\omega_1 - \omega_4)(\omega_3 + \omega_4)(\rho[1234] + \rho[2314] + \rho[3142])$ $+ (\omega_1 + \omega_4)(\omega_3 + \omega_4)(\rho[2314] + \rho[3241])$ $+ ((\omega_1 - \omega_4)(\omega_3 + \omega_4) + 2\omega_1\omega_4)(\rho[1234] + \rho[2143])]$
$\kappa_{4\gamma}^{III}$	$-\frac{i}{4\omega_1^2\omega_4^2(\omega_3+\omega_4)^2}[(\omega_1 - \omega_4)(\omega_3 + \omega_4)(\rho[1234] + \rho[2143])$ $+ ((\omega_1 - \omega_4)(\omega_3 + \omega_4) + 2\omega_1\omega_4)(\rho[1234] + \rho[3241] + \rho[3142])]$
$\tilde{\kappa}_{4\gamma}^I$	$\frac{i}{2\omega_1^2\omega_4^2(\omega_3+\omega_4)^2}[(-\omega_1(\omega_2 + \omega_1) + \omega_4(3\omega_2 + 5\omega_1))\rho[1234]$ $+ (-\omega_4(\omega_3 + \omega_4) + \omega_1(3\omega_3 + 5\omega_4))\rho[4321]]$
$\tilde{\kappa}_{4\gamma}^{II}$	$\frac{i}{2\omega_1^2\omega_4^2(\omega_3+\omega_4)^2}[(\omega_1 - \omega_4)(\rho[2314] + \rho[3241]) + (\omega_1 + \omega_4)(2\rho[1234] + \rho[2314] + \rho[2143] + \rho[3142])]$
$\mathcal{Q}_{4\gamma}^I$	$\frac{2}{\beta\omega_1^2\omega_4^2(\omega_1+\omega_3)(\omega_1+\omega_4)(\omega_3+\omega_4)^2}[(\omega_1 + \omega_4)(\omega_1^2 - 4\omega_1\omega_4 + \omega_4^2)\rho[1234] + (\omega_1 + \omega_3)(\omega_1^2 - \omega_4^2)\rho[2143]$ $- (\omega_3 - \omega_4)(\omega_4(\omega_3 + \omega_4) - \omega_1(\omega_3 + 3\omega_4))\rho[2314]$ $- (\omega_1 + \omega_3)(\omega_4(\omega_3 + \omega_4) - \omega_1(\omega_3 + 3\omega_4))\rho[3241]$ $+ (\omega_1 + \omega_4)(\omega_4(\omega_3 + \omega_4) - \omega_1(\omega_3 + 3\omega_4))\rho[3142]]$
$\mathcal{Q}_{4\gamma}^{II}$	$\frac{1}{\beta\omega_1^2\omega_2\omega_3\omega_4^2(\omega_3+\omega_4)^2}[\omega_1(-\omega_3\omega_4(\omega_3 + \omega_4)^2 + \omega_1^2(\omega_3^2 + 3\omega_3\omega_4 + \omega_4^2) + \omega_1(\omega_3^3 + 2\omega_3^2\omega_4 + \omega_3\omega_4^2 + \omega_4^3))\rho[1234]$ $+ \omega_4(\omega_3 + \omega_4)(\omega_1^3 + (\omega_1^2 + \omega_1\omega_3 - \omega_3\omega_4)(\omega_3 + \omega_4))\rho[4321]$ $- \omega_1\omega_4(\omega_1^2\omega_4 - \omega_4(\omega_3 + \omega_4)^2 + \omega_1\omega_3(\omega_3 + 2\omega_4))\rho[2143]$ $- \omega_1^2\omega_2(\omega_3 + \omega_4)^2\rho[2314] + \omega_2\omega_4(\omega_3 + \omega_4)(-\omega_1^2 + \omega_3\omega_4)\rho[3241]$ $+ \omega_1\omega_4(\omega_3 + \omega_4)(\omega_1^2 - \omega_3\omega_4 + \omega_1(\omega_3 + \omega_4))\rho[3142]]$
$\tilde{\mathcal{Q}}_{4\gamma}^I$	$\frac{1}{\beta\omega_1^2\omega_2\omega_3\omega_4^2(\omega_3+\omega_4)^2}[\omega_1(\omega_1^2(\omega_3^2 + 2\omega_3\omega_4 + 3\omega_4^2) + \omega_4(\omega_3^3 + 2\omega_3^2\omega_4 - \omega_4^3) + \omega_1(\omega_3^3 + 3\omega_3^2\omega_4 + 4\omega_3\omega_4^2 + 2\omega_4^3))\rho[1234]$ $+ \omega_4(\omega_3\omega_4(\omega_3 + \omega_4)^2 + \omega_1^2(\omega_3 + 3\omega_4) + \omega_1^2(\omega_3^2 + 3\omega_3\omega_4 + 2\omega_4^2) + \omega_1(\omega_3^3 + 3\omega_3^2\omega_4 + \omega_3\omega_4^2 - \omega_4^3))\rho[4321]$ $+ \omega_1\omega_4(\omega_3 + \omega_4)(\omega_1^2 - \omega_4^2)\rho[2143] - \omega_1\omega_2(\omega_3 - \omega_4)(\omega_4(\omega_3 + \omega_4) - \omega_1(\omega_3 + 3\omega_4))\rho[2314]$ $+ \omega_2\omega_4(\omega_3\omega_4(\omega_3 + \omega_4) - \omega_1^2(\omega_3 + 3\omega_4) + \omega_1(-\omega_3^2 - 2\omega_3\omega_4 + \omega_4^2))\rho[3241]$ $+ \omega_1\omega_4(\omega_1 + \omega_4)(-\omega_4(\omega_3 + \omega_4) + \omega_1(\omega_3 + 3\omega_4))\rho[3142]]$
$\tilde{\mathcal{Q}}_{4\gamma}^{II}$	$\frac{1}{\beta\omega_1^2\omega_2\omega_3\omega_4^2(\omega_3+\omega_4)^2}[(2\omega_3^3 + 4\omega_3^2\omega_4 + \omega_3\omega_4^2 - \omega_4^3 + \omega_1^2(\omega_3 + 4\omega_4) + \omega_1(\omega_3^2 + 3\omega_3\omega_4 + 3\omega_4^2))\rho[1234]$ $+ (2\omega_3^3 + 5\omega_3^2\omega_4 + 2\omega_3\omega_4^2 - \omega_4^3 + 2\omega_1^2(\omega_3 + 2\omega_4) + \omega_1(2\omega_3^2 + 5\omega_3\omega_4 + 3\omega_4^2))\rho[4321]$ $+ (\omega_1 - \omega_3 - \omega_4)(\omega_1 + \omega_4)(\omega_3 + 2\omega_4)\rho[2143] + \omega_2(-\omega_3^2 - 4\omega_1\omega_4 + \omega_4^2)\rho[2314]$ $+ \omega_2(-\omega_3^2 - 2\omega_3\omega_4 + \omega_4^2 - 2\omega_1\omega_3 - 4\omega_1\omega_4)\rho[3241]$ $+ (\omega_1 + \omega_4)(\omega_3^2 - \omega_4^2 + 2\omega_1\omega_3 + 4\omega_1\omega_4)\rho[3142]]$

# Bibliography

- [1] S. H. Shenker and D. Stanford, “Black holes and the butterfly effect,” *JHEP* **03** (2014) 067, [arXiv:1306.0622 \[hep-th\]](#).
- [2] S. H. Shenker and D. Stanford, “Stringy effects in scrambling,” *JHEP* **05** (2015) 132, [arXiv:1412.6087 \[hep-th\]](#).
- [3] B. Swingle and N. Y. Yao, “Seeing Scrambled Spins,” *APS Physics* **10** (2017) 82.
- [4] B. Swingle, G. Bentsen, M. Schleier-Smith, and P. Hayden, “Measuring the scrambling of quantum information,” *Phys. Rev.* **A94** no. 4, (2016) 040302, [arXiv:1602.06271 \[quant-ph\]](#).
- [5] J. Maldacena, S. H. Shenker, and D. Stanford, “A bound on chaos,” *JHEP* **08** (2016) 106, [arXiv:1503.01409 \[hep-th\]](#).
- [6] D. Stanford, “Many-body chaos at weak coupling,” *JHEP* **10** (2016) 009, [arXiv:1512.07687 \[hep-th\]](#).
- [7] J. Maldacena and D. Stanford, “Remarks on the Sachdev-Ye-Kitaev model,” *Phys. Rev.* **D94** no. 10, (2016) 106002, [arXiv:1604.07818 \[hep-th\]](#).
- [8] J. de Boer, E. Lladrés, J. F. Pedraza, and D. Vegh, “Chaotic strings in AdS/CFT,” *Phys. Rev. Lett.* **120** no. 20, (2018) 201604, [arXiv:1709.01052 \[hep-th\]](#).
- [9] R. Fan, P. Zhang, H. Shen, and H. Zhai, “Out-of-time-order correlation for many-body localization,” *Science Bulletin* **62** no. 10, (2017) 707 – 711.  
<http://www.sciencedirect.com/science/article/pii/S2095927317301925>.
- [10] Y. Huang, Y.-L. Zhang, and X. Chen, “Out-of-time-ordered correlators in many-body localized systems,” *Annalen der Physik* **529** (July, 2017) 1600318, [arXiv:1608.01091 \[cond-mat.dis-nn\]](#).

- [11] X. Chen, T. Zhou, D. A. Huse, and E. Fradkin, “Out-of-time-order correlations in many-body localized and thermal phases,” *Annalen der Physik* **529** (July, 2017) 1600332, [arXiv:1610.00220 \[cond-mat.str-el\]](#).
- [12] S. Ray, S. Sinha, and K. Sengupta, “Signature of chaos and delocalization in a periodically driven many-body system: An out-of-time-order-correlation study,” *Phys. Rev. A* **98** (Nov, 2018) 053631. <https://link.aps.org/doi/10.1103/PhysRevA.98.053631>.
- [13] S. Sahu, S. Xu, and B. Swingle, “Scrambling dynamics across a thermalization-localization quantum phase transition,” *arXiv e-prints* (Jul, 2018) [arXiv:1807.06086](#), [arXiv:1807.06086 \[cond-mat.str-el\]](#).
- [14] P. Hosur, X.-L. Qi, D. A. Roberts, and B. Yoshida, “Chaos in quantum channels,” *JHEP* **02** (2016) 004, [arXiv:1511.04021 \[hep-th\]](#).
- [15] N. Y. Yao, F. Grusdt, B. Swingle, M. D. Lukin, D. M. Stamper-Kurn, J. E. Moore, and E. A. Demler, “Interferometric Approach to Probing Fast Scrambling,” *ArXiv e-prints* (July, 2016) , [arXiv:1607.01801 \[quant-ph\]](#).
- [16] M. Gärttner, P. Hauke, and A. M. Rey, “Relating out-of-time-order correlations to entanglement via multiple-quantum coherences,” *Phys. Rev. Lett.* **120** (Jan, 2018) 040402. <https://link.aps.org/doi/10.1103/PhysRevLett.120.040402>.
- [17] M. Gärttner, J. G. Bohnet, A. Safavi-Naini, M. L. Wall, J. J. Bollinger, and A. M. Rey, “Measuring out-of-time-order correlations and multiple quantum spectra in a trapped-ion quantum magnet,” *Nature Physics* **13** (Aug., 2017) 781–786, [arXiv:1608.08938 \[quant-ph\]](#).
- [18] J. Li, R. Fan, H. Wang, B. Ye, B. Zeng, H. Zhai, X. Peng, and J. Du, “Measuring out-of-time-order correlators on a nuclear magnetic resonance quantum simulator,” *Phys. Rev. X* **7** (Jul, 2017) 031011. <https://link.aps.org/doi/10.1103/PhysRevX.7.031011>.
- [19] G. Zhu, M. Hafezi, and T. Grover, “Measurement of many-body chaos using a quantum clock,” *Phys. Rev. A* **94** no. 6, (2016) 062329, [arXiv:1607.00079 \[quant-ph\]](#).



- [20] E. Witten, “An SYK-Like Model Without Disorder,” *J. Phys. A* **52** no. 47, (2019) 474002, [arXiv:1610.09758 \[hep-th\]](#).
- [21] I. R. Klebanov and G. Tarnopolsky, “Uncolored random tensors, melon diagrams, and the Sachdev-Ye-Kitaev models,” *Phys. Rev. D* **95** no. 4, (2017) 046004, [arXiv:1611.08915 \[hep-th\]](#).
- [22] G. Mandal, P. Nayak, and S. R. Wadia, “Coadjoint orbit action of Virasoro group and two-dimensional quantum gravity dual to SYK/tensor models,” *JHEP* **11** (2017) 046, [arXiv:1702.04266 \[hep-th\]](#).
- [23] S. R. Das, A. Ghosh, A. Jevicki, and K. Suzuki, “Space-Time in the SYK Model,” *JHEP* **07** (2018) 184, [arXiv:1712.02725 \[hep-th\]](#).
- [24] S. R. Das, A. Jevicki, and K. Suzuki, “Three Dimensional View of the SYK/AdS Duality,” *JHEP* **09** (2017) 017, [arXiv:1704.07208 \[hep-th\]](#).
- [25] S. R. Das, A. Ghosh, A. Jevicki, and K. Suzuki, “Three Dimensional View of Arbitrary  $q$  SYK models,” *JHEP* **02** (2018) 162, [arXiv:1711.09839 \[hep-th\]](#).
- [26] A. Gaikwad, L. K. Joshi, G. Mandal, and S. R. Wadia, “Holographic dual to charged SYK from 3D Gravity and Chern-Simons,” *JHEP* **02** (2020) 033, [arXiv:1802.07746 \[hep-th\]](#).
- [27] A. Lala and D. Roychowdhury, “SYK/AdS duality with Yang-Baxter deformations,” *JHEP* **12** (2018) 073, [arXiv:1808.08380 \[hep-th\]](#).
- [28] R. Nandkishore and D. A. Huse, “Many-body localization and thermalization in quantum statistical mechanics,” *Annual Review of Condensed Matter Physics* **6** no. 1, (2015) 15–38, <https://doi.org/10.1146/annurev-conmatphys-031214-014726>.  
<https://doi.org/10.1146/annurev-conmatphys-031214-014726>.
- [29] S. Chaudhuri and R. Loganayagam, “Probing out-of-time-order correlators,” *Journal of High Energy Physics* **2019** no. 7, (Jul, 2019) 6. [https://doi.org/10.1007/JHEP07\(2019\)006](https://doi.org/10.1007/JHEP07(2019)006).

- [30] S. Chaudhuri, C. Chowdhury, and R. Loganayagam, “Spectral Representation of Thermal OTO Correlators,” *JHEP* **02** (2019) 018, [arXiv:1810.03118 \[hep-th\]](#).
- [31] B. Chakrabarty, S. Chaudhuri, and R. Loganayagam, “Out of Time Ordered Quantum Dissipation,” *JHEP* **07** (2019) 102, [arXiv:1811.01513 \[cond-mat.stat-mech\]](#).
- [32] B. Chakrabarty and S. Chaudhuri, “Out of time ordered effective dynamics of a quartic oscillator,” *SciPost Phys.* **7** (2019) 013, [arXiv:1905.08307 \[hep-th\]](#).
- [33] I. L. Aleiner, L. Faoro, and L. B. Ioffe, “Microscopic model of quantum butterfly effect: out-of-time-order correlators and traveling combustion waves,” *Annals Phys.* **375** (2016) 378–406, [arXiv:1609.01251 \[cond-mat.stat-mech\]](#).
- [34] F. M. Haehl, R. Loganayagam, P. Narayan, and M. Rangamani, “Classification of out-of-time-order correlators,” *SciPost Phys.* **6** (2019) 1.  
<https://scipost.org/10.21468/SciPostPhys.6.1.001>.
- [35] J. S. Schwinger, “Brownian motion of a quantum oscillator,” *J. Math. Phys.* **2** (1961) 407–432.
- [36] L. V. Keldysh, “Diagram technique for nonequilibrium processes,” *Zh. Eksp. Teor. Fiz.* **47** (1964) 1515–1527. [Sov. Phys. JETP20,1018(1965)].
- [37] R. P. Feynman and F. L. Vernon, Jr., “The Theory of a general quantum system interacting with a linear dissipative system,” *Annals Phys.* **24** (1963) 118–173. [,257(1963)].
- [38] L. Onsager, “Reciprocal relations in irreversible processes. 1.,” *Phys. Rev.* **37** (Feb, 1931) 405–426. <https://link.aps.org/doi/10.1103/PhysRev.37.405>.
- [39] L. Onsager, “Reciprocal relations in irreversible processes. 2.,” *Phys. Rev.* **38** (Dec, 1931) 2265–2279. <https://link.aps.org/doi/10.1103/PhysRev.38.2265>.
- [40] H. B. G. Casimir, “On onsager’s principle of microscopic reversibility,” *Rev. Mod. Phys.* **17** (Apr, 1945) 343–350.  
<https://link.aps.org/doi/10.1103/RevModPhys.17.343>.

- [41] R. Kubo, “Statistical mechanical theory of irreversible processes. 1. General theory and simple applications in magnetic and conduction problems,” *J. Phys. Soc. Jap.* **12** (1957) 570–586.
- [42] P. C. Martin and J. S. Schwinger, “Theory of many particle systems. 1.,” *Phys. Rev.* **115** (1959) 1342–1373. [[427\(1959\)](#)].
- [43] F. M. Haehl, R. Loganayagam, and M. Rangamani, “Schwinger-Keldysh formalism. Part I: BRST symmetries and superspace,” *JHEP* **06** (2017) 069, [arXiv:1610.01940 \[hep-th\]](#).
- [44] J. B. Johnson, “Thermal agitation of electricity in conductors,” *Phys. Rev.* **32** (Jul, 1928) 97–109. <https://link.aps.org/doi/10.1103/PhysRev.32.97>.
- [45] H. Nyquist, “Thermal agitation of electric charge in conductors,” *Phys. Rev.* **32** (Jul, 1928) 110–113. <https://link.aps.org/doi/10.1103/PhysRev.32.110>.
- [46] H. B. Callen and T. A. Welton, “Irreversibility and generalized noise,” *Phys. Rev.* **83** (Jul, 1951) 34–40. <https://link.aps.org/doi/10.1103/PhysRev.83.34>.
- [47] R. Kubo, “The fluctuation-dissipation theorem,” *Reports on Progress in Physics* **29** no. 1, (Jan, 1966) 255–284. <https://doi.org/10.1088%2F0034-4885%2F29%2F1%2F306>.
- [48] M. Schlosshauer, *Decoherence: And the Quantum-To-Classical Transition*. The Frontiers Collection. Springer, 2007. <https://books.google.co.in/books?id=1qrJUS5zNbEC>.
- [49] H. P. Breuer and F. Petruccione, *The theory of open quantum systems*. Oxford University Press, Great Clarendon Street, 2002.
- [50] U. Weiss, *Quantum Dissipative Systems*. Series in modern condensed matter physics. World Scientific, 2012. <https://books.google.co.in/books?id=qgfuFZxvGKQC>.
- [51] P. Bordia, F. Alet, and P. Hosur, “Out-of-time-ordered measurements as a probe of quantum dynamics,” *Phys. Rev.* **A97** no. 3, (2018) 030103, [arXiv:1801.08949 \[cond-mat.dis-nn\]](#).

- [52] L. García-Álvarez, I. L. Egusquiza, L. Lamata, A. del Campo, J. Sonner, and E. Solano, “Digital Quantum Simulation of Minimal AdS /CFT,” *Physical Review Letters* **119** no. 4, (July, 2017) 040501, [arXiv:1607.08560](https://arxiv.org/abs/1607.08560) [quant-ph].
- [53] L. M. Sieberer, M. Buchhold, and S. Diehl, “Keldysh Field Theory for Driven Open Quantum Systems,” *Rept. Prog. Phys.* **79** no. 9, (2016) 096001, [arXiv:1512.00637](https://arxiv.org/abs/1512.00637) [cond-mat.quant-gas].
- [54] K. chao Chou, Z. bin Su, B. lin Hao, and L. Yu, “Equilibrium and nonequilibrium formalisms made unified,” *Physics Reports* **118** no. 1, (1985) 1 – 131. <http://www.sciencedirect.com/science/article/pii/037015738590136X>.
- [55] A. Kamenev, *Field Theory of Non-Equilibrium Systems*. Cambridge University Press, 2011.
- [56] J. Berges, “Nonequilibrium Quantum Fields: From Cold Atoms to Cosmology,” [arXiv:1503.02907](https://arxiv.org/abs/1503.02907) [hep-ph].
- [57] A. Baidya, C. Jana, R. Loganayagam, and A. Rudra, “Renormalization in open quantum field theory. Part I. Scalar field theory,” *JHEP* **11** (2017) 204, [arXiv:1704.08335](https://arxiv.org/abs/1704.08335) [hep-th].
- [58] A. O. Caldeira and A. J. Leggett, “Path integral approach to quantum Brownian motion,” *Physica* **121A** (1983) 587–616.
- [59] B. L. Hu, J. P. Paz, and Y. Zhang, “Quantum brownian motion in a general environment: Exact master equation with nonlocal dissipation and colored noise,” *Phys. Rev. D* **45** (Apr, 1992) 2843–2861. <https://link.aps.org/doi/10.1103/PhysRevD.45.2843>.
- [60] B. L. Hu, J. P. Paz, and Y. Zhang, “Quantum brownian motion in a general environment. ii. nonlinear coupling and perturbative approach,” *Phys. Rev. D* **47** (Feb, 1993) 1576–1594. <https://link.aps.org/doi/10.1103/PhysRevD.47.1576>.
- [61] P. C. Martin, E. D. Siggia, and H. A. Rose, “Statistical Dynamics of Classical Systems,” *pra* **8** (July, 1973) 423–437.

- [62] C. de Dominicis and L. Peliti, “Field-theory renormalization and critical dynamics above  $T_c$ : Helium, antiferromagnets, and liquid-gas systems,” *prb* **18** (July, 1978) 353–376.
- [63] H.-K. Janssen, “On a Lagrangean for classical field dynamics and renormalization group calculations of dynamical critical properties,” *Zeitschrift fur Physik B Condensed Matter* **23** (Dec., 1976) 377–380.
- [64] F. M. Haehl, R. Loganayagam, P. Narayan, A. A. Nizami, and M. Rangamani, “Thermal out-of-time-order correlators, KMS relations, and spectral functions,” *JHEP* **12** (2017) 154, [arXiv:1706.08956](https://arxiv.org/abs/1706.08956) [hep-th].
- [65] J. Sonner and M. Vielma, “Eigenstate thermalization in the sachdev-ye-kitaev model,” *Journal of High Energy Physics* **2017** no. 11, (Nov, 2017) 149. [https://doi.org/10.1007/JHEP11\(2017\)149](https://doi.org/10.1007/JHEP11(2017)149).
- [66] R. A. Jalabert, I. García-Mata, and D. A. Wisniacki, “Semiclassical theory of out-of-time-order correlators for low-dimensional classically chaotic systems,” *Phys. Rev. E* **98** (Dec, 2018) 062218. <https://link.aps.org/doi/10.1103/PhysRevE.98.062218>.
- [67] I. García-Mata, M. Saraceno, R. A. Jalabert, A. J. Roncaglia, and D. A. Wisniacki, “Chaos signatures in the short and long time behavior of the out-of-time ordered correlator,” *Phys. Rev. Lett.* **121** (Nov, 2018) 210601. <https://link.aps.org/doi/10.1103/PhysRevLett.121.210601>.
- [68] J. Rammensee, J. D. Urbina, and K. Richter, “Many-body quantum interference and the saturation of out-of-time-order correlators,” *Phys. Rev. Lett.* **121** (Sep, 2018) 124101. <https://link.aps.org/doi/10.1103/PhysRevLett.121.124101>.
- [69] N. Tsuji, T. Shitara, and M. Ueda, “Out-of-time-order fluctuation-dissipation theorem,” *Phys. Rev.* **E97** no. 1, (2018) 012101, [arXiv:1612.08781](https://arxiv.org/abs/1612.08781) [cond-mat.stat-mech].
- [70] E. A. Calzetta and B.-L. B. Hu, *Nonequilibrium Quantum Field Theory*. Cambridge Monographs on Mathematical Physics. Cambridge University Press, 2008. <http://www.cambridge.org/mw/academic/subjects/physics/>

[theoretical-physics-and-mathematical-physics/  
nonequilibrium-quantum-field-theory?format=AR](#).

- [71] A. Kamenev and A. Levchenko, “Keldysh technique and nonlinear sigma-model: Basic principles and applications,” *Adv. Phys.* **58** (2009) 197, [arXiv:0901.3586 \[cond-mat.other\]](#).
- [72] G. Stefanucci and R. Van Leeuwen, *Nonequilibrium many-body theory of quantum systems: a modern introduction*. Cambridge University Press, 2013.
- [73] A. I. Larkin and Y. N. Ovchinnikov, “Quasiclassical Method in the Theory of Superconductivity,” *Soviet Journal of Experimental and Theoretical Physics* **28** (June, 1969) 1200.
- [74] R. Fan, P. Zhang, H. Shen, and H. Zhai, “Out-of-time-order correlation for many-body localization,” *Science Bulletin* **62** no. 10, (2017) 707 – 711.  
<http://www.sciencedirect.com/science/article/pii/S2095927317301925>.
- [75] Y. Chen, “Universal Logarithmic Scrambling in Many Body Localization,” *ArXiv e-prints* (Aug., 2016) , [arXiv:1608.02765 \[cond-mat.dis-nn\]](#).
- [76] B. Swingle and D. Chowdhury, “Slow scrambling in disordered quantum systems,” *Phys. Rev.* **B95** no. 6, (2017) 060201, [arXiv:1608.03280 \[cond-mat.str-el\]](#).
- [77] D. A. Roberts and B. Yoshida, “Chaos and complexity by design,” *JHEP* **04** (2017) 121, [arXiv:1610.04903 \[quant-ph\]](#).
- [78] N. Yunger Halpern, “Jarzynski-like equality for the out-of-time-ordered correlator,” *Phys. Rev.* **A95** no. 1, (2017) 012120, [arXiv:1609.00015 \[quant-ph\]](#).
- [79] N. Yunger Halpern, B. Swingle, and J. Dressel, “Quasiprobability behind the out-of-time-ordered correlator,” *Phys. Rev.* **A97** no. 4, (2018) 042105, [arXiv:1704.01971 \[quant-ph\]](#).
- [80] S. Caron-Huot, “Analyticity in Spin in Conformal Theories,” *JHEP* **09** (2017) 078, [arXiv:1703.00278 \[hep-th\]](#).
- [81] D. Simmons-Duffin, D. Stanford, and E. Witten, “A spacetime derivation of the Lorentzian OPE inversion formula,” [arXiv:1711.03816 \[hep-th\]](#).

- [82] L. Iliesiu, M. Kologlu, R. Mahajan, E. Perlmutter, and D. Simmons-Duffin, “The Conformal Bootstrap at Finite Temperature,” [arXiv:1802.10266 \[hep-th\]](#).
- [83] M. Blake, H. Lee, and H. Liu, “A quantum hydrodynamical description for scrambling and many-body chaos,” [arXiv:1801.00010 \[hep-th\]](#).
- [84] F. M. Haehl and M. Rozali, “Fine Grained Chaos in  $AdS_2$  Gravity,” *Phys. Rev. Lett.* **120** no. 12, (2018) 121601, [arXiv:1712.04963 \[hep-th\]](#).
- [85] F. M. Haehl and M. Rozali, “Effective Field Theory for Chaotic CFTs,” *JHEP* **10** (2018) 118, [arXiv:1808.02898 \[hep-th\]](#).
- [86] P. Basu and K. Jaswin, “Higher point OTOCs and the bound on chaos,” [arXiv:1809.05331 \[hep-th\]](#).
- [87] L. Foini and J. Kurchan, “The Eigenstate Thermalization Hypothesis and Out of Time Order Correlators,” [arXiv:1803.10658 \[cond-mat.stat-mech\]](#).
- [88] M. Garttner, J. G. Bohnet, A. Safavi-Naini, M. L. Wall, J. J. Bollinger, and A. M. Rey, “Measuring out-of-time-order correlations and multiple quantum spectra in a trapped ion quantum magnet,” *Nature Phys.* **13** (2017) 781, [arXiv:1608.08938 \[quant-ph\]](#).
- [89] S. Weinberg, *The Quantum theory of fields. Vol. 1: Foundations*. Cambridge University Press, 2005.
- [90] T. S. Evans, “THREE POINT FUNCTIONS AT FINITE TEMPERATURE,” *Phys. Lett.* **B249** (1990) 286–290.
- [91] T. S. Evans, “Spectral representation of three point functions at finite temperature,” *Phys. Lett.* **B252** (1990) 108–112.
- [92] T. S. Evans, “N point finite temperature expectation values at real times,” *Nucl. Phys.* **B374** (1992) 340–370.
- [93] J. C. Taylor, “Spectral representation of hard thermal loops,” *Phys. Rev.* **D48** (1993) 958–960.
- [94] M. E. Carrington and U. W. Heinz, “Three point functions at finite temperature,” *Eur. Phys. J.* **C1** (1998) 619–625, [arXiv:hep-th/9606055 \[hep-th\]](#).

- [95] D.-f. Hou, E. Wang, and U. W. Heinz, “n point functions at finite temperature,” *J. Phys.* **G24** (1998) 1861–1868, [arXiv:hep-th/9807118](#) [hep-th].
- [96] E. Wang and U. W. Heinz, “A Generalized fluctuation dissipation theorem for nonlinear response functions,” *Phys. Rev.* **D66** (2002) 025008, [arXiv:hep-th/9809016](#) [hep-th].
- [97] D.-f. Hou, M. E. Carrington, R. Kobes, and U. W. Heinz, “Four point spectral functions and Ward identities in hot QED,” *Phys. Rev.* **D61** (2000) 085013, [arXiv:hep-ph/9911494](#) [hep-ph]. [Erratum: *Phys. Rev.*D67,049902(2003)].
- [98] F. Guerin, “Retarded - advanced N point Green functions in thermal field theories,” *Nucl. Phys.* **B432** (1994) 281–314, [arXiv:hep-ph/9306210](#) [hep-ph].
- [99] F. Guerin, “Four point functions in Keldysh basis,” [arXiv:hep-ph/0105313](#) [hep-ph].
- [100] H. Chu and H. Umezawa, “Time ordering theorem and calculational recipes for thermal field dynamics,” *Phys. Lett.* **A177** (1993) 385–393.
- [101] P. A. Henning, “The Column vector calculus for thermo field dynamics of relativistic quantum fields,” *Phys. Lett.* **B313** (1993) 341–346, [arXiv:nucl-th/9305007](#) [nucl-th].
- [102] P. A. Henning, “Thermo field dynamics for quantum fields with continuous mass spectrum,” *Phys. Rept.* **253** (1995) 235–380.
- [103] M. E. Carrington, T. Fugleberg, D. S. Irvine, and D. Pickering, “Index summation in real time statistical field theory,” *European Physical Journal C* **50** (Apr., 2007) 711–727, [hep-ph/0608298](#).
- [104] E. Braaten and R. D. Pisarski, “Simple effective Lagrangian for hard thermal loops,” *Phys. Rev.* **D45** no. 6, (1992) R1827.
- [105] R. Baier and A. Niegawa, “Analytic continuation of thermal N point functions from imaginary to real energies,” *Phys. Rev.* **D49** (1994) 4107–4112, [arXiv:hep-ph/9307362](#) [hep-ph].



- [106] P. Aurenche and T. Becherrawy, “A comparison of the real-time and the imaginary-time formalisms of finite-temperature field theory for 2, 3 and 4-point green functions,” *Nuclear Physics B* **379** no. 1-2, (1992) 259–303.
- [107] M. van Eijck and C. G. Van Weert, “Finite-temperature retarded and advanced green functions,” *Physics Letters B* **278** no. 3, (1992) 305–310.
- [108] M. A. van Eijck, R. Kobes, and C. G. van Weert, “Transformations of real time finite temperature Feynman rules,” *Phys. Rev.* **D50** (1994) 4097–4109, [arXiv:hep-ph/9406214](https://arxiv.org/abs/hep-ph/9406214) [hep-ph].
- [109] N. Tsuji and P. Werner, “Out-of-time-ordered correlators of the hubbard model: Sachdev-ye-kitaev strange metal in the spin-freezing crossover region,” *Phys. Rev. B* **99** (Mar, 2019) 115132. <https://link.aps.org/doi/10.1103/PhysRevB.99.115132>.
- [110] R. L. Kobes and G. W. Semenoff, “Discontinuities of Green Functions in Field Theory at Finite Temperature and Density,” *Nucl. Phys.* **B260** (1985) 714–746.
- [111] R. L. Kobes and G. W. Semenoff, “Discontinuities of Green Functions in Field Theory at Finite Temperature and Density. 2,” *Nucl. Phys.* **B272** (1986) 329–364.
- [112] R. Kobes, “Retarded functions, dispersion relations, and cutkosky rules at zero and finite temperature,” *Physical Review D* **43** no. 4, (1991) 1269.
- [113] Y. Sekino and L. Susskind, “Fast Scramblers,” *JHEP* **10** (2008) 065, [arXiv:0808.2096](https://arxiv.org/abs/0808.2096) [hep-th].
- [114] R. Omnès, “On Locality, Growth and Transport of Entanglement,” *ArXiv e-prints* (Dec., 2012) , [arXiv:1212.0331](https://arxiv.org/abs/1212.0331) [quant-ph].
- [115] H. Kim and D. A. Huse, “Ballistic Spreading of Entanglement in a Diffusive Nonintegrable System,” *Physical Review Letters* **111** no. 12, (Sept., 2013) 127205, [arXiv:1306.4306](https://arxiv.org/abs/1306.4306) [quant-ph].
- [116] S. Caron-Huot, “Hard thermal loops in the real-time formalism,” *JHEP* **04** (2009) 004, [arXiv:0710.5726](https://arxiv.org/abs/0710.5726) [hep-ph].

- [117] C. P. Herzog and D. T. Son, “Schwinger-Keldysh propagators from AdS/CFT correspondence,” *JHEP* **03** (2003) 046, [arXiv:hep-th/0212072](#) [hep-th].
- [118] K. Skenderis and B. C. van Rees, “Real-time gauge/gravity duality,” *Phys. Rev. Lett.* **101** (2008) 081601, [arXiv:0805.0150](#) [hep-th].
- [119] S. Chaudhuri and R. Loganayagam, “Simplifying OTO Diagrammatics,” *To appear* .
- [120] W. Bernard and H. B. Callen, “Irreversible Thermodynamics of Nonlinear Processes and Noise in Driven Systems,” *Rev. Mod. Phys.* **31** (1959) 1017–1044.
- [121] J. A. Hertz, Y. Roudi, and P. Sollich, “Path integral methods for the dynamics of stochastic and disordered systems,” *Journal of Physics A Mathematical General* **50** no. 3, (Jan., 2017) 033001, [arXiv:1604.05775](#) [cond-mat.dis-nn].
- [122] K. H. Madsen, S. Ates, T. Lund-Hansen, A. Löffler, S. Reitzenstein, A. Forchel, and P. Lodahl, “Observation of Non-Markovian Dynamics of a Single Quantum Dot in a Micropillar Cavity,” *Physical Review Letters* **106** no. 23, (June, 2011) 233601, [arXiv:1012.0740](#) [cond-mat.mes-hall].
- [123] S. Groblacher, A. Trubarov, N. Prigge, G. Cole, M. Aspelmeyer, and J. Eisert, “Observation of non-Markovian micromechanical Brownian motion,” *Nature Communications* **6:7606** (2015) , [arXiv:1305.6942](#) [quant-phys].
- [124] X. Mi, J. V. Cady, D. M. Zajac, P. W. Deelman, and J. R. Petta, “Strong coupling of a single electron in silicon to a microwave photon,” *Science* **355** (Jan., 2017) 156–158, [arXiv:1703.03047](#) [cond-mat.mes-hall].
- [125] A. Potočnik, A. Bargerbos, F. A. Y. N. Schröder, S. A. Khan, M. C. Collodo, S. Gasparinetti, Y. Salathé, C. Creatore, C. Eichler, H. E. Türeci, A. W. Chin, and A. Wallraff, “Studying light-harvesting models with superconducting circuits,” *Nature Communications* **9** (Mar., 2018) 904, [arXiv:1710.07466](#) [quant-ph].
- [126] R. L. Stratonovich, *Nonlinear nonequilibrium thermodynamics I: linear and nonlinear fluctuation-dissipation theorems*, vol. 57. Springer Science & Business Media, 2012.

- [127] R. Stratonovich, *Nonlinear Nonequilibrium Thermodynamics II: Advanced Theory*. Springer Series in Synergetics. Springer Berlin Heidelberg, 2013.  
<https://books.google.co.in/books?id=0unnCAAQBAJ>.
- [128] A. Chakraborty and R. Sensarma, “Power-law tails and non-Markovian dynamics in open quantum systems: An exact solution from Keldysh field theory,” *prb* **97** no. 10, (Mar., 2018) 104306, [arXiv:1709.04472](https://arxiv.org/abs/1709.04472) [[cond-mat.stat-mech](https://arxiv.org/archive/cond)].
- [129] M. Bixon and R. Zwanzig, “Brownian motion of a nonlinear oscillator,” *Journal of Statistical Physics* **3** (Sept., 1971) 245–260.
- [130] R. Zwanzig, “Nonlinear generalized Langevin equations,” *Journal of Statistical Physics* **9** (Nov., 1973) 215–220.
- [131] A. Schenzle and H. Brand, “Multiplicative stochastic processes in statistical physics,” *Physics Letters A* **69** (Jan., 1979) 313–315.
- [132] T. A. Brun, “Quasiclassical equations of motion for nonlinear Brownian systems,” *Phys. Rev.* **D47** (1993) 3383–3393, [arXiv:gr-qc/9306013](https://arxiv.org/abs/gr-qc/9306013) [[gr-qc](https://arxiv.org/archive/gr)].
- [133] G. Efremov, “A fluctuation dissipation theorem for nonlinear media,” *Sov. Phys. JETP* **28** (1969) 1232.
- [134] R. Stratonovich, “Thermal noise in nonlinear resistors,” *VUZ Radiofizika* **13** (1970) 1512–1522.
- [135] R. Stratonovich, “Contribution to the quantum nonlinear theory of thermal fluctuations,” *SOVIET PHYSICS JETP* **31** no. 5, (1970) .
- [136] G. Efremov, “Contribution to theory of heat fluctuations in the nonequilibrium media,” *Izv. Vuzov (Radiofizika)* **15** (1972) 1207.
- [137] G. Bochkov and Y. E. Kuzovlev, “General theory of thermal fluctuations in nonlinear systems,” *Zh. Eksp. Teor. Fiz* **72** (1977) 238–243.
- [138] A. Sitenko, “The fluctuation-dissipation relation in nonlinear electrodynamics,” *Sov. Phys. JETP* **48** (1978) 51.

- [139] J. Gordon, “The fluctuation-dissipation relation in nonlinear electrodynamics,” *Zh. Eksp. Teor. Fiz* **75** (1978) 104–115.
- [140] D. Klyshko, *Photons Nonlinear Optics*. CRC Press, 2018.  
<https://books.google.co.in/books?id=yJdYDwAAQBAJ>.
- [141] R. Haag, N. M. Hugenholtz, and M. Winnink, “On the Equilibrium states in quantum statistical mechanics,” *Commun. Math. Phys.* **5** (1967) 215–236.
- [142] H. A. Weldon, “Two sum rules for the thermal n-point functions,” *Phys. Rev.* **D72** (2005) 117901.
- [143] T. J. Kippenberg and K. J. Vahala, “Cavity opto-mechanics,” *Optics express* **15** no. 25, (2007) 17172–17205.
- [144] A. Joshi and R. R. Puri, “Dynamical evolution of the two-photon jaynes-cummings model in a kerr-like medium,” *Phys. Rev. A* **45** (Apr, 1992) 5056–5060.  
<https://link.aps.org/doi/10.1103/PhysRevA.45.5056>.
- [145] P. Góra and C. Jędrzejek, “Nonlinear jaynes-cummings model,” *Phys. Rev. A* **45** (May, 1992) 6816–6828. <https://link.aps.org/doi/10.1103/PhysRevA.45.6816>.
- [146] W. Vogel and R. L. d. M. Filho, “Nonlinear jaynes-cummings dynamics of a trapped ion,” *Phys. Rev. A* **52** (Nov, 1995) 4214–4217.  
<https://link.aps.org/doi/10.1103/PhysRevA.52.4214>.
- [147] X.-J. Liu, J.-B. Lu, S.-Q. Zhang, J.-P. Liu, H. Li, Y. Liang, J. Ma, Y.-J. Weng, Q.-R. Zhang, H. Liu, X.-R. Zhang, and X.-Y. Wu, “The nonlinear jaynes-cummings model for the multiphoton transition,” *International Journal of Theoretical Physics* **57** no. 1, (Jan, 2018) 290–298. <https://doi.org/10.1007/s10773-017-3604-3>.
- [148] F. Barra, “The thermodynamic cost of driving quantum systems by their boundaries,” *Scientific Reports* **5** (Oct., 2015) 14873, [arXiv:1509.04223](https://arxiv.org/abs/1509.04223) [quant-ph].
- [149] G. Sadiq and S. Almalki, “Entanglement dynamics in heisenberg spin chains coupled to a dissipative environment at finite temperature,” *Phys. Rev. A* **94** (Jul, 2016) 012341.  
<https://link.aps.org/doi/10.1103/PhysRevA.94.012341>.

- [150] E. Ilievski, *Exact solutions of open integrable quantum spin chains*. PhD thesis, Ljubljana U., 2014. [arXiv:1410.1446](https://arxiv.org/abs/1410.1446) [quant-ph].
- [151] A. Das, S. Chakrabarty, A. Dhar, A. Kundu, D. A. Huse, R. Moessner, S. S. Ray, and S. Bhattacharjee, “Light-cone spreading of perturbations and the butterfly effect in a classical spin chain,” *Phys. Rev. Lett.* **121** (Jul, 2018) 024101. <https://link.aps.org/doi/10.1103/PhysRevLett.121.024101>.
- [152] T. Scaffidi and E. Altman, “Semiclassical Theory of Many-Body Quantum Chaos and its Bound,” [arXiv:1711.04768](https://arxiv.org/abs/1711.04768) [cond-mat.stat-mech].
- [153] V. Khemani, D. A. Huse, and A. Nahum, “Velocity-dependent Lyapunov exponents in many-body quantum, semiclassical, and classical chaos,” *Phys. Rev.* **B98** no. 14, (2018) 144304, [arXiv:1803.05902](https://arxiv.org/abs/1803.05902) [cond-mat.stat-mech].
- [154] E. B. Rozenbaum, S. Ganeshan, and V. Galitski, “Lyapunov exponent and out-of-time-ordered correlator’s growth rate in a chaotic system,” *Phys. Rev. Lett.* **118** (Feb, 2017) 086801. <https://link.aps.org/doi/10.1103/PhysRevLett.118.086801>.
- [155] J. de Boer, V. E. Hubeny, M. Rangamani, and M. Shigemori, “Brownian motion in AdS/CFT,” *Journal of High Energy Physics* **2009** no. 07, (Jul, 2009) 094–094. <https://doi.org/10.1088/2F1126-6708/2F2009/2F07/2F094>.
- [156] D. T. Son and D. Teaney, “Thermal Noise and Stochastic Strings in AdS/CFT,” *JHEP* **07** (2009) 021, [arXiv:0901.2338](https://arxiv.org/abs/0901.2338) [hep-th].
- [157] A. N. Atmaja, J. de Boer, and M. Shigemori, “Holographic Brownian Motion and Time Scales in Strongly Coupled Plasmas,” *Nucl. Phys.* **B880** (2014) 23–75, [arXiv:1002.2429](https://arxiv.org/abs/1002.2429) [hep-th].
- [158] P. Banerjee and B. Sathiapalan, “Holographic Brownian Motion in 1+1 Dimensions,” *Nucl. Phys.* **B884** (2014) 74–105, [arXiv:1308.3352](https://arxiv.org/abs/1308.3352) [hep-th].
- [159] J. Sadeghi, B. Pourhassan, and F. Pourasadollah, “Holographic Brownian motion in 2 + 1 dimensional hairy black holes,” *Eur. Phys. J.* **C74** no. 3, (2014) 2793, [arXiv:1312.4906](https://arxiv.org/abs/1312.4906) [hep-th].

- [160] P. Banerjee, “Holographic Brownian motion at finite density,” *Phys. Rev.* **D94** no. 12, (2016) 126008, [arXiv:1512.05853 \[hep-th\]](#).
- [161] J. de Boer, E. Llabrés, J. F. Pedraza, and D. Vegh, “Chaotic strings in AdS/CFT,” *Phys. Rev. Lett.* **120** (May, 2018) 201604.  
<https://link.aps.org/doi/10.1103/PhysRevLett.120.201604>.
- [162] J. de Boer, M. P. Heller, and N. Pinzani-Fokeeva, “Holographic Schwinger-Keldysh effective field theories,” *JHEP* **05** (2019) 188, [arXiv:1812.06093 \[hep-th\]](#).
- [163] P. Glorioso, M. Crossley, and H. Liu, “A prescription for holographic Schwinger-Keldysh contour in non-equilibrium systems,” [arXiv:1812.08785 \[hep-th\]](#).
- [164] B. Chakrabarty, J. Chakravarty, S. Chaudhuri, C. Jana, R. Loganayagam, and A. Sivakumar, “Nonlinear Langevin dynamics via holography,” [arXiv:1906.07762 \[hep-th\]](#).
- [165] M. Tsatsos, “The Van der Pol Equation,” [arXiv:0803.1658 \[math-ph\]](#).
- [166] H. J. Korsch and H.-J. Jodl, *Chaos*. Springer Berlin Heidelberg, 1999.  
<https://doi.org/10.1007%2F978-3-662-03866-6>.
- [167] Y. Ku and X. Sun, “Chaos in van der pol’s equation,” *Journal of the Franklin Institute* **327** no. 2, (1990) 197 – 207.  
<http://www.sciencedirect.com/science/article/pii/001600329090016C>.
- [168] M. Zhang and J.-p. Yang, “Bifurcations and chaos in duffing equation,” *Acta Mathematicae Applicatae Sinica, English Series* **23** no. 4, (Oct, 2007) 665–684.  
<https://doi.org/10.1007/s10255-007-0404>.
- [169] R. D. Jordan, “Effective field equations for expectation values,” *Phys. Rev. D* **33** (Jan, 1986) 444–454. <https://link.aps.org/doi/10.1103/PhysRevD.33.444>.
- [170] E. Calzetta and B. L. Hu, “Closed-time-path functional formalism in curved spacetime: Application to cosmological back-reaction problems,” *Phys. Rev. D* **35** (Jan, 1987) 495–509. <https://link.aps.org/doi/10.1103/PhysRevD.35.495>.

- [171] S. Weinberg, “Quantum contributions to cosmological correlations,” *Phys. Rev. D* **72** (Aug, 2005) 043514.  
<https://link.aps.org/doi/10.1103/PhysRevD.72.043514>.
- [172] D. Boyanovsky, “Effective field theory during inflation: Reduced density matrix and its quantum master equation,” *Phys. Rev.* **D92** no. 2, (2015) 023527, [arXiv:1506.07395](https://arxiv.org/abs/1506.07395) [[astro-ph.CO](https://arxiv.org/archive/astro-ph)].
- [173] D. Boyanovsky, “Effective field theory during inflation. II. Stochastic dynamics and power spectrum suppression,” *Phys. Rev.* **D93** (2016) 043501, [arXiv:1511.06649](https://arxiv.org/abs/1511.06649) [[astro-ph.CO](https://arxiv.org/archive/astro-ph)].
- [174] D. Boyanovsky, “Imprint of entanglement entropy in the power spectrum of inflationary fluctuations,” *Phys. Rev. D* **98** (Jul, 2018) 023515.  
<https://link.aps.org/doi/10.1103/PhysRevD.98.023515>.
- [175] D. Boyanovsky, “Information loss in effective field theory: entanglement and thermal entropies,” *Phys. Rev.* **D97** no. 6, (2018) 065008, [arXiv:1801.06840](https://arxiv.org/abs/1801.06840) [[hep-th](https://arxiv.org/archive/hep)].
- [176] R. Kubo, “The fluctuation-dissipation theorem,” *Reports on progress in physics* **29** no. 1, (1966) 255.
- [177] M. A. Nielsen and I. L. Chuang, *Quantum Computation and Quantum Information*. Cambridge University Press, 2000.
- [178] M. Rangamani and T. Takayanagi, “Holographic Entanglement Entropy,” *Lect. Notes Phys.* **931** (2017) pp.1–246, [arXiv:1609.01287](https://arxiv.org/abs/1609.01287) [[hep-th](https://arxiv.org/archive/hep)].
- [179] S. Ryu and T. Takayanagi, “Holographic derivation of entanglement entropy from AdS/CFT,” *Phys. Rev. Lett.* **96** (2006) 181602, [arXiv:hep-th/0603001](https://arxiv.org/abs/hep-th/0603001) [[hep-th](https://arxiv.org/archive/hep)].
- [180] S. Ryu and T. Takayanagi, “Aspects of Holographic Entanglement Entropy,” *JHEP* **08** (2006) 045, [arXiv:hep-th/0605073](https://arxiv.org/abs/hep-th/0605073) [[hep-th](https://arxiv.org/archive/hep)].